UNIVERSITY OF LEICESTER

The role of ActA in peptidoglycan remodelling of *Listeria monocytogenes*

Thesis Submitted for the Degree of Doctor of Philosophy at the University of Leicester

By

Ohoud Saud Al-Humaidan

(BSc, MSc)

College of Medicine, Biological Sciences and Psychology

Department of Infection, Immunity and Inflammation

University of Leicester

United Kingdom

2020

Statement of Originality

This accompanying thesis submitted for the degree of PhD entitled **"The role of ActA in peptidoglycan remodelling of *Listeria monocytogenes"*** is based on work conducted by the author in the Department of Infection, Immunity and Inflammation of University of Leicester during the period between January 2016 and December 2019.

All the work recorded in this thesis is original unless otherwise acknowledged in the text or by references.

None of this work has been submitted for another degree in this or any other University.

Signed………………………..   Date…………………………

Abstract

Listeria monocytogenes is a food-borne bacterial pathogen, which occupies different ecological niches and is responsible for a number of serious infections in humans.

L. monocytogenes has many virulence factors that enable its replication in macrophages and escape from the phagolysosome to the cytoplasm. The actin-assembly inducing protein (ActA) is one of the major virulence factors, which mediates actin polymerization, and thereby aids the intracellular motility and cell-to-cell spread, which is critical for *L. monocytogenes* pathogenesis. Recently, the ActA protein has been shown to regulate peptidoglycan (PG) biosynthesis during the replication of *L. monocytogenes* in macrophages. However, the exact mechanism for this phenomenon is unknown. The central hypothesis of the present study is that ActA possesses PG cleaving activity which controls PG biosynthesis and remodelling.

ActA is a secreted protein which consists of N-terminal, central and C-terminal domains. Three recombinant His-tagged proteins representing different domains of ActA have been successfully expressed and purified in *Escherichia coli* C41(DE3). Using a range of approaches, I have shown that the N-terminal domain of ActA has PG cleaving activity. To identify putative catalytic residues, 14 site-directed mutants where acidic residues were replaced with alanine have been generated. None of the mutants resulted in the complete elimination of cleaving activity; however, there was a reduction in activity for two mutants, the MUT 3 and MUT6 proteins. Proteomic analysis revealed the presence of ActA in the culture supernatant and the cell envelope fractions of *L. monocytogenes*, further supporting the idea that the role of this protein is in cell wall remodelling. ActA has 50 % homology with RpfA, one of the resuscitation-promoting factors found in *Mycobacteria*. However, domain swapping experiments in which the active domain in RpfA was replaced with the N-terminal domain of ActA, showed limited complementation of the triple Rpf mutant phenotype.

The identification of peptidoglycan cleaving activity of the N- terminal domain in ActA from *L. monocytogenes* would offer a novel opportunity to target and combat the virulence of this significant pathogen.

Acknowledgements

Scientific contributions

Publications:

- Jessica Loraine[1], Ohoud Alhumaidan[1], Andrew R. Bottrill, Sharad C. Mistry, Peter Andrew, Galina V. Mukamolova, Obolbek Turapov (2019) 'Efficient protein digestion at elevated temperature in the presence of sodium dodecyl sulfate and calcium ions for membrane proteomics', *Anal. Chem*, 91 (15), pp.9516-9521.

  A full version of the article can be found at the following link:
  https://www.ncbi.nlm.nih.gov/pubmed/31259536

Awards:

- **Best poster awardee**, at the 7th European Clinical Microbiology Congress held during November 01-03, 2018, in London, UK.

- **Second best placed poster**, at the third annual Midlands Academy of Medical Sciences Research Festival held on 23rd March 2018, at Loughborough University, UK.

Poster presentations:

- The third annual Midlands Academy of Medical Sciences Research Festival, held on the 23rd March 2018, at Loughborough University, UK.

- The 7th European Clinical Microbiology Congress, held during November 01-03 2018, in London, UK.

- The Microbiology Society Annual Conference, held during 10-13 April, 2018 in Birmingham.

- The 6th Midlands Molecular Microbiology Conference, held on 9th and 10th September 2019, at the University of Nottingham.

- The 6th Young Microbiologist Symposium on Microbe signalling, Organisation and Pathogenesis, held on 26th-27th August 2020, at the University of Southampton, UK.

Oral presentations:

- Post-Graduate Research Festival at the University of Leicester in 2017 and 2018.

- Flash presentation at the 6th Midlands Molecular Microbiology Conference, held on 9th and 10th September 2019, in the University of Nottingham.

Abbreviation

%	Percent
°C	Degrees centigrade
aa	Amino acid
ActA	Actin assembly inducing protein
ADC	Albumin Dextrose Catalase
Amp	Ampicillin
BCIP/NBT substrate	5-Bromo-4-chloro-3-indolyl phosphate/ nitro blue tetrazolium
bp	Base pair(s)
CFU	Colony forming unit
CSF	Cerebrospinal fluid
DMSO	Dimethyl sulfoxide
DNA	Deoxyribonucleic acid
dNTP	Deoxynucleotide
g	Gram
G + C	Guanine and Cytosine
H2O	Water
His-tag	Histidine Tag
IPTG	Isopropyl β-D-1-thiogalactopyranoside
Kan	Kanamycin
l	Litre
LA	Luria agar
LB	Luria broth
log	Logarithmic
LTGs	Lytic transglycosylase
M	Molar
M. luteus	*Micrococcus luteus*
ml	Milliliter
mM	Millimolar
Mtb	*Mycobacterium tuberculosis*
NaCl	Sodium chloride
NAG	N-Acetylglucosamine acid
NAM	N-Acetylmuramic acid
OD_{600}	Optical density reading at 600nm
PAGE	Polyacrylamide gel electrophoresis
PBS	Phosphate buffered saline
PCR	Polymerase chain reaction
PG	Peptidoglycan
PNACL	Protein nucleic acid chemistry laboratory
Rpf	Resuscitation promoting factor
RP-HPLC	Reverse phase high pressure liquid chromatography
rpm	Round per minute
Spp	Species
TAE	Tris acetic acid EDTA
v/v	Volume per volume
w/v	Weight per volume
WASP	Wiskott-Aldrich Syndrome Protein
WT	Wild type
X-gal	5-bromo-4-chloro-3-indolyl β-D-galactopyranoside

Contents

List of tables

List of Figures

xiii

Chapter 1

Introduction

1.1   *Listeria* history, taxonomy and ecology

Listeria monocytogenes was originally described in two independent studies by Murray and Pirie in 1927 (Biester and Schwarte 1939). Murray referred to it as *"Bacterium monocytegenes"* due to the characteristic monocytosis induced by the pathogen in infected laboratory rabbits and guinea pigs in Cambridge (Farber and Peterkin 1991). Pirie isolated the bacterium from rodents in South Africa and named it *"Listerella hepatolytica"* (Biester and Schwarte 1939) and suggested using the current name, *Listeria monocytogenes*, in 1940 (PIRIE 1940). In 1957, *Listeria* was classified as part of the *Corynebacteriaceae* family as a non-sporing Gram-positive rod (Farber and Peterkin 1991). Initially, *Listeria* was isolated from infected animals, however, in 1929, the first incidence of human listeriosis was reported in Denmark (Gray and Killinger 1966). Several cases of Gram-positive rods being isolated from patients in France in 1891 and in Germany in 1893 are now considered to have been *L. monocytogenes* (Gray and Killinger 1966). In 1981, a human listeriosis outbreak reported in Canada resulted in 18 deaths in 41 reported cases, involving neonates and pregnant women (Schlech III *et al.* 1983). Despite this, *L. monocytogenes* infections remain rare; nonetheless, it is still considered a problem for the food processing industry because of relatively highly mortality rates in immunocompromised individuals, fetal loss and neonatal death. In 1982 , the incidence of human listeriosis globally was reported to be 7.4 cases per million people per year, totaling to approximately 1,850 cases, with about 425 deaths reported only in the United States, the majority of cases occurring in neonates and elderly people (>70 years)(Ciesielski *et al.* 1988).

The *Listeria* genus has 17 species, including *L. aquatica, L. booriae, L. cornellensis, L. fleischmannii, L. floridensis, L. grandensis, L. grayi, L. innocua, L. ivanovii, L. marthii,L. monocytogenes, L. newyorkensis, L. riparia, L. rocourtiae, L. seeligeri, L. weihenstephanensis* and *L. welshimeri* (Weller *et al.* 2015; Orsi and Wiedmann 2016). Moreover, Hartford and Sneath suggest that *L. monocytogenes* and *L. ivanovii* are very closely related species based on DNA hybridisation studies, and that *L. grayii* is the most distantly related species of the *Listeria* genus (Schmid *et al.* 2005). Both *L. ivanovii* and *L. monocytogenes* cause human listeriosis (Guillet *et al.* 2010). However, *L. monocytogenes* is the most common pathogen, which causes listeriosis in humans (Guillet *et al.* 2010; Weller *et al.* 2015).

L. monocytogenes is a short rod with a diameter of 0.4 to 0.5 μm and a length of 0.5-2.0 μm; it tends to form a short rod-chains. A microscopic examination of old *Listeria* cultures revealed cells that that had long filaments of around 6 μm in length (Vos *et al.* 2011). It is a motile, non-

capsulated organism which can grow at a wide range of temperatures (Vázquez-Boland *et al.* 2001). *L. monocytogenes* has been found in a diversity of ecological niches such as soils, manure, sewage and the faeces of humans and animals such as cattle and sheep. It has also been found in natural water sources such as lakes, rivers and streams (Dijkstra 1982). *L. monocytogenes* is also a common food contaminant, which can be found in cabbages, cucumbers, sprouts, mushrooms, meat products, hot dogs, milk, cheese and other dairy products (Welshimer and Donker-Voet 1971; Watkins and SLEATH 1981; Colburn *et al.* 1990; Fenlon *et al.* 1996; Ramaswamy *et al.* 2007). Furthermore, *L. monocytogenes* has been isolated from fish products and seafood (Rocourt and Cossart 1997). In 1990, it was reported that 60 % of raw chicken was contaminated with *L. monocytogenes*, making poultry a major source of *Listeria* contamination (Bailey *et al.* 1990). Although *L. monocytogenes* can be killed by correctly cooking food and pasteurisation (Petran and Zottola 1989), it remains a significant problem in ready-to-eat foods that are consumed without any heat treatment or contaminated after cooking and packing (Tompkin 2002; Buchanan *et al.* 2017). It is thought that the natural habitat of this bacterium is decomposing plant matter, in which they live as saprophytes (Vázquez-Boland *et al.* 2001). Furthermore, *L. monocytogenes* has been identified in 9 out of 10 samples of wilting grass (Fenlon *et al.* 1996).

L. monocytogenes can survive freezing and is frequently detected in frozen food and ice-cream (Weagant *et al.* 1988). It can also contaminate door handles (Jarvis *et al.* 2016) and the surfaces of food processing factories (Ivanek *et al.* 2006). *L. monocytogenes* is able to form biofilms, which are highly resistant to antiseptic treatment and other stressful environmental conditions (Lundén *et al.* 2002; Ferreira *et al.* 2014). The formation of biofilms helps *L. monocytogenes* survive in very harsh environments (Travier *et al.* 2013). *L. monocytogenes* biofilms are highly problematic in the food processing industry and have been found to contaminate drains, sinks and stainless steel surfaces (Chambel *et al.* 2007). This problem is especially high in artisanal cheese dairies found in Portugal and Spain (Kongo *et al.* 2006).

Furthermore, *L. monocytogenes* biofilms are also highly significant in the clinical setting; Chrdle and Stárek reported the presence of a *L. monocytogenes* biofilm on a prosthetic hip joint, in combination with *Staphylococcus epidermidis* (Chrdle and Stárek 2011). In addition to this, *L. monocytogenes* biofilms have been reported as a complication in young children receiving ventriculoperitoneal shunts (Yakut *et al.* 2018) .

1.2 Listeriosis

1.2.1 Epidemiological situation

L. monocytogenes is a causative agent of listeriosis; the first case of human listeriosis was reported by Nyfeldt in 1929 (Nyfeldt 1929). The route of infection for human listeriosis is through the ingestion of contaminated food (Ragon *et al.* 2008; Salazar *et al.* 2016; Buchanan *et al.* 2017), and transplacentally from mother to fetus; the infant can be infected during delivery by contact with the birth canal infected with this bacterium (Colodner *et al.* 2003; Jamieson *et al.* 2006; Chaturvedi *et al.* 2015). However, no human-to-human infections have been reported (Ramaswamy *et al.* 2007; Swaminathan and Gerner-Smidt 2007).

Listeriosis, to some extent, remains relatively rare, and a noticeable decrease in listeriosis was observed in 2016 (~184 confirmed cases) according to a Public Health England (PHE) report published in May 2018 (PHE May 2018), as shown in Figure 1. The observed decrease in listeriosis reflects the increased awareness about this infection and that improvements in the manner in which *Listeria* was detected beforehand, thus it could be treated before-hand, in this way preventing the chance of infection. However, listeriosis is a severe illness and mortalities continue to occur among patients (Buchanan *et al.* 2017). Listeriosis is considered the most deadly foodborne pathogen when compared with other enteropathogenic bacteria such as *Salmonella* and *Clostridium* (Mead *et al.* 2000). Approximately 1/3 of all mortality cases associated with food-related infections are due to listeriosis (Schuppler and Loessner 2010; Buchanan *et al.* 2017). The main risk groups are elderly people and immunocompromised patients, together with pregnant women and infants (Ramaswamy *et al.* 2007).
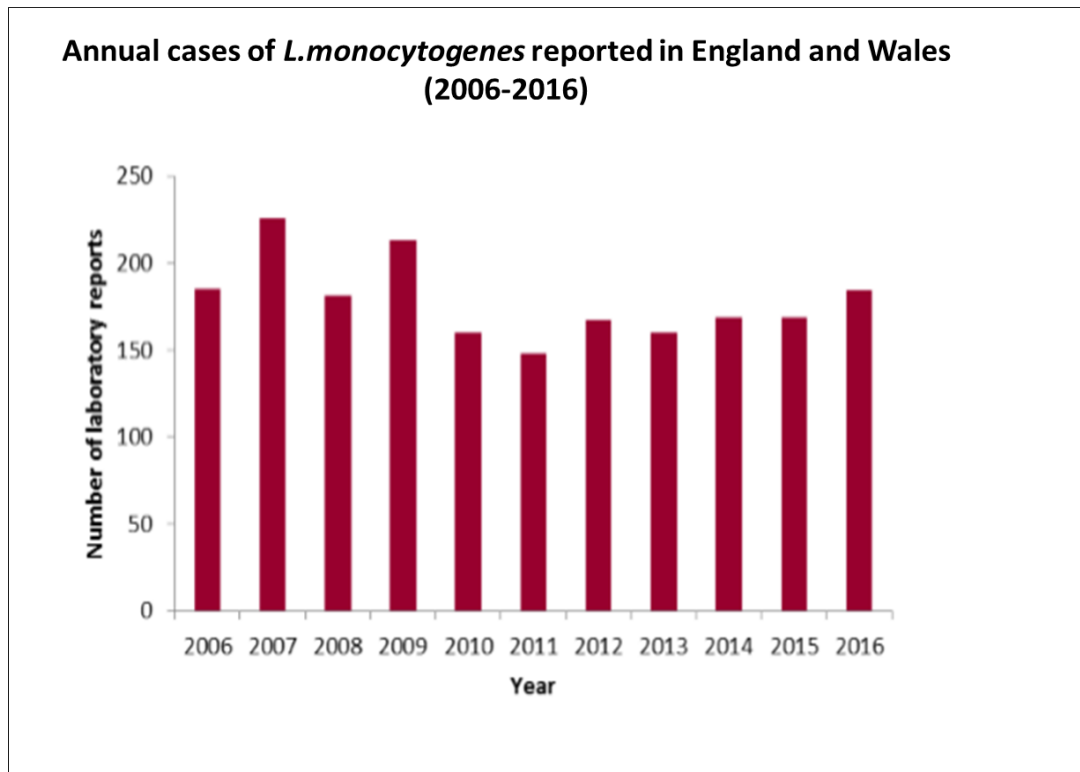
Figure 1. Number of listeriosis cases per 100, 000 people in 2006-2016 in England and Wales. This figure was published by (PHE May 2018).

Numerous human listeriosis outbreaks have occurred in many countries since the first identification of a foodborne outbreak associated with listeriosis in 1981 (Vázquez-Boland *et al.* 2001) including the UK (Dawson *et al.* 2006; Hodgkin Jun 2017), Japan (Makino *et al.* 2005), Australia (Fretz *et al.* 2010) and the United States (Wiedmann *et al.* 1996; Gottlieb *et al.* 2006). These outbreaks were related to a variety of foods such as fish, cheeses, meat, milk and salads. Moreover, it was challenging to identify the sources of these outbreaks due to the long incubation time of this organism (Vázquez-Boland *et al.* 2001).

According to the US Food Safety Inspection Service (FSIS) report in 2002, 12 severe listeriosis outbreaks were identified in the United States between 1970-2002, and a total of 466 listeriosis infections with serious complications (Williams 2010). The European Centre for Disease Prevention and Control (ECDC) reported a multi-country outbreak of listeriosis due to contaminated frozen vegetables; 47 listeriosis cases were confirmed, with 19 % of them resulting in death (Buchanan *et al.* 2017). In 2019, Public Health England reported that six patients died following a listeriosis outbreak linked to pre-packed sandwiches (Sinmaz and Tozer 2019).

Several reports have shown that *L. monocytogenes* can cause septicaemia, meningitis and endocarditis in elderly people and cause death for around 25-30 % of immunocompromised patients such as those with cancer, kidney failure and AIDS (McLauchlin 1997; Hamon *et al.* 2006; Ramaswamy *et al.* 2007). A previous study conducted on 722 listeriosis cases showed that 10-20 % of stillbirths or abortions in pregnant women were due to *L. monocytogenes*, while 68% of cases developed fetal infections or sepsis during infancy (Mylonakis *et al.* 2002) (Colodner *et al.* 2003). In 2010, 5 out of 10 immunocompromised patients died in Texas from listeriosis due to diced celery which was contaminated with *Listeria*. In 2011, according to the Food Standard Agency report (FSA 2016), *L. monocytogenes* was considered the second highest cause of foodborne disease in the UK after *Campylobacter,* and each year it causes higher mortality than *Salmonella* and *Escherichia coli* (The Food Standards Agency May 2011).

1.2.2 Clinical Signs and symptoms

The symptoms and severity of the disease depend on the mode of infection. It is estimated that the minimum dose required for infection by *L. monocytogenes* is at least 10^6 bacteria (Vázquez-Boland *et al.* 2001). The incubation period for disease development varies from hours, as in the case of *L. monocytogenes* gastroenteritis, to over 80 days, as in the case of *L. monocytogenes* septicaemia (Ooi and Lorber 2005). Individuals with non-invasive listeriosis can have an asymptomatic or mild illness; however, fever, headache, vomiting, muscle aches and gastrointestinal symptoms without serious complications like nausea and self-limiting diarrhoea can develop (Dalton *et al.* 1997; Aureli *et al.* 2000; Vázquez-Boland *et al.* 2001). In contrast, invasive listeriosis leads to life-threating systemic infections due to the ability of these bacteria to cross the intestinal barrier and reach the blood (Ooi and Lorber 2005; Ramaswamy *et al.* 2007).

Patients may suffer from loss of balance, confusion, severe headaches, stiff necks and meningitis due to the spread of this organism in the nervous system (Vázquez-Boland *et al.* 2001; Crum 2002). The other clinical forms of listeriosis are myocarditis, arthritis, pneumonia, pleuritis, hepatitis and colecystitis. In some cases, it can lead to arthritis, osteomyelitis, sinusitis, otitis, peritonitis, and localised abscesses (Vázquez-Boland *et al.* 2001; Buchanan *et al.* 2017). The following symptoms are communally seen in infants and children with listeriosis: breathing difficulties, jaundice, loss of appetite, skin rash and lethargy (Maguire and Riley Jr 1967).

1.2.3 Diagnosis and treatment

The early detection of *L. monocytogenes* is a crucial step in treating and controlling infections, especially in immunocompromised patients, fetuses and pregnant women. It can be easily misdiagnosed due to the similarity of symptoms with other diseases. Thus, various conventional tests are used to identify this organism in the lab, e.g. Gram staining, which is a basic technique to characterize the morphology of this organism (Liu 2008), growth in non-selective rich media, such as BHI or TSB and defined minimal media (Phan-Thanh and Gormon 1997). Moreover, a variety of biochemical tests can be used, such as the catalase and oxidase test, given that *L. monocytogenes* is catalase positive and oxidase negative (Farber and Peterkin 1991). However, the accuracy of the aforementioned assays and tests are low due to the similarity between *L. monocytogenes* and other Gram-positive bacteria. Thus, other sensitive methods have been developed, such as immunological tests to identify a specific antigen of *Listeria*, Listeriolysin O (Le Monnier *et al.* 2011). Various molecular techniques have also been developed, such as a polymerase chain reaction (PCR) assay to amplify specific genes of *Listeria* e,g *hly*, *prfA*, *actA* , DNA hybridization and whole genome sequencing for the rapid accurate detection of *L. monocytogenes* (Churchill *et al.* 2006; Le Monnier *et al.* 2011). Nowadays, the detection of various foodborne organisms can be done thanks to automated methods which depend on different biochemical identification tests, and the availability of identification libraries within systems such as the VITEK System (bioMerieux Vitek, Hazelwood, MO) (Churchill *et al.* 2006).

The treatment of human listeriosis with antibiotics is only required for pregnant women, newborns and immunocompromised patients (CDC 2011). Generally, the *Listeria* species are susceptible to many antimicrobial agents e.g. penicillin and gentamicin, however they are resistant to cephalosporins (Low and Donachie 1997). *L. monocytogenes* isolated from human blood culture and CSF was found to be susceptible to a variety of antibiotics such as penicillin, gentamicin, vancomycin and tetracycline (Wagner and McLauchlin 2008). Trimethoprim sulfamethoxazole is the alternative medication of choice for patients with allergies to beta-lactam antibiotics (Schaechter 2009). However, *L. monocytogenes* strains resistant to chloramphenicol, erythromycin, streptomycin and tetracycline have recently emerged (Low and Donachie 1997).

Phage therapy has been found to be efficient as an antimicrobial agent in a food processing setting, however, it cannot be used for intracellular infection (Schaechter 2009; Guenther and

Loessner 2011). For instant, phage A511 was able to destroy the *Listeria* cell wall and kill the cells within a short period of time (Lebreton *et al.* 2016). In 2011, the CDC mentioned that the most efficient way of preventing listeriosis is food pasteurization and limiting the consumption of unpasteurized milk, butter and soft cheeses. In addition, using disinfectants to clean surfaces and equipment during food processing may substantially reduce the risk of food contamination with *L. monocytogenes* and prevent listeriosis (Eklund *et al.* 1995).

1.3 Virulence and intracellular life cycle of *L. monocytogenes*

1.3.1 Intracellular Life cycle

The intracellular life cycle of *L. monocytogenes* starts from the ingestion of heavily contaminated food (McLauchlin 1997). *L. monocytogenes* have the ability to infect several types of cells and tissues within a host e,g epithelial cells , endothelial cells , macrophages , fibrblast cells , hepatocytes and dendritic cells (Lamont 2004; Schaechter 2009).

Once it reaches the bloodstream, a number of bacterial surface proteins aid *L. monocytogenes* to establish an infection and replicate inside the phagosome (Freitag *et al.* 2009). The organism uptake involves two major internalin proteins, internalin A (InlA) and internalin B (InlB) (Schuppler and Loessner 2010). Both inlA and inlB have been shown to contribute to the bacterial invasion of host cells by attaching to specific receptors on the host cell, called E-cadherin and hepatocyte growth factor (HGF) respectively (Portnoy *et al.* 2002; Schaechter 2009). Subsequent to cell entry, *L. monocytogenes* becomes encapsulated in a membrane-bound compartment as shown in Figure 2, and the internalized cells remain in vacuoles for approximately 30 minutes. Within minutes, the vacuole become acidified (Robbins *et al.* 1999) which lead to stop furthere maturation of the phagosome and help *L. monocytogenes* to survive in the vacules (Alvarez-Dominguez *et al.* 1997). The low pH inside the vacuole lead to activite several bacterial factors to allow *L. monocytogenes* to escape from the vacuole such as the metalloprotease (Mpl), the phospholipases (PLCs) and the pore-forming toxin called listeriolysin O(LLO) (Freitag *et al.* 2009; Schaechter 2009; Alvarez and Agaisse 2016). The phenomena of using an acid-activatable pore-forming proteins to mediate escape from a phagosome into the host cytosol has been reported with other intracellular organism such as *Trypanosoma cruzi* (Glomski *et al.* 2002).

The Mpl contributes in the activiation of the PLCs which lead to hydrolyse membrane phospholipids (Bitar *et al.* 2008; Alvarez and Agaisse 2016). Furthermore, LLO is very active (~10-fold more) at an acidic pH and as PLCs mediates the bacterial escape from vesicles into the cytoplasm by ruptured the phagosome membrane (Glomski *et al.* 2002). At this stage, *L. monocytogenes* starts to polymerize the host actin (Schnupf and Portnoy 2007). The actin assembly inducing protein (ActA) triggers the polymerization of actin and forms a long structure, known as the actin tail, which helps *L. monocytogenes* to move within the cytosol and from one cell to another (Pizarro-Cerdá *et al.* 2012). Then, when *L. monocytogenes* infects a new cell, the infectious cycle restarts.
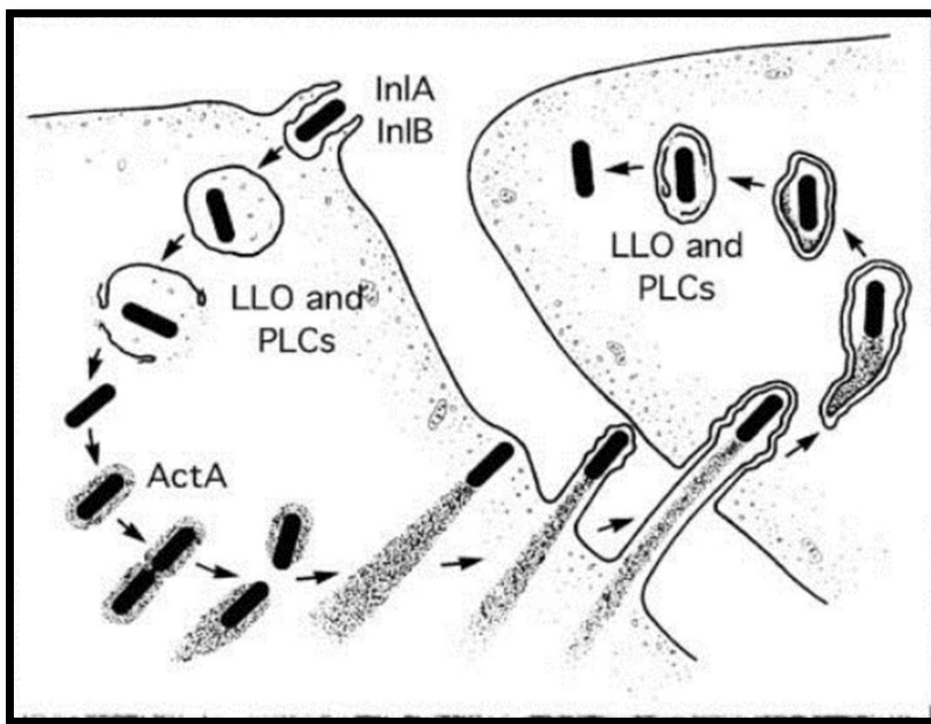
Figure 2. Scheme of intracellular invasion of *L. monocytogenes.*
In the Entry*; Listeria* manages to invade and escape from the host immune system with the use of Internalin A and B (InlA and Inl B). Inside the phagocyte, the organism lyses the phagosome using Listeriolisin O (LLO) and two phospholipases (PLCs). After being released in the cytoplasm, actin assembly inducing protein (ActA) induces actin polymerization for intracellular movment and celle to cell spread. Finally, once the bacterium reaches the cell membrane, it can rupture the cell and spread to neighbouring cells directly. The figure was published by (Portnoy *et al.* 1992).

1.3.2 Virulence factors

1.3.2.1 PrfA

PrfA stands for positive regulatory factor A (Goldfine and Shen 2007). It belongs to the family of cyclic AMP receptor protein (Crp) transcriptional regulators that can bind DNA specific sites within gene promoters, and activate transcription (Ripio *et al.* 1997; Vázquez-Boland *et al.* 2001; Lebreton and Cossart 2017). It is considered as a master switch which activates the expression of many essential virulence factors such as InlA, Hly, PlcA, PlcB and ActA, which are responsible for converting *L. monocytogenes* from an environmental saprophytic organism to an intracellular pathogen (de las Heras *et al.* 2011).

The first report of PrfA as a regulatory protein was in 1990 by Leimeister-Wachter. It was demonstrated that the *prfA* gene is required to stimulate the expression of the *hly* gene encoding for listeriolysin O (Leimeister-Wächter *et al.* 1990). Moreover, it is a temperature-dependent protein; research has found that it is maximally expressed at 37°C, while no expression at 30°C (Sheehan *et al.* 1995). The mutation of the *prfA* gene led to a defect in bacterial aggregation (Travier *et al.* 2013), intracellular growth and bacterial motility within host cells (Freitag *et al.* 1993), revealing the importance of this protein for *L. monocytogenes* virulence.

1.3.2.2 Internalins

L. monocytogenes invasion of a non-phagocytic cell occurs by internalization (Vázquez-Boland *et al.* 2001). The first internalin proteins were reported in 1991 by Gaillard *et al.* (Gaillard *et al.* 1991). Generally, internalins are surface proteins containing an N-terminal leucine-rich repeat (LRR) domain (Schaechter 2009). The analysis of *L. monocytogenes* EGDe revealed that it contained a higher number (~25) of internalins compared to other Gram-positive bacteria (Schaechter 2009). InlA and InlB are critical for *L. monocytogenes* because both play a role in the invasion of the organism into the host cell by attaching to particular receptors on the surface of host cells (Vázquez-Boland *et al.* 2001; Schaechter 2009; Sousa *et al.* 2011). InlA is a secreted protein made up of 800 amino acids, a signal sequence and a carboxy-terminal cell wall sorting signal which is necessary for peptidoglycan attachment (Mengaud *et al.* 1996). Moreover, it is required for entry into the human enterocyte and other cell lines which express the cellular receptor i.e adhesion molecule E-cadherin (Gaillard *et al.* 1991). InlB is a 630 amino acid protein with a cell surface anchor (Csa) domain responsible for association with the cell wall peptidoglycan (Vázquez-Boland *et al.* 2001). It is crucial for

bacterial entry into hepatocytic cells and other epithelial cell lines (Dramsi *et al.* 1995). In addition, other internalins such as InlC, InlH, and InlJ play a role in *L. monocytogenes* infection; however, their exact roles are unknown (Schaechter 2009).

1.3.2.3 Listeriolysin O

LLO was proposed by Geoffroy *et al.*, in 1987 (Geoffroy *et al.* 1987). LLO is a pore-forming toxin produced by *L. monocytogenes* (Schnupf and Portnoy 2007; Schaechter 2009). Moreover, the haemolytic activity of LLO requires an acidophilic environment (pH ~6) (Schaechter 2009); the reason for this remains unknown (Dramsi and Cossart 2002; Schnupf and Portnoy 2007). In *L. monocytogenes*, LLO is encoded by the haemolysin gene *hly* and is considered as one of the major virulence factors (Vázquez-Boland *et al.* 2001). It mediates the disruption of the phagosome membrane, allowing the organism to escape from the phagocytic cells during intracellular infection (Low and Donachie 1997; Vázquez-Boland *et al.* 2001).

1.3.2.4 Phospholipases

Generally, *Listeria* species secrete three PLCs proteins which have a role in the *Listeria* virulence(Vázquez-Boland *et al.* 2001).In *L.monocytogenes*,two phospholipases are produced; a phosphatidylinositol specific (PlcA), and a broad range substrate (PlcB). On the other hand, *L. ivanovii* produces an additional PLC called SmcL (Schaechter 2009). PlcA is a 33-kDa protein encoded by the *plcA* gene in *L.monocytogenes*. It has approximately 30 % identity to the PLC produced from different organisms such as *Bacillus thuringiensis, Bacillus cereus* and *Staphylococcus aureus* (Vázquez-Boland *et al.* 2001). In addition, this protein is very active in acidic conditions (pH ~5.5 - 6.5) (Vázquez-Boland *et al.* 2001). In contrast, PlcB is a protein made up of 264 amino acids, and its sequence is similar to the PLC produced by *Bacillus cereus* (38.7 % identity) and *C. perfringens* (22.4 % identity) (Vázquez-Boland *et al.* 2001). Both PlcA and PlcB with LLO promote bacterial escape from phagocytic cells during intracellular infection (Schaechter 2009).

1.3.2.5 Actin assembly inducing protein (ActA)

Host actin-based intracellular bacterial motility is coordinated by PrfA, which controls the expression of the *actA* gene (Poussin and Goldfine 2010). ActA is one of the major virulence factors which mediates bacterial escape from the phagosome by utilizing the host actin, and forming an actin tail or filaments,this process is known as actin nucleation (Poussin and

Goldfine 2010). This phenomenon is vital for bacterial motility in the infected host cell and forming pseudopod-like structures aiding the spread from one cell to another (Pistor *et al.* 1994; Portnoy *et al.* 2002). The spreading properties of *L. monocytogenes* were first noticed in 1970 by Razc *et al.* via electron microscopy (Racz *et al.*1970). Actin-mediated motility is a wide-spread mechanism used by intracellular pathogens and has been reported for *Rickettsiae tsutsugamushi, Shigella flexneri* (Tilney and Portnoy 1989), *Burkholderia pseudomallei* (*B. pseudomallei)* (Kespichayawattana *et al*. 2000) and *Mycobacterium marinum (M. marinum*) (Stamm *et al*. 2003). However, different proteins and mechanisms have been reported in these organisms (Poussin and Goldfine 2010).

ActA was first identified as a gene product necessary for actin-based motility following the generation of a transposon mutants library; one particular transposon mutant which was not motile was identified, and after sequencing, the mutation was found in the *actA* gene (Footer *et al.* 2008). In addition, the major environmental signal such as the pH , dose not effect or changed the expression of *actA* gene .However , the acidic pH can be influence the survival of *L. monocytogenes* insid the macrophages (Conte *et al.* 2002).

The ActA is a protein made up of 639 amino acids and is asymmetrically distributed on the *L. monocytogenes* surface (Pistor *et al.* 1994; Portnoy *et al.* 2002; Travier *et al.* 2013). It is composed of three domains, as shown in Figure 3, and each domain has a specific function. The first 29 amino acids represent the signal sequence which is responsible for protein secretion by the Sec system (Poussin and Goldfine 2010; Travier *et al.* 2013). Following that, the N-terminal domain (amino acids 30 to 234) is divided into three regions, and each region contributes to actin-based motility (Poussin and Goldfine 2010). The acidic region A (amino acids 32 to 45), is responsible for actin nucleation, which is the first step in actin polymerisation (Zalevsky *et al.* 2001). The second region is an actin-binding region (AB) (amino acids 59 to 102) which binds the actin monomers. The third region is the connector (C) (amino acids 145 to 156) which together with region A stimulates the actin nucleation complex called Arp2/3 (actin-related proteins) and mediates actin polymerization (Poussin and Goldfine 2010; Travier *et al.* 2013). Many scholars have observed that the deletion or mutation of the N- terminal domain results in complete abolishment of bacterial motility (Pistor *et al.* 2000; Skoble *et al.* 2000) .

The central domain (amino acids 263 to 390) has four proline-rich repeats (PPPP) (Portnoy *et al.* 2002). These proline sequences are responsible for binding to the host proteins, specifically

the enabled/vasodilator-stimulated phosphoprotein (Ena/VASP) family of proteins (Poussin and Goldfine 2010). This binding is essential for providing length for the actin tails, which are on average 1 μm in diameter and 5 μm in length (Goldberg 2001), and controls the velocity of intracellular movement (Travier *et al.* 2013). However, it is not required for actin poly-merization (Travier *et al.* 2013), and mutating this region with either a deletion or point mutation only affects the motility speed (Pistor *et al.* 2000; Auerbuch *et al.* 2003). Finally, the last domain in ActA is the C-terminal hydrophobic region which represents the area from amino acid 391 to 639. It contains a transmembrane sequence (the last 29 amino acids) for anchoring the protein on the bacterial membrane (Portnoy *et al.* 2002; Poussin and Goldfine 2010). This region is unnecessary for actin polymerization (Travier *et al.* 2013); however, besides anchoring the protein in the bacterial membrane, this domain acts as a spacer traversing the cell wall (Cicchetti *et al.* 1999).
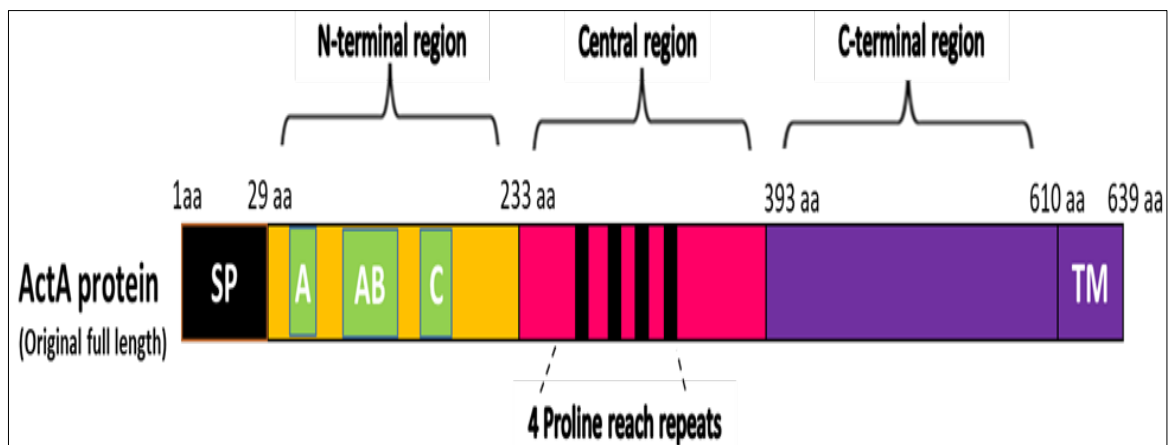
Figure 3. Actin assembly inducing protein (ActA) and its functional domains.
The ActA protein contains 639 amino acids. SP represents the signal peptide region. N-terminal region represents the N-terminal domain from amino acid 21 to 231. The central region represents amino acids 233 to 393. The C-terminal region represents the last terminal of ActA (amino acids 394 to 585) responsible for anchoring the protein to the cell wall.

Apart from intracellular motility, the ActA protein has a wide range of other functions (Rafelski and Theriot 2006), including biofilm formation, which is a significant problem in food processing as it allows the organism to attach to different surfaces, e.g. glass and stainless steel, leading to food contamination (Marie Glenn 2012; Travier *et al.* 2013). It has been reported

that this protein plays a role in bacterial persistence inside the host cell; ActA is also necessary for intestinal colonisation and bacterial aggregation (Travier *et al.* 2013). In 2010, Poussin and Goldfine reported that the acidic stretch of the ActA protein contributes to bacterial escape from the phagosome (Poussin and Goldfine 2010). Moreover, Rafelski and Theriot reported that the polarization of the ActA protein on the surface of *L. monocytogenes* is a direct consequence of cell wall growth (Rafelski and Theriot 2006). Recently in 2014, Iakobachvili (unpublished data from our laboratory) demonstrated significant PG-cleaving activity for ActA protein (Iakobachvili 2014).

1.4 Peptidoglycan hydrolases of *L. monocytogenes*

1.4.1 *L. monocytogenes* cell wall

L. monocytogenes presents with a typical Gram-positive bacterial cell wall which is made of a thick macromolecule mesh-like layer around the cytoplasmic membrane called peptidoglycan (Alonzo *et al.* 2011; Typas *et al.* 2012) , membrane and polyanionic polymers i,e teichoic acids (TAs) and lipoteichoic acid (LTAs) (Bierne and Cossart 2007). *L. monocytogenes* cell wall composed mainly 35 % peptidoglycan and 60 % to 70 % TAs and LTAs (Liu 2008). As in other non-capsulated Gram-positive bacteria, the cell wall of *L. monocytogenes* can be a target for different antibiotics (Scheurwater *et al.* 2008).

L. monocytogenes membrane contain approximately 60% protein, 30 to 35% lipid, and 1.3 to 2.3% carbohydrate e,g glucose, hexose and ribose (Bierne and Cossart 2007) . Where as , the *Listeria* peptidoglycan (also called murein) is formed by glycan chains containing alternating units of the disaccharide N-acetylmuramic acid (N- MurNAc) and N-acetyl-glucosamine (GlcNAc) linked together by a β-1,4-glycosidic bond. The stem peptide contains L-alanine-Ɣ-D-glutamic acid-meso-diaminopimelic acid-D-Ala-D-Ala bound to the MurNAc residue (Schleifer and Kandler 1972). Peptidoglycan acts as a scaffold to anchor other proteins (Goldfine and Shen 2007), endows strength, contributes to the specific shape of cells and protects against various environmental factors and stressors (Goldfine and Shen 2007; Scheurwater *et al.* 2008). Furthermore, peptidoglycan can be altered or modified to be suitable for different bacterial activities such as protein secretion, cell growth or division, and by the insertion of macromolecular structures including secretion systems, pores and flagella (Alonzo *et al.* 2011).

The TAs are covalently bound to the peptidoglycan, whereas LTAs are embedded into the plasma membrane by a diacylglycerol lipid (Bierne and Cossart 2007). TAs and LTAs are polymers in peptidoglycan with essential functions; they facilitate the attachment of different virulence proteins, stimulate responses in the host during infections and transport certain nutrients and proteins (Bierne and Cossart 2007; Wagner and McLauchlin 2008). In addition, these surface factors have a role in antibiotic susceptibility, the colonization onto surfaces and biofilm development (Gross *et al.* 2001).

1.4.2 Surface proteins anchored to the cell well of *L. monocytogenes*

L. monocytogenes genome characterised with high content of genes encoding surface proteins and these proteins contribute in the bacteria pathoginisity e,g colonization and adhesion (Glaser *et al.* 2001; Goldfine and Shen 2007). There are different types of surface proteins found in *L. monocytogenes*. Some of them are covalent associated to the cell wall and other protiens are not directly (non covalent) associated to the cell wall **,** either carry transmembane domains or N-terminal signals recognized for insertion of lipoprotein (Bierne and Cossart 2007) as shown in Figure 4.

The LPXTG protein family is an example for the covelant associated peptidoglycan protein which characterised by direct attachment to the peptidoglycan by sortase enzyme. The LPXTG proteins are present in many Gram-positive bacteria with known genome sequence (Goldfine and Shen 2007). The most common LPXTG protein in *L. monocytogenes* is InlA protein which is directly associated to peptidoglycan by sortase SrtA (Figure 4). The lmo2185 protein is a non LPXTG protein but is associated directly to peptidoglycan by sortase SrtB (Figure 4) (Bierne and Cossart 2007).

The other type of the non covalently associated cell surface proteins are characterized by present of repeated domains e,g GW modules, lysine motif and WxL domain, allow them to attache indirectly to the cell surface (Goldfine and Shen 2007). For instant, the InlB protein which promote the entery of *L. monocytogenes* inside the host cell is harbour GW modules, i.e three repetitions of 80 amino acids, (Desvaux and Hébraud 2006). GW modules allow attachment of InlB protein to LTA in the *listeria* surface (Jonquieres *et al.* 1999). P60 protein as shown in Figur 4 has a lysine motif (LysM) domain and has been dected in the cell wall fractiones of *L. moncytogenes* (Calvo *et al.* 2005). Whereas, lmo0549 protein is an example of

the non covelent surface protein carrying a WxL domain and detced in the cell surface (Bierne and Cossart 2007) .

In addition, there are surface proteins associated to the membrane by hydrophobic tail at their C-terminal such as ActA protein, which play very important role in the intracellular motility of *L. monocytogenes* (Desvaux and Hébraud 2006; Garcia-del Portillo *et al.* 2011). Furthermore, the other membrane proteins are covalent associated by thier N-terminus lipidation such as LpeA (for lipoprotein promoting entry), this protein facilitate the entry and intracellular survival in infected macrophages (Réglier-Poupet *et al.* 2003; Bierne and Cossart 2007). Finally, there are proteins detected in the supernatent fractiones of *L. monocytogenes* with unknown anchoring mechanisms such as FbpA (Lmo1829) (Bierne and Cossart 2007).
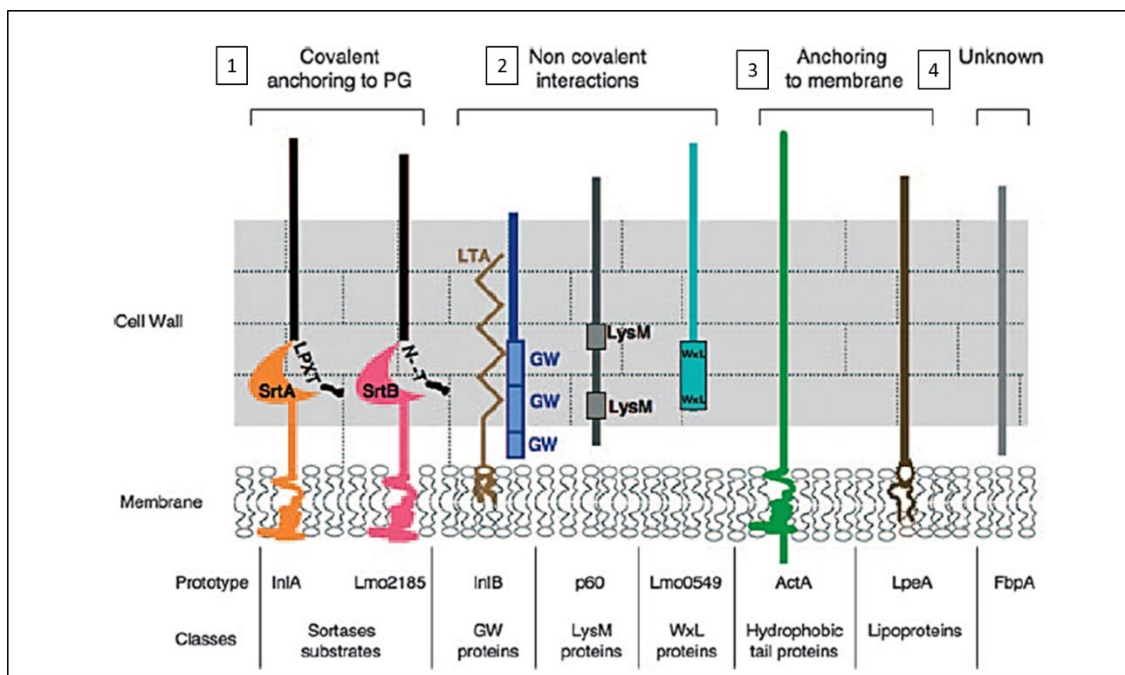
Figure 4. The classification of listerial surface proteins according to their anchoring mechanisms.
L.monocytogenes have different surface proteins anchored to the cell wall via different ways listed in the upper part. In 1 ; Surface proteins anchored covalently to the cell wall. 2 ; Surface proteins anchored non-covalently to the cell wall. 3 ; Surface proteins anchoring to the membrane.4; Proteins anchored to the cell wall by unknow mechanism. The lowe part showed an examples of proteins associated to the cell wall. InlA; internalin A, InlB; internalin B, ActA; actin assembly inducing protein. This figure was published by (Bierne and Cossart 2007).

1.4.3 Bacterial peptidoglycan hydrolases

Some surface proteins, which are characterized as murein hydrolases (autolysins), have the ability to cleave different bonds in peptidoglycan molecules. These proteins have this cleavage activity for several purpose. For example, they play a role during bacterial growth and in the splitting of daughter cells during cell division. Furthermore, in some cases in the enlargement of the saccules to allow for the insertion of different macromolecular structures such as secretion systems and flagella (Höltje 1995; Vollmer and Bertsche 2008). In addition, autolysins may help with bacterial signalling (Alonzo *et al.* 2011), autolysis (Alonzo *et al.* 2011) and recycling the products of peptidoglycan turnover, which can be been released during growth (Höltje 1995).

Generally, PG-cleaving enzymes are classified according to their cleavage sites (Figure 4): N-acetylmuramyl-L-alanine amidases, peptidases (endopeptidase and carboxy-peptidase), N-acetylglucosaminidases, muramidase (lysozymes) and lytic transglycosylases (LTGs) (Höltje 1995; Popowska 2004). The N-Acetylmuramyl-L-alanine amidases cleave the amide bond between the lactyl group of N-acetylmuramic acid (MurNAc) and the first amino acid in the stem peptide, which is L-alanine (Heidrich *et al.* 2001). This enzyme contributes to different functions such as peptidoglycan synthesis, antimicrobial resistance, cell division, cell signalling and spore formation in some organisms, such as *Bacillus subtilis* (Heidrich *et al.* 2001; Vollmer *et al.* 2008). The carboxypeptidases (CPases) and endopeptidases (EPases) cleave the peptide bonds between amino acids in the stem peptide (Höltje 1995; Vollmer *et al.* 2008). In addition, both enzymes participate in peptidoglycan biosynthesis and in the splitting of daughter cells during bacterial cell division (Höltje 1995). Whereas, the other three enzymes, N-acetylglucosaminidase, muramidase and lytic trans-glycosylases, are considered as glycan strand-cleaving enzymes.

The N-acetylglucosaminidase, as shown in Figure 5, cleaves the glycosidic bond between the N-acetyl-beta-D glucosamine residues and adjacent monosaccharides in the peptidoglycan polymer (Vollmer *et al.* 2008). They play a pivotal role in the turnover of peptidoglycan products by recycling and producing new PG precursors (Karamanos 1997), this process is essential for bacterial cell growth. Both muramidase and the lytic transglycosylase cleave the same glycosidic bond (β-1$\rightarrow$4) between the MurNAc (N-Acetylmuramic acid) and GlcNAc (N-acetylglucosamine) residues in peptidoglycan; however, they do so using different mechanisms of action (Höltje 1995).

Hydrolysis caused by lysozyme activity leads to bacterial death, while the cleavage by LTGs leads to the production of a 1,6-anhydrous ring substrate, which plays a significant role in bacterial survival (Van Asselt *et al.* 1999; Scheurwater *et al.* 2008). In addition, LTGs have different and essential functions as proteins; they create space for pores to be formed, or for the insertion of secretion systems, flagella into the peptidoglycan layer (Scheurwater *et al.* 2008). It has been hypothesised that LTGs collaborate with other peptidoglycan synthesising enzymes to remodel peptidoglycan (Vollmer *et al.* 2008). These enzymes are involved in peptidoglycan remodelling by expanding murein sacculus during cell division, which leads to the cleavage of the cells at the septum, and allows for the insertion of peptidoglycan precursors to produce new daughters cells (Vollmer *et al.* 2008). A number of LTGs from different pathogens such as *Haemophilus influenzae*, *Neisseria meningitidis* and *Pseudomonas syringae* can be uncontrolled during host infection due to the presence of LTGs reaction products which play a role in the pathogenesis (Scheurwater *et al.* 2008). Furthermore, it has been noticed that LTGs are essential in the release of toxins from *Bordetella pertussis* and *N. gonorrhoeae* during infections (Scheurwater *et al.* 2008; Typas *et al.* 2012). Nowadays, many scientists are interested in studying LTGs because the modifications of the murein proteins by these enzymes may have a significant effect on antibiotic-resistance (Scheurwater *et al.* 2008).
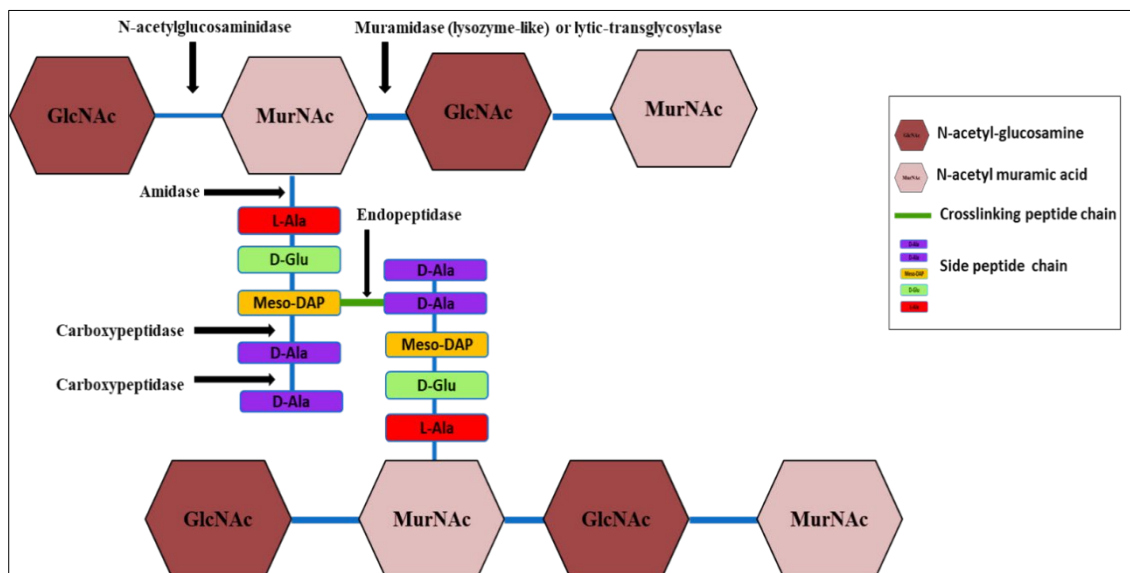
Figure 5. Peptidoglycan cleaving enzymes and their sites of action.
These enzymes include : muramidases,N-acetylglucosaminidases (glucosaminidases), peptidases (endopeptidase and carboxypeptidase) and N-acetylmuramoyl-L-alanine amidases (amidase). GlcNAc is N-acetyl-glucosamine, MurNAc is N-acetyl muramic acid, mDAP is meso-diaminopimelic acid and Ala is alanine.

1.4.4 Autolysins of *L. monocytogenes*

In *L. monocytogenes*, 133 bacterial surface proteins have been identified; these proteins are thought to contribute to virulence, biofilm formation, cell division and the attachment to and invasion of host cells (Popowska 2004). These proteins could be targets for new antibacterial drugs and other useful purposes (Bertsche *et al.* 2011). To date, seven *L. monocytogenes* autolysins have been identified with different roles: Lmo0186, Lmo2522, p60, P45, Ami (Lmo2558), MurA (Lmo2691) and Auto (lmo1076) (Popowska 2004; Popowska and Markiewicz 2006; Pinto *et al.* 2013). Genomic analysis of *L. monocytogenes* revealed the presence of 11 proteins with peptidoglycan hydrolysing domains, N-terminal signal peptides and enzymatic domains. Thus, several autolysins are still unidentified (Cabanes *et al.* 2002; Popowska and Markiewicz 2006).

P60 encoded by *iap* is an extracellular autolysin protein with a 60 kDa molecular weight, that is not controlled by PrfA. It is also known as iap (invasion-associated protein) or cwhA (cell wall hydrolase A) (Pilgrim *et al.* 2003). This protein was first identified by Kuhn & Goebe in 1989 in a culture supernatant (Kuhn and Goebel 1989). P60 contributes to the splitting of two daughter cells and the invasion of non-professional phagocytic cells, e.g. fibroblast (Bubert *et al.* 1992; Pilgrim *et al.* 2003). It has been found that mutating of p60 results in a defect in cell separation ability, a phenotypic change to a rough colony morphology along with long-chained cells and reduced intracellular motility of *L. monocytogenes* (Bubert *et al.* 1992; Popowska 2004). However, Δ*iap* strains did not affect the escape of cells from the phagosome or the intracellular growth rate of cells (Pilgrim *et al.* 2003). Structural analysis of the p60 protein revealed two LysM domains; these domains are found in many enzymes involved in bacterial cell wall degradation (Cabanes *et al.* 2002). Moreover, overexpression of *iap* in *L. monocytogenes* resulted in bacteriolytic activity, which provides evidence that p60 is one of the peptidoglycan hydrolases of *L.monocytogenes* (Pilgrim *et al.* 2003; Popowska 2004). Similarly, this activity was reported with the overexpression of *iap* in *Bacillus subtilis* (Pilgrim *et al.* 2003). Lenz *et al.* proposed that p60 digests the peptide bond linking D-glutamine and Meso-DAP of the peptide side chain in *L. monocytogenes* peptidoglycan. This suggestion was based on the similarity of this protein with the peptidoglycan endopeptidase (LytF) in *Bacillus subtilis* (Lenz *et al.* 2003). The sequence homology of p60 with the autolysin protein in *Enterococcus faecium* provides further evidence validating that p60 has hydrolytic activity (Pilgrim *et al.* 2003).

P45 is one of the cell surface proteins of *L. monocytogenes* with a size of 45 kDa, encoded by the *spl* gene (Schubert *et al.* 2000; Cabanes *et al.* 2002). It has been detected in culture supernatants similarly to p60, as well as cell surface extracts (Schubert *et al.* 2000; Popowska 2004). In addition, sequence similarity was identified between P54 of *L. monocytogenes* and Usp45 of *Lactococcus lactis*. Also a 55 % similarity and 38 % identity with p60 was found (Schubert *et al.* 2000). Schubert *et al.* showed that P45 hydrolyzed the cell wall of *L. monocytogenes* and thus is considered as a peptidoglycan hydrolases (Schubert *et al.* 2000; Popowska 2004).

Ami (Lmo2558) is a 102 kDa autolytic amidase, and is encoded by the amidase gene (*ami)* (McLaughlan and Foster 1998). It has only been detected on the bacterial surface (Milohanic *et al.* 2001). Ami plays a role in the adhesion of *L. monocytogenes* inside eukaryotic cells with its cell wall-binding domain and motility (Foster 1995; Popowska 2004). Interestingly, there is high sequence homology (~49 % identity) of the N-terminal domain of Ami of *L. monocytogenes* with the amidase domain of the *S. aureus* autolysin At1. Furthermore, the C-terminal domain of Ami 54% has homology with the InlB surface-anchoring domain of *L. monocytogenes* (Foster 1995). In addition, the predicted structure of this protein shows the presence of two domains (a catalytic domain and cell wall binding domain) which is very common in autolysins (Mclaughlan and Foster 1998). Given all the aforementioned evidence, along with findings from HPLC obtained by McLaughlan and Foster, it is evident that Ami has amidase activity (Mclaughlan and Foster 1998).

The *murA* gene encodes the muramidase protein (MurA) or Lmo2691, which is a 66-kDa molecular weight protein (Goldfine and Shen 2007). However, the naming of this protein is unfortunate, as murA is used for the designation of other genes, which can cause confusion. The MurA protein contains an amidase domain in the N-terminal region, followed by 4 LysM domains (Carroll *et al.* 2003) and shares homology with enzymes that cleave the bond between MurNAc and GlcNAc (Popowska 2004). For instance, 46 % identity and 59 % similarity was found between the N-terminal region of MurA from *L. monoctyogenes* and muramidase-2, which is the major autolysin of *E. faecalis* and *Lactococcus* (Carroll *et al.* 2003). A mutant murA strain (Δ*murA*) showed a similar phenotype to Δ*iap* mutants in that they formed as a long chain of cells (Goldfine and Shen 2007). Moreover, it has been found that MurA is involved in cell separation and cell wall turnover or remodelling (Carroll *et al.* 2003).

Lmo1076 (also known as Auto) is a 64 kDa surface-associated protein of *L. monocytogenes* encoded by the *aut* gene (Popowska 2004). It contains three domains: a signal sequence, the

N-terminal autolysin domain that is comparable to domains found in many cell wall hydrolases, and the C-terminal cell wall-anchoring domain which is similar to the InlB and Ami proteins (Cabanes *et al.* 2002). When studied, the Δ*aut* strain did not display any change in colony morphology, cell separation ability or in cell to cell motility (Cabanes *et al.* 2004). However, Auto is required for the entry or invasion of *L. monocytogenes* in many different non-phagocytic eukaryotic cells (Cabanes *et al.* 2004).

Recently, Lmo0186 and Lmo2522 were characterised as proteins with digesting activity, due to their ability to cleave crude cell wall preparations and an artificial lysozyme substrate (NAG)3-MUF (Pinto *et al.* 2013). However, they were found to be unnecessary for bacterial growth. In addition, both proteins are homologous to the *actinobacterial* Rpf proteins, which are considered as a lytic transglycosylases with the ability to increase the viable count of dormant cultures and stimulate the growth of vegetative cells. Thus, it has been suggested that Lmo0186 and Lmo2522 may possess lytic transglycosylase activity (Pinto *et al.* 2013).

1.5   Resuscitation promoting factor (Rpf)

Rpf was first identified in *Micrococcus luteus (M. luteus)* by Mukamolova *et al.* (Mukamolova *et al.* 1998). Later, it was identified in other Gram-positive bacteria with high GC content (Telkov *et al.* 2006) such as *Mycobacterium tuberculosis*, *Mycobacterium avium*, *Mycobacterium bovis*, *Mycobacterium marinum*, *Mycobacterium smegmatis* and *Streptomyces coelicolor* (Gupta and Srivastava 2012). The analysis of the *M. luteus* Rpf protein demonstrated that the N-terminal region which contains 75 amino acid residues, has sequence similarity (up to 75 % identical residues) with *M. tuberculosis* and all other Rpf like proteins (Telkov *et al.* 2006).

In *M. tuberculosis*, five Rpf-like proteins were identified: RpfA (Rv0867c), RpfB (Rv1009), RpfC (Rv1884c), RpfD (Rv2389c) and RpfE (Rv2450c) (Kana *et al.* 2008; Rosser *et al.* 2017). Both RpfA and RpfD are secreted proteins, while RpfB, RpfC and RpfE are membrane anchored proteins (Gomez *et al.* 2000; Romano *et al.* 2012). All *M.tuberculosis rpf* gene products exhibit similar biological activity to the *M. luteus* Rpf (Mukamolova *et al.* 2002). The structure of the Rpf domain from *M. tuberculosis* revealed that it possesses a lysozyme-like domain (Cohen-Gonsaud *et al.* 2005; Kana and Mizrahi 2010). Therefore, it was proposed that all Rpf-like proteins are peptidoglycan digesting enzymes (Telkov *et al.* 2006). Furthermore, it has been found that the Rpf from *M. luteus* can stimulate the growth of viable cells of *M. tuberculosis* (Shleeva *et al.* 2002) and vice versa, suggesting that there is a conserved

mechanism of action (Mukamolova *et al.*, 2002). Rpf proteins possess transglycosylase activity, which is essential for their biological functions (Rosser *et al.* 2017). This activity allows for the cleavage of the beta-1,4-glycosidic bond in the glycan backbone of peptidoglycan (Kana and Mizrahi 2010). Furthermore, the transglycosylase activity is key in cell wall remodelling through the hydrolysis of the glycan backbone of peptidoglycan (Kana and Mizrahi 2010).

All Rpf's have similar biological methods of action and are implicated in the resuscitation of dormant cells (Kana and Mizrahi 2010). In addition, various *rpf* mutant strains of *M. tuberculosis*, which had deletion mutations on different individual Rpf proteins, had no significant phenotypic defects. This indicates that there is a functional redundancy within this protein family (Kana *et al.* 2008; Kana and Mizrahi 2010). In contrast, many scholars have proposed that there is functional variation between these proteins (Kana and Mizrahi 2010). For instance, Gupta *et al*. noticed that all the *rpfs* genes were expressed in the early stages of resuscitation from a non-culturable state (Gupta *et al.* 2010). However, *rpfC* was found to be consistently expressed at a high level in comparison to the other *rpfs* at all stages during bacterial growth. In the same study, *rpfE* and *rpfD* were highly expressed under acidic stress, while *rpfC* and *rpfE* were highly expressed under hypoxic condition (Gupta *et al.* 2010). In *M. bovis*, *rpfE* was associated with the transition of *M. bovis* from slow to fast growth in *vitro* (Tufariello *et al.* 2004). On other hand, the deletion of three *rpfs* genes in *M. tuberculosis* in different combinations showed a growth defect *in-vivo* and affected *in-vitro* resuscitation (Downing *et al.* 2005; Kana *et al.* 2008). In *L. monocytogenes*, the two Rpf proteins mentioned previously (section 1.4.4), Lmo0186 and Lmo2522, were studied. Individual mutations of these Rpfs had no effect on bacterial growth, whereas double mutations showed an extension of the lag phase for *L. monocytogenes* when grown in minimal media (Gupta and Srivastava 2012).

Finally, all the aforementioned PG cleaving enzymes that have been described above are usually secreted proteins; therefore, secretory systems are further discussed in detail below.

1.6   Protein secretory systems of *Listeria* spp.

In general, most pathogenic organisms secrete various virulence factors such as proteins, enzymes and toxins which are already present on the cell wall into the extracellular environment, or inject these factors directly into the host cell to cause infections.

However, non-pathogenic organisms also secrete proteins which are essential to their survival (Desvaux and Hébraud 2006). In *Listeria* spp, six different secretion systems have been identified; these are the Secretory (Sec) pathway, Tat pathway (Twin-arginine translocation), FEA (Flagella Export Apparatus), FPE (Fimbrilin Protein Exporter), Wss (WXG100 secretion system) and the Holin proteins. These are further explained in Figure 6 (Bierne and Cossart 2007; Wooldridge 2009). All of the mentioned secretion pathways allow for virulence factors to be translocated either from the cytoplasm or membrane to the cell surface (Wooldridge 2009). Moreover, the proteins which have been synthesised in the bacterial ribosome can be transported by different pathways depending on the presence or absence of the N-terminal signal peptide. The Sec, Tat and FEP pathway secreted proteins required specific secretion signals present in the N-terminal end (Bierne and Cossart 2007). In contrast, the other secretion systems i.e. FEA, Holins and Wass are responsible for the secretion of proteins lacking signal peptides(Desvaux and Hébraud 2006).

The Sec pathway is the most common system used to secrete most of the virulence proteins in *Listeria* species (~508, as shown in Figure 6) in the unfolded manner (Desvaux and Hébraud 2006). The proteins are exported through the Sec pathway via their N-terminal signal sequence, which is cleaved by signal peptidases upon translocation (Forster and Marquis 2012). In addition, several translocation factors participate in the transportation of proteins via this pathway, e.g. SecY (translocon subunit), SecE (translocon subunit), SecG (translocon subunit), SecDF(translocon associated complex) andYajC (translocon associated complex) (Wooldridge 2009; Halbedel *et al.* 2014). The proteins exported by the Sec system can be localized to three different sites, as shown in Figure 6. First, the protein may be anchored to the cell membrane via the transmembrane segment, or covalently attached through the N-terminal domain to long-chain fatty acids of the bacterial cell membrane. Second, the proteins can be anchored to the cell wall; the third possibility is that they can be secreted into the extracellular milieu. Examples of proteins secreted by this pathway in *L. monocytogenes* are InlA, InlB, ActA, Hly and PlcB. These proteins are actual secretory proteins because they all possess signal peptides (Desvaux and Hébraud 2006; Halbedel *et al.* 2014).

The second secretory system is the Tat pathway, which contributes to the transport of different metal-containing enzymes after their folding in the cytoplasm (Figure 6) (Wooldridge 2009). The proteins intended for transport through the TAT contain a distinctive twin-arginine motif within the N-terminal signal sequence, which is cleaved by signal peptidases during translocation (Forster and Marquis 2012). These proteins are most likely secreted into the

extracellular milieu (Desvaux and Hébraud 2006). Protein FepB (Lmo0367), which is required for the oxidation of ferrous to ferric iron, is an example of a predicted Tat pathway dependent protein based on bioinformatic analysis (Bagnoli and Rappuoli 2017).

The proteins which form pilin-like structures are exported by the FEP pathway (Desvaux and Hébraud 2006). Similarly to the Sec and Tat pathway secreted proteins, pilin-like proteins have an N-terminal signal sequence that is cleaved by a Type 4 prepilin peptidase during translocation (Forster and Marquis 2012). On the other hand, the FEA pathway is responsible for secreting proteins that form the flagella hook and filament (Forster and Marquis 2012). In *L. monocytogenes*, the FlaA (Flagellin A) protein, which contains the listerial flagellar filament and has been shown to possess digesting activity, is secreted by this pathway (Desvaux and Hébraud 2006).

Holins are small membrane proteins that allow for the translocation of proteins lacking the signal peptide via the cytoplasmic membrane. Holins are responsible for the secretion and activation of proteins with muralytic activity (Rydman and Bamford 2003). Lastly, the Wss pathway was first identified in *M. tuberculosis* (Sutcliffe 2011), and is known to translocate some of the virulence factors of pathogenic bacteria into the extracellular milieu (Forster and Marquis 2012).
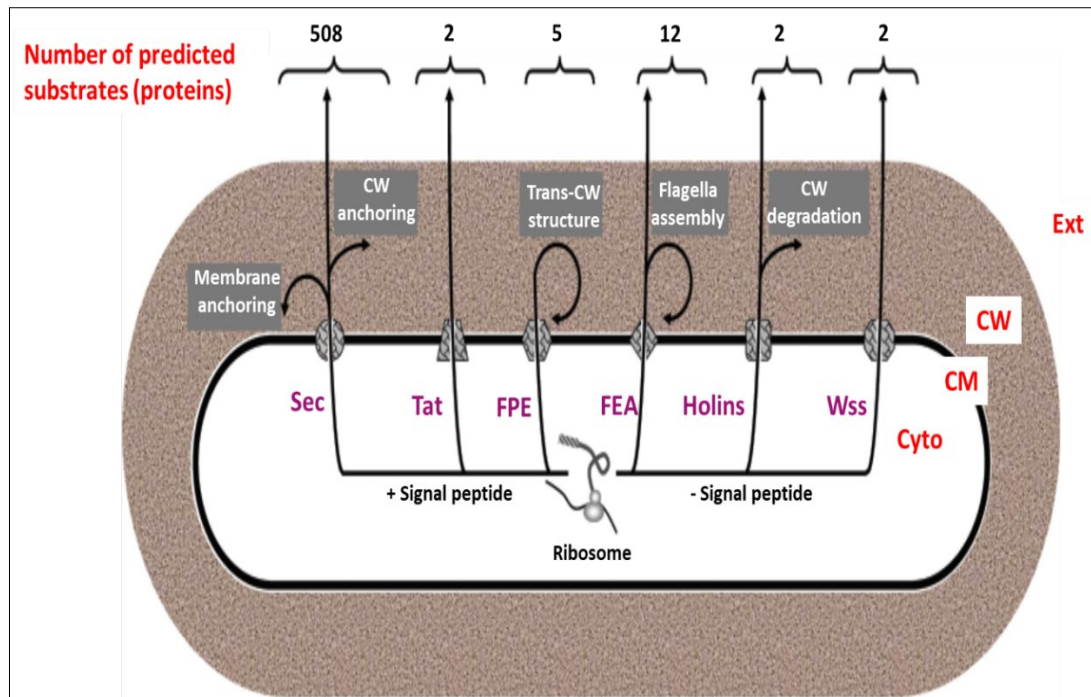
Figure 6. Protein secretion pathways in *Listeria* spp.
The six different protein secretion systems found in *Listeria* spp are shown above, along with the manner in which they secrete proteins. The pathways are: Sec pathway (Secretion apparatus) system, Tat pathway (Twin-arginine translocation), FPE pathway (Fimbrilin-Protein Exporter), FEA pathway (Flagella Export Apparatus), Wss pathway (WXG100 proteins with WXG motif of 100 amino acyl residues) and Holins pathway. Ribosomal synthetised proteins can be exported to different destinations depending on the presence (+) and absence (-) of the signal peptide. Proteins secreted by the Sec pathway could be localized in membrane or cell wall (CW) or secreted to extracellular milieu (Ext). While, proteins secreted by Tat pathway exported to the extracellular medium. FEP is involved in the formation of trans-cell wall structures and FEA is involved in flagella assembly. Proteins exported by Holins pathway can be involved in CW degradation or secreted into the extracellular milieu. The estimate number of virulence proteins secreted by each pathway are mentioned in the top. Cyto is cytoplasm. CM is cytoplasmic membrane. CW is cell wall. Ext is extracellular milieu. This figure was published by (Desvaux and Hébraud 2006).

1.7 Previous work

Previous work in our laboratory has identified significant PG cleaving activity for the ActA protein (ActA$_{A30-N639}$) (Iakobachvili 2014). Iakobachvili was able to purify ActA$_{A30-N639}$ protein after laborious optimisation (Iakobachvili 2014). Moreover, the signal sequence has been

removed from ActA$_{A30-N639}$ protein. The rationale behind this strategy was that the signal sequence might influence the expression and the stability of the construct in *E.coli*, because the signal peptides of other organisms, e.g. *L. monocytogenes* are not compatible with *E. coli*. In addition, it could affect protein folding and possibly lead to the production of inclusion bodies. (Choi and Lee 2004). Iakobachvili, identified a new function for the ActA protein, this being the peptidoglycan cleaving activity which was shown using two different methods: a zymogram assay and MUF Tri-NAG (4-Methylumbelliferyl β-D-N, N′, N′-triacetylchitotrioside) cleavage (Iakobachvili 2014). The actual structure for the ActA protein is not known and has not yet been resolved, therefore it is not possible to study the crystal structure and find the active sites responsible for the identified enzymatic activity. Thus, the alignment of homologous proteins from different organisms was previously carried out (Iakobachvili 2014), and the conserved positions with a high probability of amino acids considered essential for the enzymatic activity were highlighted, this is shown in Figure 7.
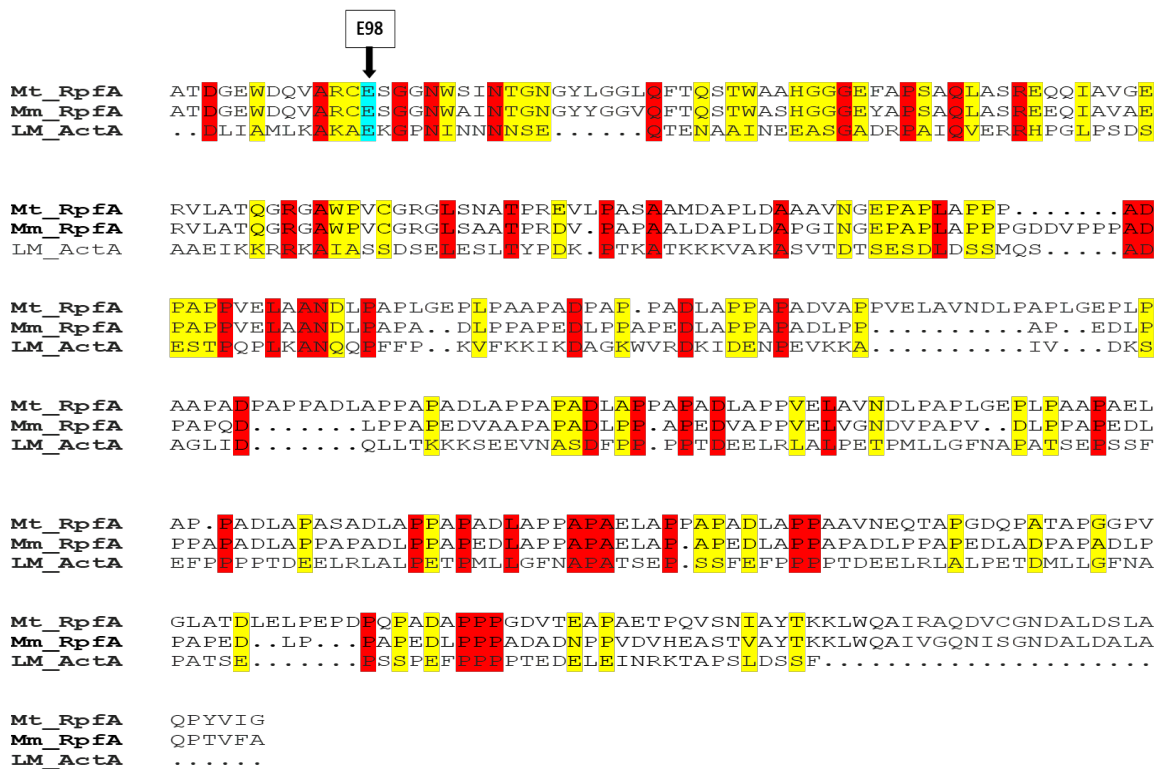
Figure 7. Multiple Sequence Alignment of the RpfA protein from *M. tuberculosis* and *M. marinum,* and the ActA protein from *L. monocytogenes.*
The absolutely conserved residues are highlighted in red, and similarly grouped amino acids are in yellow. The blue colour highlights the catalytic glutamate (E98) that is conserved in all three proteins (Iakobachvili 2014).

Following this, it has been shown that ActA of *L. monocytogenes* has 50 % similarity in terms of amino acid sequence with RpfA of *M. tuberculosis* and *M. marinum*. The alignment predicated that E98 (glutamic acid number 98), which is located in the N-terminal domain of ActA, could be the catalytic residue, as it was conserved in all three proteins. In *Mycobacteria*, all the Rpf proteins possess lytic transglycolysis activity (Gupta and Srivastava 2012), and it is known that a single acidic residue (often glutamate) within the active centre mediates catalysis (Weaver *et al.* 1995; G. V. Mukamolova *et al.* 2006). Moreover, the similarity between RpfA and ActA in the roles that they play in intracellular movement via actin tail formation , and the evidence presented by Iakobachvili (Iakobachvili 2014), supports the hypothesis that the ActA protein could be a bifunctional protein. We therefore believe this warrants further investigation.

1.8 Hypotheses

ActA is a well-studied virulence factor, which is essential for actin-base mobility of *L. monocytogenes.* However, a recently published study indicated that it also plays a role in remodelling of peptidoglycan during intracellular replication. Based on previous findings from our laboratory we hypothesise that ActA possesses PG cleaving activity and this activity is critical for peptidoglycan remodelling during infection. Establishment of catalytic residues, enzyme specificity and putative partners will aid development of therapeutic agents to prevent *L. monocytogenes* replication in infected individuals. ActA has 50% sequence homology with RpfA, we therefore suggest that both proteins have similar functions in bacterial growth and virulence; moreover, ActA is likely to be a lytic transglycosylase enzyme.

1.9 Project aims

1. Expression and purification of the entire ActA protein and truncated forms of ActA.
2. Investigate the activity *in-vitro* of the truncated proteins and site-directed mutagenesis generated protein forms using different assays.
3. A major effort will be made to investigate the structure of ActA and try to successfully crystallise ActA.
4. Use recombinant ActA to raise polyclonal ActA-specific antibodies for localisation experiments and pull-down assays.
5. Generate a chimeric construct containing portions of *rpfA* and *actA* genes by domain swapping to invistigate ActA function in bacterial growth.

Chapter 2

Materials and Methods

Unless stated in the text, all chemicals were purchased from Sigma (Sigma-Aldrich, UK Ltd) or Fisher (Fisher Scientific, UK Ltd) and PCR reagents were purchased from Promega (UK, England) or Fisher (Fisher Scientific, UK Ltd).

2.1   Media and buffers

2.1.1   Media

All media were prepared according to the suppliers' instructions.

2.1.1.1   Tryptone soya broth (TSB)

TSB was prepared by dissolving 30 g of powder in 1 litre of milliQ grade water, then autoclaved at 121 °C for 30 minutes.

2.1.1.2   Tryptone soya agar (TSA)

TSA was prepared by suspending 40 g of powder in 1 litre of milliQ grade water, then autoclaved at 121 °C for 30 minutes and poured into sterile Petri dishes.

2.1.1.3   Lysogeny broth (LB)

LB was prepared by adding 20 g of powder to 1 litre of milliQ grade water, then autoclaved at 121 °C for 30 minutes.

2.1.1.4   Luria Agar (LA)

The one litre of LA (Sigma-Aldrich) was prepared by adding the 37 g of powder to 1 litre of milliQ grade water, which was then autoclaved at 121 °C for 30 minutes and poured into sterile Petri dishes.

2.1.1.5   Modified Welshimer's broth (MWB)

MWB is a chemically defined minimal medium used to support the growth of *L. mono-cytogenes* (Premaratne *et al.* 1991). It was prepared as published elsewhere (Premaratne *et al.* 1991); Table 1 illustrates all of the components used for the preparation of MWB. The media was sterilized by autoclaving at 121 °C for 30 minutes. The amino acids and vitamins were filter sterilized.

Table 1. MWB ingredients

Ingredient	g/l
KH_2PO_4	6.56 g
Na_2HPO_4	30.96 g
$MgSO_4$	0.41 g
Ferric citrate	0.088 g
Glucose	10.0 g
L-Leucine	0.1 g
L-Isoleucine	0.1 g
L-Valine	0.1 g
L-Methionine	0.1 g
L-Arginine	0.1 g
L-Cysteine	0.1 g
L-Glutamine	0.6 g
Riboflavin	0.5 mg
Thiamine	1 mg
Biotin	1 mg
Thioctic acid	0.005 mg

2.1.1.6   Brain Heart Infusion Broth (BHI)

The one litre of BHI was prepared by adding the 37 g of powder into 1 litre of milliQ grade water, then autoclaved at 121 °C for 30 minutes.

2.1.1.7   Buffered *Listeria* Enrichment Broth (BLEB)

BLEB was prepared in 500ml by dissolving 23 g of powder into 500 ml milliQ grade water. Then, the contents of one vial of *Listeria* Selective Enrichment Supplement, which was provided with the media, was added. The broth was sterilised by autoclaving at 121 °C for 30 minutes.

2.1.1.8   Albumin-Dextrose-Complex (ADC) broth

One litre of 10 % ADC was prepared by dissolving 50 g of bovine serum albumin, 20 g of D-glucose and 8.5 g of sodium chloride in milli-Q grade water. The broth was filter sterilize in a 0.22μm filter.

2.1.1.9 7H9 Middlebrook broth

The 7H9 (Becton, Dickinson and Company Ltd) was prepared according to the manufacturer's instructions by adding 2.35 g of 7H9 powder and 2 ml of 50 % glycerol in 450 ml milliQ grade water. The media was autoclaved at 121 ˚C for 15 minutes and allowed to cool to 55 °C. Then, ADC (final concentration of 10 %, section 2.1.1.8) and Tween 80 (final concentration of 0.1 %) were added to the 7H9 medium.

2.1.1.10 7H11 Middlebrook agar

The 7H11 (Becton, Dickinson and Company Ltd) was prepared by dissolving 21 g of media powder in to 900 ml milliQ grade water containing 5 ml of 100 % glycerol. The media was sterilized by autoclaving at 121°C for 30 minutes. Finally, the media was allowed to cool to 55 °C, and 100 ml of ADC was added.

2.1.1.11 Sauton's media

Sauton's media was prepared by dissolving 0.5 g of KH_2PO_4, 0.5 g of $MgSO_4$, 4 g of L-aspartate, 2 g of citric acid, 0.1 ml of 1 % $ZnSO_4$, 0.05 g ferric ammonium citrate and 10 ml of 100 % glycerol in 1 litre of milliQ grade water. Finally, this was then sterilized by autoclaving at 121 °C for 30 minutes.

2.1.2 Buffers

2.1.2.1 Phosphate Buffered Saline (PBS)

PBS was prepared by dissolving one PBS tablet in 100 ml of milliQ grade water. The final buffer contained 0.01 M phosphate buffer (pH 7.4), 0.0027 M potassium chloride and 0.137 M sodium chloride. After that, the solution was autoclaved at 121°C for 30 minutes.

2.1.2.2 50X Tris-acetic acid EDTA (TAE)

This buffer was made by dissolving 48.4 g of Tris base in 800 ml of milliQ grade water and then by adding 11.4 ml of glacial acetic acid (17.4 M) and 3.7 g of ethylene-diamine-tetra-acetic acid (EDTA). The solution was adjusted to 1 litre with milliQ grade water. This solution was diluted 1 in 10 (10x) with milliQ grade water, which was distilled before use.

2.1.2.3 10X SDS buffer

SDS buffer was prepared by dissolving 144 g of glycine, 10 g of SDS and 30.3 g of Tris base in 1 litre of milliQ grade water. For the running gel, 1X SDS was prepared by mixing 100 ml of 10X SDS with 900 ml of milliQ grade water.

2.1.2.4 10X Western blot buffer (transfer buffer)

The Western blot buffer was prepared by adding 144 g of glycine and 30.3 g Tris base in 1 litre of milliQ grade water.

2.1.2.5 Colloidal Coomassie stain

A stock solution was prepared by mixing 0.1 % (w/v) Coomassie Brilliant Blue G-250, 10 % (w/v) ammonium sulphate and 2 % (w/v) phosphoric acid. For the working solution, 80 ml of Colloidal Coomassie stain solution was added to 20 ml of methanol.

2.1.2.6 Isopropyl β-D-1-thiogalactopyranoside (IPTG)

The IPTG was used at a concentration of 100 mM. It was prepared by dissolving 240 mg of IPTG in 10 ml of milliQ grade water. The solution was filter sterilized using a 0.2 mm syringe filter and aliquoted to sterile 1.5 ml tubes.

2.1.2.7 10 % (w/v) Tween 80

The 10 % (w/v) Tween 80 was prepared in a glass beaker by adding 2 g of Tween 80 to 18 ml of milliQ grade water. Then, the solution was mixed on a stirrer until dissolved. Finally, the solution was filter sterilized.

2.1.3 Antibiotic solutions

Ampicillin was used at a 100 μg/ml concentration (AMP100). AMP100 was prepared by dissolving 1 g of ampicillin in 10 ml of milliQ grade water. The solution was then filter sterilized using a 0.2 mm syringe filter, aliquoted into sterile 1.5 ml tubes and stored at -20°C. Kanamycin was used at a 50 μg/ml concentration (Kan50). Kan50 was prepared by dissolving 1 g of kanamycin in 20 ml of milliQ grade water. The solution was filter sterilized using a 0.2 mm syringe filter, aliquoted into sterile 1.5 ml tubes and stored at -20°C.

2.2 Bacterial strains and plasmids

The plasmids in this research are listed in Table 2. All bacterial strains used in this project are summarised in Table 3.

Table 2. Plasmids used in this study

Plasmid	Resistant	Characteristics	Reference
pET15b- TEV	AmpR	6 x His-tagged recombinant protein expression.Construct for the overexpression of ActA into the *E. coli* periplasm	(Canova *et al.* 2008)
pGEM-T-Easy vector	AmpR	*E. coli* T-A cloning vector	Promega UK, England
pMV306	KmR	Integrating vector for cloning.	(Stover *et al.* 1991)
pMV261	KmR	Overexpression vector	

Table 3. Bacterial strains used in this study

Strain	Description	Reference
BL21(DE3) pET-15bTEV::*actA* (this strain lacked the signal sequence, predicted to be at the amino acid residues 1 to 29 or 30)	Expression of recombinant ActA$A_{30-N639a.a}$ containing pET15b::*actA*	Collection of Lab 227, University of Leicester. UK. Preliminary data from Iakobachvili (Iakobachvili 2014)
C41(DE3) pET-15b::*actA*	Expression of recombinant ActA $_{A30-N639a.a}$ containing pET15b::*actA*	This study
C41(DE3) pLEICS-01 ::*actA* $_{A30-S157\ a.a}$	Expression of recombinant ActA $_{A30-S157\ a.a}$ (N-terminal short version)	This study
C41(DE3) pLEICS-01 ::a*ctA* $_{A30-N233\ a.a}$	Expression of recombinant ActA $_{A30-N233\ a.a}$	This study
C41(DE3) pLEICS-01::*ActA* $_{G393-N639\ a.a}$	Expression of recombinant ActA $_{G393-N639\ a.a}$	This study

Strain	Description	Reference
C41(DE3) pLEICS-01::a*ctA* E98A	Expression of recombinant ActA $_{A30-S157 a.a}$ containing a site directed mutation (SDM) in glutamate 98 to alanine	This study
C41(DE3) pLEICS-01::a*ctA* E42A	Expression of recombinant ActA $_{A30-S157 a.a}$ containing a SDM in glutamate 42 to alanine	This study
C41(DE3) pLEICS-01::a*ctA* E44A	Expression of recombinant ActA $_{A30-S157 a.a}$ containing a SDM in glutamate 44 to alanine	This study
C41(DE3) pLEICS-01::a*ctA* E45A	Expression of recombinant ActA $_{A30-S157 a.a}$ containing a SDM in glutamate 45 to alanine	This study
C41(DE3) pLEICS-01::a*ctA* E46A	Expression of recombinant ActA $_{A30-S157 a.a}$ containing a SDM in glutamate 46 to alanine	This study
C41(DE3) pLEICS-01::a*ctA* E49A	Expression of recombinant ActA $_{A30-S157 a.a}$ containing a SDM in glutamate 49 to alanine	This study
C41(DE3) pLEICS-01::a*ctA* E49A-E50A	Expression of recombinant ActA $_{A30-S157 a.a}$ containing a SDM in glutamate 49 and glutamate 50 to alanine	This study
C41(DE3) pLEICS-01::a*ctA* E44A-E45A-E46A	Expression of recombinant ActA $_{A30-S157 a.a}$ containing a SDM in glutamate 44, glutamate 45 and glutamate 46 to alanine	This study
C41(DE3) pLEICS-01::a*ctA* MUT1	Expression of recombinant ActA $_{A30-S157 a.a}$ containing a scanning mutation to alanine	Generated by Thermo-Fisher
C41(DE3) pLEICS-01::a*ctA* MUT2	Expression of recombinant ActA $_{A30-S157 a.a}$ containing a scanning mutation to alanine	Generated by Thermo-Fisher

Strain	Description	Reference
C41(DE3) pLEICS-01::actA MUT3	Expression of recombinant ActA A30-S157 a.a containing a scanning mutation to alanine	Generated by Thermo-Fisher
C41(DE3) pLEICS-01::actA MUT4	Expression of recombinant ActA A30-S157 a.a containing a scanning mutation to alanine	Generated by Thermo-Fisher
C41(DE3) pLEICS-01::actA MUT5	Expression of recombinant ActA A30-S157 a.a containing a scanning mutation to alanine	Generated by Thermo-Fisher
C41(DE3) pLEICS-01::actA MUT6	Expression of recombinant ActA A30-S157 a.a containing a scanning mutation to alanine	Generated by Thermo-Fisher
E. coli DH5α	For DNA cloning	Bioline ,UK
E. coli BL21(DE3)	Competent cell for protein expression	New England Biolabs
E. coli C41(DE3)	Competent cell for protein expression	Lucigen , UK
E. coli LMG	For peptidoglycan purification	Invitrogen™
L. monocytogenes EGD-e	Wild type strains of *L. monocytogenes* (EGD-e stains, isolated from a rabbit listeriosis)	Dr. Sarah Glenn, University of Leicester.
ΔactA L. monocytogenes	Deficient strains of *L. monocytogenes* (EGD-e strains, with a deleted *actA* gene)	Dr D. Portnoy, University of Pennsylvania, Philadelphia, USA
Micrococcus luteus	Wild type strains of *Micrococcus luteus,* used in the zymogram assay	Collection of Lab 227, University of Leicester.
M. marinum	Wild type strains of *M. marinum*, isolated from human	Collection of Lab 227, University of Leicester.

2.3 Preparation of frozen stocks, starter cultures and competent cells

2.3.1 *Listeria monocytogenes*

L. monocytogenes EGD-e wild type and $\Delta actA$ (*actA* gene deletion) strains were cultured from frozen stocks which were made by mixing 250 µl of 75 % (v/v) sterile glycerol with 750 µl of bacterial culture in a 1.5 ml cryogenic tube and stored at -80°C. The starter culture of *L. monocytogenes* was prepared from frozen stocks by inoculating the frozen stock into 10 ml of appropriate media (either TSB, MWB or BLEB media), then incubating it at 37°C overnight in a shaking incubator.

2.3.2 *Escherichia coli*

E. coli strains were cultured from frozen stocks, which were made by mixing 250 µl of 75 % (v/v) sterile glycerol with 750 µl of bacterial culture in a 1.5 ml cryogenic tube, and stored at -80°C. The starter culture of *E. coli* was prepared from frozen stocks by inoculating the frozen stock into 10 ml of LB media with an appropriate antibiotic and then incubated at 37°C overnight in a shaking incubator. The *E. coli* C41 (Lucigen, UK) and *E. coli* BL21 (DE3) (New England Biolabs) commercial strains were stored at -80°C so that they can be used freshly when required, as described in section 2.5.8.

2.3.3 *Mycobacterium marinum*

M. marinum cultures were prepared from frozen stocks which were made by mixing 250 µl of 75 % (v/v) sterile glycerol with 750 µl of bacterial culture in a 1.5 ml cryogenic tube and stored at -80°C. The starter culture was prepared by inoculating a frozen stock culture into 7H9 medium supplemented with refreshment media (45 ml 7H9, 5 ml ADC and 250 µl 10 % Tween 80). *M. marinum* was incubated at 32 °C for 2 weeks. Bacterial cultures were grown to an OD_{600nm} of 0.7 and subcultured into 100 ml of 7H9 media (section 2.1.1.9) supplemented with 10 % ADC (section 2.1.1.8) and 0.05 % Tween 80 (section 2.1.2.7).

2.3.4 *Micrococcus luteus*

The *M. luteus* strain was cultured from frozen stocks which were prepared in the same manner as the *L. monocytogenes* stocks (section 2.3.1).The *M. luteus* starter cultures were prepared using frozen stocks by inoculating the frozen stock into 5 ml of LB, then incubating at 37 °C in a shaking incubator at 200 rpm overnight.

2.3.5 Competent *E. coli* C41 (DE3) cells

E. coli C41 (DE3) (Lucigen, UK) competent cells were prepared for protein expression using the calcium chloride ($CaCl_2$) treatment method (Chang *et al.* 2017). In brief, a starter culture of *E. coli* C41 (DE3) was prepared from frozen stock as mentioned in section 2.3.2, but with 2 ml of LB media without any antibiotics. Then, 2 ml of starter culture was inoculated into 200 ml of LB and grown at 37 °C with shaking at 200 rpm, until the culture reached an OD_{600nm} of 0.2 to 0.4 (~1.5 hours). The culture was chilled on ice for 15 minutes. After that, the cells were harvested at 2500 x g for 15 minutes at 4°C; the supernatant was discarded and pellet re-suspended in 50 ml of pre-chilled 100 mM $CaCl_2$. The resuspended cells were incubated on ice for 5 minutes. The centrifugation and the resuspending step were repeated twice. Finally, the cells were suspended in 2 ml of 100 mM $CaCl_2$ and used for heat shock transformation.

2.3.6 Competent *M. marinum* cells

M. marinum cells were grown in 100 ml of 7H9 supplemented with refreshment media (45 ml 7H9, 5 ml ADC and 250 µl 10 % Tween) until an $OD_{600\ nm}$ of 0.6-0.8 (~10 days). Cells were harvested by centrifugation at 2,000 x g for 20 minutes at room temperature. The supernatant was removed, and the bacterial pellet was washed 3 times with 10 % (v/v) sterile glycerol at room temperature. The volume used for washing was reduced each time (starting with 30 ml, then 20 ml, and ending with 10 ml). Finally, the pellet was resuspended in 2 ml of 10 % glycerol and 400 µl aliquots were used for electroporation (section 2.5.10).

2.4 Investigation of bacterial growth

L. monocytogenes wild type and Δ*actA* strains were grown in 5 ml TSB and MWB as mentioned in section 2.3.1. Afterwards, the OD_{600nm} of all cultures was adjusted to 0.01. Then, 150 µl of culture was pipetted into a well of a 96-well plate. The Varioskan instrument was used for optical density measurements every 30 minutes for a period of 30 hours. Each growth curve experiment was replicated (~3 times), and the CFU values were calculated where stated. The data was collected and analysed using GraphPad Prism version 7.0.

2.5   Molecular biology

2.5.1   Primers

All primers used in this study were ordered from Sigma-Aldrich (stocks of 100 μM) and all sequences used in this study are shown in Table 4.

Table 4. Primers used in this study

Primer name	Sequence (5'-3')	Purpose
ActALeic-F1	TACTTCCAATCCATGGCGACAG ATAGCGAAGATTCTA	To amplify a gene fragment encoding a short version of ActA $_{A30\text{-}S157\ a.a}$
ActALeic-R1	TATCCACCTTTACTGTCAACTAT CCGATGATGCTAT	
ActALeic-F1	TACTTCCAATCCATGGCGACAG ATAGCGAAGATTCTA	To amplify a gene fragment encoding a long version of ActA $_{A30\text{-}N233\ a.a}$
ActALeic-R2	TATCCACCTTTACTGTCAATTTT CGTCGATTTTATCA	
ActALeic-F4	TACTTCCAATCCATGGGTAGACC AACATCTGAAGA	To amplify a gene fragment encoding ActA $_{G393\text{-}N639\ a.a}$
ActALeic-R4	TATCCACCTTTACTGTCAATTAT TTTTTCTTAATT	
E98A- F	ATGTTGAAAGAAAAAGCAGCAA AA GGTCCA AAATCAAT	Site direct mutagenesis of E98A in ActA $_{A30\text{-}S157\ a.a}$
E98A-R	ATTGATATTTGGACCTTTTGCTG CTTTTTCTTTCAACAT	
E42A-F	TCTAGTCTAAACACAGATGCAT GG GAA GAAGAAAAAACA	Site direct mutagenesis of E42A bin ActA $_{A30\text{-}S157\ a.a}$
E42A-R	TGTTTTTTCTTCTTCCCATGCATC TGTGTTTAGACTAGA	
E44A-F	CTAAACACAGATGAATGGGCAG AAGAAAAAACAGAAGAG	Site direct mutagenesis of E44A in ActA $_{A30\text{-}S157\ a.a}$
E44A-R	CTCTTCTGTTTTTTCTTCTGCCCA TTCATCTGTGTTTAG	

Primer name	Sequence (5'-3')	Purpose
E45A-F	AACACAGATGAATGGGAAGCAG AAAAACAGAAGAGCAA	Site direct mutagenesis of E45A in ActA $_{A30-S157\ a.a}$
E45A-R	TTGCTCTTCTGTTTTTCTGCTTC CCATTCATCTGTGTT	
E46A-F	ACAGATGAATGGGAAGAAGCAA AAACAGAAGAGCAACCA	Site direct mutagenesis of E46A in ActA $_{A30-S157\ a.a}$
E46A-R	TGGTTGCTCTTCTGTTTTGCTTC TTCCCATTCATCTGT	
E49A-F	TGGGAAGAAGAAAAAACAGCA GAGCAACCAAG GAGGTA	Site direct mutagenesis of E49A in ActA $_{A30-S157\ a.a}$
E49A-R	TACCTCGCTTGGTTGCTCTGCTG TTTTTTCTTCTT CCCA	
E49A-E50A-F	GAAGAAGAAAAAACAGCAGCG CAACCAAGCGAGGTAAAT	Site direct mutagenesis of E49A -E50A in ActA $_{A30-S157\ a.a}$
E49A-E50A-R	ATTTACCTCGCTTGGTTGCGCTG CTGTTTTTTCTTCTTC	
E44A-E45A-E46A-F	AACACAGATGAATGGGCAGCAG CAAAAACAGAAGAGCAA	Site direct mutagenesis of E44A-E45A-E46A in ActA $_{A30-S157\ a.a}$
E44A-E45A-E46A-R	TTGCTCTTCTGTTTTTGCTGCTGC CCATTCATCTGTGTT	
tb_rpf_c4- Fw	CTTGGTACCGGCCATGTGACATT ACCC	To isolate and amplify upstream of rpfA in *M. tuberculosis*
rpfAR2	ACAGGATCCGGTCGCCTGAGCG GCCAT	
ActAcom-F1	ACAGGATCCGCGACAGATAGCG AAGAT	To isolate and amplify the N-terminal of actA gene
ActA com-R1	CAGCTGCAGACTATCCGATGAT GCTAT	
rpfA-F2	GATCTGCAGAACGCAACACCCC GCGAA	To isolate and amplify downstream of rpfA in *M. tuberculosis*
tb_rpf_-RV	CGGGAATTCTCAGCCGATGACG TACGG	
pMV261-F	TGCGCCCGGCCAGCGTAAGTA	Diagnostic primers for the pMV261 vector, used for colony PCR
pMV261-R	TGATCACCGCGGCCATGATGG	
pMV306- F	CCT TTGAGTGAGCTGATAC	Diagnostic primers for the pMV306 vector, used for colony PCR
pMV306 -R	CGTTCGCCCTGTCGTTCA	

Primer name	Sequence (5'-3')	Purpose
Act test- F2	AAGAGTTGAACGGGAGAGGC	Confirmation of the *actA* deletion in *L .monocyto - genes*, gene-specific primers used for colony PCR
Act test- R2	TCACTTATCAGAGCCGGTGC	
ActA test -F	AGCTAATTAAGAAGATAACTAACTG	Confirmation of the *actA* gene deletion in *L. mono- cytogenes*,test primer used for colony PCR
ActA test -R	CAAGCACATACCTAGAACCACCTTT	
pET15b-Tev:: *actA*-F	CTAATACATATGGCGACAGATAGCGAAGAT	To isolate and amplify the *actA* gene (Iakobachvili 2014)
pET15b-Tev :: *actA*-R	ATCGGATCCTTAATTATTTTTCTTAATG	
PLEICS -01-F	TAATACGACTCACTATAGGG	Used for the sequencing of all constructs generated by PROTEX
PLEICS-01-R	ATTAACATTAGTGGTGGTGGT	

2.5.2 Colony PCR

Colony PCR was used for strain confirmation. For template preparation, the desired colony from an agar plate was streaked on to a fresh agar plate before resuspending in 100 μl RNAse/ DNAse free water in a 1.5 ml sterile tube. The sample was heated at 95°C for 15 minutes, then cooled down on ice for 5 minutes. The sample was then centrifuged for 5 minutes at 12,000×g, and 1 μl of the resulting supernatant was used as a template for PCR (Table 5). A master mix was prepared, as shown in Table 6.

The PCR amplification was performed using the following steps. Initially subjecting the DNA to a high temperature (95°C) allows the separation of DNA strands by breaking the hydrogen bonds. Then, the annealing step, which is performed at 55°C enables the primers to bind to the complementary DNA sequence. Finally, the extension step takes place at 68°C, which is the optimal temperature to activate the Taq polymerase and build the complementary new strand. These cycles were repeated 30 times, in which the products of each cycle served as a template for the next cycle, resulting in an exponential increase in the PCR product. The Go Taq DNA polymerase was used with the 5x reaction buffer (Promega).

Table 5. Preparation of PCR mixture

For 25µl PCR reaction	× 1
RNAse/DNAse free water	14.4µl
5X Green GoTaq® Reaction buffer	5.0µl
dNTPs (2mM)	2.5µl
Reverse primer (10 pmol/µl)	1.0µl
Forward primer (10 pmol/µl)	1.0µl
Go TAQ G2 (5 U/µl)	0.1µl
Template (boiled sample)	1.0 µl
Final volume	25.0µl

Table 6. PCR condition of colony PCR

Step		Temperature	Time
Initial denaturation		95°C	2 minutes
Denaturation	30 cycles	95°C	30 seconds
Annealing		55°C	30 seconds
Extension		68°C	2 minutes
Final Extension		68°C	5 minutes
Infinite hold		15°C	∞

2.5.3 High fidelity PCR

High fidelity PCR was used to amplify the target DNA to be used for cloning. The reaction was performed as listed in Table 7, using high fidelity Platinum Taq DNA polymerase (Invitrogen™). In addition, the PCR condition used are summarized in Table 8.

Table 7. Preparation of High-Fidelity PCR reaction

For 50µl PCR reaction	
RNAse/DNAse free water	50 µl
5X Q5 Reaction buffer	10 µl
dNTPs (2 mM)	5 µl
10 µM reverse primer	2.5 µl
10 µM forward primer	2.5 µl
5X Q5 High GC Enhancer	10 µl
Template (boiled bacteria)	1.0 µl
Q5 High-Fidelity DNA Polymerase (0.02 U/µl)	0.5 µl
Final volume	50.0 µl

Table 8. PCR condition used for High-Fidelity PCR

Steps		Temperature	Time
Initial denaturation		95°C	2 minutes
Denaturation		95°C	30 seconds
Annealing	31 cycles	55°C	30 seconds
Extension		68°C	35 seconds
Final Extension		68°C	5 minutes
Infinite hold		12°C	∞

2.5.4 Agarose gel electrophoresis

DNA samples were routinely separated by gel electrophoresis using a 1 % (w/v) gel. The 1 % (w/v) agarose solution was prepared by dissolving 1 g of agarose into 100 ml of 1× TAE buffer, which was later supplemented with 5 µl of SYBR Safe DNA Gel stain (Thermo Fisher Scientific). The solution was used to make the gel. A loading dye (Thermo Fisher Scientific) was added to samples before loading them in the gel. The GeneRuler™ 1kb (Thermo Fisher

Scientific) ladder was always used with each sample. Finally, electrophoresis was performed at 80 V for 1 hour, and bands were visualized using a gel documenting system (Bio-Rad).

2.5.5   Purification of PCR products

PCR products were purified using the QIAquick PCR Purification Kit (Qiagen, UK) according to the manufacturer's instructions. DNA was eluted using 50 µl RNAse and DNAse free water. The desired DNA band based on size was extracted from the 1 % (w/v) agarose gel and purified using the Qiagen PCR purification kit (Qiagen, UK) according to the manufacturer's instructions if contaminating bands were present following PCR or digestion. DNA was eluted using 80 µl RNAse/DNAse free water.

2.5.6   Restriction enzyme digestion

Restriction enzymes and buffers (New England Biolabs) were used to digest purified DNA. The digestions reactions were performed using enzymes, the recommended buffers, according to the manufacturer's protocols and the purpose. For molecular cloning digestions 3 µg of DNA was used in a final volume of 50 µl, whereas, 500 ng DNA was used for a final volume of 10 µl for diagnostic digestion. In both types of digestions, 1 x CutSmart buffer, 10 units of restriction enzyme, DNA templates and RNAse/DNAse free water to the final volume of 10 µl were used. The digestion mixture was incubated at 37°C for 2 hours. In this study, several restriction enzymes were used, these are as follows: *Bam*HI, *NdeI, PstI, KpnI and EcoRI.*

2.5.7   Ligation reaction

The T4 DNA ligase (Promega) was used to set up ligation reactions between the vector (plasmid), e.g. pGEM-T-Easy, pMV261, pMV306 and the DNA insert to be used in the cloning. Reactions were done as recommended by the suppliers. The linearized vector (100 ng) was ligated with ~150 ng of insert DNA in the presence of 1 µl T4 DNA ligase and 1 µl ligase 10 x buffer made up to a final volume of 10 µl. The mixture was incubated overnight at room temperature.

2.5.8   Heat shock transformation

DH5α™ (Alpha-select competent *E. coli*) cells (Bioline) were used in the heat shock transformation for cloning, whereas *E. coli* C41 (DE3) (Lucigen) and *E. coli* BL21 (DE3) (New England Biolabs) competent cells were used for protein expression.

The stored cells (at -80°C) were thawed on ice and 1 µl of plasmid was added to the competent cells, which were then incubated for 30 minutes on ice. The bacteria were heat shocked at 42°C for 45 seconds and immediately returned on ice for 2 minutes. Pre-warmed LB medium (970 µl) containing 10 mM MgSO4 was added to the mixture and incubated at 37°C for one hour with shaking. Finally, the mixture was plated on to LA containing an appropriate antibiotic for plasmid selection.

2.5.9 Plasmid extraction and purification

E. coli cultures were grown overnight in 5 ml of LB with the appropriate antibiotic at 37°C, with shaking. Plasmid DNA extraction was done using the GeneElute™ Plasmid Miniprep kit according to the manufacturer's protocol. DNA was eluted with 80 µl RNase /DNAse free water. Finally, the plasmid purity was checked by agarose gel electrophoresis.

2.5.10 Electroporation

M. marinum competent cells (400 µl, prepared as described in section 2.3.6) were transferred into 2 mm long-electrode electroporation cuvettes (GeneFlow) and 5 µl (~500 ng) of the purified plasmid with the insert was added. Electroporation was carried in the transformation mixture at 2500 V, 1,000 Ω and 25 µF using the Bio-Rad Gene Pulser system.

The electroporated cells were transferred to a universal tube; the original cuvette was washed twice with 1 ml refreshment media (45 ml 7H9, 5 ml ADC and 250 µl 10 % Tween) and added to the competent cells. The competent cells were incubated overnight at 32°C in a static incubator to recover. Then, 200 µl of the mixture and serial dilutions (10^{-1}, 10^{-2}, 10^{-3}, 10^{-4}, 10^{-5} and 10^{-6}) were plated on 7H11 agar supplemented with the appropriate antibiotic (in this study, 50 µg/ml kanamycin was used). In addition, 200 µl of competent cells that were not electro-porated with DNA was plated as a negative control. Finally, all plates were incubated at 32°C for 2-3 weeks (until colonies appeared).

2.5.11 DNA Sequencing

The DNA sequencing was carried out by using the Sanger sequencing SUPREMERUN service at GATC biotech to verify the target inserts or clones. The resulting sequences were compared with published references using a basic local alignment search tool (BLAST).

2.5.12 Site-Direct Mutagenesis (SDM)

SDM was performed using the GeneArt® Site-Directed Mutagenesis System (Invitrogen™) according to the manufacturer's instructions to generate mutated constructs. The primers contained a changed codon sequence designed (mentioned in Table 4, section 2.5.1) to substitute the acidic residue of interest in the *actA* gene to alanine (alanine scanning). DNA was methylated first at 37°C for 20 minutes before mutagenic primers bound to and amplified the entire plasmid during the PCR. The PCR cycling conditions used were : denaturation for 2 minutes (94°C), annealing for 30 seconds (57°C) and primer extension for 30 seconds (68°C) for a total of 18 cycles. A control PCR that did not contain any template DNA was carried out to check for any DNA contamination.

Then, the PCR product was analysed on a 1 % agarose gel before carrying out the recombine-tion reaction. Afterwards, the recombination reaction step was done to circulized the plasmid which help and enhances the colony output and DH5α™-T1R E (Bioline) was used for transformation. After transformation, random colonies were selected for plasmid extraction and sequencing. Finally, the clone containing the correctly sequenced insert was used for protein purification and activity experiments. This method is shown schematically in Figure 8.
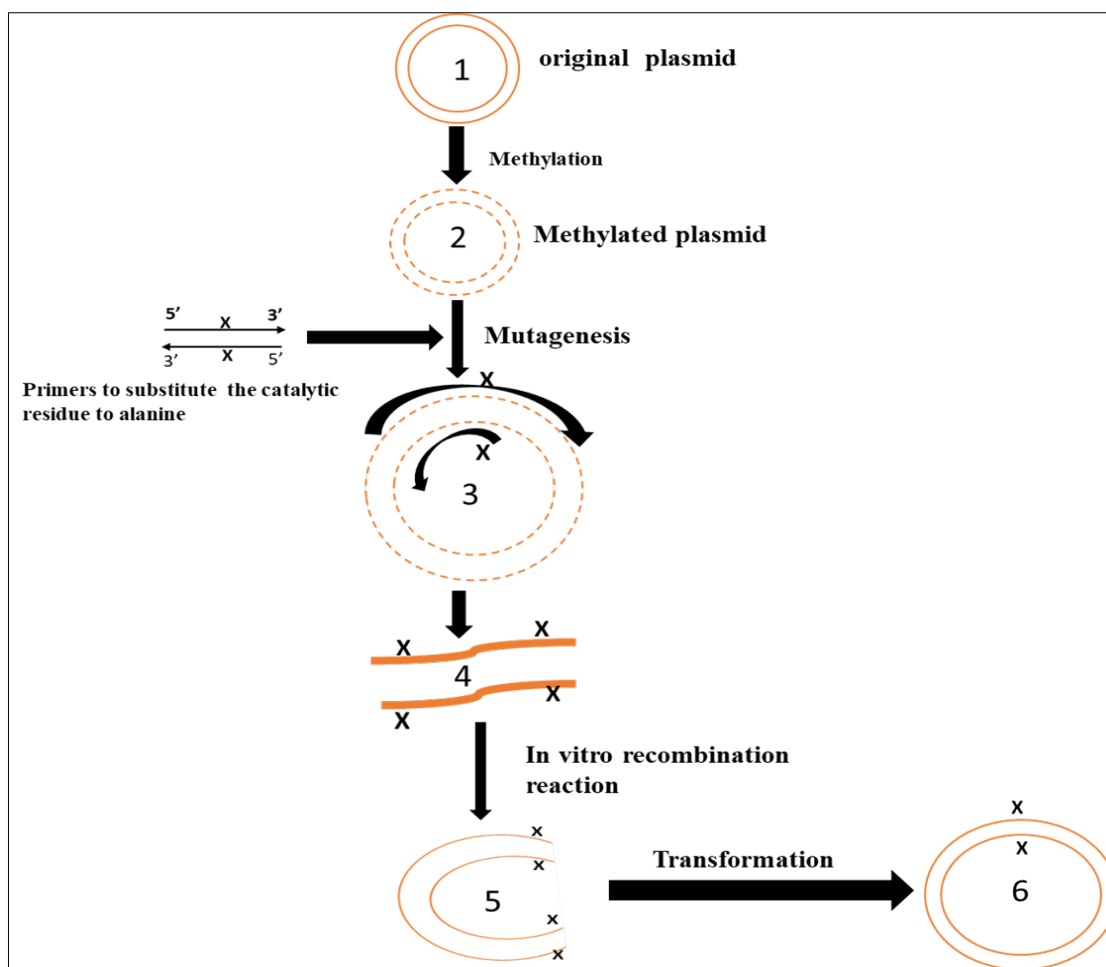
Figure 8. Schematic representation of the process to generate an SDM mutant using the GeneArt® Site-Directed Mutagenesis System (Invitrogen™).

In step 1: the plasmid templet mixed with PCR reagents and Methyl transferase reagents. Step 2: the methylated plasmid amplified in mutagenesis reaction with two overlapping primers contain the target mutation. Step 3: mutagenic primers bind and amplify the entire plasmid. Step 4: after PCR reaction, 5 µL of linear PCR product visualised on a 1% agarose gel. Then recombination reaction allows for the formation of a circular plasmid. Step 5: the circular plasmid used in transformation of DH5α. Step 6: three to five colonies have been selected, analysed by plasmid isolation and sequencing.

2.6   Sodium dodecyl sulfate-polyacrylamide gel electrophoresis (SDS-PAGE)

Precast polyacrylamide gels (SERVAGel™TG PRiME™) were used for the analysis of proteins. Gels were assembled into SDS-PAGE tanks and electrophoresis was performed in SDS-PAGE running buffer (14.4 g of glycine, 3.03 g of Tris base and 1 g of SDS dissolved in 1 litre of milliQ grade water).

Protein samples were diluted in 4x sample buffer (8 ml of glycerol, 4.8 ml of 1 M Tris HCl (pH 6.8), 1.6 g SDS, 8 mg bromophenol blue, 6.2 ml water and 10 mM dithiothreitol), and ran at 200 V. The protein sizes were determined by comparing them with the BLUeye prestained Protein Ladder (GeneFlow) which has a size range of 10-245 kDa.The protein visualised after staining with Colloidal Coomassie (amonium sulfate 10 %, Coomassie G-250 0.1 %, ortho-phosphoric acid 3 %, methanol 20 %), and destained in water.

2.7   Western blotting

The Western blot method was used to detect proteins using different antibodies (Table 9). The Western blot machine Bio-RAD Trans-Blot® TurboTM Transfer system was used to transfer proteins to a nitrocellulose membrane (AmershamTM ProtranTM supported 0.45 µm NC, GE Healthcare Life Sciences) after separation on SDS-PAGE. Sigma Fast BCIP/NBT or peroxidase substrate for enhanced chemiluminescence (ECL) were used to visualise proteins on the C-Digit system (Li-Cor) according to the manufacturer's instructions.

Table 9. Antibodies and reagents used in this study

Reagent	Source	Application
Monoclonal Anti-polyHistidine antibody	Sigma	Detection of His-tagged proteins expression
Custom polyclonal anti-ActA antibody raised in rabbit	Gemini Biosciences Ltd	Detection of the ActA protein
Alkaline-phosphatase conjugate anti-mouse IgG	Sigma	Secondary antibodies
Alkaline-phosphatase conjugated anti-rabbit IgG	Sigma	Secondary antibodies
Anti-rabbit IgG, HRP-linked antibody	Cell Signaling Technology	Secondary antibodies
BCIP®/NBT Liquid Substrate System	Sigma	Detection of proteins bands on the nitrocellulose membrane

2.8 Expression and purification of recombinant ActA protein

2.8.1 Cloning of recombinant ActA$_{A30-N639 a.a}$

To assess and investigate the hypothesis of this study, the plasmid pET15b-Tev:: *actA* was used to express and purify the ActA$_{A30-N639}$ protein. The pET15b-Tev:: *actA*, where *actA* lacks the signal sequence (an average length of ~ 29 amino acid) has previously been generated in our laboratory(Iakobachvili 2014). The culture of pET15b-Tev::*actA* was prepared from frozen stocks, and plasmid extraction was performed as mentioned in section 2.5.9. After plasmid sequencing, the correct clone was transformed into a suitable competent cell, either *E. coli* BL21 (DE3) or *E. coli* C41 (DE3) for protein expression and purification. The map of the pET15b-Tev plasmid can be seen in Appendix 8.1.

2.8.2 Cloning of recombinant truncated forms of ActA$_{A30-N639 a.a}$

To generate truncated versions of the ActA$_{A30-N639 a.a}$ protein, the specific primers were desing (Table 4). The cloning of *actA* into pLEICS-01 was performed by the protein expression laboratory PROTEX at the University of Leicester. In PROTEX, a ligation of the free cloning method was used. The plasmid pLEICS-01 (map can be found in Appendix 8.2) containing an ampicillin resistance gene and the hexa-histidine tag, was used for the expression of a different version of ActA$_{A30-N639}$.

The plasmids pLEICS-01–ActA $_{A30-S157 a.a}$, pLEICS-01–ActA $_{A30-N233 a.a}$, pLEICS-01–ActA $_{G393-N639 a.a}$ and pLEICS-01-ActA $_{E235-N639a.a}$ were sequenced using pLEICS-01 primers (Table 4). The truncated ActA forms were used to identify the protein domain associated with peptidoglycan cleavage activity, which was previously found in ActA $_{A30-N639}$ (Iakobachvili 2014). Thus, two versions of the N-terminal *actA* gene were generated: a short version pLEICS-01–Acta $_{A30-S157 a.a}$, with the amino acid residues from 30 to 157 in the N-terminal domain, and a long version pLEICS-01–ActA $_{A30-N233 a.a}$ (amino acids 30-233) also in the N-terminal domain (Figure 9). The reason behind generating two clones from the same domain was based on a prediction of fragments with different activities. In addition, a previous study (Iakobachvili ,2014) predicted a glutamate residue (E98) to be responsible for peptidoglycan digestion activity. Other constructs included pLEICS-01–ActA $_{G393-N639}$ (amino acids 393-639) to represent the C-terminal region of ActA and pLEICS-01-ActA $_{E235-N639}$ (amino acids 235-639) to represent the central domain. These were generated to be used as a control in the activity assay. Figure 9 shows the basic constructs generated in the study.
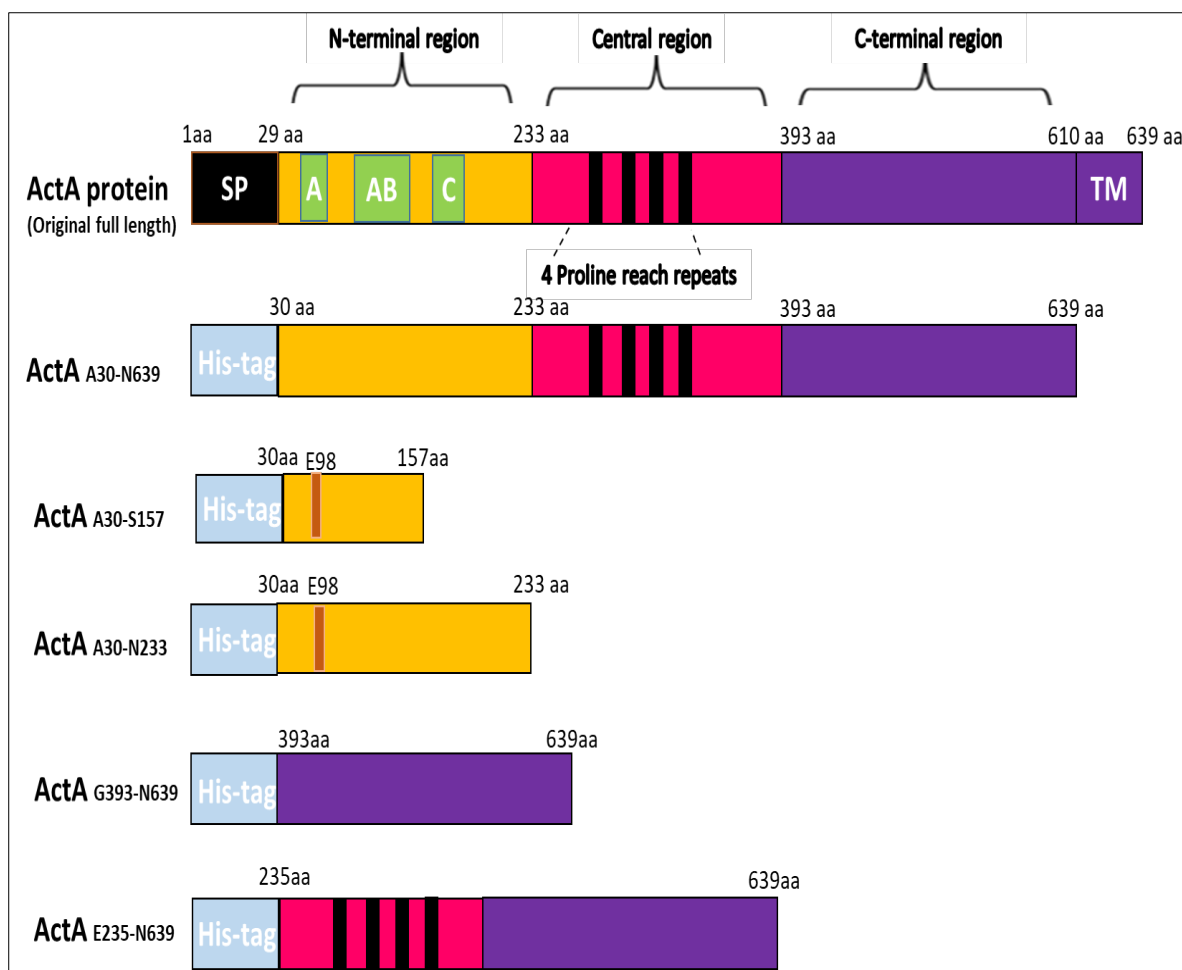
Figure 9. Schematic representation of the variants of ActA generated in the study.

The original structure of the full-length ActA protein is shown at the top (639 aa). The position of the SP (signal peptide domain) and TM (transmembrane domain) are indicated. The yellow area represents the N-terminal domain starting from residue 30 to 233. The pink area represents the Central domain from 232 to 393, containing an area of 4 proline rich repeats. The purple area represents the C-terminal domain from 394 to 610. Highlighted in green are: (A) region with a stretch of acidic residues (32-45 aa), (AB) an actin monomer-binding region (59-102 aa), and (C), a cofilin homology sequence (145-156 aa). E98 is a glutamic acid predicated previously (Iakobachvili 2014) as a catalytic residue.

2.8.3 Generation of site-directed mutants of ActA

In total, 14 proteins were generated in this study using directed mutagenesis (SDM). The plasmid pLEICS-01 (Appendix 8.2) was used as a template for the generation of the E98A, E42A, E44A, E45A, E46A, E44A-E45A-E46A, E49A and E49A-E50A protein variants.

The constructs for the expression of these variants were generated using the GeneArt® Site-Directed Mutagenesis System (Invitrogen™) as mentined in section 2.5.12 and the pLEICS-

01–ActA $_{A30\text{-}S157}$ plasmid as a template. The SDM constructs of ActA_MUT1, ActA_MUT2, ActA_MUT3, ActA_MUT4, ActA_MUT5 and ActA_MUT6 were generated by Thermo-Fisher. In the Thermo-Fisher synthetic constructs, the pET151/D-TOPO plasmid (Appendix 8.3) with an N-terminal 6x histidine tag and a TEV protease site was used.

2.8.4   Expression trials

Small scale trials were used to confirm protein expression and for the optimization of the expression conditions. Cultures of *E. coli* BL21 (DE3) or *E. coli* C41 (DE3) were grown from frozen stocks, as mentioned in section 2.3.2. , in 5 ml of LB. Cultures were grown to an OD$_{600nm}$ of 0.6-0.8 at 37°C with shaking. Different concentrations of IPTG were used to induce protein expression as following; 0.1 mM, 0.5 mM and 1 mM. Post-induction and incubation for 4 hours at 37ºC or 18 hours at 18ºC were tested. The protein expression patterns were analyzed using SDS-PAGE and Western blot as described in sections 2.6 and 2.7.

2.8.5   Protein purification

Large scale protein expression and purification was performed after establishing optimal expression conditions as described in section 2.3.2. *E. coli* cultures (2 ml) were inoculated in to 500 ml LB containing 50 µg/ml ampicillin. Cultures were incubated at 37 ºC with shaking at 200 rpm until the OD$_{600nm}$ reached 0.6. Soluble protein production for all the protein variants was performed by inducing the protein expression with 0.5 mM IPTG, followed by 4 hours incubation at 37°C with shaking. The cell pellets were collected by centrifugation at 6,000 x g for 35 minutes at 4°C (Beckman JA 25.5 rotor, Beckman Coulter Avanti J-30I centrifuge). Then, PBS was used to wash the cell pellet, after which the mixture was centrifuged at 20,000 x g for 15 minutes at 4°C and stored at -20°C. The pellets were re-suspended in 30 ml binding buffer (20 mM KCl, 150 mM NaCl, 20 mM Tris base, pH 8.5) and lysed via sonication with 4 10 seconds bursts (amplitude 9) using a sonicator (Soniprep 150 Plus Digital Ultrasonic Disintegrator) with 2 minutes of cooling on ice between sonication bursts. *E. coli* lysates were centrifuged at 20,000 x g for 40 minutes at 4°C (Beckman JA 25.5 rotor, Beckman Coulter Avanti J-30I centrifuge); the pellet was discarded. The supernatant was used for protein purification using immobilized metal affinity chromatography (IMAC) and size exclusion chromatography.

For affinity chromatography, a Ni^{2+} chelating column (Ni-Sepharose 6 Fast Flow, GE Healthcare Life Sciences) was pre-equilibrated with a binding buffer (20 mM KCl, 150 mM

NaCl, 20 mM Tris base, pH 8.5.), and the purification process was performed at 4°C. The supernatant was allowed to pass through the Ni^{2+} chelating column, and 5 washing steps were conducted with 15 ml binding buffer. Then, the Ni^{2+}chelating column was washed with 15 ml of 20 mM of imidazole with binding buffer. Finally, all proteins were eluted with different concentrations of imidazole as shown in Table 10. The collected fractions containing the protein of interest were analysed on SDS-PAGE and confirmed by Western blot using anti-polyhistidine antibodies (1:2.000 dilution).

Table 10. Imidazole concentrations used for the elution of proteins in the IMAC.

Protein	Imidazole concentration used for elution in IMAC
ActA $_{A30-N639}$	500 mM , based on previous work (Iakobachvili 2014)
ActA $A_{30-S157}$	60 mM
ActA $A_{30-N233}$	60 mM
ActA $_{G393-N639}$	100 mM
All SDM proteins (14 proteins generated in this study)	60 mM

The second step of protein purification was size exclusion chromatography. In this chromatography step, a Superdex 200 (10/300 HiLoad) column was used with the ÄKTA™ Purifier system (GE Healthcare Life Science, UK). The column was equilibrated with a buffer made up of 150 mM NaCl and 20 mM Tris base at a pH of 8.5. The protein sample was loaded into the AKTA purifier loop. The fractions of interest were collected and analysed by SDS-PAGE and Western blot. The identities of the purified proteins were confirmed using mass-spectrometry analysis by the Protein-Nucleic Acid Chemistry Laboratory (PNACL) at the University of Leicester.

2.9   ActA crystallization trials

Pooled fractions of purified proteins were concentrated using Millipore Amicon® Ultra- 43 kDa Centrifugal Filter Units to reach a final concentration of at least 3 mg/ml. Protein concentrations were determined using the Nanodrop instrument. In current study, the sitting drop vapour diffusion method was used for crystallization trials. The liquid handling for the crystallization was done using the Mosquito® Crystal Nanolitre Protein Crystallization Robot

51

(TTP Labtech). For the screening of the crystallization conditions, formulated buffer systems such as ProPlex™, Morpheus®, PACT premier™ and JCSG-plus™ of Molecular Dimensions were used. Each screen had 96 different buffers. For the preliminary crystallization trials, a drop of protein (0.1 μl) was mixed with 0.1 μl of the buffer from the screens (1:1 ratio) and placed on the MRC 96-well crystallization plate. One plate was set up at room temperature and another at 4°C, and sealed with plastic film (3M Hampton Research) to prevent any contamination or evaporation. After preparing the crystallization screens, each well was examined for the presence of any crystals. The first step of crystal formation is supersaturation (Figure 10), which is achieved by evaporating the water from the mixture (protein and precipitant) into the reservoir solution, leading to concentration, precipitation and nucleation of proteins (Smith *et al.* 1996). Further experiments were performed with larger drops by using 1.2 μl of protein and 1.2 μl of buffer from the most promising crystallization conditions.
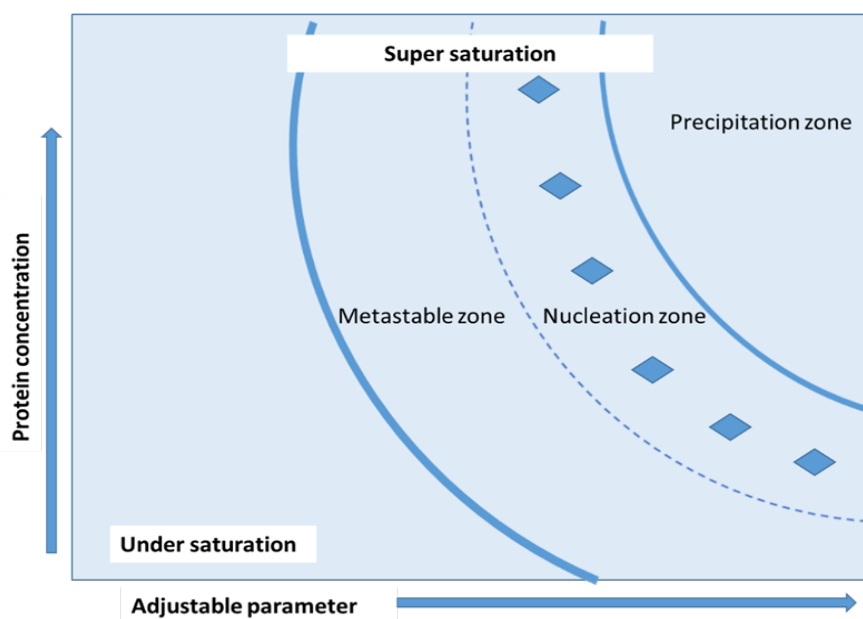
Figure 10. Diagram showing the phases of protein crystallisation.

Four stages can be considered in the crystallisation process: Stage 1: is the unsaturated stage; this is where the concentration of protein and precipitants are too low for nucleation or crystal growth. Stage 2: is the metastable stage, where protein growth can occur but is too dilute for nucleation. Stage 3: this is the nucleation stage, where both nucleation and crystal growth occurs. Stage 4: the final step is the precipitation step, which is when disordered aggregates are formed.

2.10 Protein activity assays

2.10.1 Zymography

The PG cleavage activity of the ActA proteins was investigated by zymography assays as previously described (Mukamolova *et al.* 2006) with some minor modifications. A starter culture of *M. luteus* was prepared as mentioned in section 2.3.4, and was inoculated in 500 ml of LB media. This was incubated overnight at 37°C (shaking at 200 rpm) to the optical density of 1.5 - 2. The bacteria were harvested by centrifugation at 6,000 x g for 30 minutes. The pellet was frozen at -20°C before being lyophilised. The lyophilised *M. luteus* was ground into a fine powder and stored at room temperature before analysis via zymography. Lyophilized *M. luteus* 0.2 % (w/v) was incorporated into a polyacrylamide gel by mixing it with 9.7 ml of the SDS-PAGE gel mixture. For the zymogram assay, 15 µl (2 µg/ml) of purified protein, 3 µl (0.5 µg/ml) of lysozyme (positive control) and 15 µl of the negative control (pET15b-Tev) were loaded onto the gel and ran at 200 V for 1 hour. The gels were washed twice in water, and incubated in refolding buffers with different pH values containing 0.2 % (w/v) Triton x 100, to replace SDS at room temperature for one hour. The following refolding buffers were used to find the optimal refolding conditions: 20 mM potassium phosphate at pH 6.5 or 7.8, and 20 mM Tris at pH 5.7, 6.6 and 8.0 with and without magnesium (1 mM). The gel was incubated further in the same buffers without Triton for 24 hours at 37°C. Finally, the clearance band which indicated peptidoglycan degradation was visualised by staining gels with 0.2% methylene blue for 60 minutes, and destaining with water for 45–60 minutes (Zahrl *et al.* 2005).

2.10.2 Preparation of peptidoglycan from *E. coli* for FITC labelling

This subsection will describe the steps used to purify and label *E. coli* PG for activity assays.

2.10.2.1 Generation and purification of *E. coli* peptidoglycan

The purification of PG from *E. coli* cells was carried out by using the well-established protocol from Glauner's group (Glauner *et al.* 1988). Briefly, a starter culture of *E. coli* (LMG) was prepared as mentioned in section 2.3.2 in 5 ml LB, reinoculated into 400 ml of LB without antibiotics and incubated at 37°C with agitation until an OD $_{600nm}$ of 0.8-0.9 was reached. The growing culture was rapidly cooled on ice for 10 minutes and cells were harvested by centrifugation at 4,000 x g at 4°C for 30 minutes. The supernatant was removed, and the pellet was resuspended in 6 ml of cold water. The cell suspension was boiled in the presence of 6 ml of 8 % SDS to prevent the activation of muralytic enzymes and to remove proteins.

The culture was continuously boiled with stirring for 30 minutes and cooled down to room temperature. Then, the sample was centrifuged at 100,000 x g for 1 hour. The supernatant was carefully discarded, and the pellet resuspended in MilliQ H2O and centrifuged at 100,000 x g for 1 hour. This washing procedure was repeated between 10 to 12 times to remove SDS, and the Hayashi test was carried out to determine the conce-ntration of SDS (explained in section 2.10.2.2).

After the removal of SDS, the sample was resuspended in 900 µl of buffer containing 100 mM Tris HCl (pH 7.0) and 10 mM NaCl and transferred into 2 ml tubes. Then, 100 µl of 3.2 M imidazole (pH 7.0) was added to the sample. Following that 15 µl of 10 mg/ml α-amylase was added to the sample. This was incubated for 2 hours at 37°C. After incubation, 20 µl of 10 mg/ml Pronase E (pre-incubated at 60°C for 2 hours) was added to the sample and incubated for 1 hour at 60°C. After incubation, 1 ml of 4 % (w/v) SDS was added, and the sample was heated to 100°C for 15 minutes. Further washing was done as described above. Finally, the purified PG was ready for activity assays e.g., experiments with the digestion of FITC labelled PG or the analysis of PG via HPLC.

2.10.2.2 Hayashi test

The Hayashi test was performed as described by Hayashi (Hayashi 1975). This test is used to assess the level of SDS in the preparation. The sample (335 µl) was mixed with 7 µl of 0.5 % methylene blue, 170 µl 0.7 M sodium phosphate (pH 7.2) and 1 ml of chloroform. Then, the sample was mixed vigorously and briefly centrifuged. Finally, if SDS had been removed, a transparent or pinkish layer would appear at the top of the chloroform phase.

2.10.2.3 PG labelling with FITC

FITC (1 mg) was dissolved in 100 µl of DMSO using a vortex. Purified PG (section 2.10.2.1) was resuspended in 900 µl of phosphate buffer (40 mM KH_2PO_4, pH 8.5). Then, FITC was added to the PG sample. The final volume of the precipitate was 1 ml, and the mixture was incubated overnight at 4°C. After incubation, the FITC was covalently bound to PG, and the unbound FITC was removed by several washing steps (10 times) with milliQ grade water via ultracentrifugation at 100,000 g for 1 hour. In all the washing steps, the pellet was resuspended in milliQ grade water. After the last washing step, 100 µl of supernatant was tested for unbound FITC with the Varioskan instrument (excitation/emission spectra of 495/521 nm). The sample free of un-bound FITC was used for further experimentation.

2.10.2.4 FITC experiment

After the removal of SDS in the preparation, 100 µl of purified protein was mixed with 2 µl of PG labelled with FITC and incubated at 32°C for 24 hours. Then, the mixture was centrifuged at 20,000 x g for 30 minutes. The supernatant was filtered using 0.22 µm filter units. Finally, the muralytic activity was tested by measuring the fluorescence in relative fluorescence units (RFU) using a Varioskan. This experiment is quantitative, simple and highly sensitive (Sogawa and Takahashi 1978; Maeda 1980). However, in the labelling step, it is not possible to calculate the exact amount of FITC required as PG has a variable structure and the molecular weight is not known.

2.10.3 Analysis of peptidoglycan fragments

Digested peptidoglycan samples were analysed using a ProntoSIL C18 AQ column (Bischoff Chromatography) on an AKTA Purifier System. The detailed analysis of peptidoglycan fragments was carried out by Prof. W. Vollmer's group at Newcastle University. For the analysis on the C18 AQ columns, the ActA$_{A30-S157}$ protein (3 µM) was incubated with *L. monocytogenes* peptidoglycan overnight at 37°C. Samples were boiled for 5 minutes, followed by the addition of cellosyl, after which samples were incubated at 37˚C for 5 hours and then analysed via HPLC.

2.11 Production and purification of Anti-ActA antibodies

A recombinant truncated ActA$_{A30-S157}$ protein was used to generate anti-ActA polyclonal antibodies (Gemini Biosciences Ltd). Two rabbits were immunized with the protein using the Titremax adjuvant. During a 90-day immunisation schedule, a pre-immune serum (1st bleed) was supplied before immunization, with serum being days 21, 35, 49, 63 and 93. The poly-clonal Anti-ActA antibody was purified using a pre-packed FliQ Protein A Sepharose column (Generon). The column was equilibrated with 10 column volumes (CV) of loading buffer (50 mM tris buffer, pH 7.5). 5 ml of loading buffer was used with an equal amount of polyclonal sera for loading onto the column. The flow-through was collected in a clean tube before the column was washed with 10 CV of loading buffer.

The bound antibodies were eluted using 0.1 M Glycine buffer (pH 3). Then, 1 ml fractions were collected into Eppendorf tubes containing 100 µl of 1 M Tris HCl (pH 8.5). The eluted fractions were concentrated using Amicon Ultra Centrifugal filters (100 kDa). The concentrated antibodies were analysed by SDS-PAGE and aliquoted for long term storage at-80°C.

55

2.12 Dot blots to determine the affinity of anti-ActA antibody to *L. monocytogenes* ActA

The purified recombinant ActA protein (~1 µg) was spotted directly onto the nitrocellulose membrane and dried. The membranes were blocked for 30 minutes using 5 % milk in PBS. After blocking, the membrane was washed three times with PBST buffer (PBS with 0.05 % Tween 20). Then, the membrane was incubated with anti-ActA antibodies for 1 hour at room temperature. The membrane was then washed with PBST and incubated with the secondary anti-rabbit alkaline phosphatase conjugated antibody (1:2,000) at room temperature for 1 hour. Following another wash step, the membranes were exposed to the alkaline phosphatase substrate (BCIP/NBT), and the reaction was stopped by washing the membrane with water.

2.13 ActA localization in *L.monocytogenes*

In an attempt to optimise the detection of the ActA protein *in-vitro* from *L. monocytogenes* (native host), several different methods were used to detect the ActA protein in the cellular fraction to be used in the immunoprecipitation experiment. These methods are detailed below.

2.13.1 Detection of ActA in culture supernatant and membrane/cell wall fractions

This was carried out as described previously by Bierne *et al.* (Bierne *et al.* 2004). *L. mono-cytogenes* wild type and Δ*actA* were grown as mentioned in section 2.3.1. The starter culture was inoculated into 100 mL BHI medium and incubated at 37°C to an OD_{600nm} of approximately 1. The supernatant fraction was prepared by centrifugation at 16,000 x g, 4°C for 20 minutes. Then, the supernatant was collected and filtered with a 0.22 µm Millipore filter to remove remaining cells or debris. The supernatant was concentrated using a 100 kDa cutoff membrane on an Amicon ultrafiltration device (Millipore). Then, the sample was pelleted by centrifugation x2000 for 30mins at 4°C and supernatant was discarded. The proteins were precipitated by10% trichloroacetic acid-acetone (TCA) following the protocol described previously (Bierne *et al.* 2004). Finally, the sample was boiled at 92C°C for 2 minutes before analysed by SDS-PAGE and Western blot with anti-ActA as the primary antibody (1:2,000) and anti-rabbit alkaline phosphatase conjugated as the secondary antibody (1:2,000).

2.13.2 Detection of ActA in cell wall and membrane fractions using differential ultra-centrifugation

This was done as described previously by Mawuenyega *et al.* (Mawuenyega *et al.* 2005), with minor modifications.

Culture of wild type *L. monocytogenes* was grown in 1 litre of BHI until an OD_{600} of 0.9. Then, the bacteria were pelleted by centrifugation at 5,000 x g, at 4°C for 20 minutes. The pellet was re-suspended in TBS buffer (20m mM TrisHCl (pH 8.0), 150 mM NaCl, 20 mM KCl and 10 mM $MgCl_2$) with proteinase and phosphatase inhibitors (Roche) and lysed via sonication using 3 bursts of 45 seconds (amplitude 9) in a sonicator (Soniprep 150 Plus Digital Ultrasonic Disintegrator), with pauses of 2 minutes on ice. Following that, bacterial lysate was centrifuged at 2,500 x g, 4°C for 15 minutes. The supernatant was further centrifuged at 27,000 x g, at 4°C for 1 hour. The pellet was washed in carbonate buffer (pH 11). The supernatant was subjected to 4 hours of centrifugation at 100,000 x g at 4°C. The supernatant contained cytoplasmic proteins (cytoplasmic fraction). The pellet representing the membrane fractions was washed twice in TBS buffer with proteinase and phosphatase inhibitors and once in carbonate buffer (pH 11). Proteins from the cellular fractions were analysed by SDS-PAGE. Finally, the analysis of the proteins was carried out by Western blot using anti-ActA antibodies and by mass spectrometry.

2.13.3 Optimisation of digestion protocol for detection of membrane proteins

The obtained membrane fractions from section 2.13.2 were digested by our new developed method called Digestion at Elevated Temperature, DIET, (Loraine *et al.* 2019). In each experiment, approximately 250 μg of membrane proteins was used in a final volume of 50 μL. Each sample contained 10 mM Tris HCl buffer, pH 8.5, 5 mM dithiothreitol, 0.1% (w/v) SDS, and 10 mM $CaCl_2$. The trypsin was added in the ratio of 1 molecule of enzyme to 50 molecules of the substrate immediately before placing samples in a heating block. The samples were incubated at 52°C for 30 minutes and have been sent to mass spectrometry.

2.13.4 Detection of ActA in cell surface and intracellular fractions grown in BLEB media

Lathrop *et al.* (Lathrop *et al.* 2008) published localization method different to Mawuenyega *et al.* (Mawuenyega *et al.* 2005). Briefly, starter cultures of *L. monocytogenes* wild type and Δ*actA* were grown in 20 ml BLEB broth overnight at 37°C, in a shaking incubator. The cells were centrifuged at 2000 x g at 10°C for 15 minutes, then washed and re-suspended in 20 ml PBS. Thereafter, 5 ml of each culture was centrifuged at 2000 x g at 10°C for 15 minutes. The supernatants were discarded, and the cell pellets were used for both surface and intracellular protein extraction. For surface protein isolation, cell pellets were suspended in 100 μl PBS buffer (pH 7.0) containing 5 % (w/v) SDS, vortexed, and incubated at 37°C for 1 hour. The sample was then centrifuged at 12,000 x g at 5°C for 5 minutes, and the supernatant containing

the surface proteins was removed. After this, the cell pellets were used for intracellular protein isolation by ultrasonication. The pellet was resuspended in 100 µl of PBS, sonicated for 1 minute using the Soniprep 150 Plus Digital Ultrasonic Disintegrator and centrifuged at 12,000 xg at 4°C for 5 minutes. The supernatant containing the intracellular proteins was collected. Finally, both the surface and intracellular proteins extraction were analyzed by SDS-PAGE, Western blot and mass spectrometry.

Chapter 3

Expression, purification, and structural characterisation of the recombinant ActA proteins

3.1 Introduction

The generation of recombinant proteins has proven very important for scientific research; they have played significant roles in structural biology research, in the investigation of protein functions, antibody generation and for the development of diagnostic kits (Palomares *et al.* 2004; Dennison 2013). However, the production of large amounts of soluble recombinant proteins is challenging. Several factors may directly affect recombinant protein expression, for instance: bacterial strain, expression vector, culture media, purification buffer and expression temperature (Rosano and Ceccarelli 2014; Chhetri *et al.* 2015).

Bacteria, in particular *E. coli*, are considered as ideal expression hosts due to their ability to tolerate as well as accommodate recombinant protein production. *E. coli* expression hosts have several advantages; they are reasonably cheap to work with, can be used to produce high protein yields, and they can replicate to the optimal expression condition within a short period of time (Marston 1986; Baneyx and Mujacic 2004; Rosano and Ceccarelli 2014). Furthermore, genetic manipulations in *E. coli* are well-established and do not pose any significant health risks (Kleiner-Grote *et al.* 2018). Recombinant proteins fold better in *E. coli* compared to mammalian hosts (Makino *et al.*2011). However, using this bacterium as an expression host can be problematic, as some proteins may be degraded or generated as inclusion bodies (Lilie *et al.* 1998). The steps required to obtain a recombinant protein are straightforward, however, protocol optimisation is usually necessary to achieve satisfactory yields of soluble recombinant protein. This task can be complicated by several influential factors; poor growth of the host (Rosano and Ceccarelli 2014), toxicity of the protein or lack of protein expression (Dumon-Seignovert *et al.* 2004), formation of insoluble proteins called inclusion bodies (Wingfield 2015), reduced stability of the protein (Maurizi 1992) and loss of enzymatic activity (Rosano and Ceccarelli 2014).

As described in detail in Chapter 1 (section 1.9), previous work in our laboratory has identified peptidoglycan cleaving activity of the $ActA_{A30-N639}$ protein (Iakobachvili ,2014) which warranted further investigation. Thus, this chapter describes the process of the generation, expression and purification of different versions of the ActA protein (shown in Chapter 2 , Figure 9, section 2.8.2) to be used in structural studies and activity assays (described in Chapter 4). In addition, this chapter will describe the generation and purification of 14 site-directed mutagenesis (SDM) proteins to identify potential catalytic residues within $ActA_{A30-S157}$, which

are important for PG cleaving activity. Furthermore, several attempts to solve the structure of the NH2-terminal region of the ActA protein will be shown in this chapter. The determination of protein structures is crucial because it reinforces our knowledge about a protein's function, and provides insight into the mechanism by which these proteins work (Dessau and Modis 2011).

3.2 Results

3.2.1 ActA$_{A30-N639}$ protein could not be purified from *E. coli*

It was previously shown that an ActA$_{A30-N639}$ protein (no signal sequence) could be expressed in *E. coli* (Iakobachvili 2014). Consequently, a pET15b-Tev::*actA*$_{A30-N639}$ construct which was previously generated (Iakobachvili 2014) was used to express this protein (ActA$_{A30-N639}$). The plasmid was purified from *E. coli* DH5α using the GeneElute™ Plasmid Miniprep (Sigma) kit and digested with the *NdeI* and *Bam*HI enzymes (mentined in Chapter 2,section 2.5.6). Figure 11 shows the undigested pET15b-Tev::*actA*$_{A30-N639}$ construct (lane 1) and digested plasmid (lane 2). The digested sample yielded two bands: a bigger fragment corresponding to the linearised pET15b-Tev plasmid (calculated size of 5,708 bp) and a smaller band corresponding to the *actA* insert (calculated size of 1,902 bp). The plasmid was sequenced, and the analysis of the sequence confirmed that there were no mutations or deletions in the plasmid. Using a previously established protocol,this recombinant plasmid was transformed into *E.coli* BL21 (DE3) and the resultant strain was used for the expression of the protein (Iakobachvili 2014). However, multiple attempts to express the protein under different conditions (e.g. various concentrations of IPTG, temperatures and media) were unsuccessful. Therefore, an alternative expression host *E. coli* C41 (DE3) was used, as this is designed for the expression of toxic proteins (Glauner *et al.* 1988).
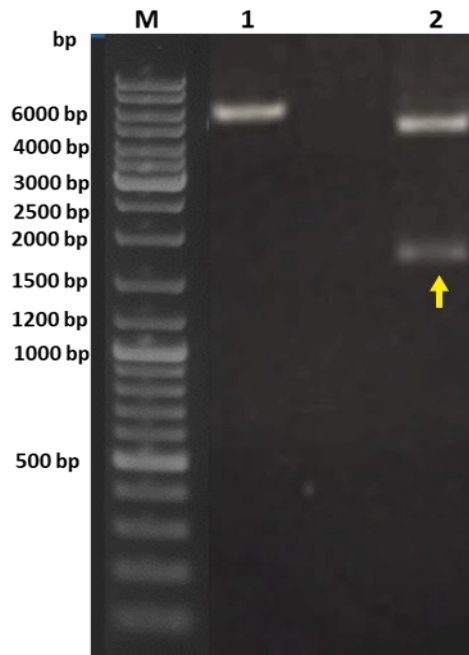
Figure 11. Agarose gel electrophoresis showing the diagnostic digest of pET15b-Tev::*actA* A30-N639.

The *actA* gene was cloned between the *NdeI* and *Bam*HI sites of the pET15b-TEV plasmid. [M] Is 1 kb DNA ladder. Lane (1) Undigested plasmid and (2) Plasmid digested with *NdeI* and *Bam*HI. The *actA* insert is indicated by a yellow arrow (~1,900 bp).

Figure 12 shows the results of the expression trial for the ActA$_{A30-N639}$ protein using *E. coli* C41 (DE3) induced with 0.5 mM IPTG at different incubation temperatures. In Figure 12A, the SDS-PAGE shows multiple bands for the crude extracts of the following samples: pET15b-TEV (pET15b), soluble ActA$_{A30-N639}$ (S) and insoluble ActA$_{A30-N639}$ (US), expressed at different temperatures i,e 37 ºC and 18 ºC. SDS-PAGE was performed for all the lysates to analyse protein expression. As shown in Figure 12A, there is no evidence of an additional band around 67 kDa (the predicated size for ActA$_{A30-N639}$) in both soluble (S) and insoluble(US) fractions. Therefore, a Western blot (Figure 12B) was used to detect protein presence. The blot in Figure 12B shows no band in the empty pET15b vector lane (negative control) with the anti-His antibody. However, in both soluble and insoluble fractions, multiple bands were recognised with a specific antibody. It shows that ActA$_{A30-N639}$ is expressed in all conditions, but is aggregated (upper bands) and degraded (lower bands). Moreover, Figure 12B shows multiple bands present in the soluble fractions and a substantial amount of bands present in the insoluble fractions. Changing the temperature did not make any difference, and the problem was not solved.
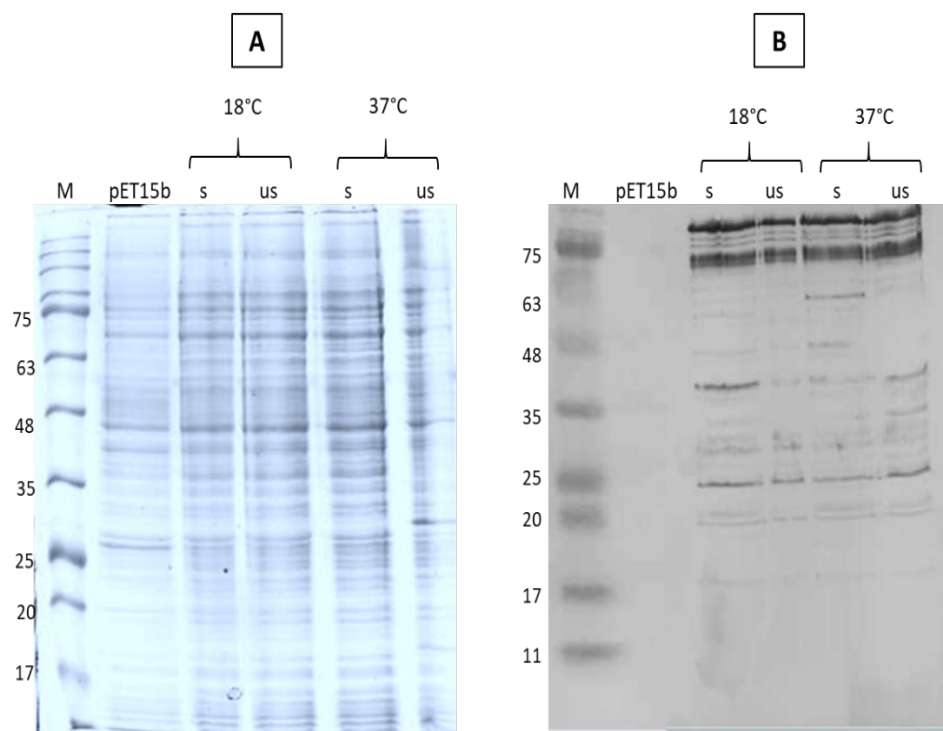
Figure 12. Expression trials for the recombinant ActA$_{A30-N639}$ protein.
Expression of ActA$_{A30-N639}$ protein in *E. coli* C41 (DE3) was induced with 0.5 mM IPTG using different temperatures (18ºC and 37ºC). Both soluble (S) and insoluble (US) fractions were tested for ActA$_{A30-N639}$ expression. (A) 12 % SDS-PAGE with multiple bands in all lanes. (B) Western blot with anti-polyHis antibodies (1:2,000) showing bands in all the lanes except the negative control lane (pET15b). [M] Prestained Protein Ladder (Geneflow, UK).

ActA$_{A30-N639}$ purification was performed in two steps, using affinity chromatography and gel filtration (as described in section 2.8.5). Figure 13A shows a representative elution profile for the ActA$_{A30-N639}$ protein obtained from the gel filtration step. The fractions were collected at approximately 62 minutes, which corresponds to a 67 kDa protein based on the elution position of the molecular weight standard. In addition, multiple peaks were present in the gel filtration profile, showing protein aggregation and degradation. The fractions collected at 62 minutes from both the expressed ActA$_{A30-N639}$ and the negative control (empty pET15b) samples were analysed via SDS-PAGE. The result of the SDS-PAGE (Figure 13B) shows multiple bands in all the lanes for the collected fractions (lanes 1 to 6), with no evidence of a pure single protein band around the corresponding size (67 kDa) of the ActA$_{A30-N639}$ protein. Therefore, a Western blot was performed to confirm whether the bands obtained corresponded to ActA$_{A30-N639}$ by using anti-polyHis antibodies. As illustrated in Figure 13C, no band was detected in the negative control (pET15b) lane, while multiple bands were recognised with the anti-polyHis

63

antibody. This result confirmed that the ActA$_{A30-N639}$ protein was expressed but in multiple forms. It was not possible to purify the ActA$_{A30-N639}$ protein and therefore, we focused on the expression and purification of truncated forms of ActA.
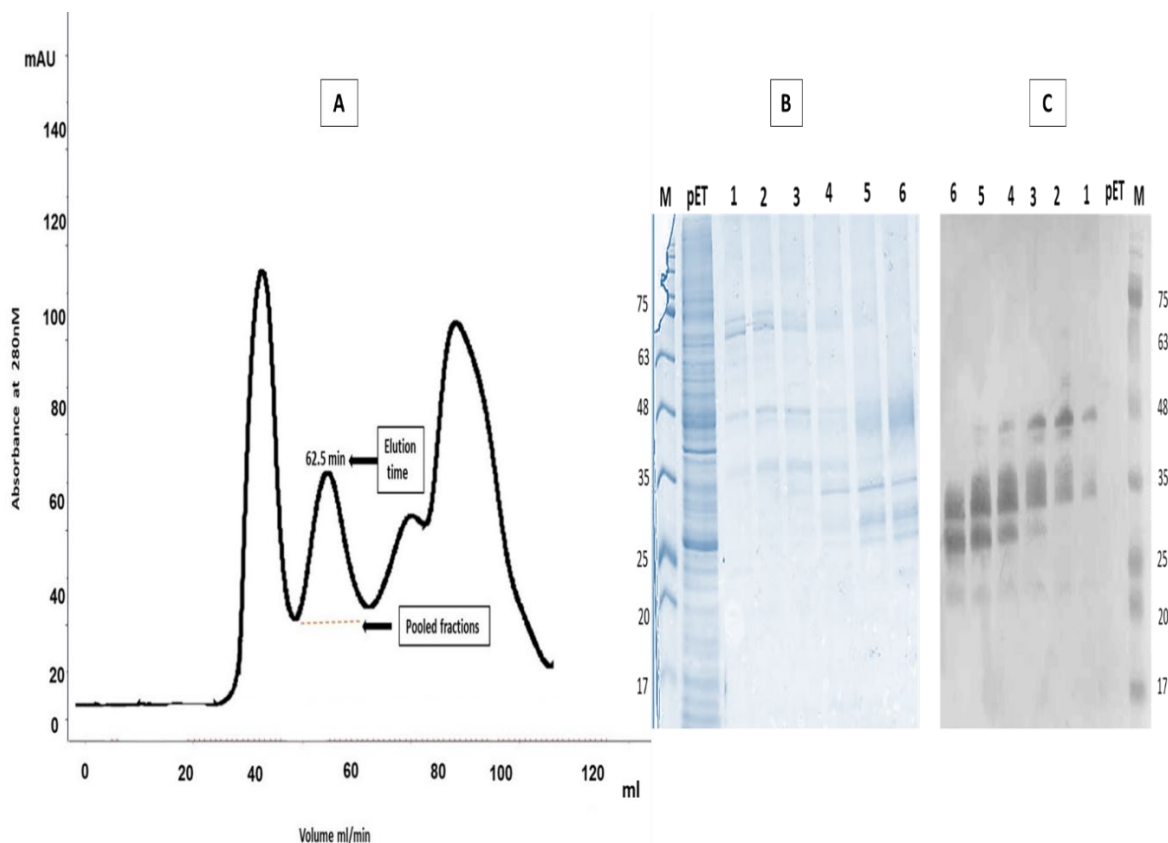
Figure 13. Purification and analysis of ActA $_{A30-N639}$.
(A) Gel filtration profile of ActA$_{A30-N639}$. (B) SDS-PAGE analysis of the fractions at around 62 minutes from gel filtration chromatography. pET: stand for the empty vector pET15b-TEV, and it used as a negative control. The numbered lanes represent the fractions collected from the gel filtration at around 62 minutes. (C) Western blot with anti-poly-His antibody (1:2,000) for the protein fractions and the empty vector (pET15b-TEV). Both (A) and (B) show multiple bands for the ActA$_{A30-N639}$ protein after gel filtration. The SDS-PAGE gel was stained with Colloidal Coomassie blue. [M] Marker (Prestained Protein Standards obtained from Geneflow, UK).

3.2.2 Truncated forms of ActA protein

The three constructs were generated successfully by PROTEX for the expression of truncated versions of ActA: ActA $_{A30\text{-}S157}$, ActA$_{A30\text{-}N233}$ and ActA $_{G393\text{-}N639}$. The plasmids for the three constructs were sequenced at GATC biotech (section 2.5.11) to confirm that there were no mutations and that the plasmids had the correct inserts. The sequencing did not reveal any mutations in any plasmids. Morover, the BLAST analysis was shown in the Appendix (8.4, 8.5 and 8.6) and the identity for each clone matched the original sequences in the database. Therefore, all plasmids were purified as illustrated in Figure 14. The expected plasmid sizes of PLEICS-01-ActA$_{A30\text{-}S157}$, PLEICS-01-ActA$_{A30\text{-}N233}$ and PLEICS-01-ActA$_{G393\text{-}N639}$ were 8,131, 8,260 and 8,830 bp respectively. The purified plasmids were then used for transformation into the expressing host, *E. coli* C41 (DE3).
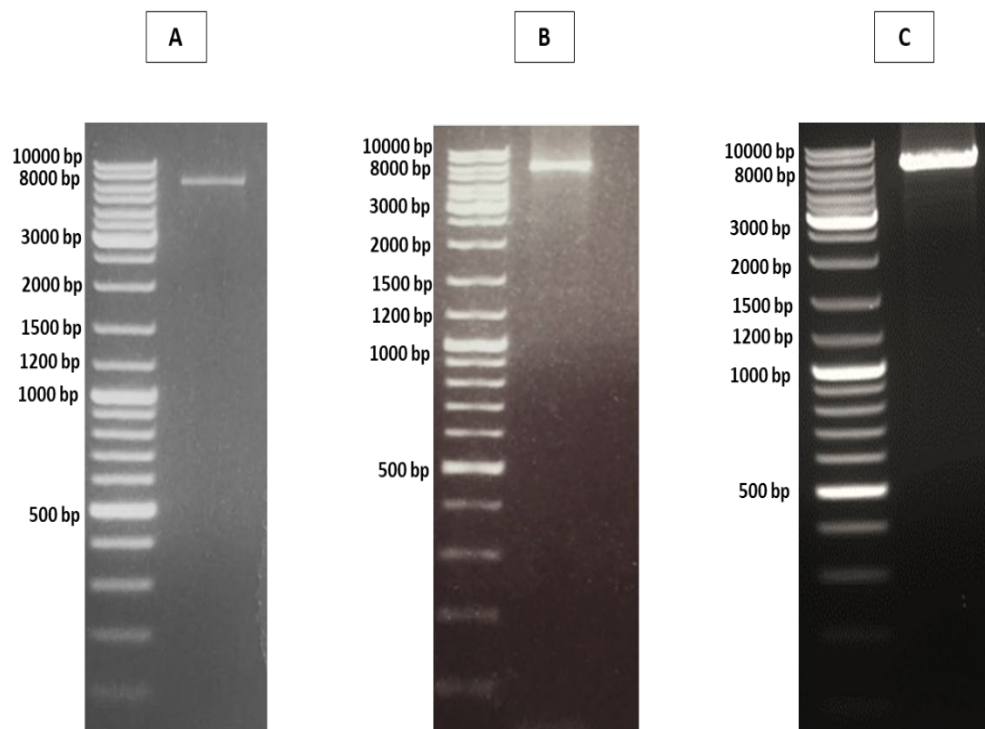
Figure 14. Agarose gel analysis showing the DNA profile of the PLEICS-01-ActA$_{A30\text{-}S157}$, PLEICS-01- ActA$_{A30\text{-}N233}$ and PLEICS-01- ActA $_{G393\text{-}N639}$ plasmids.
The sequence confirmation of all the constructs was performed by GATC. (A) PLEICS-01-ActA$_{A30\text{-}S157}$ with the expected size of 8,131 bp. (B) PLEICS-01- ActA$_{A30}$-N233 plasmid with the size of 8,260 bp. (C) PLEICS-01-ActA$_{G393\text{-}N639}$ plasmid with the size of 8,830 bp. The 1 kb DNA size markers (Thermo Scientific™ O'GeneRuler, UK) were used in all agarose gels.

Expression trials for ActA$_{A30-S157}$ and ActA$_{A30-N233}$ were done on a small scale as described in Chapter 2 (section 2.8.4). The 0.5 mM IPTG was used for the expression of both proteins, and the cultures were incubated at different temperatures. Proteins from the soluble fractions were analysed by SDS-PAGE and Western blot using the anti-polyhistidine antibody (Figure 15). Figure 15A shows the SDS-PAGE of the crude extracts before the induction of ActA$_{A30-S157}$ (pre) and the soluble ActA$_{A30-S157}$ after induction at different temperatures. Numerous bands of proteins with different sizes were present in all lanes. However, an additional band around 24 kDa was in the 37ºC lane (indicated by a black arrow), which corresponds to the expected size of the ActA$_{A30-S157}$ protein. To confirm the presence of ActA$_{A30-S157}$, a Western blot was carried out using the anti-polyHis antibody, as illustrated in Figure 15B. No band was detected in the pre-induction lysate, which was used as a negative control. A good yield of ActA$_{A30-S157}$ with the size of 24 kDa was observed in the samples expressed at 37ºC. In the samples expressed at 18ºC (Figure 15B) there was a faint band around 24 kDa in size corresponding to the ActA$_{A30-S157}$ protein, which was not visible on the gel obtained from SDS-PAGE (Figure 15A). This indicates that the protein is not expressed at high levels in this condition.

The ActA$_{A30-N233}$ protein was expressed in the same way as the ActA$_{A30-S157}$ protein. The SDS-PAGE result shown in Figure 15C shows multiple bands for the pre and post induced soluble lysate fractions at different temperatures. A very faint additional band around 35 kDa (indicated by an arrow) shows that ActA$_{A30-N233}$ protein was present at 37ºC (Figure 15C). Therefore, a Western blot using the anti-polyHis antibody was performed on all the samples, as illustrated in Figure 15D. The pre-induced (pre) lysate lane was empty, as shown in Figure 15D. In contrast, a single band which was approximately 35 kDa, corresponding to the ActA$_{A30-N233}$ protein, was detected in both lanes. Overall, the results of the trials indicate that the ActA$_{A30-S157}$ and ActA$_{A30-N233}$ proteins were successfully expressed, and that the optimal expression condition was incubation at 37ºC for 4 hours. The amount of protein expressed was greater in this condition compared to expression at 18ºC.
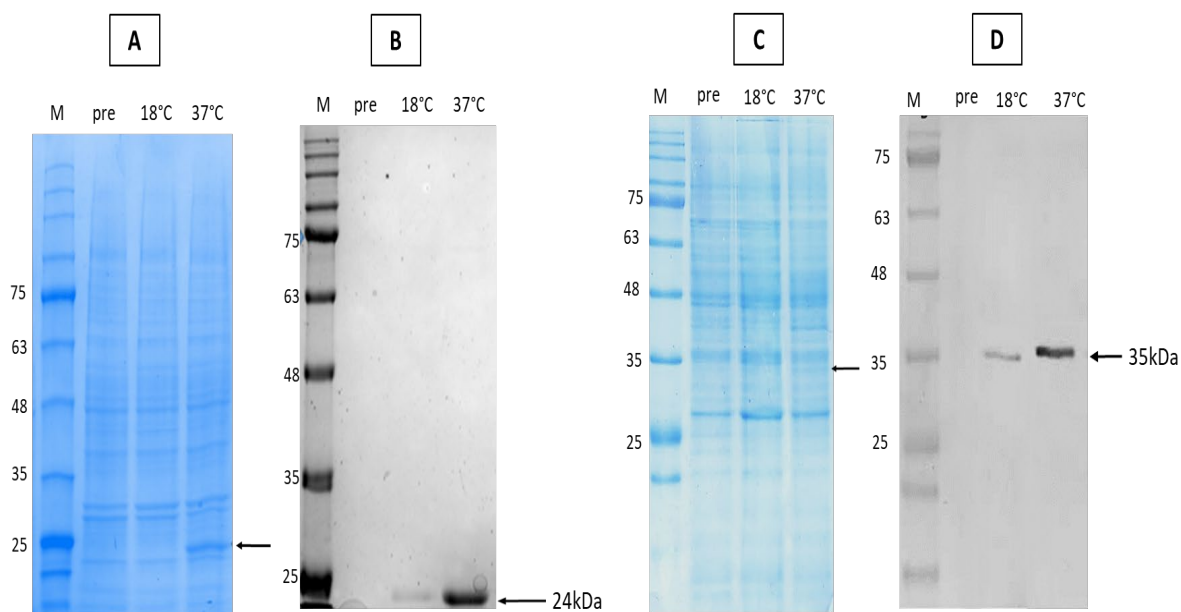
Figure 15. Expression trials for the recombinant ActA$_{A30-S157}$ and ActA$_{A30-N233}$ proteins. SDS-PAGE and Western blot showing the small-scale protein expression of ActA$_{A30-S157}$ and ActA$_{A30-N233}$ in *E. coli* C41 (DE3). (A) SDS-PAGE gel stained with Coomassie blue for both the pre and post-induced soluble lysates of ActA$_{A30-S157}$ (expected size 24 kDa) at different temperatures. (B) Western blot with anti-polyHis antibody (1:2,000) for the same samples (A); it shows the expression of soluble ActA$_{A30-S157}$, at the expected size of around 24 kDa in both temperatures. (C) SDS-PAGE gel for the pre and post-induced soluble lysates of ActA$_{A30-N233}$ at different temperatures. (D) Western blot with anti-polyHis antibody (1:2,000) for the same samples as (C); it shows the expression of soluble ActA$_{A30-N233}$ at the expected size of 35 kDa. Pre. lane corresponds to the pre-induction lysate. Cells were cultured at room temperature, 200 rpm in LB media to an OD$_{600nm}$ of 0.7 before being induced with 0.5 mM IPTG. [M] The marker was the Prestained Protein Standard (Geneflow, UK).

A two-step purification was employed to purify the ActA$_{A30-S157}$ (Figure 16) and ActA$_{A30-N233}$ (Figure 17) proteins, as indicated in section 2.8.5. The SDS-PAGE in Figure 16A shows the eluted nickel column fractions for the soluble ActA$_{A30-S157}$ protein. The ActA$_{A30-S157}$ protein was visible, and migrated to the expected size of 24 kDa (bands highlighted in black). After that, the protein was further purified using gel filtration chromatography. Figure 16B shows the elution profile of the ActA$_{A30-S157}$ protein obtained from the gel filtration purification step.

Further, ActA$_{A30\text{-}S157}$ protein was eluted at 80 minutes (indicated by the black line), which is the expected size of 24 kDa. The fractions of the eluted peak were collected and analysed by SDS-PAGE and Western blot using the anti-polyHis antibodies, as shown in Figure 16 C .Both the SDS-PAGE and Western blot analysis show the pure ActA$_{A30\text{-}S157}$ protein at the correct size (24 kDa). For further confirmation, the pure band of ActA$_{A30\text{-}S157}$ protein was analysed by mass spectrometry. The result obtained is shown in Figure 16D; it revealed that the ActA$_{A30\text{-}S157}$ protein matched the original protein sequence in the database. The red peptides represent the identified peptides.
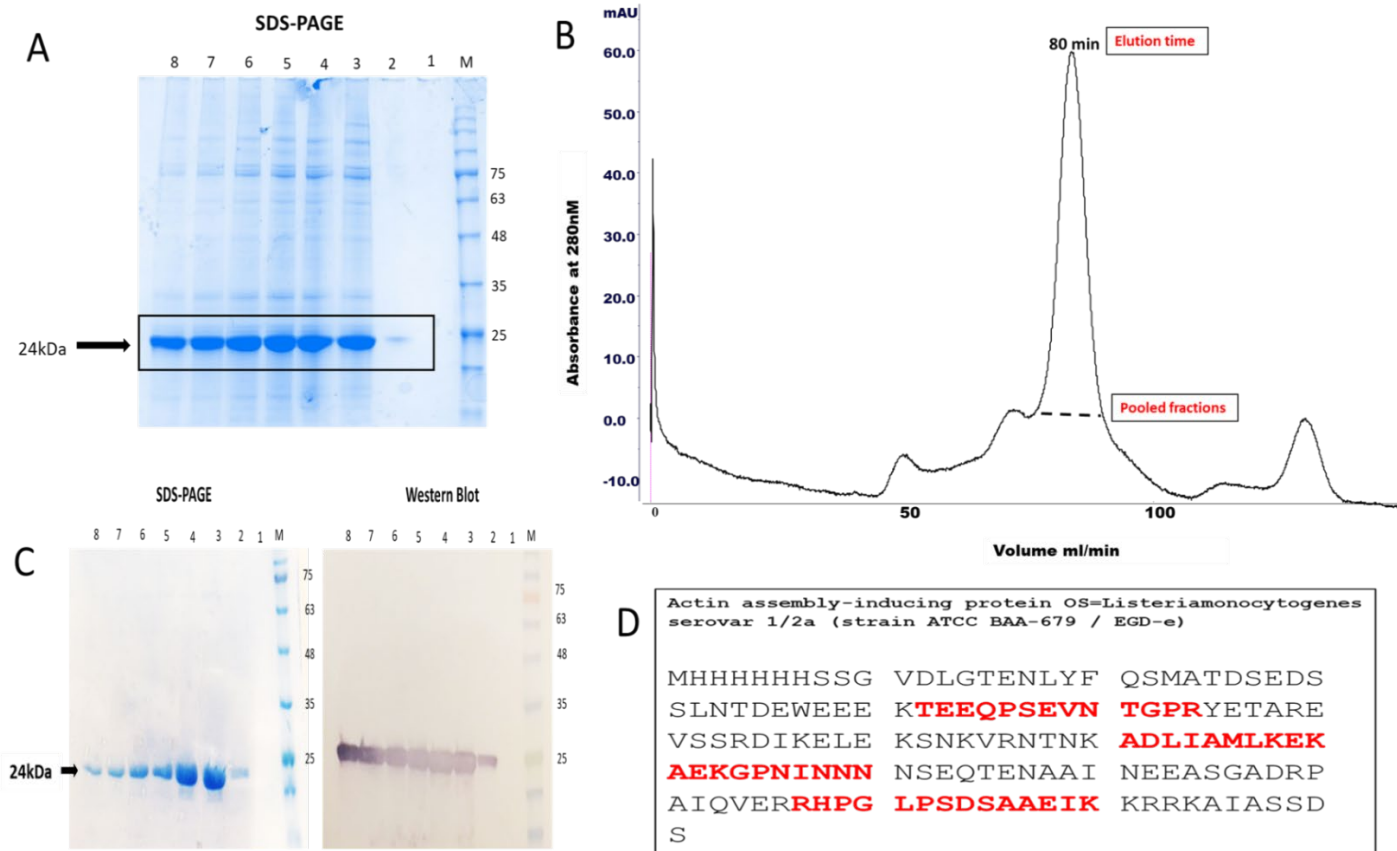
Figure 16. Purification and confirmation of the His-tagged ActA_{A30-S157} protein.
(A) SDS-PAGE gel of the fractions obtained from the purification of ActA_{A30-S157} by affinity chromatography. The protein was eluted with 60 mM imidazole and the bands are present at expected molecular weight of 24 kDa. (B) Gel filtration purification results showing a peak at 80 minutes corresponding to a protein of 24 kDa size. (C) SDS- PAGE and Western blot with anti-polyHis antibodies for the eluted fractions after gel filtration. (D) Conformation of ActA_{A30-S157} by mass-spectrometry. The red colour shows the identified peptides, which matched the peptides in the database. The Prestained Protein Standard (Geneflow, UK) labelled as [M] was used.

69

The purification process of the ActA$_{A30-N233}$ protein was similar to ActA$_{A30-S157}$. The eluted fractions of ActA$_{A30-N233}$ from the nickel column were separated using SDS-PAGE. The protein migrated to the correct size of around 35 kDa (highlighted in black), as seen in Figure 17A. Then, gel filtration was conducted as a further purification step; the elution profile is presented in Figure 17B. The single peak at 77 minutes corresponds to a 35 kDa protein. After that, the desired fractions of the eluted proteins were analysed using SDS-PAGE, stained with Coomassie blue and confirmed by Western blot using the anti-His antibody (1:2,000), as shown in Figure 17C. The gel and Western blot provide evidence that the ActA$_{A30-N233}$ protein obtained was pure and had the correct size of 35 kDa. The identity of the protein was also confirmed by mass spectrometry, and it was found to match the peptide sequence in the database (Figure 17D).
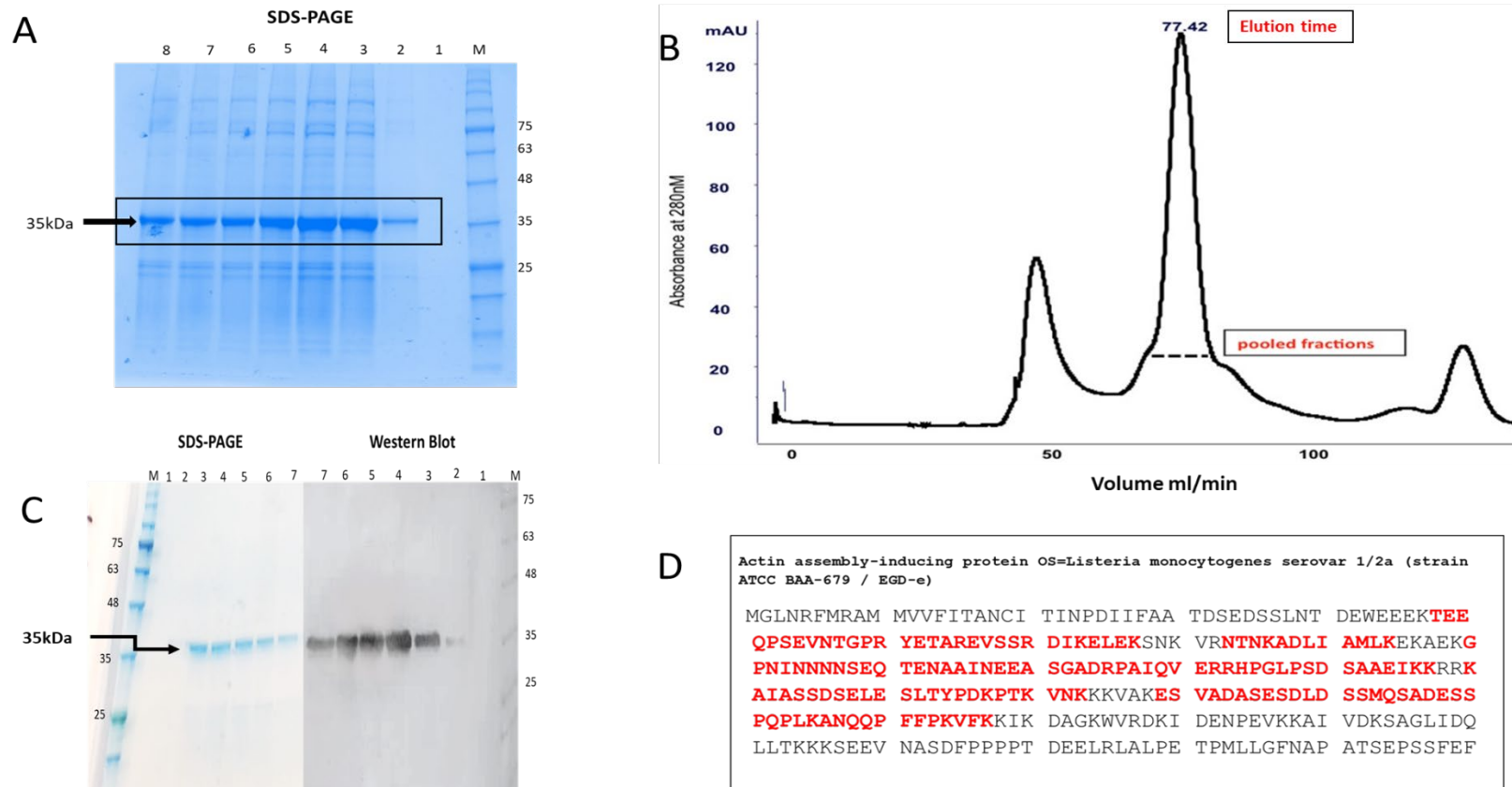
Figure 17. Purification and confirmation of the His-tagged ActA_{A30-N233} protein.
(A) SDS-PAGE gel showing the eluted fractions of ActA_{A30-N233}; the protein was eluted with 60 mM imidazole. The molecular weight of this protein is 35 kDa; bands corresponding to this size were present and are highlighted in black. (B) Gel filtration data showing a peak at 77 minutes, corresponding to a protein 35k Da in size. (C) Shows SDS-PAGE gel and Western blot for the eluted fractions after gel filtration. (D) The identity of ActA_{A30-N233} was confirmed by mass spectrometry. The red colour shows the identified peptides. [M] Prestained Protein Standard (Geneflow, UK).

The ActA $_{G393-N639}$ protein was expressed and purified as mentioned in Chapter 2 (sections 2.8.4 and 2.8.5). The expressed ActA $_{G393-N639}$ was purified by affinity chromatography and Figure 18A shows the data obtained from SDS-PAGE for the fractions obtained. The gel shows a band around 27 kDa (highlighted in black) which represents the expected size of the ActA $_{G393-N639}$ protein. Thereafter, gel filtration chromatography was performed; the elution profile is presented in Figure 18B. The fractions were collected and analysed further. Figure 18C shows the SDS-PAGE and Western blot data for the fraction obtained after gel filtration, and shows that the purified ActA $_{G393-N639}$ protein migrated to the expected size (27 kDa). Similar to the other mentioned truncated proteins, the identity of ActA $_{G393-N639}$ was confirmed by mass spectrometry, as it matched the peptides of the ActA protein found in the database (Figure 18D).
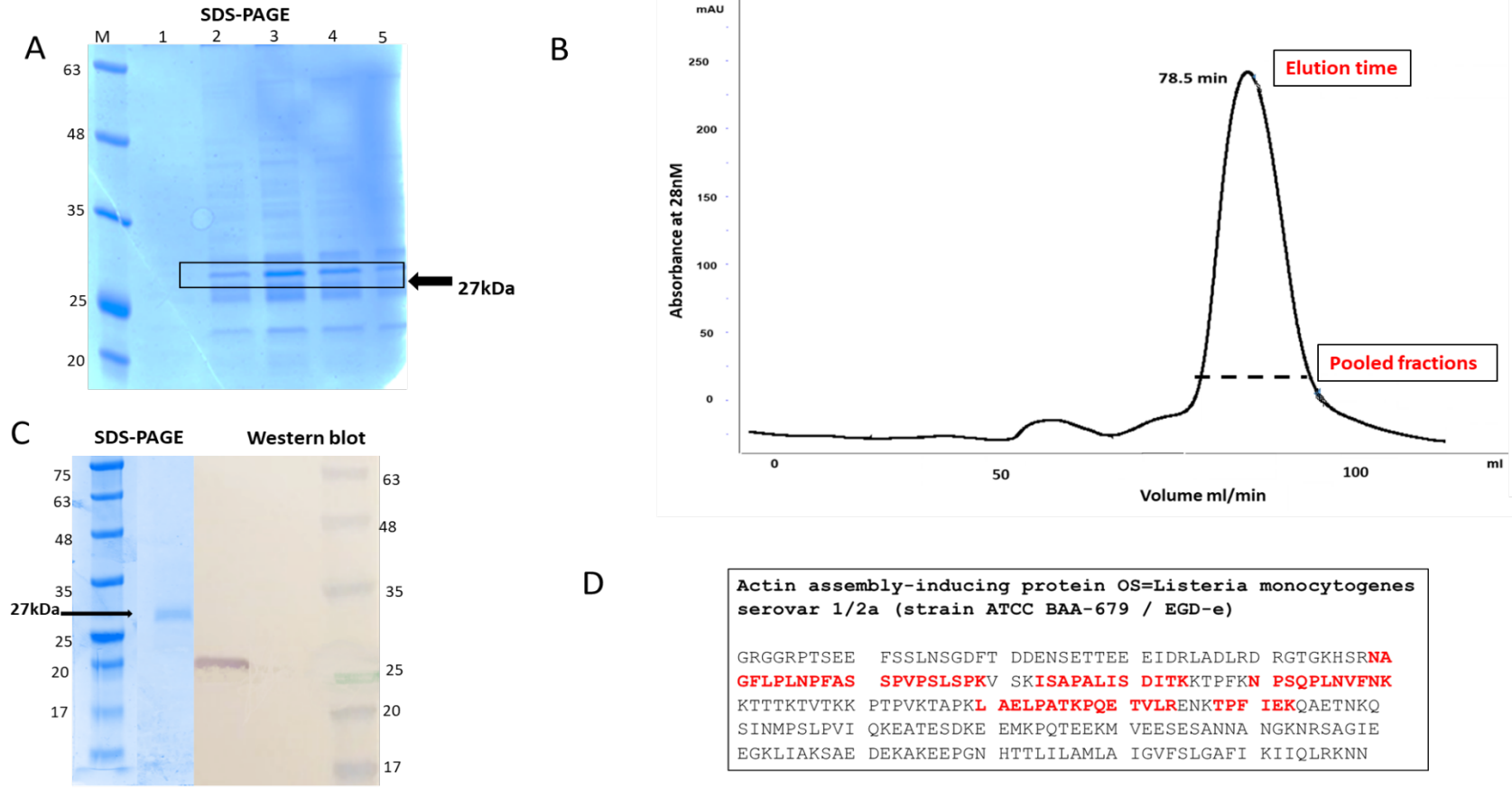
Figure 18. Purification and confirmation of the His-tagged ActA$_{G393-N639}$ protein.
(A)SDS-PAGE gel showing the purified fractions of ActA$_{G393-N639}$ protein obtained by affinity chromatography which was eluted with 100 mM imidazole. The molecular weight of the protein is 27 kDa, which is reflected by the band highlighted in black. (B) Gel filtration results showing the eluted peak at 78.5 minutes, corresponding to a 27 kDa protein. (C) SDS-PAGE gel and Western blot with anti-polyHis antibody for eluted fraction after gel filtration . (D) Mass-spectroscopy data confirming the identity of the ActA $_{G393-N639}$ protein; the red colour shows the identified peptides. [M] Prestained Protein Standard (Geneflow UK).

3.2.3 Site-Directed Mutagenesis (SDM) generated proteins

The main reason for generating proteins using SDM (shown in Table 11) was to investigate enzymatic activity. The mutagenesis procedure was carried out on the pLEICS-01::*actA* $A_{30-S157}$ plasmid due to its importance in the current study (further explained in the discussion). The predicted catalytic residues (the prediction strategy is mentioned in Chapter 4) were substituted with alanine. This is because alanine is a small, non-polar, inert residue that would be unlikely to cause unwanted disturbances to protein structure.

Table 11. Summary of all ActA mutagenesis used.

Mutant #	Strain	Sequencing	Type of mutation	Source
1	ActAE98A	100 %	Single point mutation at E98A in ActA$_{A30-S157}$	This study
2	ActAE42A	100 %	Single point mutation at E42A in ActA$_{A30-S157}$	This study
3	ActAE44A	100 %	Single point mutation at E44A in ActA$_{A30-S157}$	This study
4	ActAE45A	100 %	Single point mutation at E45A in ActA$_{A30-S157}$	This study
5	ActAE46A	100 %	Single point mutation at E46A in ActA$_{A30-S157}$	This study
6	ActAE49A	100 %	Single point mutation at E49A in ActA$_{A30-S157}$	This study
7	ActAE49A-E50A	100 %	Duple mutation at E49A and E50A in ActA$_{A30-S157}$	This study
8	ActAE44A-E45A-E46A	100 %	Triple mutation for E44, E45A and E46A in ActA$_{A30-S157}$	This study
9	ActA_Mut1	100 %	Scanning mutation for D32A ,E34A , D35A and D41A in ActA$_{A30-S157}$	Thermo-Fisher
10	ActA_MUT2	100 %	Scanning mutation for E54A, E62A, E66A and D71A in ActA$_{A30-S157}$	Thermo-Fisher
11	ActA_MUT3	100 %	Scanning mutation for E74A, E76E and D88A in ActA$_{A30-S157}$	Thermo-Fisher
12	ActA_MUT4	100 %	Scanning mutation for E95A, E98A , E109A and E112A in ActA$_{A30-S157}$	Thermo-Fisher
13	ActA_MUT5	100 %	Scanning mutation for E118A, E119A, E123A, D124A and E131A in ActA$_{A30-S157}$	Thermo-Fisher
14	ActA_MUT6	100 %	Scanning mutation for D140A, E144A and D56A in ActA$_{A30-S157}$	Thermo-Fisher

All SDM constructs were generated successfully and confirmed by sequencing at GATC (data not shown). After confirming the correct sequences, all recombinant mutated proteins were obtained by transforming the mutated plasmids into *E. coli* C41(DE3), and the proteins obtained were purified (as mentioned in section 2.8.5) alongside the wild type (ActA$_{A30-S157}$ protein). The SDS-PAGE gel in Figure 19 shows that all protein variants (from lane 1 to 14) were successfully purified, and migrated similarly to the wild type ActA$_{A30-S157}$ protein (lane 15), with no noticeable effect on mobility. However, the difference between these proteins was in the concentration of protein obtained after purification.
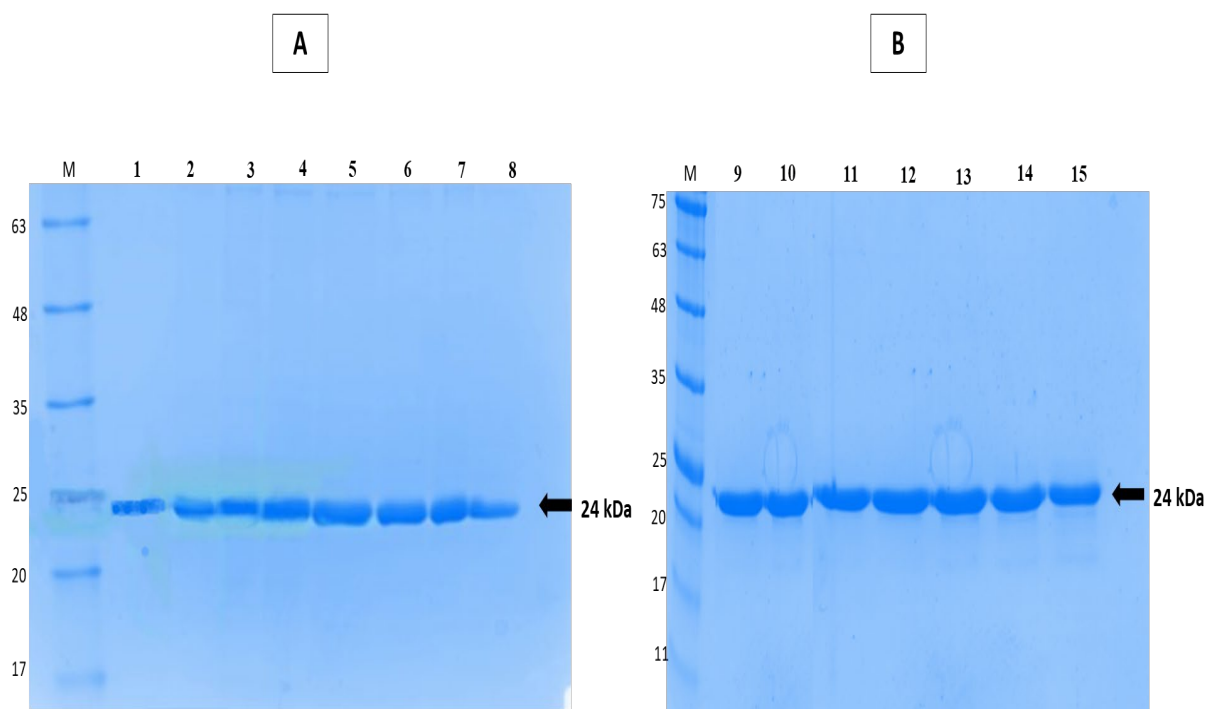
Figure 19. Purification of all the proteins obtained from SDM.
SDS-PAGE gel showing all the purified recombinant mutated proteins generated in the lab or synthesised by Thermo-Fisher. (A) Lanes 1 to 8 represent the proteins mutated in the lab using the GeneArt® Site-Directed Mutagenesis System: E98A, E42A, E44A, E45A, E46A, E49A, E49AE50A, E44AE45AE46A respectively. (B) Lanes 9 to 14 represent the purified proteins mutated by Thermo-Fisher: MUT1, MUT2, MUT3, MUT4, MUT5 and MUT6 respectively. Lane 15 represents the wild type ActA$_{A30-S157}$ protein. All proteins migrated to the expected size of 24 kDa. [M] Prestained Protein Standard (Geneflow, UK).

3.2.4 Attempts to solve the structure of ActA$_{A30-S157}$ and ActA$_{A30-N233}$

Following the successful purification of ActA$_{A30-S157}$ and ActA$_{A30-N233}$, several attempts with different conditions were conducted to solve the structure of the NH2-terminal domain of the ActA protein, using various crystallisation techniques. Many conditions were used, including different concentrations of pure proteins (3, 5, 7.5 and 11 mg/ml) and temperatures, as well as with and without the His-tag; other conditions used are listed in Appendix 8.7 and 8.8.

As shown in the images in Figure 20, blobs (a drop of a thick liquid or viscous substance) were obtained instead of clear crystals: His-ActA$_{A30-S157}$ (Figure 20A), ActA$_{A30-S157}$ without the His-tag (Figure 20B) and the His-ActA$_{A30-N233}$ protein (Figure 20C). These images show the unsuccessful crystallisation for all of the mentioned proteins.

His-ActA$_{A30-S157}$ ActA$_{A30-S157}$ without His-tag   His-ActA$_{A30-N233}$
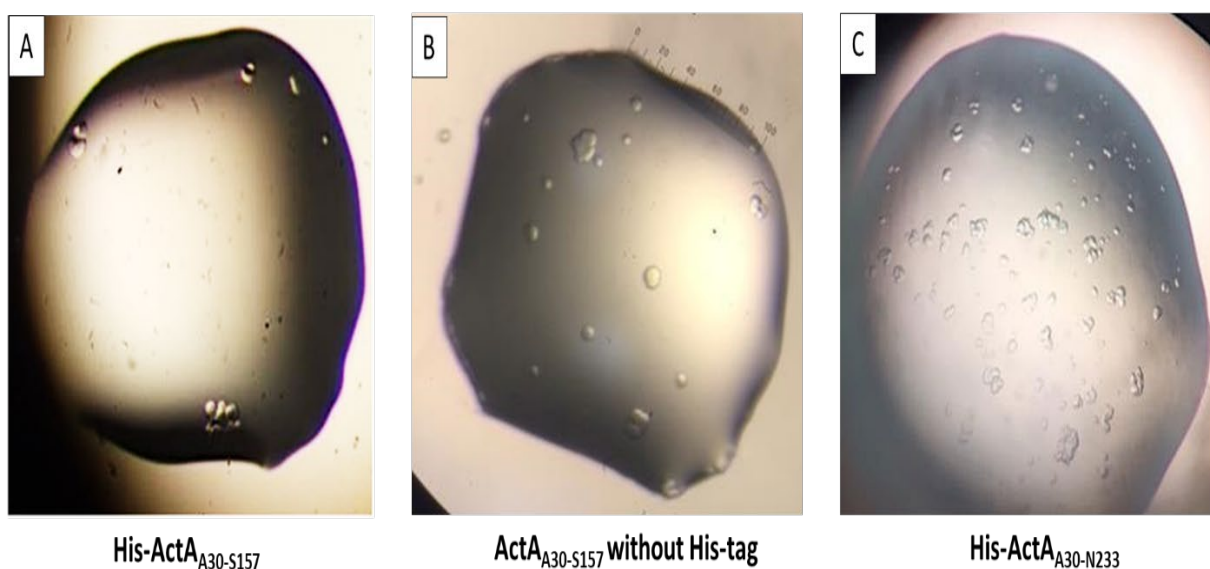
Figure 20. Blobs instead of actual crystal for ActA$_{A30-S157}$ and ActA$_{A30-N233}$ proteins.
(A) Small blobs were obtained from His-ActA$_{A30-S157}$. The condition for this was a protein concentration of 5 mg/ml in 0.1 M Na HEPES (pH 7.0) and 15 % w/v PEG 4,000. (B) Blobs of ActA$_{A30-S157}$ without the His-tag, obtained with 5 mg/ml protein concentration in 0.1 M Na HEPES (pH 7.0) and 15 % w/v PEG 4,000 condition. (C) Blobs of the His-tagged ActA$_{A30-N233}$. The protein concentration for this condition was 5 mg/ml in 0.1 M Na HEPES (pH 7.0) and 15 % w/v PEG 4,000.

3.1 Discussion

A large quantity of pure protein is required for both functional and structural characterization (Rosano and Ceccarelli 2014). As described in this chapter, several challenges were encountered during the expression and purification of the $ActA_{A30-N639}$ protein (Iakobachvili 2014). While the $ActA_{A30-N639}$ protein was expressed at a good level (as shown in Figure 13), it was not possible to purify the protein because it either aggregated or degraded during purification. As shown in section 3.2.1, $ActA_{A30-N639}$ failed to purify as a soluble protein with the expected size. It is likely that the $ActA_{A30-N639}$ protein did not fold properly, which led to protein instability. In addition, a protease inhibitor was during the purification because there was s study for Alvarez and Agaisse (Alvarez and Agaisse 2016) proposed that metalloprotease (Mpl) in *L.monocytogenes* has the ability to cleave the full length ActA protein at a specific region. The specific region is between AVC domain i.e encompassing the *a*cidic stretch, *v*erprolin homology, and *c*entral region, and the proline-rich region (PRR) of ActA .Thuse, the inhibitor was used but it did not change the result.

Protein degradation and aggregation is very common and is frequently reported in literature (Villaverde and Carrió 2003; Baneyx and Mujacic 2004; Pina *et al.* 2014). Moreover, large multi-domain recombinant proteins are more challenging to produce in their native conformation (folding) because they are not in their native environment (Baneyx and Mujacic 2004). Furthermore, the central domain of ActA protein includes four proline-rich repeat sequences which might cause the anomalous migration of $ActA_{A30-N639}$ protein (Footer *et al.* 2008). The phenomenon of higher migration than the expected size on SDS-PAGE has been reported with other proteins (Werten *et al.* 2001; Footer *et al.* 2008); for instance, Ruggiero *et al.* found that *Mycobacterial* Rpfs migrated further than their actual size after SDS-PAGE and RpfA in particular is rich in proline (Ruggiero *et al.* 2009), like ActA.

The cloning of gene fragments coding the truncated forms $actA_{A30-S157}$, $actA_{A30-N233}$ and $actA_{G393-N639}$ was successfully carried out by the PROTEX service. However, attempts to clone the $actA_{E235-N639}$ gene fragment (coding the central domain of ActA) failed. Although the exact reason for this is unclear, it has been suggested that the presence of sequences coding for the proline-rich repeat (PPPP) in this domain contributed to the failure. It is also possible that this particular version of the protein was toxic for *E. coli.* Perhaps an application of an alternative vector or expression host could have been used to solve this technical challenge; this is something that can be considered for future work.

This project focused on optimizing the expression of $ActA_{A30-S157}$, $ActA_{A30-N233}$ and $ActA_{G393-N639}$. The optimal concentration of IPTG was found to be 0.5 mM, and proteins were successfully expressed at 37ºC with a good yield (~0.2 mg/ml). Many scholars have proposed that the induction of recombinant protein expression with lower concentrations of IPTG and at lower temperatures (~18°C) may prevent the formation of inclusion bodies and aid the production of a soluble form of the protein (Gräslund *et al.* 2008; Rosano and Ceccarelli 2014). However, for the proteins described in this chapter, the formation of inclusion bodies at 37ºC was not observed; it was therefore not necessary to use a lower temperature.

The purification of $ActA_{A30-S157}$, $ActA_{A30-N233}$ and $ActA_{G393-N639}$ was carried out in two stages; affinity chromatography and gel filtration. As shown in Figures 15, 16 and 17, all proteins were successfully purified in a soluble form and produced single bands at the predicted sizes of 24kDa, 35kDa and 27kDa, respectively. Similarly, all ActA protein variants (generated via SDM) were purified successfully, as shown in the SDS-PAGE data (section 3.2.3); none of the mutations affected protein expression, solubility or stability. All SDM generated proteins behaved like the wild type ($ActA_{A30-S157}$) and produced bands of the same size on the SDS-PAGE gels. Thus, the purification results for all the truncated and SDM proteins prove that the generation of truncated proteins was an ideal strategy to use for the current study. The present findings are consistent with other research (Baneyx and Mujacic 2004), which found that the short domain proteins (<100 residues) are easier to express and purify due to their fast-folding kinetics in comparison with multi-domain proteins. For instance, Rigi *et al.* found that the truncated form of recombinant *Staphylococcal* protein A (SpA), a major surface protein from *Staphylococcus aureus,* was expressed at higher levels and retained IgG-binding activity when produced in *E.coli* BL21 (DE3), while the full length protein was challenging to express and purify (Rigi *et al.* 2015). Ching *et al.* reported that the truncated recombinant protein r56 from *Orientia tsutsugamushi* was more stable and easily purified in large amounts, as opposed to the full length version (Ching *et al.* 1998). However, truncated recombinant proteins might show an adverse effect in terms of purification when compared with the full length versions (Jennings *et al.* 2016), as deleting small domains of some proteins might affect the folding or the solubility of the desired protein (Dyson 2010). Although the ActA protein has been known for many years, its structure has not yet been solved. Only the structure of a small fragment of this protein in complex with WASP (Wiskott-Aldrich syndrome protein) has been solved. Unfortunately, all attempts to crystallise $ActA_{A30-S157}$ and $ActA_{A30-N233}$ have failed, as shown in section 3.2.4. In the future, ActA proteins could be crystallised using a natural ligand or

substrate e.g. actin (Niebuhr *et al.* 1997) or peptidoglycan fragments. However, it was not possible to test this due to time limitations.In the following chapter, all the purified proteins will be utilised for the assessment of PG- cleaving activity by zymography and the cleavage of FITC labelled PG.

Chapter 4

Investigation of the peptidoglycan-cleaving activity of recombinant ActA proteins

4.1 Introduction

PG biosynthesis, degradation and remodelling are essential parts of the bacterial life cycle. All bacteria, including *L. monocytogenes*, have a significant number of surface proteins covalently bound to PG, and these proteins play a crucial role in cell growth, cell metabolism, peptidoglycan synthesis and degradation, and virulence. Some of these proteins possess PG cleaving activity which is essential for various processes such as the formation of flagella, protein secretion, PG recycling and actin polymerisation (Popowska 2004). One protein which possesses the ability to cleave PG is the ActA protein.

As stated in Chapter 1, ActA is a crucial virulence factor because it is indispensable for the actin-mediated mobility of *L. monocytogenes*. It has also been shown to control peptidoglycan biosynthesis during macrophage infection (Siegrist *et al.* 2015). The molecular mechanism of this regulation is currently unknown; however ActA has previously been shown to possess PG cleaving activity as assessed by zymography and in the degradation of an artificial lysozyme substrate (Iakobachvili 2014). In the previous study preceding this work, a non-secreted recombinant version of ActA ($ActA_{A30-N639}$) was generated (Iakobachvili 2014). However, it was not clear which particular domain of ActA was responsible for the PG cleaving activity.

Thus, within the current project, several truncated forms of ActA were produced and their activity assed by zymography and it was investigated whether or not these proteins can cleave of FITC-labelled PG. Additionally, with the use of SDM, variants of the N-terminal domain of ActA were generated and used for PG cleavage assays. This chapter will focus on the identify-cation of the domain which possesses PG cleaving activity and the characterization of this activity. In section 4.2.4, the activity of the SDM generated variants will be described, along with the identification of potential catalytic residues.

4.2 Results

4.2.1 Zymography for the truncated ActA proteins

Several truncated forms of ActA were generated and purified as described in Chapter 3. Initially, the PG cleaving activity of purified $ActA_{A30-S157}$, $ActA_{A30-N233}$ and $ActA_{G393-N639}$ was tested by using zymography assays, as described in Chapter 2 (section 2.10.1).

Figure 21 shows results from SDS-PAGE and zymography analyses for the aforementioned truncated forms of ActA, which were carried out in order to detect any enzymatic or cleaving activity. The purified $ActA_{A30-S157}$ (~2 µg/ml) produced a single band at the predicted size of ~24 kDa on an SDS-PAGE gel (Figure 21A) and clearance band at the same size (24kDa) was present in a zymogram (Figure 21B). Suggesting that $ActA_{A30-S157}$ has the ability to cleave the cell wall of *M. luteus*, which was supplemented within the zymogram gel. Moreover, no clearance was detected in the lane containing an elution fraction from the *E. coli* cells transformed with the empty vector control (Figure 21B). The lysate from *E. coli* transformed with an empty vector was subject to the same purification steps and used as a negative control in the zymogram gel, in order to validate any findings and confirm that no false positive results (random or non-specific activity) were present.

Similarly, purified $ActA_{A30-N233}$ (~2 µg/ml) was assessed using SDS-PAGE (Figure 21C) and zymography (Figure 21D). The protein was pure, and produced a single band which was 35 kDa in size, according to SDS-PAGE (Figure 21C), along with a zone of clearance band in the zymogram gel (Figure 21D). The empty vector negative control (Figure 21D) did not produce any clearance on the zymogram gel. The optimum renaturation buffer used for the zymography assay for both proteins contained 20 mM potassium phosphate (KH_2PO_4) at a pH of 6.5. Different buffers ranging in pH (pH 5, 6, 7, 7.5 and 8) were used for the renaturation of proteins, however the clearance bands were either very faint or completely disappeared, indicating that these buffers did not support renaturation or activity of these proteins (data not shown). Figure 21E shows purified $ActA_{G393-N639}$ (~2 µg/ml) at the predicted size of ~27 kDa on an SDS-PAGE gel, however, this protein corresponds to the C-terminal domain of the ActA protein, and did not produce any clearance on the zymogram gel (Figure 21F). As in previous experiments, the negative control fraction (Figure 21E) from *E. coli* that had the empty vector did not cleave the *M. luteus* cell wall.
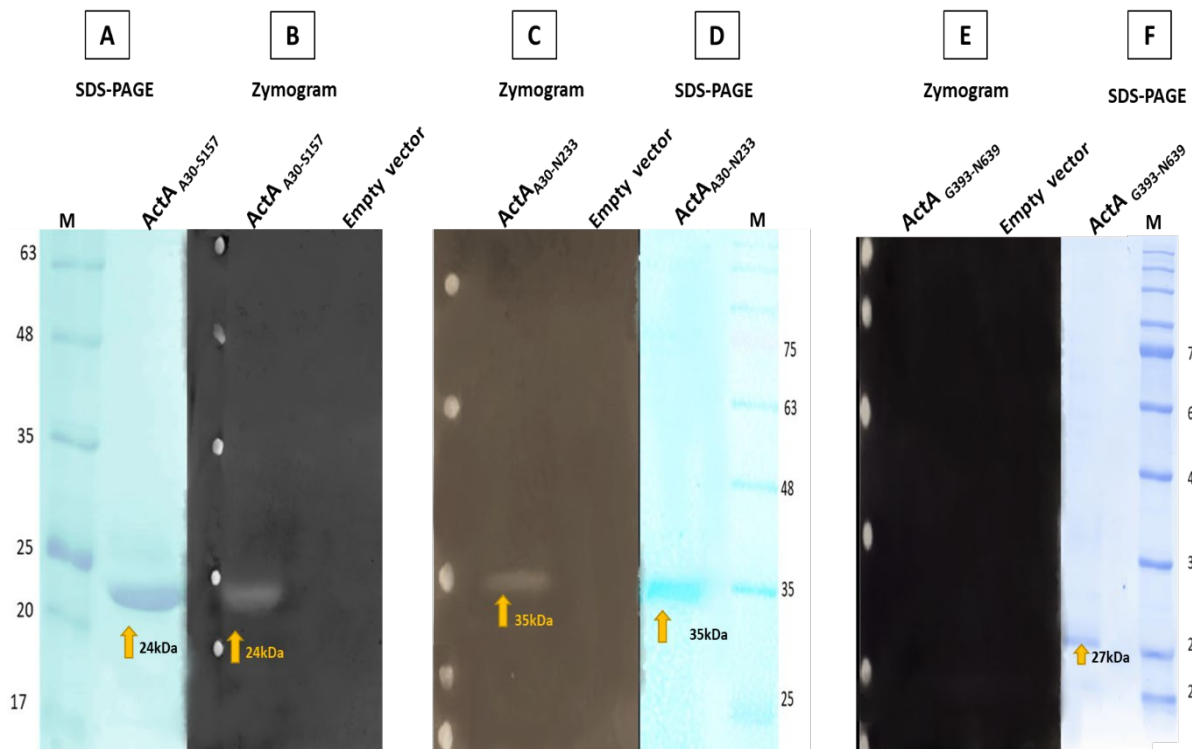
Figure 21. Assessing the PG cleaving activity of purified ActA$_{A30-S157}$, ActA$_{A30-N233}$ and ActA$_{G393-N639}$ via zymography.

(A) Purified ActA$_{A30-S157}$ protein ran on a 12 % SDS-PAGE gel migrating to the expected size of 24 kDa. (B) Zymogram gel for purified ActA$_{A30-S157}$, a clearance band corresponding to the ActA$_{A30-S157}$ band on the SDS-PAGE is present**.** No band detected in the negative control in the zymogram (extract from *E. coli* cells transformed with an empty vector). (C) Zymogram gel for the purified ActA$_{A30-N233}$ protein, which produced a clear band at the right size of 35 kDa, along with the lack of a band in the negative control (empty vector). (D) SDS-PAGE gel for the ActA$_{A30-N233}$ protein (35 kDa). (E) Zymogram gel; the first lane represents the purified ActA$_{G393-N639}$ protein, with no clear band at the expected size. The second lane represents the empty vector control fraction. (F) SDS-PAGE gel of purified ActA$_{G393-N639}$ which migrated at the expected size of 27 kDa. The result above indicates that both the NH2- terminal proteins were enzymatically active, while no band was detected with the C-terminal protein. The aforementioned assays were repeated five times (biological replicates).

Consequently, further zymography experiments using purified ActA$_{G393-N639}$ were performed to confirm that this version of ActA had no PG cleaving activity (Figure 22). For instance, the experiment was repeated with the use of purified ActA$_{A30-S157}$ as a positive control, as illustrated in Figure 22A. SDS-PAGE analysis of this experiment (Figure 22B) revealed that both proteins were pure and migrated as single bands to the predicted size.

In addition, both protein preparations were found to have the same protein concentration (~2 µg/ml). The zymography assay for these samples revealed a visible band of clearance for ActA$_{A30-S157}$ (Figure 22A), corresponding to the ActA$_{A30-S157}$ band on the SDS-PAGE gel (Figure 22B). However, no clearance was detected with ActA$_{G393-N639}$ protein (Figure 22A). Furthermore, different renaturation buffers were tested, including 40 mM KH$_2$PO$_4$ (pH 6.5), 20 mM KH$_2$PO$_4$ (pH 7) and 20mM Tris (pH 6.5), as shown in Figures 22C, 22D and 22E. However, no clearance bands were detected with ActA$_{G393-N639}$ in the zymography assays with any of the conditions used, indicating that this protein does not have the ability to cleave PG. Lysozyme (~0.5 µg/ml) was used as a positive control in all of the optimisation experiments, but due to its high level of activity and the risk of cross-contamination, it was loaded and ran on a separate gel (Figure 22F). As expected, lysozyme produced a strong clearance band in the zymography assays at the expected size of 14.4 kDa, in all of the conditions tested.
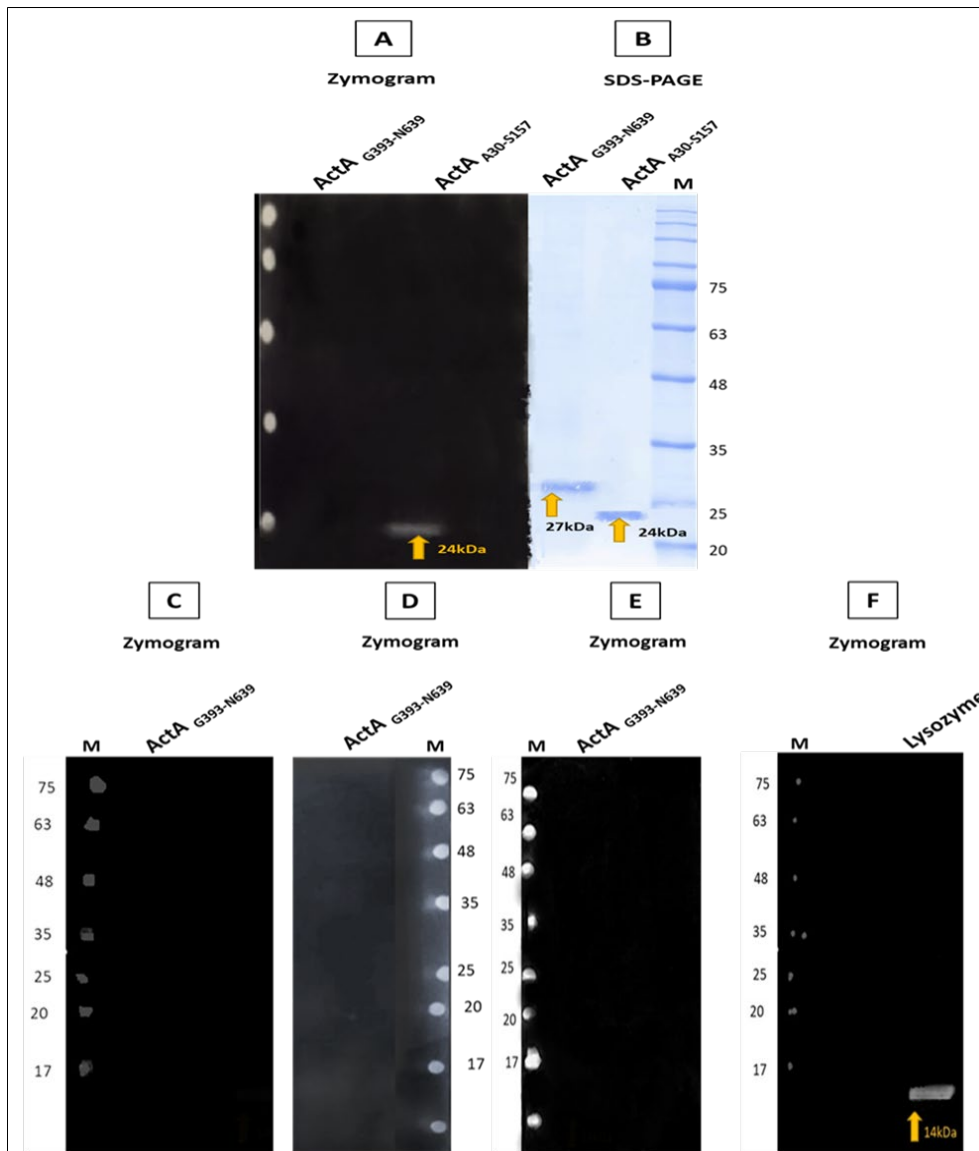
Figure 22. Testing various conditions to detect whether ActA$_{G393-N639}$ is able to cleave PG using zymography.

(A)ActA$_{G393-N639}$ protein with no band of clearance, and ActA$_{A30-S157}$ protein with apparent clearance activity in the zymogram gel .(B) Represents both ActA$_{G393-N639}$ and ActA$_{A30-S157}$ on a 12 % SDS-PAGE stained with Coomassie blue. Zymograms were performed with purified ActA$_{G393-N639}$ using different renaturation buffers; 20 mM KH$_2$PO$_4$ (pH 7) was used in (C), 20 mM KH$_2$PO$_4$ (pH 7) was used in (D), and finally, 20mM Tris (pH 6.5) was used in (E). In the three assays using the different renaturation buffers, no clearance band in the zymogram was detected for ActA$_{G393-N639}$. (F) Zymography assay performed with lysozyme (~0.5μg/ml) which was used as positive control; the expected zone of clearance is visible. This result shows that ActA$_{G393-N639}$ has no cleaving activity. These assays were repeated with five biological replicates.

4.2.2 Cleavage of *E. coli* PG labelled with FITC

To further evaluate the activity of the truncated versions of ActA, an alternative experiment was performed by using the PG of *E. coli* labelled with FITC (as described in Chapter 2, section 2.10.2). PG was purified and tested using the Hayashi test (Chapter 2, section 2.10.2.2) to confirm that PG preparations were not contaminated with SDS, which could interfere with PG cleavage and FITC labelling. Figure 22 represents the results of the Hayashi test performed on purified *E. coli* PG prepared in the lab. Various controls were also included: MilliQ H_2O as a negative control, and solutions with different concentrations of SDS; 1 % (w/v), 0.1 % (w/v), 0.01 % (w/v) and 0.001 % (w/v) were used to compare with the prepared *E. coli* PG samples. The results shown in Figure 23 confirmed that extracted PG sample (tube labelled 'sample') was free from SDS as it had a colorless bottom layer, indicating that the PG sample was ready and suitable to be labelled with FITC.
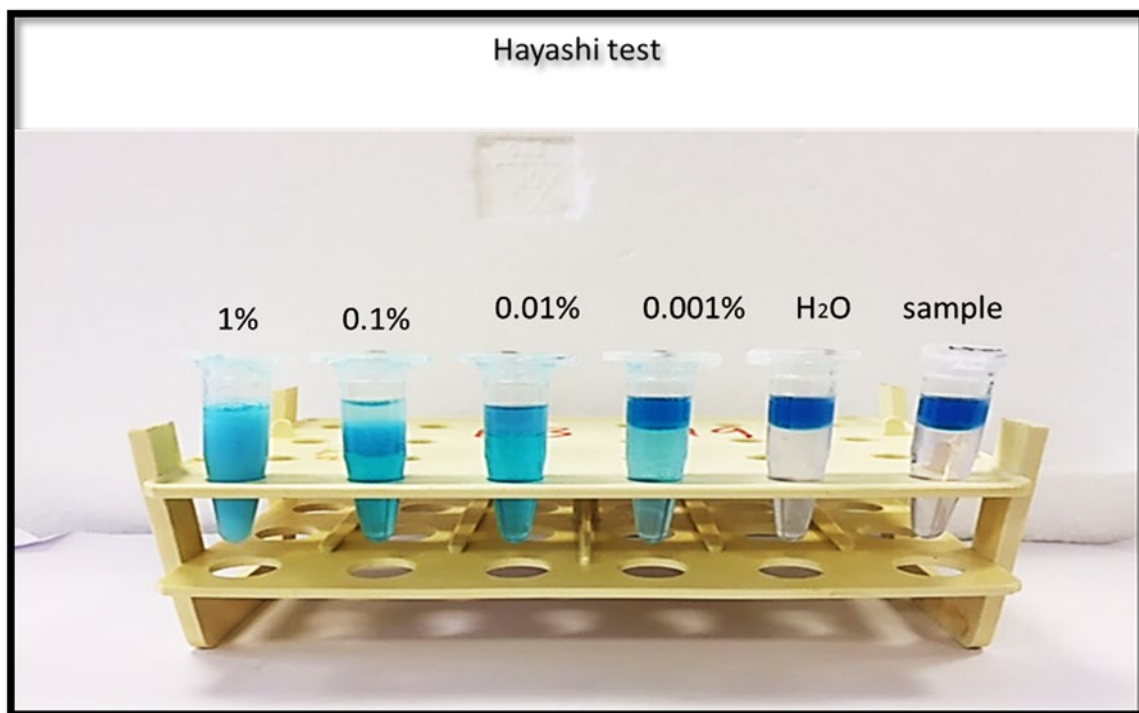
Figure 23. Hayashi test to ensure the complete removal of SDS from the extracted *E. coli* PG.
Different concentrations of SDS were prepared (1 %, 0.1 %, 0.01 %, 0.001 % w/v) to be used as positive controls. MilliQ H_2O was used as a negative control to indicate the complete absence of SDS. The clear/pink bottom layer in the sample indicates the complete removal of SDS, and the blue colour of the bottom layer indicated the presence of SDS in the preparation.

Following this, the *E. coli* PG was labelled with FITC and was used to assess the PG cleaving activity of freshly purified ActA$_{A30-S157}$, ActA$_{A30-N233}$ and ActA$_{G393-N639}$. In addition, purified empty vector elution fractions and lysozyme were used as negative and positive controls. All samples were filter-sterilised before use to prevent any bacterial contamination that may result in false positive results. All the data obtained were normalized to 1 mg of protein used in the assays. Figure 24 illustrates the fluorescence measurements (excitation/emission spectra of 495/521nm) of FITC-PG incubated with ActA$_{A30-S157}$ (2µg/ml), ActA$_{A30-N233}$ (2µg/ml), ActA$_{G393-N639}$ (2 µg/ml), boiled ActA$_{A30-S157}$ (2 µg/ml), boiled ActA$_{A30-N233}$ (2 µg/ml), lysozyme (2 µg/ml) and the empty vector elution fraction after normalization to 1 mg of protein. PG is insoluble, however, if digested in this case, it would result in the release of soluble fluorescent muropeptides. A higher fluorescence signal corresponds to an increased amount of PG cleaving activity.

As shown in Figure 24, the lysozyme sample showed the highest fluorescence reading (50,445 RFU/mg) when compared to the other samples. This is because lysozyme is active hydrolytic enzyme, indicating that this assay is suitable to measure PG cleaving activity. Both ActA$_{A30-S157}$ and ActA$_{A30-N233}$ also released soluble fluorescent PG fragments corresponding to 42,018 RFU/mg and 35,071 RFU/mg, respectively. This suggests that both proteins are actively able to cleave PG, and the observed activity was well above that which was present in the *E. coli* harbouring the empty expression vector. Importantly, the PG cleaving activity of ActA$_{A30-S157}$ and ActA$_{A30-N233}$ was completely abolished by boiling. Moreover, the activities of these proteins were similar and showed no statistically significant difference ($p > 0.05$, unpaired t-test). In contrast, a FITC-PG sample treated with ActA$_{G393-N639}$ protein had very low fluorescence (2,676 RFU/mg), which was comparable with fluorescence levels detected in the boiled samples and negative control (Figure 24). However, it was significantly different from the fluorescence detected the ActA$_{A30-S157}$ and ActA$_{G393-N639}$ treated samples ($p<0.0001$, unpaired t-test). All experiments were repeated with three biological and technical replicates and Figure 24 shows the mean values from these experiments.
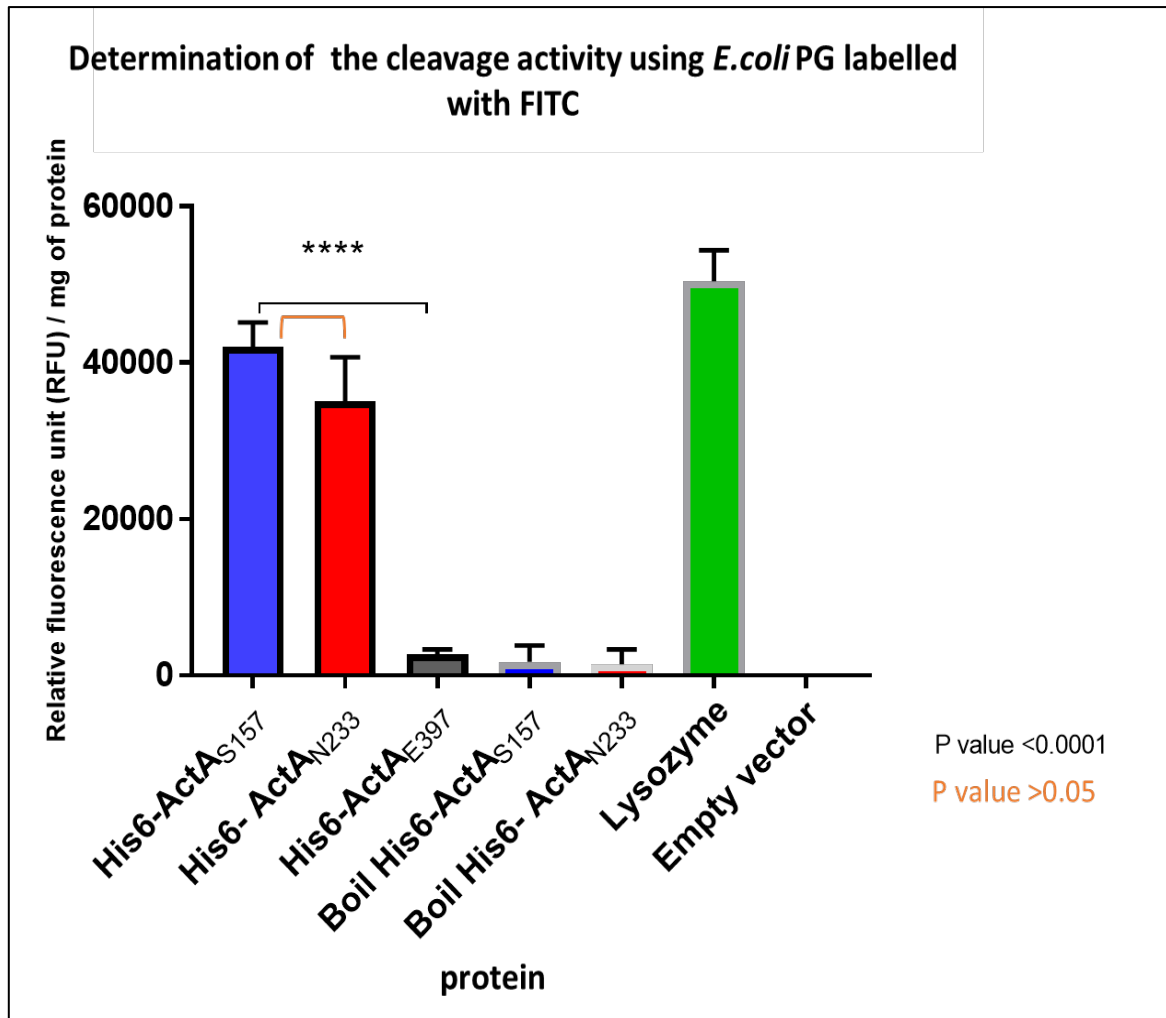
Figure 24. Assessing the ability of truncated versions of ActA to cleave FITC labelled PG.

PG obtained from *E. coli* labelled with FITC (2 µl) was incubated with truncated versions of the ActA protein (2 µg/ml) overnight at 32°C. The amount of solubilized muropeptide was estimated by assessing fluorescence at 495/521 nm. $ActA_{A30-S157}$, $ActA_{A30-N233}$, $ActA_{G393-N639}$ and lysozyme were used at a concentration of 2 µg/ml. Boiled $ActA_{A30-S157}$ and $ActA_{A30-N233}$ were used to detect whether boiling inhibits cleavage activity. Lysozyme was used as a positive control, whereas fractions from *E. coli* cells containing an empty vector were used as a negative control. The error bars represent the standard deviation of the mean. All samples were assayed via three independent experiments and with triplicate samples, the columns shows the mean values from these replicates. (****$p < 0.0001$).

4.2.3 Attempts to analyse the muropeptides released by ActA$_{A30-S157}$ using HPLC

Purified *E. coli* PG was treated in the lab with the following samples for muropeptides analysis; purified ActA$_{A30-S157}$ protein, elution fractions prepared from the empty vector *E. coli* C41 (DE3) or boiled ActA$_{A30-S157}$. The treated PG was loaded on to a ProntoSIL C18 AQ column (Bischoff Chromatography). The analysis of the peaks obtained were not consistent (data not shown), and it was not possible to prove whether these peaks were muropeptides and not any contaminating peptides. In addition, a sufficient positive control, e.g. mutanolysin, was not used when the experiment was performed. Therefore, the purified ActA$_{A30-S157}$ protein was sent to Newcastle University for further analysis.

Dr. Jad Sassine at Newcastle University performed HPLC analysis using a Prontosil 120 C18 column; the results obtained are shown in Figure 25. In these experiments, purified PG from *L. monocytogenes* was digested with cellosyl (a muramidase enzyme from *Streptomyces coelicolor*) which hydrolyses the glycosidic bond in PG (Figure 25A). Panels B and C show the peaks obtained for the *L. monocytogenes* PG digested with ActA$_{A30-S157}$ at pH 7.5 and pH 5.0, respectively. Untreated PG was used as a negative control; this sample was not found to have significant amounts of soluble muropeptides (Figure 25D). The cellosyl sample released several muropeptides, as shown in Figure 25B. No peaks relating to muropeptides were detected in the ActA$_{A30-S157}$ treated sample with two different buffers (Figure 25B and Figure 25C), indicating that no muropeptides were detected with the ActA$_{A30-S157}$ protein.
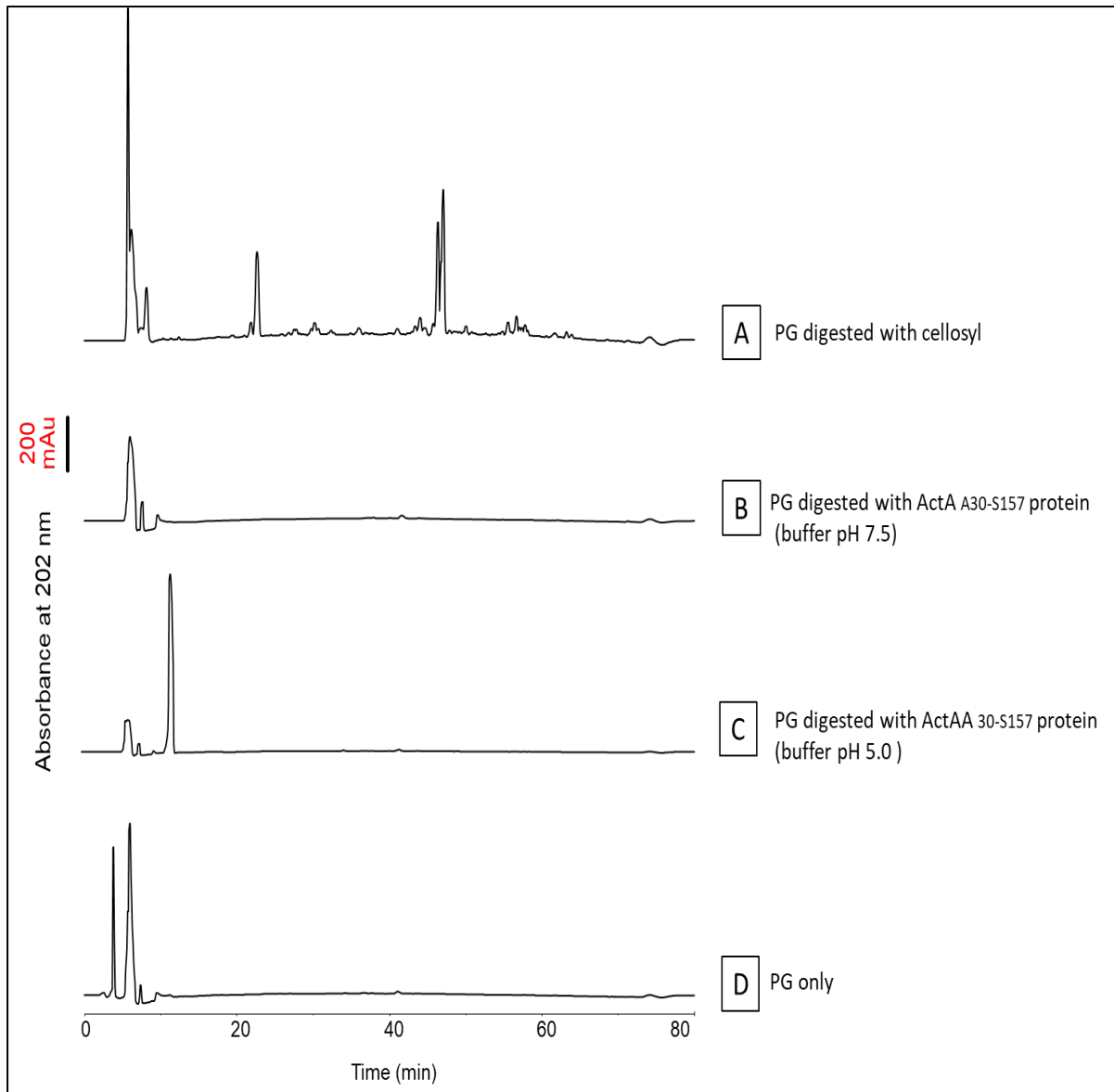
Figure 25. Separation of *L. monocytogenes* muropeptides via reverse-phase liquid chromatography'using a Prontosil 120 C18 column.
(A) *L. monocytogenes* PG digested with Cellosyl, resulting in the production of several muropeptides; this used as a positive control for comparison with the ActA$_{A30-S157}$ protein. (B) Represents PG digested with ActA$_{A30-S157}$; no peak was detected when a buffer made up of 20 mM Tris/HCl (pH 7.5) was used. (C) PG digested with ActA$_{A30-S157;}$ no peaks were detected when 20 Mm Na acetate (pH 5.0) was used as a buffer. (D) Undigested *L. monocytogenes* PG. To avoid having four Y axes for each of the 4 HPLC chromatograms, the scale bar (200 mAu with the black bar below) is the equivalent of the Y axis. The experiments were done by Dr. Jad Sassine at Newcastle University.

90

4.2.4 The activity of proteins generated using SDM

4.2.4.1 The prediction strategies used to produce SDM constructs

Initially, the prediction strategy to identify the residues to be mutated via SDM was based on bioinformatic data obtained from a previous study (Iakobachvili 2014). Glutamate 98 (E98) in the ActA N-terminal domain was predicted to be a putative catalytic residue.

The second method for the prediction of the catalytic residues created in this study was based on the study by Lauer *et al.* in which scanning mutagenesis of different domains in ActA was performed (Lauer *et al.* 2001). ActA protein variants (SDM) were used for the complementation of an *actA* deletion mutant in order to study the effect of mutations on bacterial shape, actin polymerisation and actin-mediated intracellular motility. Separately, the stability of the mutated proteins was tested. However, the cleaving activity was not investigated in this study.

Interestingly, Lauer *et al.* found that several regions in the NH2-terminal domain produced unusual motility phenotypes associated with amino acid changes, e,g slow or no movement rate in the cells, discontinuous actin tails. One of these regions which produced novel functions in actin-based motility was the stretch of multiple glutamate residues, starting from position E42 to E50 (Lauer *et al.* 2001) as shown in Figure 26. For instance, mutating this region affected the protein by a reduction in stability and in changes to the motility rate *in vivo*, with a slow movement rate noticed. In addition, a mutation within this region had a negative impact on the cell-to-cell spread of *L. monocytogenes* and lead to a decreased amount of binding to the actin monomer, all of which are very important factors in the pathogenesis of *L. monocytogenes*.

Moreover, as previously described, the main hypothesis of this project is that ActA may be able to hyrdolyse PG (Iakobachvili 2014). Furthermore, due to the similarity of ActA with RpfA (Iakobachvili 2014), it has been predicted that ActA could be a lytic transglycosylase protein, as glutamate is essential for the cleaving activity of lytic transglycosylases (Smith *et al.* 1996; Baneyx and Mujacic 2004). Therefore, based on the findings of Lauer *et al.* (2001) and Iakobachvili (2014), eight-point mutations to different glutamic acid (E) residues (Figure 26) in the stretch of multiple glutamates which showed a motility phenotype (Lauer *et al.* 2001).

In the current study, mutations made on plasmid pLEICS-01::*actA* $A_{30-S157a.a}$ encoding for ActA$_{A30-S157}$ using the GeneArt® Site-Directed Mutagenesis System (Invitrogen™) as described in Chapter 2 (section 2.5.12). The following selected glutamate residues were located

in the region i.e. stretch of multiple glutamate in NH2-nterminus domain, which showed a motility phenotype: E42 E44, E45, E46, E44, E45, E46, E49, E49 and E50 (Figure 26).
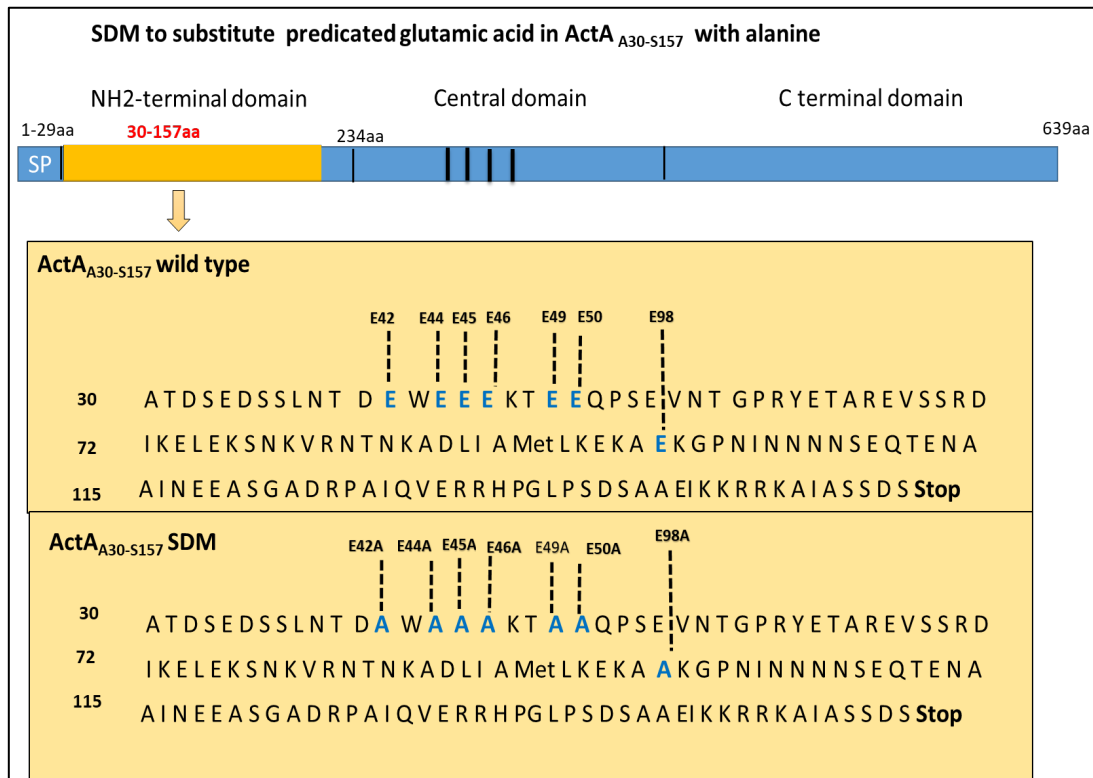
Figure 26. SDM to substitute the predicated gluatamic acid residues in ActA$_{A30-S157}$ protein.
The glutamic acid (E) residues in ActA$_{A30-S157}$ (highlighted in blue) were mutated to alanine to generate various ActA variants.

Finally, several constructs designated as ActA_MUT1, ActA_MUT2, ActA_MUT3, ActA_ MUT4, ActA_MUT5 and ActA_MUT6 were generated by Thermo Fisher (Figure 27). In these variants, scanning mutations for particular glutamatic and aspartate residues were performed by replacing them with alanine, following the strategy proposed by *Lauer et al.* (Lauer *et al.* 2001).
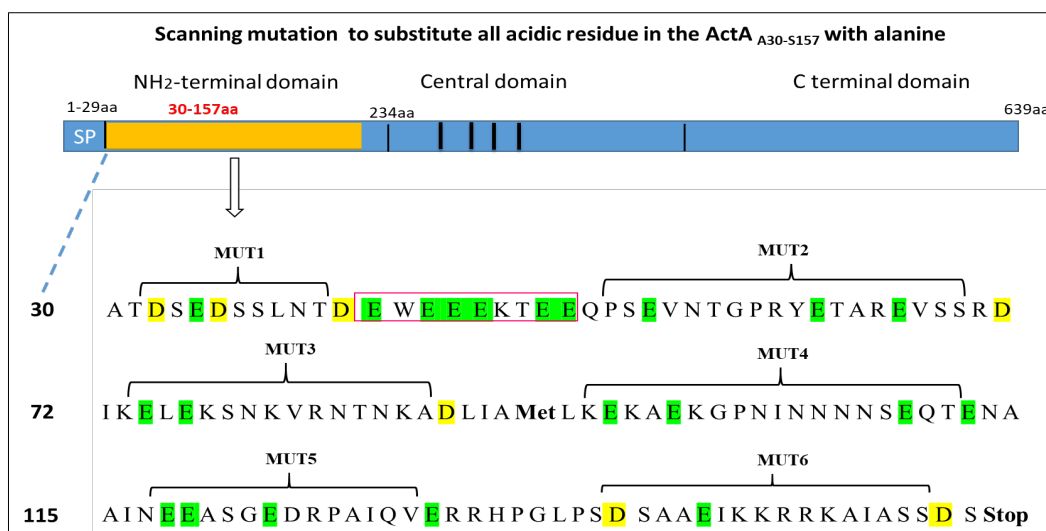
Figure 27. Scanning mutation approach to substitute all acidic residues in ActA_{A30-S157} protein.

All highlighted acidic residues (aspartate [D] & glutamic acid [E]) were mutated to alanine. The six protein variants were generated as follows: MUT1 (ActA_MUT1), MUT2 (ActA_MUT2), MUT3 (ActA_MUT3), MUT4 (ActA_MUT4), MUT5 (ActA_MUT5) and MUT6 (ActA_ MUT6). The red box indicates the region which was previously scanned in Figure 26.

4.2.4.2 Assessing the activities of the mutated protein variants generated via SDM

The activity of the purified SDM generated proteins (mentioned in Chapter 3, section 3.2.3) was assessed by zymography and by the ability to cleave FITC labelled PG in the same manner with the wild type ActA_{A30-S157} protein (Chapter 2, sections 2.10.1 and 2.10.2). Figure 28 shows the results of the SDS-PAGE and zymography assays for all the generated mutants. Moreover, Western blot assays with anti-His antibodies were performed for all ActA protein variants (these results are shown in the Appendix 8.9). The purpose of performing SDS-PAGE was to ensure that the mutated amino acid residues did not have a deleterious effect on protein expression, solubility and stability. Both the SDS-PAGE gel (Figure 28) and Western blot (Appendix 8.9) analysis revealed that all the proteins were purified successfully with a good yield, and the blot confirmed the presence of the protein of interest. As shown in Figure 28, all proteins produced a single band at the expected size of ~24 kDa.

Although all proteins were used at the same concentration of ~2 µg/ml, the intensity of the bands were different. In some point mutations e, g E44A, E46A and E44AE45AE46A (Figure 28C), the intensity of the bands were low. Whereas in E98A (Figure 28A), E42A (Figure 28B),

E49A (Figure 28B), and E49A and E50A (Figure 28D), the band intensity was higher. This difference may be related to protein stability, as Lauer *et al.* noticed that scanning mutations in the region with the stretch of glutamate residues reduced protein stability (Lauer *et al.* 2001). In the zymography assay, all the proteins generated via SDM had comparable activity to the wild type protein (Figure 28) and produced a single band at the same position (~24 kDa). However, it is difficult to deduce information about the intensity of the band because the zymography assay only provides a qualitative measurement of cleavage activity.
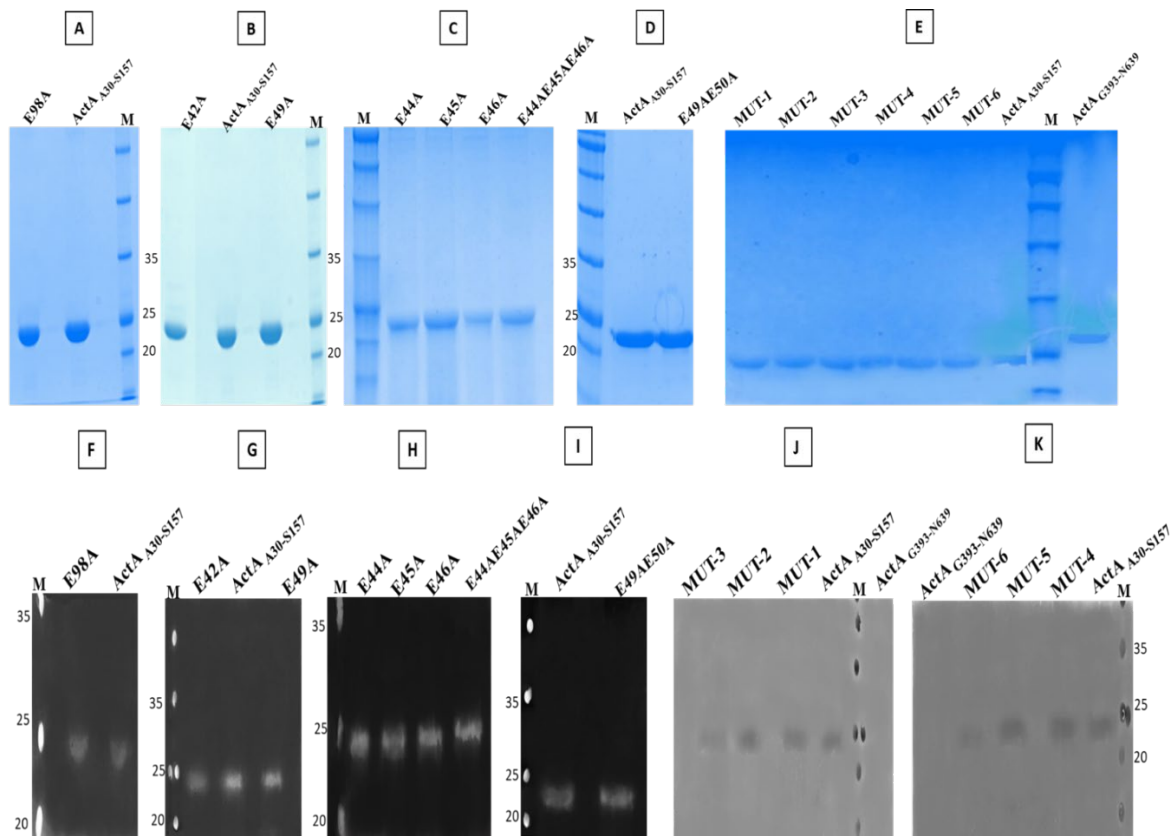
Figure 28. Purification and assessment of the activity of all the ActA protein variants via zymography assays.
All purified proteins were ran on a 12 % SDS-PAGE and zymogram gel. **(A)** SDS-PAGE purified E98A and ActA$_{A30-S157}$ protein. **(B)** E42A, E49A and ActA$_{A30-S157}$ proteins. **(C)** E44A, E45A, E46A and E44AE45AE46A **(D)** E49AE50A and ActA$_{A30-S157}$. **(E)** Shows the proteins generated via Thermo-fisher: ActA$_{A30-S157}$, MUT1, MUT2 , MUT3, MUT4, MUT5, MUT6 and ActA$_{G393-N639}$ which was used as a negative control. All SDM generated proteins migrated similarly to the ActA$_{A30-S157}$ protein to 24 kDa in the SDS-PAGE gel. (F), (G), (H), (I), (J), and (K) are images of the zymograms for the mentioned proteins. [M] represents the colour Prestained Protein Standard (Geneflow, UK) marker used. This experiment was repeated with three biological replicates.

94

Following the PG-cleaving activity, the cleavage of FITC labelled PG was assessed for all the SDM mutated proteins (Figure 29). The substitution of the presumptive catalytic residues did not completely abolish the enzymatic activity, as shown in Figure 29. The percentage activity was calculated from the normalized fluorescence obtained from each mutant, relative to the activity observed with the wild type protein (ActA$_{A30-S157}$). However, four mutants showed reduced cleavage activity in comparison to the wild type protein.

There was an 80 % reduction for E42A, 83 % reduction for E49A, 81 % reduction for MUT3 and a 73 % reduction in activity for MUT6. Previously, E42A and E49A were shown to be unstable *in vitro* by Lauer *et al.* (Lauer *et al.* 2001) and this provides an explanation for their low cleaving activity. In contrast, MUT3 and MUT6 proteins were previously found to be stable (Lauer *et al.* 2001), and in this study, sufficient protein was obtained from each mutant. Moreover, both mutants (MUT3 and MUT6) showed very faint clearance bands in the zymography assays (Figure 29J and Figure 29H), thus, probably both might be involved in the enzymatic activity. On other hand, a higher amount of activity was noticed with the other mutants i.e E44A, E45A, E44AE45AE46A, E49AE50A, E98A and MUT5, this is possibly due to these proteins being more stable.
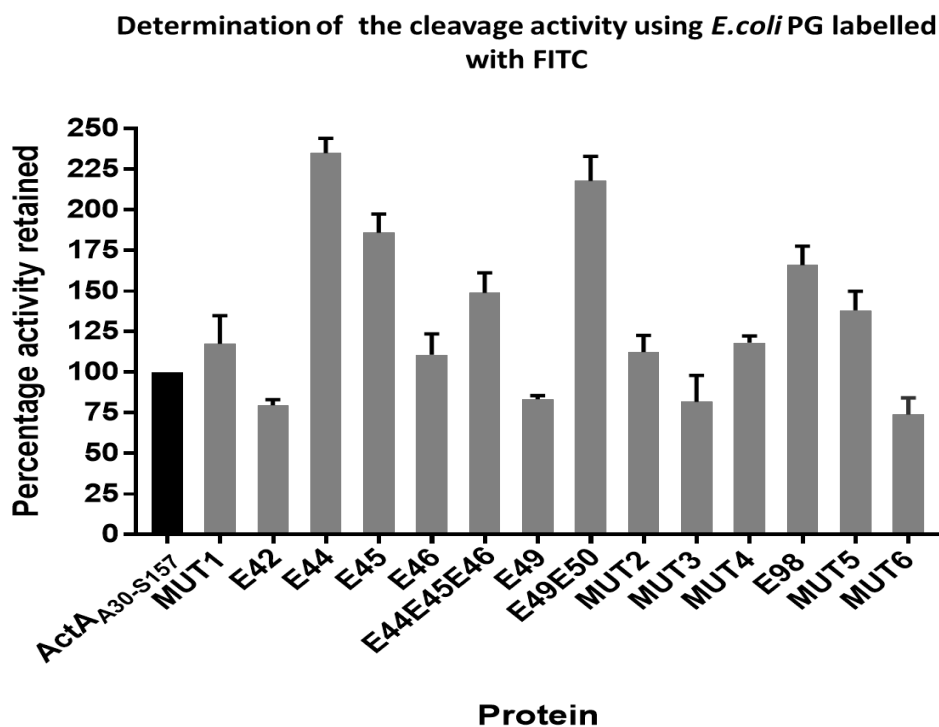
Figure 29. Assessing the cleaving activity of all the ActA protein variants in being able to cleave FITC labelled PG.
The black column shows the percentage activity of the wild type $ActA_{A30-S157}$ as 100 %. The grey columns represent the percentage activity of the following ActA protein variants; E42A (80%), E44A (243%), E45A (185%), E46A (110 %), E44AE45AE46A (148 %), E94A (83 %), E94AE50A (217 %), MUT1 (117 %), MUT2 (112 %), MUT3 (81 %), MUT4 (118 %), MUT5 (138 %) and MUT6, with the lowest activity of 73%. The percentage activity was calculated using the normalized fluorescence obtained from each mutant relative to the wild type $ActA_{A30-S157}$. The findings show that none of the mutations completely abolished activity. All the proteins were assayed in triplicate and the average value of three independent experiments with different protein preparations are shown. The error bar represents the standard deviation of the mean.

4.3   Discussion

The results of this chapter have addressed the hypothesis that the ActA protein from *L. monocytogenes* has PG cleaving activity and that this activity may be related to specific domains. The investigation of NH2-terminally truncated versions of ActA revealed that both $ActA_{A30-S157}$ and $ActA_{A30-N233}$ were able to cleave PG; this activity was confirmed via two

independent methods. The N-terminal variants of ActA were able to digest the *M. luteus* cell wall in zymography assays and cleave *E. coli* PG in FITC digestion experiment. In contrast, the zymogram analysis of ActA$_{G393-N639}$ demonstrated clearly that the C-terminal of ActA is inactive after laborious optimisation steps. Moreover, ActA$_{G393-N639}$ did not showed an obvious activity in FITC experiment. This finding was not surprising, as a number of functions have previously been attributed to the N-terminal domain in the ActA protein. Suggesting the importance of this domain in actin tail formation, which is essential for the pathogenesis of *L. mono*cytogenes (Lasa *et al.* 1997), motility rate of intracellular bacteria (Lauer *et al.* 2001) and for the stability of ActA in mammalian cells (Moors *et al.* 1999).

The attempts made to analyse muropeptides which were released after the cleaving activity of ActA were unsuccessful. The use of HPLC to understand the mechanisms by which peptidoglycan cleaving enzymes work would be informative. This technique would help us to understand the function of such proteins and give an insight as to how they work. Despite the doubt relating to the true nature of the peaks demonstrated in the initial HPLC experiment performed for ActA$_{A30-S157}$ with the *E. coli* PG, further optimisation would need to be performed in order to obtain further datasets. This optimization could be in the form of using different buffers, columns and protocols. In addition, an explanation for the findings obtained from the HPLC assay performed at Newcastle University are could be that the released muropeptide products were too large, and therefore did not bind well to the column and could not be detected. Previously, the inability of numerous PG hydrolases to release soluble muropeptides has been reported with different bacterial species (Jorgenson *et al.* 2014; Schaub *et al.* 2016). Moreover, several proteins which were identified as having peptidoglycan cleaving activity did not show the presence of soluble muropeptides, which could be detected via HPLC, e.g. LtgG (lytic transglycosylase G) from *B. pseudomallei* (Jenkins et al. 2019). The Cwp19 protein (Cell wall protein) from C. *difficile* and RlpA protein (lipoprotein A) from *Pseudomonas aeruginosa* (*P. aeruginosa*), all were LTGs and they failed to generate detected soluble fragment in the HPLC (Jorgenson *et al.* 2014; Wydau-Dematteis *et al.* 2018; Jenkins *et al.* 2019). Testing the activity of the NH2-terminal ActA using PG from *L. monocytogenes* would be an area of research for the future. However, the procedure for isolating PG from *Listeria* spp. is challenging and would need the aid of a specialist, as the procedure requires an incubation with step 48% hydrofluoric acid, which is a safety concern for many laboratory settings.

The mutation of the wild type amino acid residue may provide an insight into the role of said residue in a different aspect, such as protein structure (Bordo and Argos 1991), protein function, e.g., active sites or binding sites and protein stability (Bordo and Argos 1991; Betts and Russell 2003). In this chapter, the replacement of different amino acid residues with alanine did not abolish the cleaving activity of the proteins tested, and all the SDM generated proteins showed distinctive activity in two different assays. The zymography assay is a simple to perform yet valuable technique which is commonly used to measure the activity of various cleaving enzymes (Ren *et al.* 2017). However, the intensity of the band of interest cannot be calculated. All the ActA protein variants produced a clear band virtually indistinguishable in size from the activity seen with the wild type protein via the zymography assays. This finding indicates that all the mutated residues are not essential for PG-cleaving activity.

It should be noted that cleaving activity was by no means completely abolished in the FITC labelled PG assay for all the variant proteins, and the substitution of presumptive residues did not completely abolish activity. Interestingly, slightly impaired cleaving activity was noticed with four mutants; E42A, E49A, MUT3 and MUT6, in comparison with the wild type protein. E42A and E49A were excluded from being responsible for PG-cleaving activity due to instabilities noticed previously (Lauer *et al.* 2001). While MUT3 and MUT6 mutants were possibly responsible for the PG activity because both mutants produced a stable and good yield protein in Lauer *et al* study (Lauer *et al.* 2001) and showed a very faint band in the zymogram gel in comparison with the wild type and the other protein variants in current study. Furthermore, both MUT3 and MUT6 showed the lowest activity in the FITC assay in relation to the wild type, and the mutation within these regions showed unusual motility phenotype (Lauer *et al.* 2001). For example, the mutation within the MUT3 region produced long pseudopod-like protrusions during intracellular infection in comparison with the wild type *L. monocytogenes*; these protrusions aid the bacteria in being able to invade host cells (Lauer *et al.* 2001). Thus, all of the mentioned reasons support the fact that MUT3 and MUT6 may play an important role in the cleavage of PG in the ActA protein. A similar observation with regards to a partial reduction in activity has been reported with the Rpf protein from *M. luteus* (Mukamolova *et al.* 2006), the muralytic activity and physiological activity e.g. resuscitation and growth stimulatory, were attenuated but not completely abolished when the presumptive catalytic residue was altered. Furthermore, PG hydrolysing activity of the FlgJ (flagellum) protein from *Salmonella typhimurium* (*S. typhimurium*) was reduced partially with amino acid

substitutions (Nambu *et al.* 1999). Whereas in other studies, complete inactivation was reported (Mushegian *et al.* 1996; Bayer *et al.* 2001).

The main advantages of FITC based assays are that they are simple and rapid to perform, provide quantitative data and are reasonably sensitive (Sogawa and Takahashi 1978; Maeda 1980). On the other hand, in this study one of the disadvantages of the FITC procedure was the difficulty in being able to determine the exact concentration of labelled PG used in the experiment. This may have affected the amount of activity noticed, given the complicated and variable structure of PG. However, in all experiments performed, the same volume of FITC labelled PG (2 µl) was used when comparing the activity of different proteins.

Finally, the obtained results were as expected with regards to the prediction of catalytic residues, as the actual structure of the ActA protein is still yet to be solved and the precise position of the active site has not yet been determined. Although the prediction was not random and the hypothesis generated was based on previous work (Lauer *et al.* 2001; Iakobachvili 2014), however the prediction strategies was most likely not enough and is an area where further work is needed. Thus, the characterisation of the precise activity of ActA, and the products of its activity on bacterial peptidoglycan, as well as their possible influence on different functions are challenges to be undertaken in future. The following chapter (Chapter 5) outlines the generation of specific polyclonal anti-ActA antibodies, aiming to facilitate the study of protein localization and pull dawn assay.

Chapter 5

Investigation of ActA
localization in
L. monocytogenes

5.1 Introduction

Investigating the subcellular localisation of proteins is important for understanding their interactions with other proteins and other functions (Garcia-del Portillo *et al.* 2011; Peng and Gao 2014). Generally, bacterial surface proteins are synthesized in the cytoplasm, and a specialized secretion system will assist in their transposition to the exterior face of the lipid bilayer (Carvalho *et al.* 2014). Surface proteins are known to be important for colonisation and for the virulence of many microorganisms (Desvaux and Hébraud 2006). Furthermore, they play a fundamental role in antibiotic resistance, interactions with the environment and in nutrient transport (Hu *et al.* 2017).

In *Listeria* spp., six-protein secretion systems have been recognized, of which is the Sec pathway, the most common pathway to secrete virulence proteins, as mentioned in Chapter 1 (section 1.6). The proteins processed by the Sec pathway can become membrane-associated through an anchor molecule like lipoproteins, e.g. LpeA, which allows such proteins to be covalently attached to the long chain fatty acids of the cytoplasmic membrane. Another manner in which proteins can become membrane-associated is by possessing transmembrane domains (integral membrane proteins), one example being ActA. Alternatively, proteins can associate with cell wall components through covalent interactions, as seen with internalin A (InlA), or through non-covalent interactions, as with internalin B (InlB) (Desvaux *et al.* 2006; Desvaux and Hébraud 2006; Carvalho *et al.* 2014).

The ActA protein of *L. monocytogenes* is secreted by the Sec secretion system, and remains anchored in the cytoplasmic membrane via a C-terminal hydrophobic tail (Desvaux and Hébraud 2006). This project was focused on investigating the role of ActA in PG modification, and performing experiments into the localization of ActA would help provide an insight into function. The aims of this chapter are to first optimise the protocols for the digestion of the membrane and cell envelope proteins from *L. monocytogenes*. Secondly, to detect the ActA protein from *L. monocytogenes* in the subcellular fractions i.e culture supernatant, cell wall, membrane, and cytosol), then use this fraction to find putative partners of ActA in *L. monocytogenes*. Finally, to confirm the localization result of ActA by using anti-ActA antibodies which were generated specifically for this purpose as well as by performing mass-spectrometry.

5.2 Results

5.2.1 Generation and validation of anti-ActA antibodies

The production of polyclonal ActA antibodies has been described in Chapter 2 (section 2.11). Figure 30 shows the dot blot analysis (described in Chapter 2, section 2.12) for the pre-immune serum and post-immune serum (received from Gemini Biosciences Ltd). The sample (Figure 30A) shows no recognition of the $ActA_{A30-S157}$ protein at the indicated dilutions (1:10,000 and 1:20,000). This proves that the pre-immune serum did not contain any antibodies that could recognize ActA (Figure 30A). The non-purified post-immune serum was able to recognize the recombinant $ActA_{A30-S157}$ protein at different dilutions (1:5000 to 1:160,000) and showed differences between spot intensities (Figure 30B) The rationale behind performing the dot blot was to establish the affinity between the generated antibody and the recombinant ActA protein, the findings of which are shown in Figure 30B. It is evident that the antibody is highly sensitive to the recombinant $ActA_{A30-S157}$ protein; the antibodies were able to detect the protein even at high dilution ratios, such as the 1:160,000 dilution ratio.
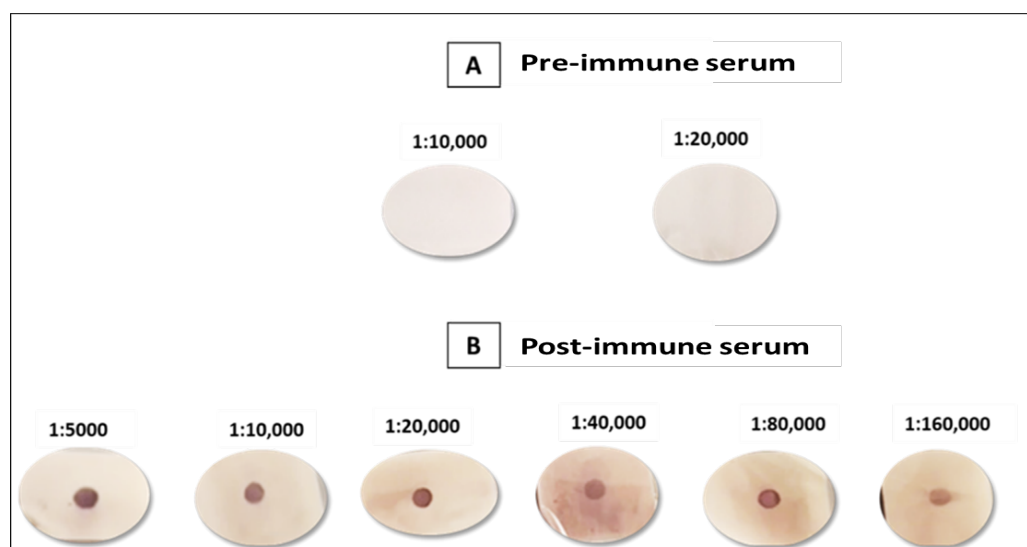
Figure 30. Dot blot of the anti-ActA polyclonal antibodies before purification.
Recombinant $ActA_{N30-S157}$ (1 µg) was spotted onto the nitrocellulose membrane, dried and incubated with pre-immune (A) and post-immune serum (B) samples. (A) Represents the pre-immune serum tested at 1:10,000 and 1:20,000 dilutions against $ActA_{N30-S157}$ and no recognition of the $ActA_{A30-S157}$ protein. (B) Shows non-purified post-immune serum tested using various dilutions (1:5,000, 1:10,000, 1:20 000, 1:40000, 1:80,000 and 1:160,000) against $ActA_{N30-S157}$ and the antibodies were able to detect $ActA_{N30-S157}$ protein in all mentioned dilution.

After initial confirmatory experiments, the anti-ActA antibody was purified using Protein A-Sepharose beads as described in Chapter 2. The eluted relevant fractions from the Protein A-Sepharose purification step containing the antibody (Figure 31A) were analysed by SDS-PAGE (Figure 31B). The heavy chain (~50 kDa) and light chain (~30 kDa) of the purified immunoglobulin G (IgG) were visible on an SDS-PAGE gel, as illustrated in Figure 31B. The purified antibody was aliquoted and frozen at -80ºC.
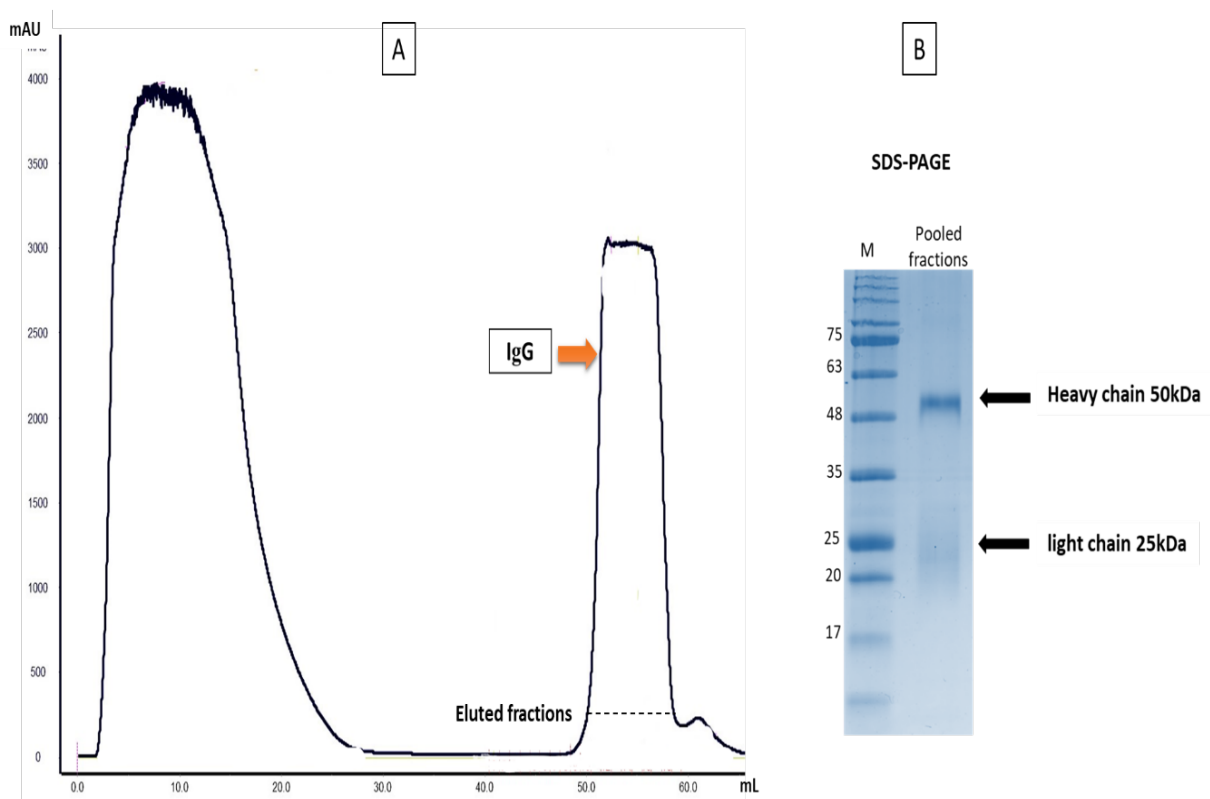
Figure 31. Purification of the anti-ActA antibodies using Protein A Sepharose beads and SDS-PAGE analysis.
(A) Gel filtration result for purified antibody (IgG) eluted by a low pH buffer. The orange arrow highlights the peak corresponding to the antibodies. (B) SDS-PAGE analysis for the pooled fractions from the ion/gel filtration. Highlighted are the bands corresponding to the heavy and light chains of IgG at ~50kDa and ~25kDa, respectively. The ladder [M] used was the Prestained Protein Standard (Geneflow, UK).

The sensitivity of the purified anti-ActA antibody was characterized via a Western blot assay (Figure 32). The purified ActA$_{A30-S157}$ (3 µg/ml) protein was ran on an SDS-PAGE gel (Figure 32A). The gel shows a pure protein evident by a single band at the relevant size of 24 kDa and with sufficient concentration to be used for a Western blot. Varying dilutions of the anti-ActA antibody (1:2,000, 1:40,000 and 1:200,000) were used in the Western blot analysis against 3 µg/ml of recombinant ActA$_{A30-S157}$ (Figure 32B, Figure 32C and Figure 32D). The results of the three panels (Figure 32B, Figure 32C and Figure 32D) revealed that the antibodies are highly sensitive towards the recombinant ActA$_{A30-S157}$, and that they can detect the protein at both low (1:2,000 and 1:40,000) and high dilutions (1:200,000). The difference in spot intensities in the threes panel (Figure 32B, Figure 32C and Figure 32D) was due to the different dilution used.
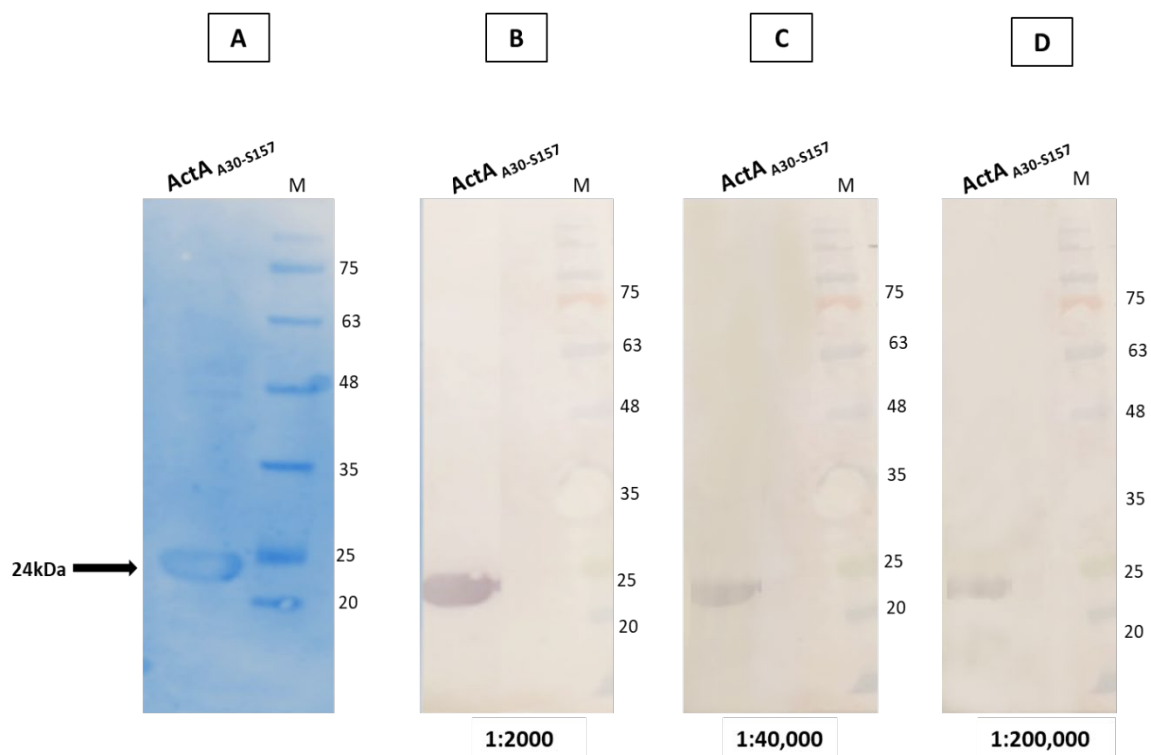
Figure 32. Validation of the anti-ActA antibody via Western blot.
(A) SDS-PAGE analysis of 3 µg/ml of the recombinant ActA$_{A30-S157}$ protein. The same protein amount was used for Western blot analysis with varying antibody dilutions (B: 1:2,000, C: 1:40,000 and D: 1:200,000). [M] Prestained Protein Standard (Geneflow, UK).

5.2.2 Detection of ActA in culture supernatants and membrane/cell wall fractions prepared from *L. monocytogenes*

The method described in Chapter 2, section 2.13.1, was used to determine the fractions, which contained the ActA protein. The secreted ActA was expected to be released in the culture supernatant as previously described (Garcia-del Portillo *et al.* 2011).

Both *L. monocytogenes* EGD-e wild type and *ΔactA* mutant (strain with the *actA* gene deleted) were cultured in TSB, as described in Section 2.3.1. The culture supernatant and membrane/cell wall fraction preparations from the wild type and *ΔactA* mutant strains were ran on an SDS-PAGE gel (Figure 33). As expected, all the lanes on the SDS-PAGE gel presented with multiple bands for the culture supernatant preparation and membrane/cell wall fractions. The protein patterns were similar for both of the strains (Figure 33).
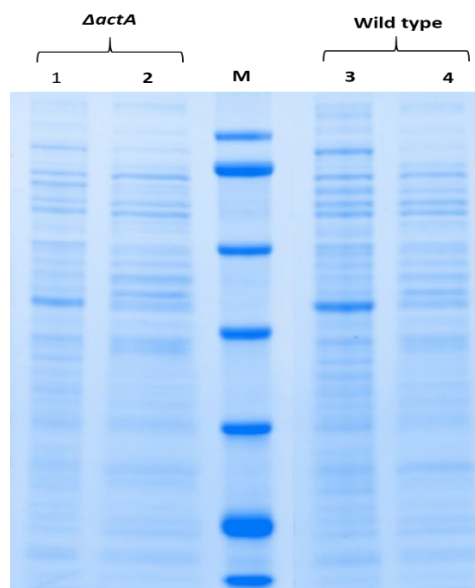
Figure 33. SDS-PAGE gel stained with Coomassie blue to analyse the culture supernatant and membrane/cell wall fractions from wild type and *ΔactA L. monocytogenes* strains.

(1)*ΔactA* culture supernatant fraction. (2) *ΔactA* membrane/cell wall fraction. (3) Wild type culture supernatant fraction. (4) Wild type membrane/cell wall fraction. [M] Represents the Prestained Protein Standard (Geneflow, UK).

Western blot analyses using the anti-ActA antibody were performed with all of the obtained fractions. The blot analysis using the anti-ActA antibody (Figure 34) revealed the presence of bands at around 35 kDa and 48 kDa in the culture supernatants fractions of both the *ΔactA*

mutant (Lane 1) and wild type (Lane 3) strains. The band present at around ~65 kDa was observed in all the samples. As all the mentioned bands were identified both in the wild type and in the mutant strain, they can be considered as non-specifically recognized protein bands. Interestingly, a band (circled in blue) with the expected molecular size of ActA (90 kDa) as previously reported (Lathrop *et al.* 2008; Garcia-del Portillo *et al.* 2011) was clearly observed in the culture supernatant fraction of the wild type strain only (Lane 3). This said molecular weight band was absent in the *ΔactA* strain (Lane 1), suggesting that the antibodies recognize the wild type ActA. In addition, no ActA band was detected in the membrane/cell wall fractions of the wild type strain. These results confirm previously published data on the detection of ActA in culture supernatant (Garcia-del Portillo *et al.* 2011). However, the main aim of this chapter is to identify the partners of ActA in the membrane or cell wall fraction, thus, different protocols were used for this purpose.
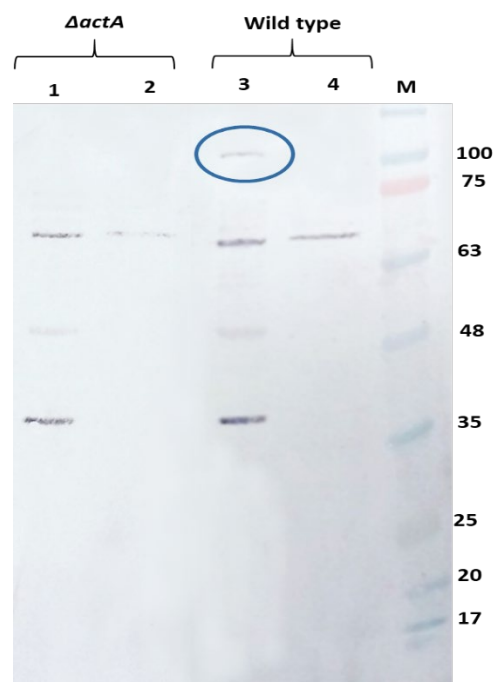
Figure 34. Western blot of the anti-ActA antibody for the culture supernatants and membrane fractions from *L. monocytogenes* wild type and *ΔactA* strains.

(1)*ΔactA* culture supernatant fraction. (2) *ΔactA* membrane/cell wall fraction. (3) Wild type culture supernatant fraction. (4) Wild type membrane/cell wall fraction. The blue circle in Lane 3 highlighting a band at approximately 90kDa corresponds to the size of the ActA protein. [M] Represents the Prestained Protein Standard (Geneflow, UK).

5.2.3 Detecting the presence of ActA in the cell wall and membrane fractions using differential ultracentrifugation

The fractionatation of *L. monocytogenes* was performed as previously described by Mawuenyega *et al.* (Mawuenyega *et al.* 2005) in Chapter 2 (Section 2.13.2). Several proteome-ics studies have shown that the ActA protein is present either in the cell wall or membrane fractions (Kocks *et al.* 1992; Lathrop *et al.* 2008; Garcia-del Portillo *et al.* 2011). Thus, the cell wall, cytoplasm and membrane fractions were obtained from wild type *L. monocytogenes* and analysed via SDS-PAGE and Western blot to detect the presence of ActA. Figure 35A shows the SDS-PAGE gel with various cellular fractions obtained from wild type *L. monocytogenes,* and Figure 35B shows the Western blot results for the same samples. The SDS-PAGE gel (Figure 35A) shows multiple bands present in all the fractions representing different proteins, while the Western blot (Figure 35B) shows the detection of an unknown band with a molecular weight of 35 kDa in all the lanes. Notably, similar bands of approximately 35 kDa in size were detected previously in the Western blot for section 5.2.2 in both wild type and *ΔactA L.monocytogenes*. It was thus concluded that this was a non-specific band. This result indicates that this procedure was not sensitive, as ActA could not be detected via Western blot assays using the anti-ActA antibody.
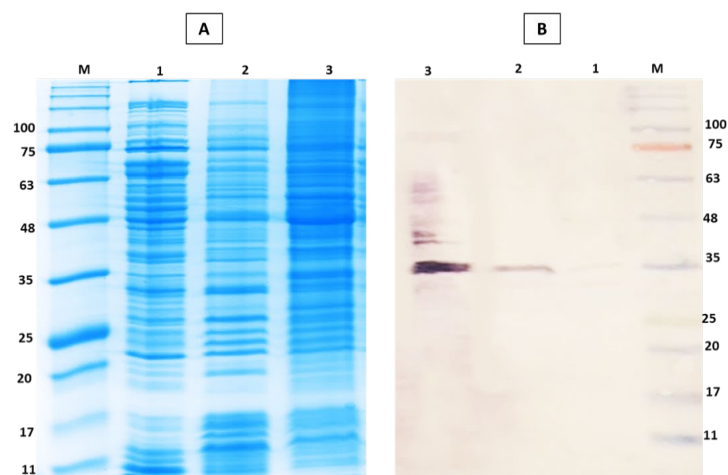
Figure 35. Analysis of the localisation of ActA via differential centrifugation.
SDS-PAGE and Western blot showing subcellular fractions from wild type *L. monocytogenes*. (A) SDS-PAGE gel of different cellular compartments: (1) Cytoplasmic fraction. (2) Membrane fraction. (3) Cell wall fraction. (B) Western blot with the anti-ActA antibody for the same samples mentioned in (A). [M] Prestained Protein Standard (Geneflow, UK).

Subsequently, mass spectrometry analysis was performed for the fractions obtained from both wild type and *ΔactA L. monocytogenes* samples. The mass spectrometry data showed that the ActA protein was present in the membrane fraction of the wild type strain only. Furthermore, one peptide fragment of ActA was identified via mass spectrometry (Figure 36) with low confidence (Appendix 8.10) which indicates that this method is not the ideal method for ActA localization due to the low detection of ActA protein. In addition, ActA was not detected in the fractions from the *ΔactA L.monocytogenes* strain as expected (Appendix 8.10).


```
P33379 (64%), 70,351.5 Da
Actin assembly-inducing protein OS=Listeria monocytogenes serovar 1/2a (strain ATCC BAA-679 / EGD-e) OX=169963
1 exclusive unique peptides, 1 exclusive unique spectra, 1 total spectra, 9/639 amino acids (1% coverage)

MGLNRFMRAM  MVVFITANCI  TINPDIIFAA  TDSEDSSLNT  DEWEEEKTEE
QPSEVNTGPR  YETAREVSSR  DIKELEKSNK  VRNTNKADLI  AMLKEKAEKG
PNINNNNSEQ  TENAAINEEA  SGADRPAIQV  ERRHPGLPSD  SAAEIKKRRK
AIASSDSELE  SLTYPDKPTK  VNKKKVAKES  VADASESDLD  SSMQSADESS
PQPLKANQQP  FFPKVFKKIK  DAGKWVRDKI  DENPEVKKAI  VDKSAGLIDQ
LLTKKKSEEV  NASDFPPPPT  DEELRLALPE  TPMLLGFNAP  ATSEPSSFEF
PPPPTDEELR  LALPETPMLL  GFNAPATSEP  SSFEFPPPPT  EDELEIIRET
ASSLDSSFTR  GDLASLRNAI  NRHSQNFSDF  PPIPTEEELN  GRGGRPTSEE
FSSLNSGDFT  DDENSETTEE  EIDRLADLRD  RGTGKHSRNA  GFLPLNPFAS
SPVPSLSPKV  SKISAPALIS  DITKKTPFKN  PSQPLNVFNK  KTTTKTVTKK
```

Sequence	Observed	Actual Mass	Charge
(R)DRGTGKHSR(N)	507.2563	1,012.50	2

Figure 36. Mass spectrometry analysis for the membrane fraction obtained from the wild type *L. monocytogenes*.
Trypsin digestion for the membrane fraction of the wild type produced one peptide (highlighted by yellow colour) which matched the predicted profile of ActA. The yellow color shows the identified peptide (DRGTGKHSR).

We developed a new digestion method to detect membrane bound proteins (Section 5.2.4) instead of the conventional method of digestion used at the University of Leicester Proteomics Facility (PNACL, University of Leicester). This was due to the low level of detection for the ActA protein in the membrane fraction via mass spectrometry, as well as due to the known fact

that the detection of membrane proteins is challenging given their hydrophobic nature (Mirza *et al.* 2007).

5.2.4 Optimisation of the digestion protocol to detect membrane proteins

The membrane fraction analysis by mass spectrometry is extremely difficult (Mirza *et al.* 2007). Thus, we developed a novel method for analysis membrane proteins by using an ionic detergent, sodium dodecyl sulfate (SDS), at high temperature and we call it DIET (digestion at elevated temperature.

The method itself was described in Chapter 2 (section 2.13.3) and all details are summarized in our manuscript (Loraine *et al.* 2019). Briefly, the membrane fractions of *L. monocytogenes* were prepared in three biological replicates, and each replicate was split in two parts. In addition, each part was digested with DIET method and conventional method to compare the efficiency of two different methods. The result of mass spectrometry of the membrane fractions showed that no ActA protein detected in both method. However, the result showed that this method is more efficient in detection of membrane proteins compared to the conventional method (Figure 37). As shown in Figure 37A, the total number of proteins identified using the conventional method of digestion was 304 with 51 uniquely identified proteins. Whereas, the amount of proteins identified by DIET method was 401 in total, with 148 uniquely identified proteins. Figure 37B, shows an example of 21 proteins (17 trans-membrane or membrane/cell wall associated proteins) identified by DIET only and no peptide was identified at all by the traditional method of digestion. In regards to ActA, it has been conclude that ActA protein is expressed at very low level or/and degraded in the media used to grow.

Accession nubmer	Membrane/Cell Wall Localisation
Q8Y614	Cell wall enzyme PBP1 associated cell cycle protein
Q8Y936	Flagellar hook-associated protein 1
Q8Y9B5	Putative lipoprotein
Q8Y467	Transmembrane protein. Multidrug transporter
Q8Y3X9	Uncharacterised protein
Q7AP75	Transmembrane protein. Choline transport
Q8Y6Q8	Transmembrane protein
Q8Y7K8	Transmembrane protein. Peptidase family
Q8Y6P7	Transmembrane protein
P0DJM1	Metal-binding, heat response chaperone
Q8Y7D2	Transmembrane protein. Rhodanese-like protein
Q8Y7E9	Uncharacterised protein
Q8Y876	Outer membrane-bounded periplasmic space protein
Q8Y7B4	Membrane oxidoreductase
P0DJP1	30S ribosomal protein S21
Q8Y980	Transmembrane protein
Q929P4	Carbohydrate transmembrane transporter
Q8Y5W4	Transmembrane protein
Q8Y679	ATP-binding protein, integral component of membrane
Q8Y732	Uncharacterised protein
Q92DA4	Transmembrane formate transporter

Figure 37. Analysis of the mass spectrometry data of membrane digestion using the traditional method vs the developed DIET method.
(A) The total number of proteins identified using the conventional method was 304 while 401 proteins were identified via DIET. The amount of uniquely identified proteins by DIET was 148, while that of the traditional method was 51. (B) Examples of protein identified via the DIET method only.

5.2.5 Detection of ActA in the cell surface and intracellular fractions prepared from *L. monocytogenes* grown in BLEB media

Lathrop *et al.* (2008) published a method to study the expression and localization of ActA and InlB proteins from *L. monocytogenes* using a selective enrichment broth called buffered BLEB (Lathrop *et al.* 2008).

The method mentioned in Chapter 2 (Section 2.13.4) was used for experiments described in this section. Cell surface and intracellular fractions obtained were analysed by SDS-PAGE, Western blot and mass spectrometry for both wild type and *ΔactA* strains. The SDS-PAGE gel in Figure 38A shows cell surface and intracellular fractions obtained from both strains. There were multiple bands in all the lanes, and the gels were similar to the SDS-PAGE gels in Figure 33 and Figure 35A.

Of note, there was a band present corresponding to a molecular weight of ~90 kDa (indicated by a black box) in the cell surface fraction of the wild type strain, which was absent in the cell surface fraction of the *ΔactA* mutant. The Western blot with anti-ActA antibodies in Figure 38B confirmed the presence of the single band which was ~90 kDa in the cell surface fraction of the wild type strain.
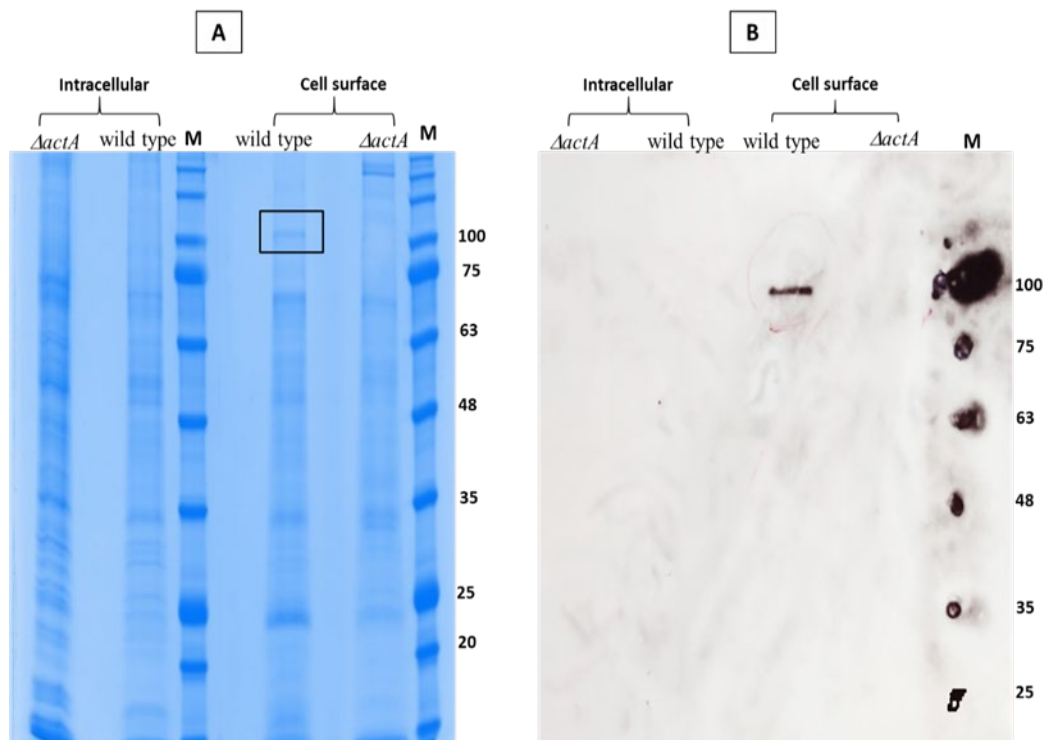
Figure 38. Analysis of ActA localization in *L. monocytogenes* grown in BLEB media.
SDS-PAGE and Western blot showing the localization of ActA in *L. monocytogenes* wild type and mutant strains. (A) SDS-PAGE gel showing proteins from the intracellular and cell surface fractions. (B) Western blot performed with anti-ActA antibodies of the same samples as (A). A single band at around 90 kDa is visible in the cell surface fraction of the *L. monocytogenes* wild type strain, corresponding to the expected size of the ActA protein. [M] Prestained Protein Standard (Geneflow, UK).

For further confirmation, all the mentioned fractions were analysed via mass spectrometry. The results revealed that 9 peptides of ActA with high levels of confidence (Appendix 8.11) have been identified in the surface fraction of the wild type strain, as shown in Figure 39 and that they matched the predicted profile. In addition, ActA was not detected in the fractions obtained from the *ΔactA L.monocytogenes* strain (Appendix 8.11).

ACTA_LISMO (100%), 70,351.5 Da

Actin assembly-inducing protein OS=Listeria monocytogenes serovar 1/2a (strain ATCC BAA-679 / EGD-e) OX=169963 GN=a

9 exclusive unique peptides, 10 exclusive unique spectra, 10 total spectra, 131/639 amino acids (21% coverage)

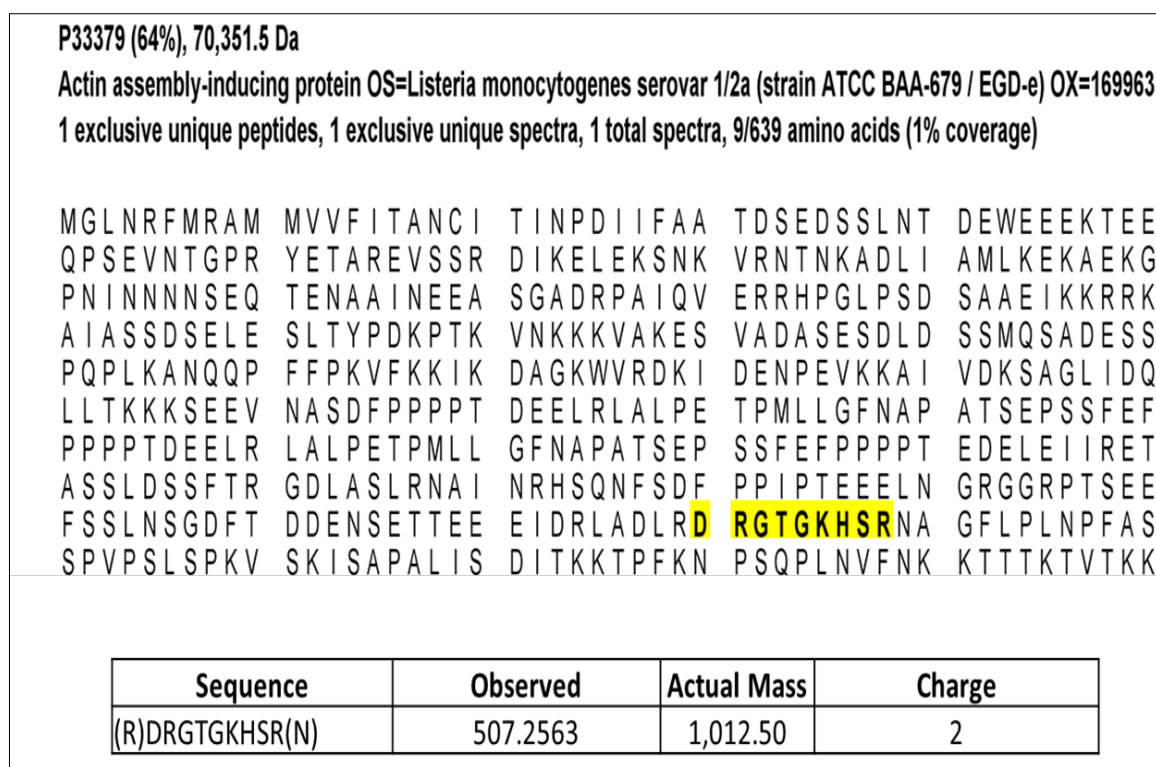| Sequence	Observed	Actual Mass	Charge
(R)RHPGLPSDSAAEIK(K)	493.2634	1,476.77	3
(K)AIASSDSELESLTYPDKPTK(V)	718.0267	2,151.06	3
(K)ESVADASESDLDSSmQSADESSPQPLK(A)	942.7417	2,825.20	3
(K)ANQQPFFPK(V)	538.7798	1,075.55	2
(R)DKIDENPEVKK(A)	657.8486	1,313.68	2
(R)DKIDENPEVKK(A)	438.9015	1,313.68	3
(K)SAGLIDQLLTK(K)	579.8401	1,157.67	2
(R)ETASSLDSSFTR(G)	650.8044	1,299.59	2
(K)ISAPALISDITK(K)	614.861	1,227.71	2
(K)LAELPATKPQETVLR(E)	555.9893	1,664.95	3

Figure 39. Mass spectrometry analysis of the cell surface fraction obtained from wild type *L. monocytogenes*.
The trypsin digestion for the cell surface fraction of the wild type produced 9 peptides (highlighted by yellow colour) which matched the predicted profile of ActA. The yellow colour shows the identified peptides.

5.3 Discussion

In this chapter, different procedures were used to detect and study the localization of the ActA protein. In all of the techniques, it was essential to use antibodies specific for ActA for the detection of this protein, in particular subcellular fractions (Dahl *et al.* 2001). Therefore, rabbit polyclonal antibodies were raised against the ActA protein. These antibodies were produced because of their ability to recognize multiple conformational epitopes (LEDER *et al.* 1994; Read *et al.* 2009). The results demonstrated that the polyclonal anti-ActA antibodies bound specifically to the ActA protein. On the other hand, the detection of the ActA protein in native hosts was extremely challenging because the cellular fractionations of Gram-positive organisms are known to be complex and difficult to work with (Tavares and Sellstedt 2000; Cole *et al.* 2008), due to the presence of the thick cell wall compared to Gram-negative bacteria (Tavares and Sellstedt 2000). In addition, ActA is known to be expressed well inside infected cells (*in vivo*) compared to extracellular environments (*in vitro*) (Garcia-del Portillo *et al.* 2011). All the mentioned reasons therefore make the detection of cell wall associated proteins like the ActA protein very challenging. However, the localization of a protein is very important for determining and explaining its predicted function (Wang *et al.* 2005).

First, it was important to show that the ActA is a secreted protein released into the culture media (Desvaux and Hébraud 2006). This is not an easy task as the expression of extracellular ActA protein is affected by many conditions such as growth temperature, glucose concentration, selective antimicrobial agents and salts (Lathrop *et al.* 2008). Interestingly, the Western blot analysis confirmed that the ActA is a secreted protein (Figure 34). This was consistent with other studies where ActA was shown to be a secreted protein (Lathrop *et al.* 2008; Garcia-del Portillo *et al.* 2011).

Differential centrifugation was used to study the subcellular fractionation of *L. monocytogenes* grown in BHI and BLEB media. In both cases, ActA was detected using anti-ActA antibodies and via mass spectrometry analysis. It was expected that ActA would be detected in the cell wall or membrane fractions (Kocks *et al.* 1992; Lathrop *et al.* 2008; Garcia-del Portillo *et al.* 2011), as it is known that ActA spans both the bacterial membrane and peptidoglycan (Rafelski and Theriot 2006). In the case where the bacteria were grown in BHI broth media, modest amounts of ActA were found in the membrane fraction, as shown via mass spectrometry. We concluded that *L. monocytogenes* grown in BHI media does not produce enough ActA protein. Thereafter, attempts were made to find the conditions where ActA is produced at an appropriate

amount. One of the major goals of this chapter was to find the best method to study the localization of ActA and the further analysis of any ActA partners. Sokolovic *et al.* reported that ActA expression in strains from serogroup 4 of *L. monocytogenes* was significantly higher in mammalian cell culture medium and MEM (minimum essential medium) compared to BHI broth (Sokolovic *et al.* 1996). Furthermore, Lathrop *et al.* and Niebuhr *et al.* also observed low levels of ActA in different strains of *L.monocytogenes* grown in BHI (Niebuhr *et al.* 1993; Lathrop *et al.* 2008). The reason for this poor detection of ActA was attributed to the glucose content in the BHI medium (Greene and Freitag 2003), which might be indirectly responsible for the lowering of the media pH, subsequently affecting expression (Behari and Youngman 1998). It has been previously reported that high concentrations of sugar, specifically glucose, in the media influences the expression level of some virulence proteins in *L. monocytogenes* e.g. LLO and phospholipase C (Milenbachs *et al.* 1997). However, other research groups have suggested that the reason for the difficulty in expressing *actA* in *L. monocytogenes* strains was due to the 5′ untranslated region (5′ UTR) of the *actA* gene, which affects the translation efficiency and is unrelated to glucose in culture media (Wong *et al.* 2004).

The identification of the bacterial membrane proteins is generally very difficult. Therefore, we developed a new digestion method to digest membrane proteins. Named the DIET method, it is very simple and efficient for the investigation of membrane proteins using mass spectrometry (Loraine *et al.* 2019). It results in the detection of a higher amount of membrane and cell wall proteins when compared to the traditional method of digestion. Despite using this efficient method, the identification of ActA in *L. monocytogenes* grown in BHI media was still not possible. However, when cultures were grown in BLEB broth, the localisation of ActA was confirmed with very high confidence. Approximately nine peptides of ActA were identified with 99.99% confidence in the membrane fraction.

This finding is in agreement with Lathrop *et al.* (Lathrop *et al.* 2008), which showed that the expression of ActA *in-vitro* was stronger in 12 serotypes of *L. monocytogenes* grown in BLEB compared to non-selective broth (BHI and LB), which showed weak or no ActA expression (Behari and Youngman 1998; Greene and Freitag 2003; Wang *et al.* 2005). Generally, the expression of various virulence factors in *L. monocytogenes* is affected by environmental conditions (Smith and Portnoy 1997). The reason for the higher expression of ActA in BLEB media and lower expression in BHI is not clear (Lathrop *et al.* 2008). However, high concentration of salts could have an effect on protein expression. In addition, unpublished data

from Lathrop *et al.* (Lathrop *et al.* 2008) points to fact that the pH of BHI broth sharply dropped to 2.11 after *L. monocytogenes* growth, whereas BLEB broth is a highly buffered medium, favouring the increased expression of peptidoglycan modifying proteins. The presence of ActA in the cell surface supports the main hypothesis of this study, explaining the role of this protein in cell wall assembly and turnover. Unfortunately, due to time constraints, no immunoprecipitation assays could be performed. Finally, further methods need to be used in future to standardize the identification of membrane proteins and for the identification of ActA protein partners.

Chapter 6

Domain swapping experiments to probe the function of ActA in bacterial growth

6.1 Introduction

Domain swapping refers to the genetic rearrangement of proteins by combining two or more genetic elements that code for domains or subdomains (Ostermeier and Benkovic 2001). Generally, the main goal of domain swapping is to create a novel protein that has improved or novel properties; this can be achieved by exchanging amino acid sequences With an existing protein (Nixon *et al.* 1998). Domain swapping has been developed for different purposes, e.g. to understand proteins' novel functions, enhance their stability and expression, improve or alter their catalytic functions and for better therapeutic properties (Nixon *et al.* 1998; Béguin 1999).

In *Mycobacterium tuberculosis*, five resuscitation promoting factor (Rpf) proteins have been identified (Telkov *et al.* 2006). These Rpfs have been shown to have muralytic activity *in-vitro* against crude cell wall preparations and against an artificial lysozyme substrate (Telkov *et al.* 2006). Moreover, it has been found that this activity is responsible for the resuscitation of dormant cells and promotion of growth (Mukamolova *et al.* 1998; Gupta and Srivastava 2012). Previously, significant amino acid sequence homology (up to 50 %) and conservation of a key acidic residue E98, between RpfA of *Mycobacterium marinum* and *M. tuberculosis* and ActA of *L. monocytogenes* has been identified (Iakobachvili 2014) as mentioned in Chapter 1 (section 1.9). Based on their conserved amino acid architecture (Iakobachvili 2014), it was hypothesised that ActA may have Rpf-like activity.

First, this chapter will describe the effect of deleting *actA* on the growth of *L. monocytogenes*. Then, the domain swapping strategies used to investigate any possible complementation of ActA activity in the *rpf* deletion mutants of *M. marinum* will be explained. Furthermore, the method in which a chimeric protein was expressed and generated, where the Rpf domain was replaced with the N-terminal domain of ActA, will be explained. Finally, details will be provided about how this chimeric construct was used for the complementation of phenotype in a Δ*rpfABE M. marinum strain*. This Δ*rpfABE Mycobacterium marinum* was generated previously in the lab by Dr. Mariam Noor (University of Leicester). The rationale behind using this triple mutant was due to the fact that it has an obvious phenotype (growth defect) when compared with wild type *M. marinum*, and this defect was completely improved when *rpfA* from *M. tuberculosis* was introduce to the strain (unpublished data, Dr. Mariam Noor).

In other words, *rpfA* was completely complemented with *M. marinum* Δ*rpfABE*. Therefore, the chimeric construct was used alongside *rpfA* for the complementation of phenotype in *M. marinum* Δ*rpfABE* to see whether a similar effect on the growth of Δ*rpfABE M. marinum* occurs.

6.2   Results

6.2.1   The deletion of *actA* (Δ*actA*) does not affect the growth of *L. monocytogenes,* with no specific phenotype being observed

It was essential to study the growth behaviour of wild type *L. monocytogenes* (WT) and Δ*actA* mutants *in vitro*. The reason behind this experiment was to examine any potential growth defects caused by the deletion of *actA* in the mutant strain when compared to WT *L. monocytogenes*.

Firstly, the identity of WT and *ΔactA* strains was confirmed by colony PCR using two types of primers (listed in Table 4, Chapter 1). Test primers were designed to identify sequences upstream and downstream of the *actA* gene, as shown in Figure 40A. On the other hand, gene-specific primers were designed to confirm the presence of the *actA* gene (Figure 40C). The predicted sizes of the PCR products obtained with the test primers for the WT and Δ*actA* strains were 2,000 bp and 233 bp, respectively (Figure 40B). However, the application of gene-specific primers produced a 230 bp PCR product for the WT strain (Figure 40D) and no product, as expected, with theΔ*actA* strain (Figure 40D). These predictions were confirmed by PCR, as shown in Figure 40.
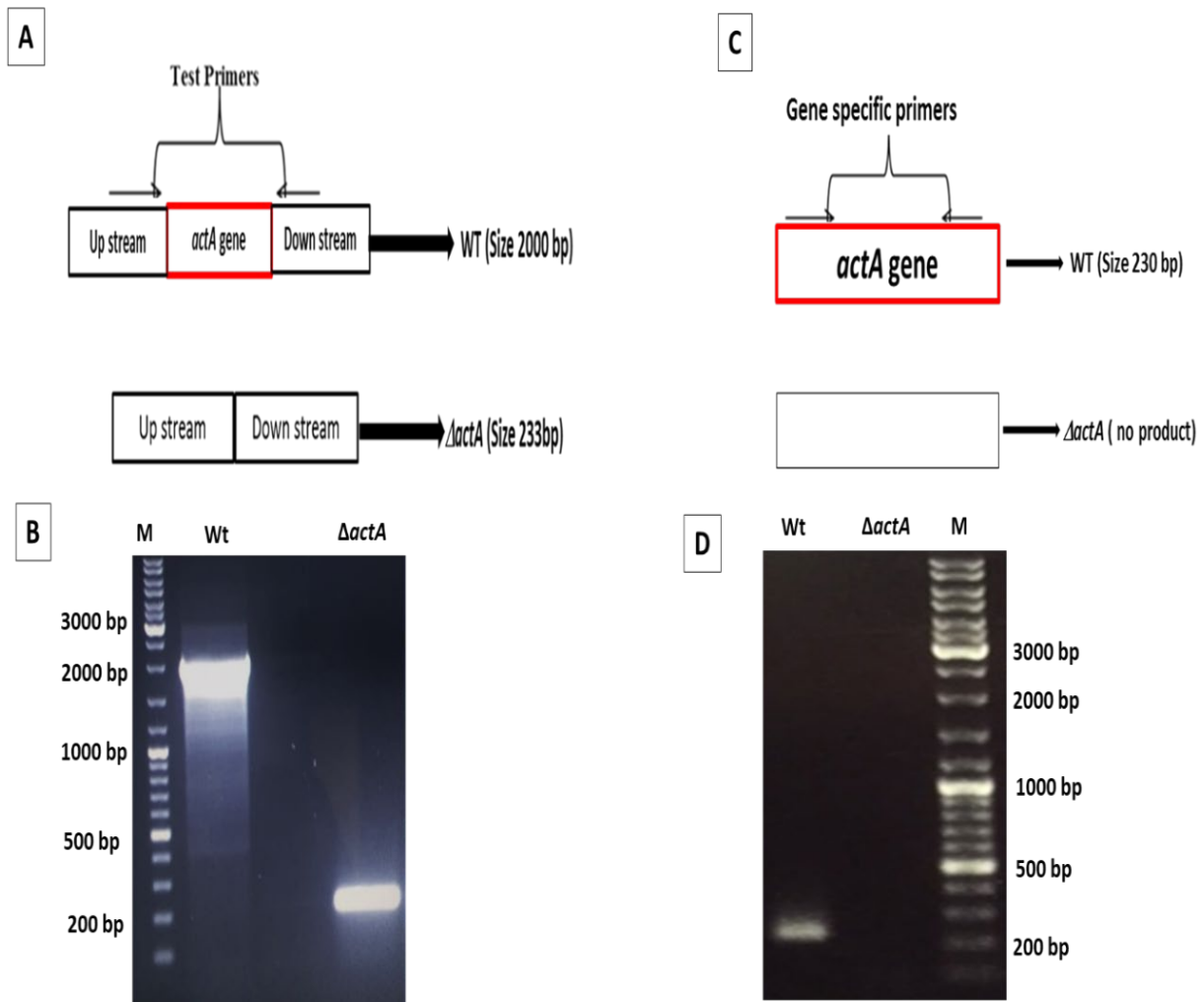
Figure 40. Agarose gel electrophoresis showing the confirmation of the presence and absence of *actA* gene in both strain of *L. monocytogenes* by using test and gene specific primers.

(A) Schematic representation of the test primers used for confirmation. (B) Gel electrophoresis for the *L. monocytogenes* tested; the WT strain PCR product migrated to the expected size of approximately 2,000 bp, whereas the Δ*actA* product migrated to the expected size of 233 bp. (C) Schematic representation for gene specific primers used for conformation. (D) Gel electrophoresis for the WT strain PCR product which migrated to ~ 230 bp, as expected, with no band detected for the Δ*actA* strain. [M] Is a 1 kb DNA ladder (Thermo Scientific™ O' GeneRuler, UK).

Thereafter, the growth patterns of both strains were tested using the method described in Chapter 2 (section 2.4). Different mediums were used for these experiments; TSB as a general non-selective medium and MWB as a chemically defined medium. Figure 41A and 40B show

119

the growth curve of the two strains at OD_{600nm} over 24 hours. In Figure 41A, the optical density for both the strains in TSB did not reveal any statistically significant differences for any of the time points (calculated via an unpaired t-test, revealing a p-value of 0.5). Similarly, there was no statistically significant difference between both strains when cultured in MWB at any of the time points (calculated via an unpaired t-test, revealing a p-value of 0.6), as illustrated in Figure 41B. Furthermore, the CFU counts (Figure 41C) for both strains were also performed by plating on TSA media. The results of the CFU counts revealed no statistically significant difference between both strains at any of the time points (calculated via unpaired t-test, revealing a p-value of 0.3), as shown in Figure 41C.

Furthermore, the colony morphology did not appear to be affected in the $\Delta actA$ mutant at any of the time points; Figure 41D shows the identical colony morphology of both strains at the one-hour time point. Overall, the results indicate that the deletion of the *actA* gene does not result in any phenotypic changes in terms of growth, as judged by OD and CFU counts. Thus, the $\Delta actA$ *L. monocytogenes* strain could not be used for further investigation and complementation of growth defects.
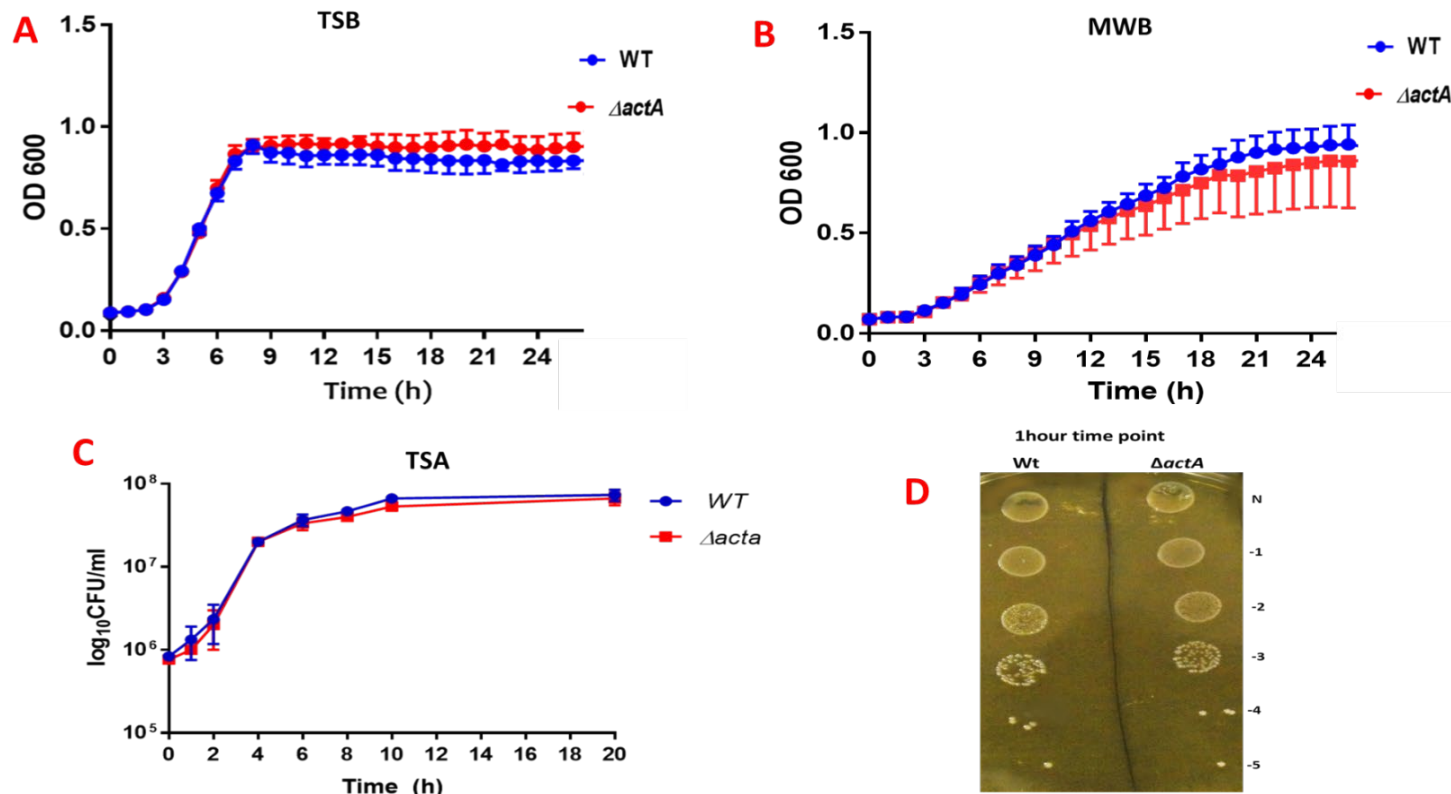
Figure 41. *L. monocytogenes* **WT and Δ*actA* growth curves.**
(A) Growth curves of the wild type and Δ*actA* mutants in TSB. No differences between optical densities (OD_{600nm}) at any of the time points. (B) Growth curves of the wild type and Δ*actA* mutant in MWB at OD_{600nm}; no difference present between the strains for any of the time points. In (A) and (B), each data points represent the mean of 11 replicates for both strains in TSB and MWB, respectively. (C) CFU counts for the WT and Δ*actA* strains cultured on TSA. Each data point represents the mean of 3 biological replicates. The error bars represent the standard deviation of the mean. (D) Colony morphologies of the two strains at the 1-hour time point, both strains presenting with similar morphologie.

6.2.2 Generation of the chimeric construct

The experimental strategy used to generate the chimeric gene (*rpfA-actA*) is detailed in Figure 42. Briefly, the chimeric construct was created by domain swapping a gene fragment encoding the active part of RpfA from *M. tuberculosis* (Mtb), with a gene fragment encoding the N-terminal domain of ActA from *L. monocytogenes*.

In the first step, primers were designed (shown in Chapter 1, Table 4) to amplify the upstream region of *rpfA* (F1), the downstream region of *rpfA* (F3) and the NH2–terminal region of *actA* (F2). Moreover, for the purposes of cloning, additional specific endonuclease restriction sites illustrated in Table 12, were introduced to the primer sequences. As the second step, high fidelity PCR (Chapter 2, section 2.5.3) was performed to amplify the F1 and F3 using the genomic DNA of Mtb as a template. On the other hand, the pLEICS-01::*actA* $_{A30-S157 \, a.a}$ plasmid was used as a template to amplify the F2.

Table 12. Gene-specific primers for the amplification of F1, F2 and F3.

Primer name	Restriction site introduced	Fragment description	Molecular size of fragment
tb_rpf_c4 Fw	*KpnI*	To amplify the upstream region of *rpfA* gene (F1)	573 bp
rpfAR2	*Bam*HI		
ActAcomF1	*Bam*HI	To amplify the NH2 terminal region of the *actA* gene (F2)	397 bp
ActA comR1	*PstI*		
rpfAF2	*PstI*	To amplify the down-stream region of *rpfA* gene(F3)	814 bp
tb_rpf_RV	*EcoRI*		
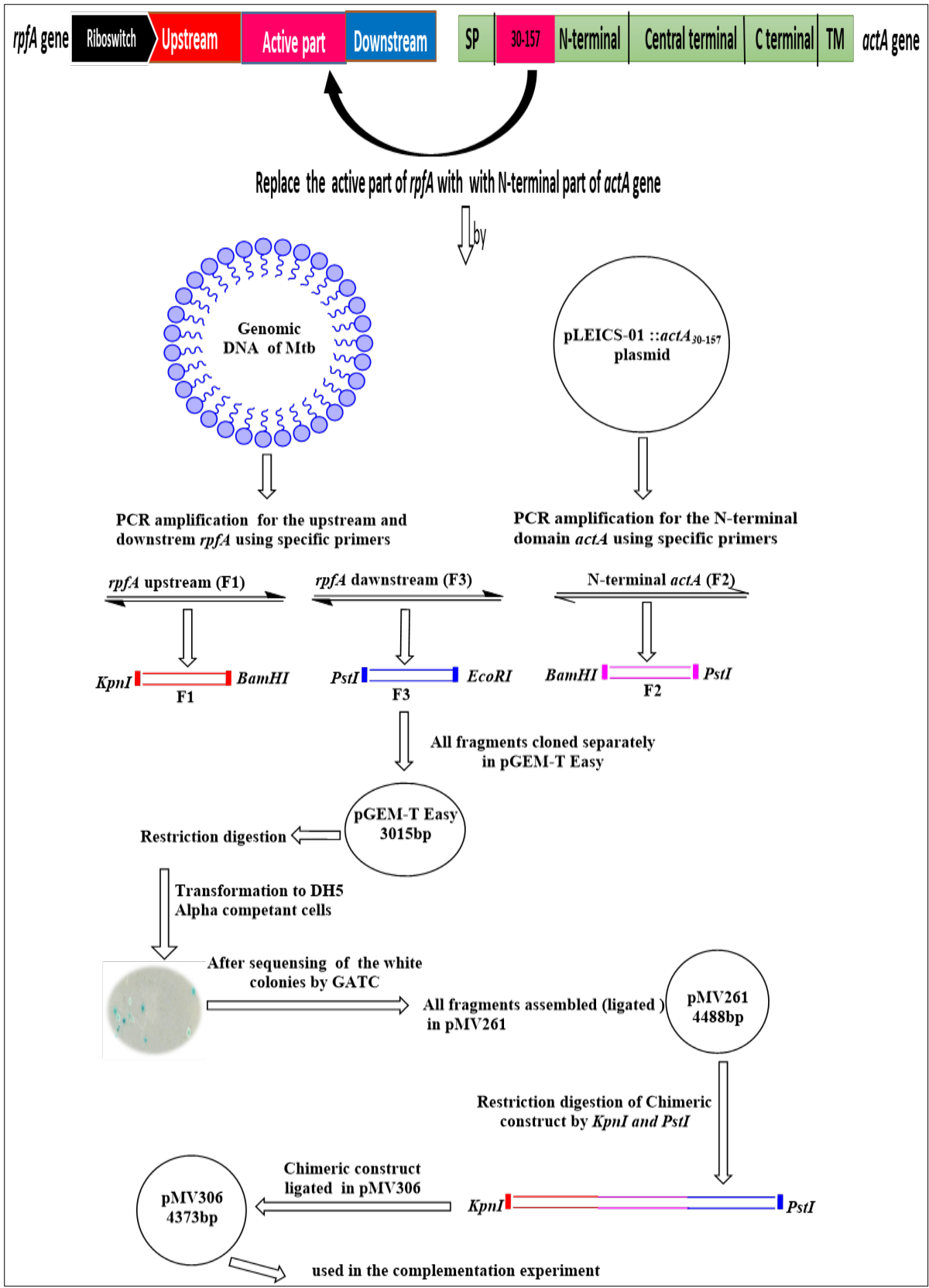
Figure 42. Schematic showing the strategy for the generation of the chimeric construct (*rpfA-actA*).

The PCR products were analysed by agarose gel electrophoresis. As shown in Figure 43, the F1 and F3 regions of *rpfA* generated single bands of approximately 573 bp and 814 bp in size, whereas the F2 region of *actA* (F2) generated a band of approximately 397 bp in size.
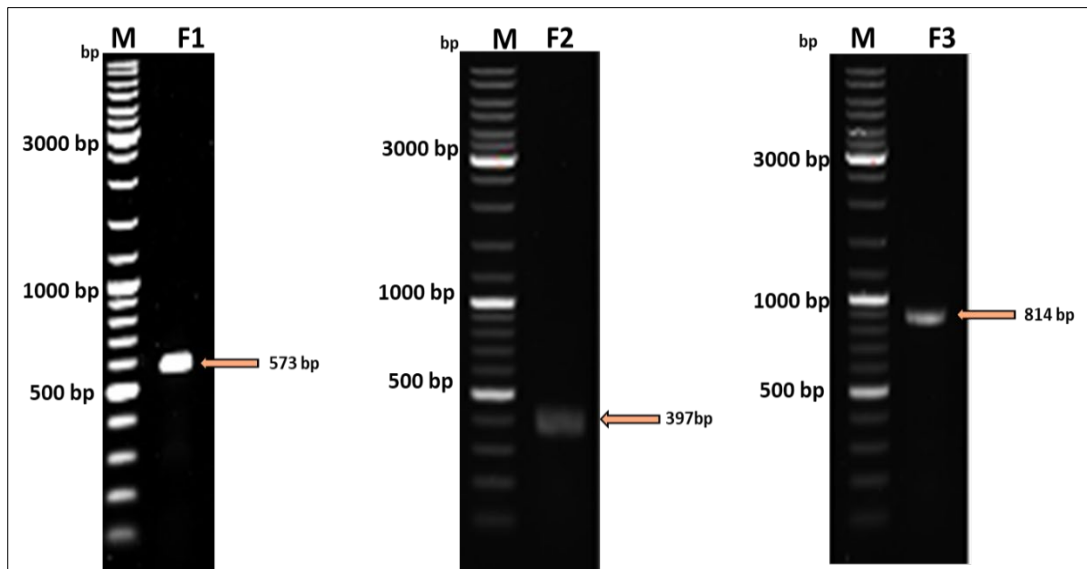
Figure 43. Agarose gel electrophoresis of the amplified F1, F2 and F3 fragments.
The upstream region of *rpfA* (F1), N-terminal region of *actA* (F2) and the downstream region of *rpfA* (F3) were amplified via a PCR performed with the high fidelity Platinum Taq DNA polymerase (Invitrogen™). All PCR products were migrated to expected sizes of 573 bp, 397 bp and 814 bp for F1, F2 and F3 respectively. [M] 1kb DNA ladder size marker (Thermo Scientific™ O'GeneRuler, UK).

Following this, PCR products were purified using the QIAquick PCR Purification Kit (Chapter 2, section 2.5.5) and initially cloned separately into pGEM-T Easy (Promega) cloning vectors (3,015 bp). The pGEM-T Easy (Promega) vector was chosen as the T-overhangs in the vector prevent vector recircularization which can lead to an increased efficiency of ligation with the PCR product (Tao *et al.* 1994). Furthermore, this vector allows the LacZ bases blue-white screening strategy, meaning the clones successfully transformed with the insert can be easily identified on agar plates based on their colour. The successful ligation of each fragment was verified by restriction digests using specific restriction enzymes. As shown in Figure 44, the digestion of each construct resulted in the generation of 2 bands. The band approximately 3,000 bp in size present in all the lanes represents the pGEM-t-Easy vector. The smaller band around 537 bp in size in lane 1 represents the F1when digested with *KpnI* and *Bam*HI, this band

124

migrated to the expected size of 537 bp. Lane 2 represents a 397 bp fragment coding the F2. The band approximately 814 bp in size in lane 3 represents the F3.
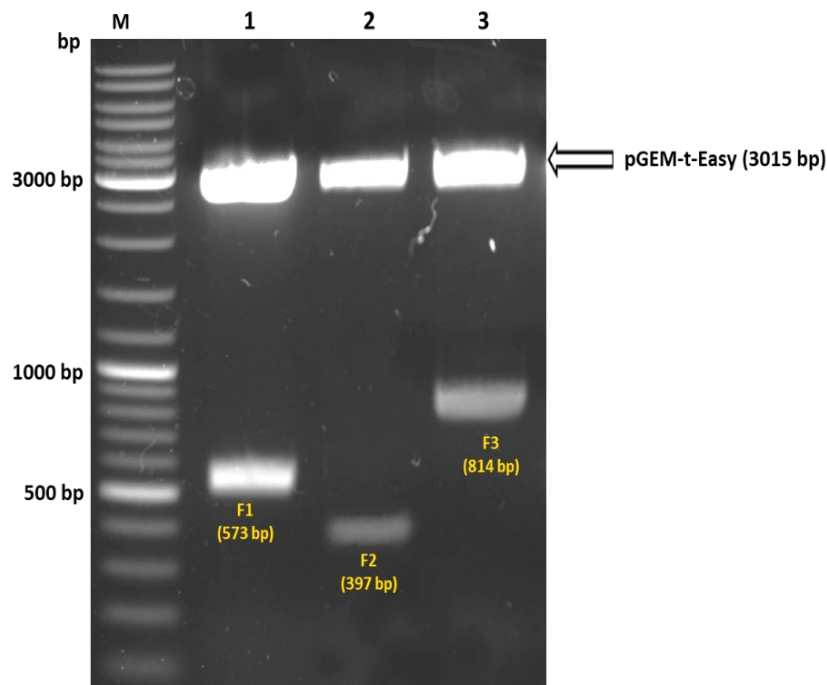
Figure 44. Agarose gel electrophoresis for restriction digests performed on the three fragments cloned into pGEM-T Easy vectors.
The plasmid of each fragment was digested with specific enzymes. (1) Restriction digest of the F1 with *KpnI* and *Bam*HI (573 bp product). (2) Restriction digest of the F2 with *PstI* and *Eco*R1 (397 bp product). (3) Restriction digestion of the F3 with *PstI* and *Bam*HI (814 bp). The band approximately ~3 kb in size present in all of the lanes represents the pGEM-T-Easy vector. [M] 1kb DNA ladder size markers (Thermo Scientific™ O'GeneRuler, UK).

The bands representing each of the inserted fragments were extracted from the agarose gel, purified using a Qiagen PCR purification kit (Qiagen, UK) and transformed into DH5α™ cells (Bioline) via heat shock transformation (Chapter 2, Section 2.5.8). The transformed cells were plated onto LA agar plates containing (100 mg/ml ampicillin, 100 mM IPTG and 50 mg/ml X-gal) and incubated overnight at 37°C. Moreover, plasmid extraction was performed on the white colonies, and the confirmation of each clone was performed by sequencing (GATC biotech) to ensure no mutations were introduced during the PCR amplification steps. The sequencing results revealed the presence of no mutations in all of the fragments, and the identity

of each clone was 100 %, as shown in Appendices 8.12, 8.13 and 8.14. Following sequencing, two vectors were used to ligate the chimeric construct (*rpfA-actA*). The first vector was pMV261 and the second was pMV306. The pMV261 vector is a replicative plasmid (multicopy & extrachromosomal) for *Mycobacterial* spp. It contains a DNA cassette encoding a kanamycin resistance, along with a heat shock promotor (hsp60) which allows for a high level of gene expression. The pMV261 plasmid has been used for complementation on certain occasions (Stover *et al.* 1991; Joseph *et al.* 2010; Movahedzadeh *et al.* 2011). In contrast, the pMV306 plasmid is a single copy plasmid which integrates into the *Mycobacterial* chromosome; it does not have a promotor and is most commonly used for complementation, as integrative plasmids have proved to be more advantageous for complementation experiments (Stover *et al.* 1991; Kumar *et al.* 1998; Movahedzadeh *et al.* 2011). The rationale behind using both of the aforementioned vectors is that it was not known which vector would suit the chimeric construct in the complementation experiment, and how the construct would behave in both of the vectors.

The ligation strategy used to insert the three fragments into pMV261 is illustrated in Figure 45. Briefly, pMV261 was digested with *PstI* and *EcoRI* in order to ligate the plasmid firstly with F3, which was digested with the same restriction enzymes (Figure 45). The digested pMV261 plasmid and F3 were electrophoresed on an agarose gel, extracted from said gel, purified using a Qiagen PCR purification kit (Qiagen, UK) and ligated following the protocol mentioned in Chapter 2 (section 2.5.7). After the ligation step, the clones were transformed into DH5α™ (Bioline) cells via heat shock transformation. The transformed cells were plated onto LA agar supplemented with kanamycin (50 mg/ml) and incubated overnight at 37°C. Thereafter, several colonies were selected, on which plasmid extraction was performed. Furthermore, restriction digests were performed using the restriction enzymes (*PstI* and *EcoRI*) relevant to the F3 fragment to confirm the presence of the insert in the vector, as illustrated in Figure 46. As displayed in the figure, lane 1 shows the undigested plasmid and Lane 2 shows the result of the double digestion for the pMV261-F3 construct; single bands at the expected sizes for both the pMV261 vector (~4,000 bp) and the F3 insert (~800 bp) are visible.

After confirming the correct insert was present, the pMV261-F3 plasmid was used as a template to ligate the second fragment (F2). F2 was ligated using the same strategy illustrated in Figure 45, but with different restriction enzymes. *PstI* and *Bam*HI were used in the restriction digest of the pMV261-F3 and F2 plasmids. The successful cloning of the pMV261-F3-F2 construct was confirmed via a double digestion reaction. Lane 3 of Figure 46 shows the undigested

pMV261-F3-F2 plasmid, whereas lane 4 shows pMV261-F3-F2 digested with *PstI* and *Bam*HI
. As can be seen, two single bands were obtained, with 4,488 bp product for pMV261 and a
397 bp product for the F2 fragment. The third fragment, F1, was cloned into pMV261-F3-F2
in a similar manner to the other fragments (Figure 45), however, with the use of *KpnI* and
*Bam*HI as the restriction enzymes. Within Figure 46, Lane 5 shows undigested pMV261::*rpfA-actA*, which is a chimeric construct cloned in pMV261. Lane 6 represents the digestion of the
final clone pMV261::*rpfA-actA* with *KpnI* and *Bam*HI producing two single bands at the
expected sizes of 4,488 bp (pMV261) and 537 bp (F3) respectively.
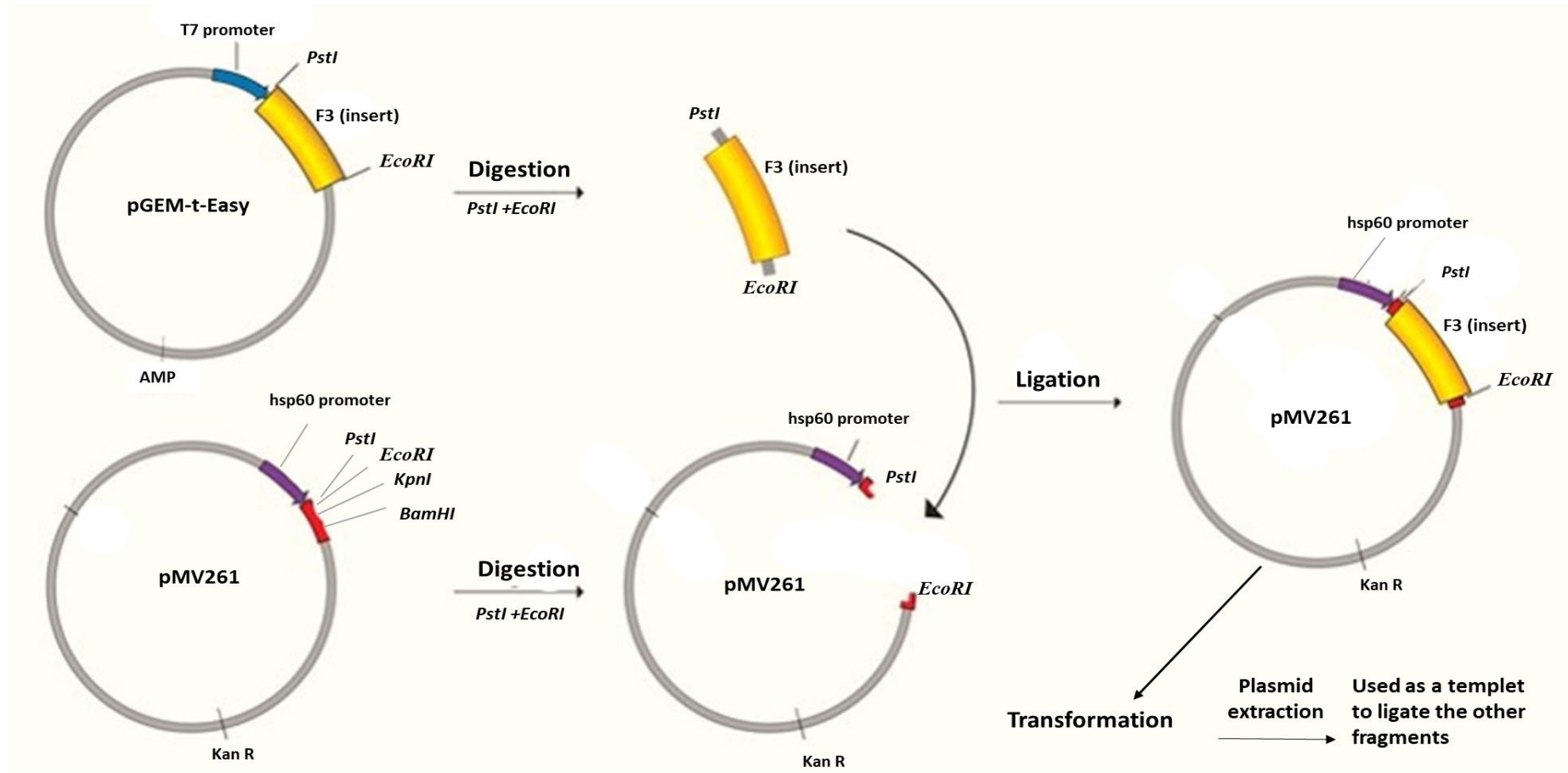
Figure 45. Schematic showing the cloning strategies to insert the F3 fragment into the pMV261 vector.
Shown here is the technique used to ligate and subclone F3 (downstream *rpfA* fragment) from the pGEM-T-Easy vector into the pMV261 vector.

Both the fragment and vector have the same restriction sites for cloning purposes.
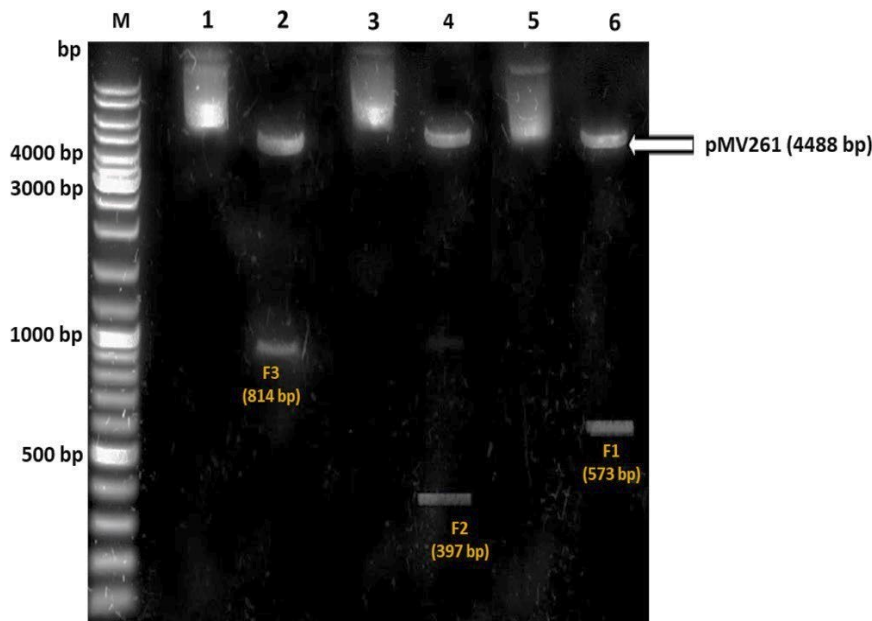
Figure 46. Agarose gel electrophoresis for the restriction digestion of the pMV261 cloned with fragments F1, F2 and F3.

The purified plasmid encoding the F1, F2 and F3 fragments were subcloned into the pMV261 vector. The three clones were verified by digestion with specific restriction enzymes. (1) Undigested pMV261-F3 insert. (2) pMV261-F3 digested with *PstI* and *EcoRI* resulting in the release of F3 (~800 bp). (3) Undigested pMV261-F3-F2. (4) pMV261-F3-F2 digested with *PstI* and *Bam*HI resulting in the release of a product approximately ~397 bp in size corresponding to the F2 insert. (5) Undigested pMV261::*rpfA-actA*. (6) pMV261::*rpfA-actA* digested with *KpnI and Bam*HI resulting in the release of the F1 (~573 bp). The band approximately 4,000 bp in size in lanes 2, 4 and 6 represents the pMV261 plasmid. [M] 1 kb DNA ladder size marker (Thermo Scientific™ O'GeneRuler, UK).

The successful cloning of the three fragments into pMV261, as shown in Figure 47A, was confirmed by a diagnostic restriction digest with different restriction enzymes. As illustrated in Figure 47B, single and double digestions were performed, and the products were ran on agarose gels. Lane 1 of Figure 47B represents the undigested pMV261::*rpfA-actA*. Lane 2 shows pMV261::*rpfA-actA* digested with *KpnI* and *EcoRI;* these restriction enzymes were selected as the chimeric insert contained the endonuclease restriction site *KpnI* at the 5' end and an *EcoR1* site at the 3' end, as shown in Figure 47A.

After the digestion, the expected products for the insert (1,800 bp) and vector (4,488 bp) were observed. Lane 3 of Figure 47B represents the products obtained after the double digest of pMV261::*rpfA-actA* with *KpnI* and *Bam*HI, resulting in the release of the F1 fragment (~573 bp) and the pMV261plasmid (4,488 bp). Lane 4 (Figure 47B) shows pMV261::*rpfA-actA* digested with *PstI* and *EcoRI*, which confirmed the presence of F3 with the correct molecular size of 814 bp. On the other hand, lanes 5, 6, 7 and 8 show the single digest of pMV261::*rpfA-actA* with *KpnI, Bam*HI, *PstI* and *EcoRI* respectively. All the single digests resulted in the production of clean single bands. The final lane (lane 9), shows the digestion of pMV261::*rpfA-actA* with *EcoRI* and *Bam*HI, resulting in the production of a single band approximately 1,200 bp in size representing the F2-F3 fragment, and a second band for the pMV261 plasmid (4,488 bp). Overall, the analysis of the agarose gel electrophoresis data in Figure 47B shows the successful ligation of all the fragments into pMV261, as the different restriction enzymes digested the chimeric construct (pMV261::*rpfA-actA*) as expected, resulting in bands corresponding to the correct molecular sizes of the chimeric insert and vector.
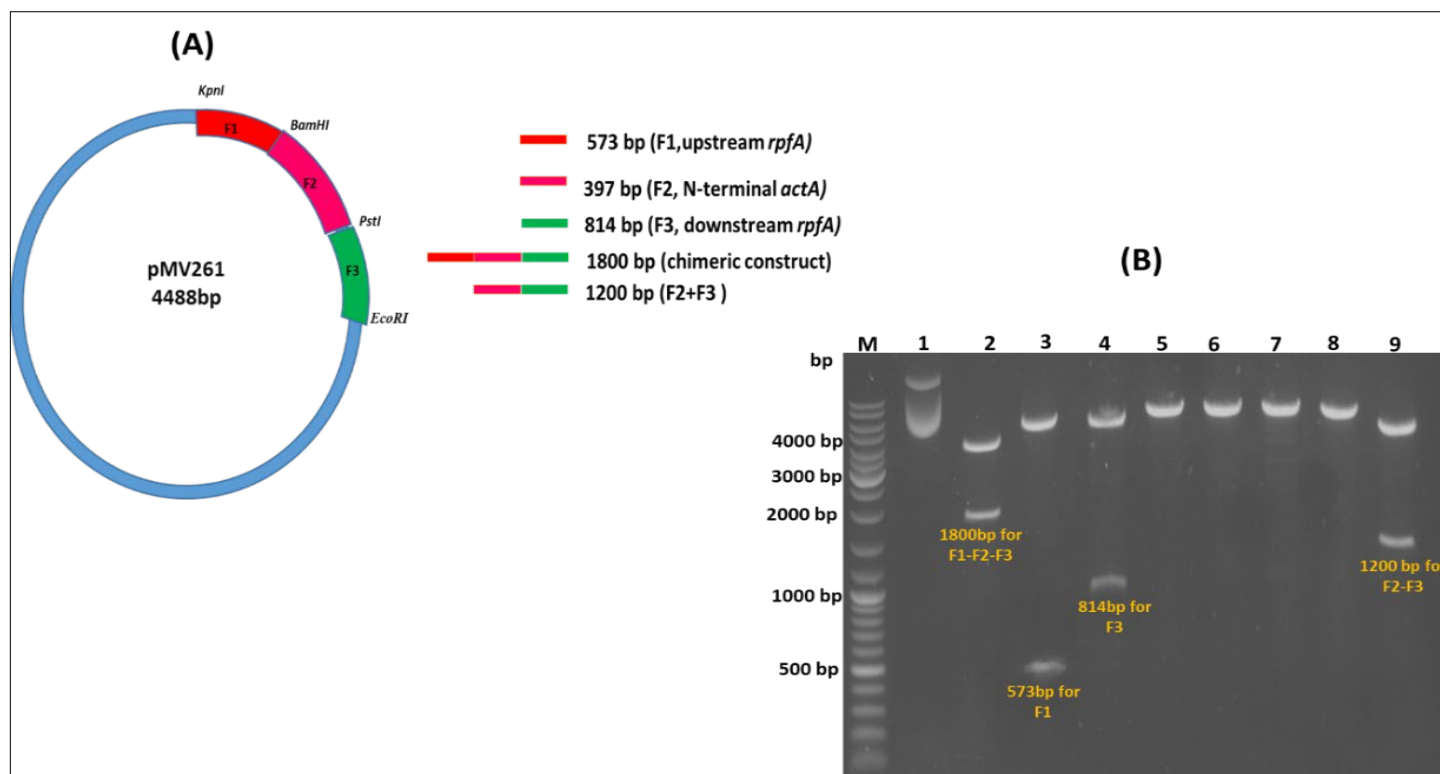
Figure 47. Diagnostic digest of the pMV261::*rpfA-actA* with different restriction enzymes.
(A) Schematic showing the *rpfA-actA* gene cloned into pMV261. (B) Restriction digest of pMV261::*rpfA-actA* with different restriction enzymes: (1) undigested pMV261. (2) pMV261::*rpfA-actA* digested with *KpnI* and *EcoRI* resulting in product at the expected size of 1,800 bp. (3) Double digest of pMV261::*rpfA-actA* with *KpnI* and *BamHI* producing fragments corresponding to F1 (573 bp) and pMV261(4,488 bp). (4) Digestion of *PstI* and *EcoRI* showing the F3 fragment (814 bp). (5), (6), (7) and (8) show the single digest of pMV261::*rpfA-actA* with *KpnI, BamHI, PstI* and *EcoRI*, respectively. (9) Digestion of pMV261::*rpfA-actA* with *EcoRI* and *BamHI* firstly resulting in the production of a band approximately 1,200 bp in size for the ligated inserts of F2 with F3, and secondly a band for the pMV261 vector. The upper bands in (2), (3), (4) and (9) correspond to the pMV261 plasmid (~4,000 bp). (M) 1 kb DNA ladder size marker (Thermo Scientific™ O'GeneRuler, UK).

131

The final cloning step was to use the alternative pMV306 vector to ligate the chimeric insert (*rpfA-actA*) by digesting pMV261::*rpfA-actA* with *KpnI* and *EcoRI* in order to subclone *rpfA-actA* into the pMV306 vector (which was digested with the same restriction enzymes). The pMV306 vector was ligated with the *rpfA-actA* gene and then transformed into DH5α™ cells (Bioline). In order to confirm that the chimer was correctly inserted, the restriction enzymes *KpnI* and *EcoRI* were used as illustrated in Figure 48. Lane 1 (Figure 48) shows the undigested pMV306::*rpfA-actA* plasmid, and lane 2 shows the result of the digestion of pMV306::*rpfA-actA*, which produced a small single band of approximately 1,800 bp corresponding to the expected size of the *rpfA-actA* insert, and another band approximately ~4,000 bp in size representing the pMV306. This generated construct was then used for the complementation experiments.
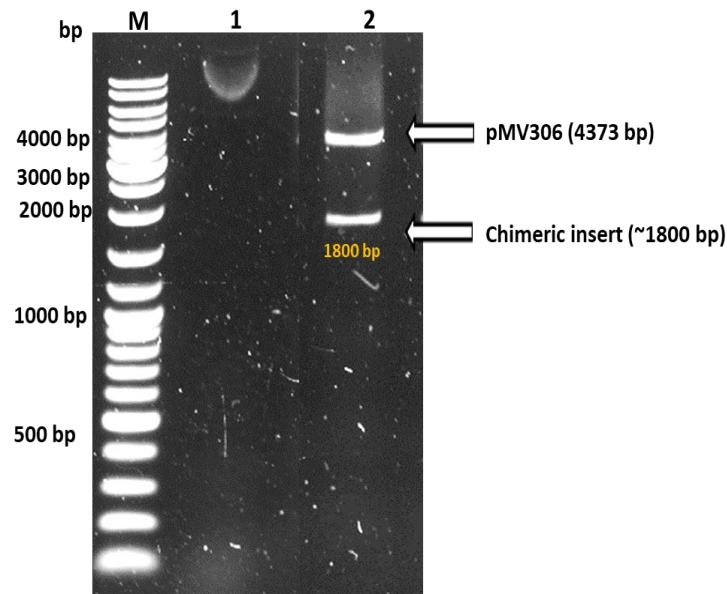
Figure 48. Agarose gel electrophoresis for the restriction digests of pMV306::*rpfA-actA*. (1) Undigested pMV306::*rpfA-actA* (2) Digestion of pMV306::*rpfA-actA* with *KpnI* and *EcoRI*, resulting in the release of a band approximately 1,800 bp in size relating to *rpfA-actA* (chimeric insert) and a second band corresponding to the pMV306 vector (~4 kb).

6.2.3 Complementation of ΔrpfABE and wild type *M. marinum* with pMV306::*rpfA-actA*

A triple deletion mutant (Δ*rpfABE*) *M. marinum* strain was generated previously by Dr. *Mariam Noor* (University of Leicester); this was chosen to be used alongside wild type *M. marinum* to study the effects of complementation with *rpfa-actA*. The reason for this is that the Δ*rpfABE* strain showed a significant growth defect when plated on Middlebrook 7H11 in comparison with the *M. marinum* wild type strain (unpublished data, Dr. Mariam Noor). Additionally, the introduction of the *rpfA* gene from Mtb into the Δ*rpfABE* strain complemented the initially observed growth defect. Thus, the effect of the chimeric construct on the growth of *M. marinum* strains (wild type and Δ*rpfABE*) was investigated by introducing the pMV306::*rpfA-actA* plasmid into *M. marinum* wild type and Δ*rpfABE* competent cells, as described in Chapter 2 (Sections 2.3.6 and 2.5.10).

Several plasmids were used in the complementation experiment as follows: (i) pMV306::*rpfAMtb*, which was used as a positive control. It was generated by Dr. Sarah Glenn (University of Leicester). The reason for using this plasmid was to show the effect of the *rpfA* gene. According to unpublished data from Dr. Mariam Noor, the plasmid completely complemented the Δ*rpfABE M. marinum* and improved growth. (ii) Empty plasmid (pMV306); this was used as a negative control to ensure that any effects noticed after complementation was not due to other components of the plasmid. (iii) The pMV306::*rpfA-actA*, this is a chimeric plasmid which have the upstream region of *rpfA* (F1), the downstream region of *rpfA* (F3) and the NH2–terminal region of *actA* gene (F2). All strains were electroporated and tested for their ability to grow on 7H11. Moreover, Δ*rpfABE* and wild type *M. marinum* control strains (cells not electroporated with the plasmids) were plated to visualise the growth differences between those which had been observed previously (unpublished data, Dr. Mariam Noor).

After 12 days of incubation on 7H11, the confirmation of the successful electroporation of all the strains with the plasmids was performed by colony PCR using pMV306 F&R primers (Chapter 1, Table 4). Analysis of the PCR products was performed by agarose gel electrophoresis as shown in Figure 49, along with the purified plasmids (pMV306::*rpfAMtb*, pMV306 and pMV306::*rpfA-actA*). The first three lanes in Figure 49A show the different controls used: Lane 1 shows the pMV306 plasmid which migrated to the expected size of ~250 bp.

Lane 2 represents the un-electroporated pMV306::*rpfA-actA* plasmid which migrated to the expected size of 1,800 bp. Lane 3 shows the un-electroporated pMV306::*rpfAMtb* plasmid migrating to the expected size of 1,500 bp. The other three lanes in the same figure (Figure 49A) show the PCR products of the electroporated plasmids in *M. marinum ΔrpfABE* as follows: Lane 4 shows a single band approximately 250 bp in size for pMV306 transformed into *ΔrpfABE*. Lane 5 shows a band approximately 1,800 bp in size for the pMV306::*rpfA-actA* electroporated into Δ*rpfABE*. Lane 6 shows the band (~1,500 bp) for the pMV306::*rpfAMtb* plasmid electroporated into Δ*rpfABE*. The results shown in Figure 41A indicate that all the plasmids were electroporated successfully into *M. marinum ΔrpfABE*, as all the constructs produced bands corresponding to the expected size when screened with the pMV306 the primers. Furthermore, Figure 49B shows similar data to Figure 49A, but for the constructs electroporated into the wild type *M. marinum*. Overall, the results revealed that the electroporation of the plasmids into both strains was successful.
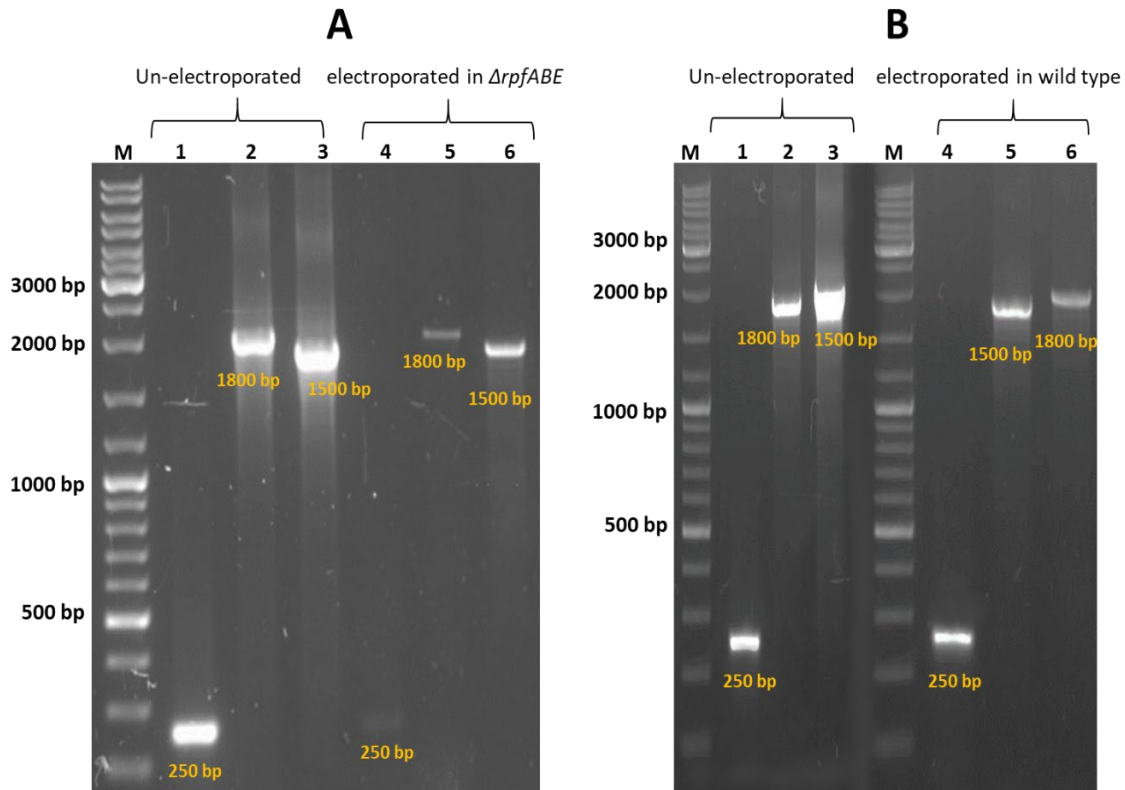
Figure 49. Agarose gel electrophoresis showing the successful electroporation of the different plasmids into *M. marinum ΔrpfABE* wild type.

Colony PCR screening using the pMV306 F&R primers was performed for all the constructs which were electroporated into both *M. marinum ΔrpfABE* and the wild type *M. marinum*. (A) represents different controls and constructs electroporated into the *ΔrpfABE M. marinum* strain are as follows: (A1) Un-electroporated pMV306 plasmid (~250 bp). (A2) Un-electroporated pMV306::*rpfA-actA* plasmid migrating to the expected size of 1,800 bp. (A3) Un-electroporated pMV306:: *rpfAMtb* (1,500 bp). (A4) Single band approximately 250 bp in size for *ΔrpfABE* transformed with pMV306. (A5) Single band approximately 1,800 bp in size for *rpfA-actA* electroporated into *ΔrpfABE*. (A6) Single band (~1,500 bp) for pMV306:: *rpfAMtb* electroporated into *ΔrpfABE*. In (B) : from B1 to B3 Similar controls to that used in (A). The B4 to B6 are pMV306, pMV306::*rpfAMtb* and pMV306::*rpfA-actA* electroporated into the wild type *M. marinum* strain.

After successful electroporation, the strains were used for growth experiments. The *ΔrpfABE M. marinum* and wild type *M. marinum* strains were serially diluted and plated on 7H11, as illustrated in Figure 50A. The *ΔrpfABE* mutant *of M. marinum* (Figure 50A, lane 4) displayed a pronounced plating phenotype, with delayed colony formation and a growth defect when compared with the wild type *M. marinum* (Figure 50A, lane 5). The delay in colony formation was also observed with the *ΔrpfABE* strain electroporated with the pMV306 plasmid (negative control vector), as shown in lane 2 (Figure 50A).

The chimeric construct had a toxic effect on the triple mutants by inhibiting growth, as illustrated in lane 3 (Figure 50A). These toxic effects are thought to be due to the expression of the chimeric construct as opposed to influencing factors on the plasmid backbone. This is because the *ΔrpfABE::*pMV306 empty vector in lane 2 showed the same colony phenotype as the *ΔrpfABE M. marinum* (lane 4). Conversely, the pMV306:: *rpfAMtb* in lane 1 (Figure 50A), which was used as a positive control, resulted in a colony formation similar to that observed in the wild type *M. marinum* (Figure 50A, lane 5) and resulted in the complete reversal of the delayed colony forming phenotype observed in the *ΔrpfABE M. marinum*, as expected. The final lane in Figure 50A (lane 6) shows the colony morphology of the wild type *M. marinum* containing pMV306::*rpfA-actA*; the growth appeared to be equivalent to the wild type *M. marinum* in lane 5. Given this, the results indicate that the chimeric construct has no toxic effect in the wild type strain, but it was not able to complement *ΔrpfABE M. marinum.*

Furthermore, the growth of all the plated strains in Figure 50A were also assessed by CFU counts, as shown in Figure 50B. The results of the CFU counts revealed an approximately two-fold decrease in growth between the *M. marinum* wild type (Figure 50A, column 5) and *ΔrpfABE* (Figure 50A, column 4) throughout the 12 days of incubation on 7H11. The two-fold CFU reduction observed with the *ΔrpfABE* strain was statistically significant with a P value of 0.0076 (unpaired t-test analysis, P-value of <0.05 to be significantly different). This result supports the observed phenotype (growth defect) between the two strains when plated out (Figure 50A). In addition, there was a significant difference in CFU counts between the *ΔrpfABE* strain electroporated with pMV306::*rpfA-actA* (Figure 50A, column 3) and *ΔrpfABE* containing pMV306 (Figure 50A, column 2), the p-value was 0.02 (unpaired t-test analysis, P-value of <0.05 to be significantly different). This result is consist with what is shown in Figure 50A, and explains the major growth defect observed with the *ΔrpfABE* strain electroporated with pMV306::*rpfA-actA* when compared to *ΔrpfABE* electroporated with pMV306 (empty

vector). Column 1 of Figure 50B shows the CFU counts of the *ΔrpfABE* strain electroporated with pMV306::*rpfAMtb*. A substantial increase in CFU counts can be observed when compared to *ΔrpfABE* electroporated with pMV306 (empty vector), suggesting that the pMV306::*rpfAMtb* plasmid could have induced the same phenotype as the wild type. However, the cells may have needed more incubation time in order to present with a similar phenotype to the wild type strain.

Therefore, the plates shown in Figure 51 were incubated for a further two weeks (Figure 51A) and three weeks (Figure 51B), as it was thought that a further incubation period may aid to see more obvious morphological differences in the complemented strains. The further incubation of ΔrpfABE complemented with pMV306::*rpfA-actA* did not improve the colonies growth, as shown in Figure 51.

In Figure 51A and Figure 51B, the delayed colony formation of *ΔrpfABE* (lane 4), Δ*rpfABE* electroporated with pMV306 (lane 2) and Δ*rpfABE* electroporated with pMV306::*rpfA-actA* (lane 3), was more pronounced when given further incubation time. In contrast, the colony morphologies of the *M. marinum* cells electroporated with pMV306::*rpfAMtb* in lane 1 in both Figure 51A and Figure 51B were similar to the wild-type strain, which showed no delayed in colony formation. In addition, it was not possible to carry out the CFU counts for the plates incubated for two and three weeks as the colonies merged and became uncountable, as shown in Figure 51A and Figure 51B.
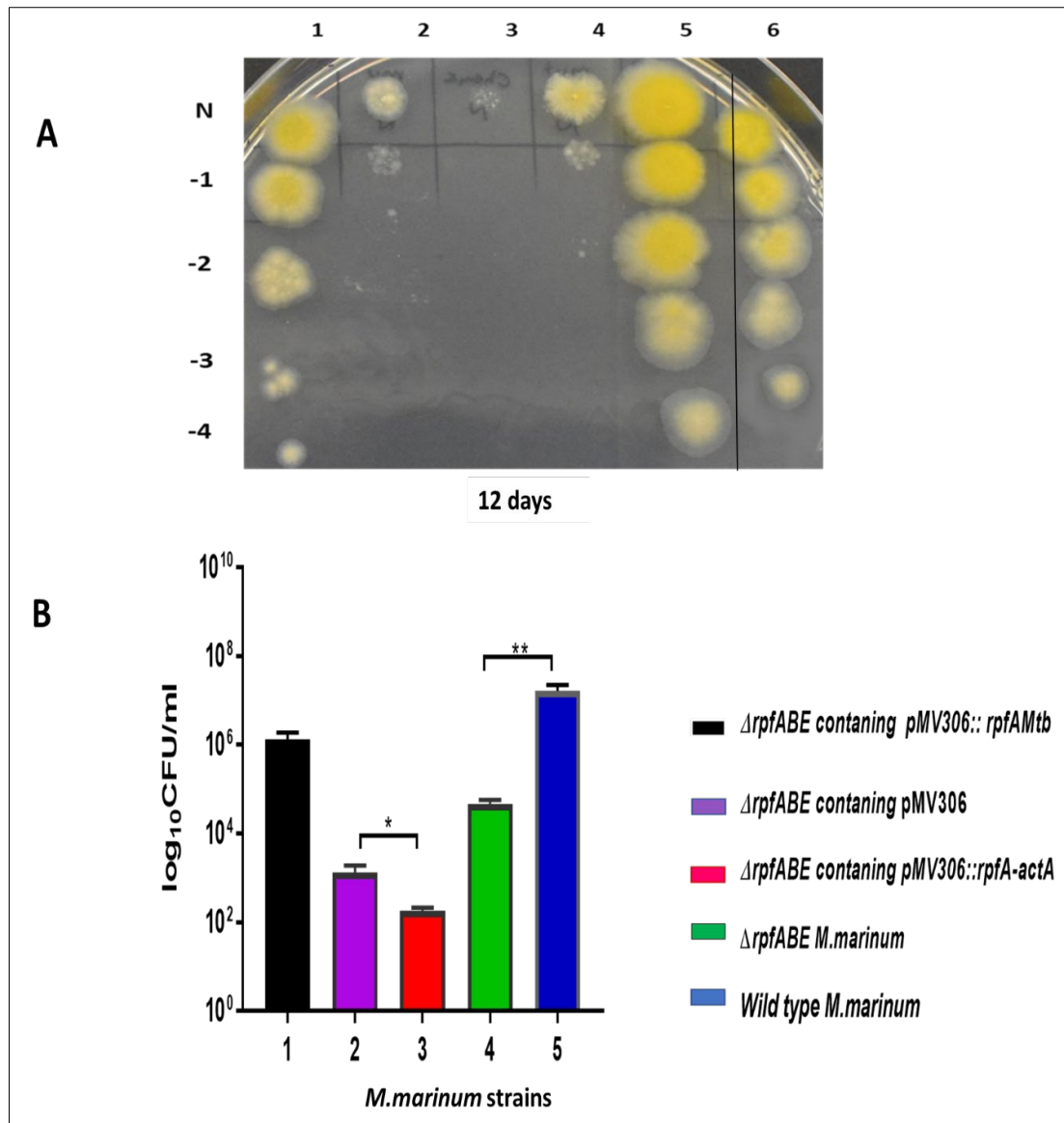
Figure 50. Growth of *M. marinum* WT and *ΔrpfABE M. marinum* in 7H11 media.
(A) Colony morphology of the selected strainsw hich were serially diluted, plated onto
Middlebrook 7H11 agar plates and incubated for 12 days before analysing growth. (1) *M.
marinum ΔrpfABE* with pMV306::*rpfAMtb*. (2) *M. marinum ΔrpfABE* with pMV306. (3) *M.
marinum ΔrpfABE* with pMV306::*rpfA-actA*. (4) *M. marinum ΔrpfABE*. (5) Wild type *M.
marinum*. (6) Wild type *M. marinum* with pMV306::*rpfA-actA*. (B) CFU counts over 12 days
on the complemented strains. The graph represents data of three independent experiments.
Unpaired t-test analysis performed to show any statistically differences (* = p <0.05, ** = p
<0.01).
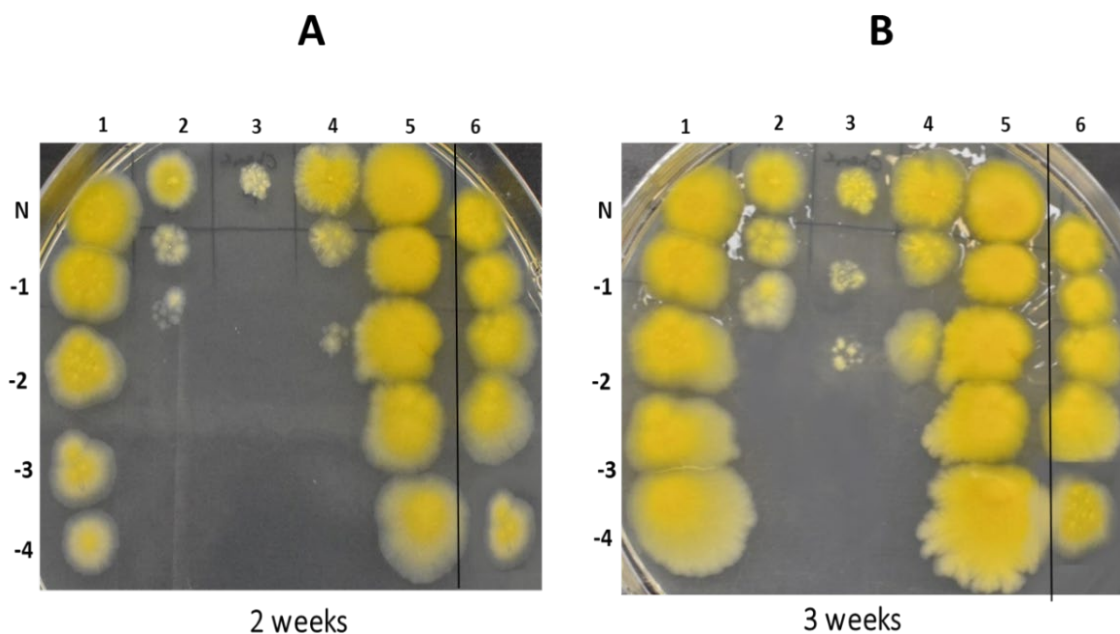
Figure 51. Growth of *M. marinum* WT and *ΔrpfABE M. marinum* in 7H11 media incubated for two and three weeks.

The cultures of selected strains were serially diluted, plated onto Middlebrook 7H11 agar plates and incubated for two weeks (A) and three weeks (B) before analysing growth. (1) *M. marinum ΔrpfABE* with pMV306::rpfAMtb. (2) *M. marinum ΔrpfABE* with pMV306. (3) *M. marinum ΔrpfABE* with *rpfA-actA*. (4) *M. marinum ΔrpfABE*. (5) Wild type *M. marinum*. (6) Wild type *M. marinum* with *rpfA-actA*.

To confirm expression of RpfA and RpfA-ActA chimeric protein culture supernatants (done by Dr.Vivak, University of Leicester) were prepared from *M. marinum* strains and used for Western bolt analysis as previously described (Mukamolova *et al.* 2002). Briefly, wild type M. *marinum*, *ΔrpfABE* containing pMV306::*rpfA-actA, ΔrpfABE* containing pMV306:: *rpfAMtb* and *ΔrpfABE* were grown Sauton's medium to OD_{580} 1.0 following the protocol mentioned in (Mukamolova *et al.* 2002)**.** As Figure 52, shows RpfA appeared in WT supernatant as ~48kDa band which was recognised by anti-Rpf polyclonal antibody (lane 2). This band was missing in *ΔrpfABE* mutant (lane 1). However *ΔrpfABE* strains containing either pMV306::*rpfAMtb* (lane 3) or pMV306::*rpfA-actA* (lane 4) also produced 48kDa band, suggesting that these strains produced RpfA or chimeric RpfA-ActA.
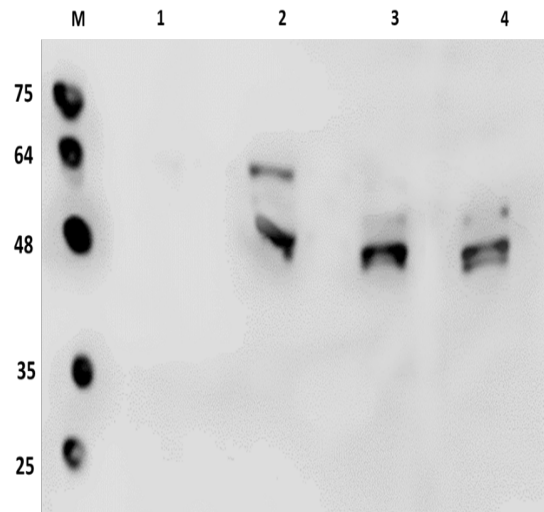
Figure 52. Detection of the RpfA and RpfA-ActA proteins in culture supernatants from *M. marinum* strains via a Western blot.
Western blot with primary polyclonal anti-Rpf antibodies (1:3,000) and secondary anti-sheep antibodies (1:10,000) used to detect RpfA protein in the culture supernatant of *M. marinum* strains. (1) Culture supernatant of *M. marinum ΔrpfABE*. (2) Culture supernatant of *M. marinum* wild type. (3) Culture supernatant of *M. marinum ΔrpfABE* containing pMV306:: *rpfAMtb* .(4) Culture supernatant of *M. marinum ΔrpfABE* containing pMV306:: *rpfA-actA*. Lane (2), (3) and (4) show the expression of RpfA protein at the expected size of ~48 kDa. [M] Prestained Protein Ladder (Geneflow, UK).

6.3 Discussion

In this chapter, the growth of a wild type and an Δ*actA* mutant strains of *L. monocytogenes* was assessed. The results revealed that the deletion of the *actA* gene had no impact on the growth of *L. monocytogenes* when assayed in a rich medium (TSB) and minimal medium (MWB). Both strains grew similarly according to optical density measurements and CFU counts for all the mentioned time points. This phenomenon has been mentioned before in several articles, where the growth of two strains i.e wild type and Δ*actA L. monocytogenes* were compared intracellularly (Guzman *et al.* 1995; Mitchell *et al.* 2015).

The great challenge faced in the work mentioned in this chapter was in generating the novel chimeric construct by merging portions of two genes from different organisms to form a new gene. Moreover, many scholars have reported the success of this technique for generating novel

genetic material (Voigt *et al.* 2002; Rogers *et al.* 2009; Rogers and Hartl 2011). Examples of useful advantages of domain swapping include: improving protein structure or function, enhancing the catalytic and non-catalytic properties of proteins and creating a protein with novel activity (Nixon *et al.* 1998; Ostermeier and Benkovic 2001). Nixon *et al.* reported a hybrid b-glucosidase that conferred special properties i.e being optimally active at pH 6.6-7.0 and 45-50 °C, in comparison with the parent enzymes, of which the *Agrobacterium tumefaciens* b-glucosidase had optimal activity at pH 7.2–7.4 and 60°C and the *Cellvibrio gilvus* b-glucosidase had optimal activity at pH 6.2–6.4 and 35°C (Nixon *et al.* 1998). In addition, domain swapping between two highly homologous enzymes from different species is very common, this is done in order to ameliorate certain undesireable properties, such as insufficient thermal stability (Olsen *et al.* 1991). For instance, the hybrid *Bacillus* β-glucanase, which has a high level of thermostability and tolerance towards acidic conditions, was generated by domain swapping between two homologous β-glucanase enzymes (74% homology) from *Bacillus amyloliquefaciens* and *Bacillus macerans* (Olsen *et al.* 1991). However, the role and behavior of chimers as a source of phenotypic novelty is unpredictable (Rogers and Hartl 2011). Unfolded proteins or low levels of activity have been observed with some hybrid enzymes (Hosseini-Mazinani *et al.* 1996; Nixon *et al.* 1998).

In this study, the purpose of domain swapping was to investigate the phenotypic effects of the chimeric construct (pMV306::*rpfA-actA*) originating from *rpfA* and *actA* genes (specifically the NH2-terminal domain). This would help to characterize the activity detected in ActA, by proving the functional redundancy between the *rpfA* and *actA* genes. The pMV306::*rpfA-actA* construct was successfully generated, and the effect on cell phenotype was studied in the complementation experiments with the *M. marinum* Δ*rpfABE* strain. Previously, a triple mutant of *M. marinum* lacking three genes (*rpfA, rpfB* and *rpfE*) was generated in our Lab (unpublished data, Dr. Mariam Noor, University of Leicester). The *M. marinum* Δ*rpfABE* strain displayed a distinct plating phenotype, evident by the delayed colony formation on Middlebrook 7H11 agar, in comparison with wild type *M. marinum*. Furthermore, Dr. Mariam Noor showed that the *rpfA* gene of *Mycobacteria tuberculosis* had the ability to completely complement the *M. marinum* Δ*rpfABE* phenotype by improving the growth defect observed (unpublished data, Dr. Mariam Noor, University of Leicester). Thus, it was used as a positive control in this study.

The complementation results obtained in the current study confirmed the previous unpublished findings of Dr. Mariam Noor, these being that the *ΔrpfABE* strain electroporated with

pMV306:: *rpfAMtb* grew similarly to the *M. marinum* wild type. Importantly, the growth defect of *M. marinum* ΔrpfABE was not reversed by genetic complementation with the pMV306:: *rpfA-actA* chimeric construct. In addition, the growth of the ΔrpfABE strain containing pMV306::*rpfA-actA* in 7H11 was not as good as the growth of ΔrpfABE strain with pMV306 (empty vector control), which indicates the toxic effect of the chimer on the ΔrpfABE strain. Furthermore, Western blot analysis was performed on culture supernatants obtained from M.*marinum* strains. Results confirmed that RpfA protein was expressed in both ΔrpfABE strain containing pMV306::*rpfA-actA* and ΔrpfABE strain containing pMV306:: *rpfAMtb*. However, the results mentioned above suggests that the chimeric protein RpfA::ActA protein could not substitute the RpfA protein.

The effect of the chimeric construct on the growth of *M. marinum ΔrpfABE* was not entirely surprising, because, as mentioned previously by Arguello *et al*. (Arguello *et al.* 2007) and others (Rogers and Hartl 2011), less is known about the behavior of chimeric genes through recombination events at the DNA level (Foster *et al.* 2002). Moreover, the generated chimeric gene could behave differently from the parent genes in terms of localization, regulation and even function (Rippey *et al.* 2013).

Chapter 7

Final discussion

Peptidoglycan remodelling is important for many physiological processes such as cell growth, division, and adaptation to stressful conditions (Höltje 1995; Popowska 2004; Vollmer and Bertsche 2008). Therefore, the enzymes involved in PG remodelling are attractive targets for the development of antibiotics, especially with the increasing prevalence of multidrug-resistant bacterial strains (Han *et al.* 2011; Jenkins *et al.* 2019). Characterisation of the proteins involved in PG synthesis, hydrolysis and remodelling, as well as understanding the functional interactions of these proteins, will help to establish these novel drug targets.

To date, seven *L. monocytogenes* autolysins have been identified, including two Rpf-like proteins, Lmo0186 and Lmo2522 (Popowska 2004; Popowska and Markiewicz 2006; Pinto *et al.* 2013). It is likely that Lmo0186 and Lmo2522 are lytic transglycosylases, similar to the Rpf proteins. LTGs are enzymes that cleave the β-1,4-glycosidic bond between N-acetylmuramic acid and N-acetylglucosamine in PG to permit the remodelling of the cell wall and the insertion of newly synthesised material during cell elongation and division (Ravagnani *et al.* 2005; Scheurwater *et al.* 2008; Vollmer *et al.* 2008). We propose that the ActA protein is also a lytic transglycosylase and that it aids PG biosynthesis and remodelling in *L. monocytogenes.*

ActA is a well-studied protein with many functions (shown in Figure 53). Beyond the polymerisation of host cell actin, ActA facilitates bacterial escape from the phagosome (Poussin and Goldfine 2010), mediates bacterial escape from host autophagic recognition (Yoshikawa *et al.* 2009) and has a role in epithelial cell invasion (Suárez *et al.* 2001). Strikingly, the deletion of *actA* affected cell aggregation, which led to the inhibition of biofilm formation and decreased ability of *L. monocytogenes* to persist for long periods within the cecum and colon lumen of mice (Travier *et al.* 2013). In addition, ActA has been shown to mediate the PG biosynthesis of *L. monocytogenes* during macrophage infection (Siegrist *et al.* 2015). These different roles are presumably associated with the different domains of ActA. In particular, ActA contains three domains: first is the the N-terminal domain, which is important in actin polymerization (Kocks *et al.* 1992; Lauer *et al.* 2001). Second is the central domain, which has proline-rich repeats that are critical for the *L. monocytogenes* actin-mediated motility (Footer *et al.* 2008; Travier *et al.* 2013). Last is the C-terminal domain, which has a hydrophobic region which anchors the protein to the bacterial surface (Poussin and Goldfine 2010; Travier *et al.* 2013). ActA is a secreted protein and is produced during growth both *in vitro* and *in vivo* (Lathrop *et al.* 2008; Garcia-del Portillo *et al.* 2011; Halbedel *et al.* 2014).
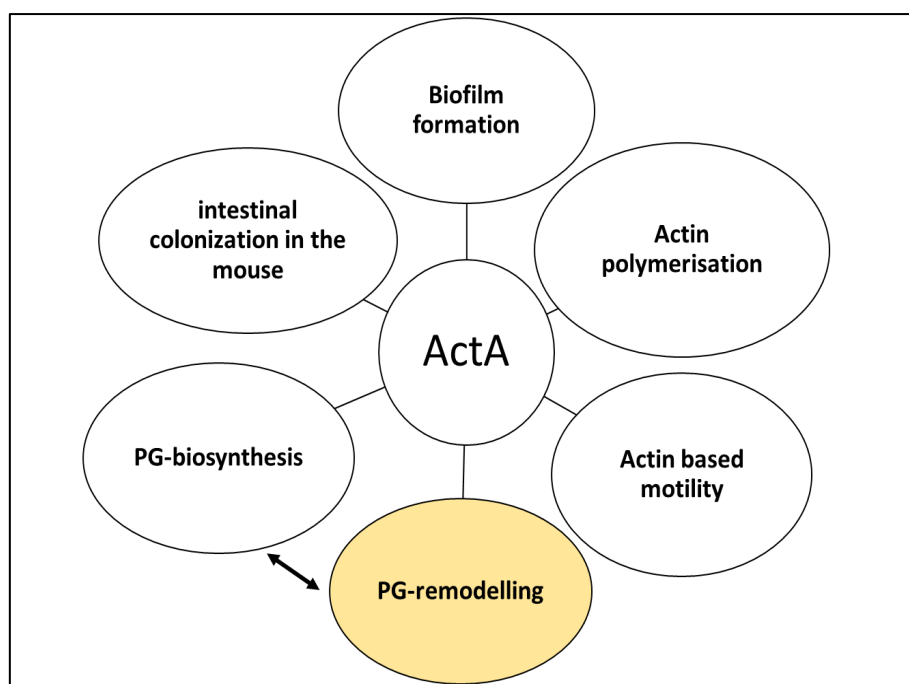
Figure 53. Schematic depicting the proposed functions of ActA from *L. monocytogenes.*

This project aimed to characterise the previously observed PG cleaving activity of ActA (Iakobachvili 2014) and establish the biological role of this activity in the growth of *L. monocytogenes*. To achieve this goal, a multidisciplinary approach was taken to generate and purify three truncated recombinant ActA proteins and establish the specific domain responsible for the cleavage of PG. Furthermore, 14 protein variants of the N-terminal domain of ActA (Chapter 3) were generated and their activity was assessed (Chapter 4). Other approaches included crystallisation attempts to solve the structure of the N-terminal domain of the ActA protein (Chapter 3), ActA localisation studies (Chapter 5) and domain swapping experiments to probe the role of ActA in growth by attempting to complement the growth defects of a triple mutant strain of *M. marinum* ($\Delta rpfABE$) (Chapter 6).

To determine the specific domain of ActA responsible for the PG cleaving activity, three recombinant truncated versions of ActA (ActA$_{A30-S157}$, ActA$_{A30-N233}$ and ActA $_{G393-N639}$) were successfully expressed, purified and studied *in-vitro*. PG cleaving activity was detected in the N-terminal domain of ActA, which was able to cleave the cell wall of *M. luteus* when studied via zymography assays and it was also found to be active against FITC-labelled PG of *E. coli*. Moreover, the cleavage activity of the N-terminal proteins abolished when it was subjected to heat inactivation. The protein lysate extracted from control cells transformed with an empty control vector were not found to have any of this cleavage activity. Moreover, the C-terminal

domain (ActA$_{G393-N639}$) was found to have no PG cleaving activity. This phenomenon is common in PG cleaving proteins, where the activity is allocated to a specific domain. For example, the N-terminal domain of the *M. luteus* Rpf possesses PG cleaving activity, and the C-terminal LysM domain is necessary for binding to the cell wall (Mukamolova *et al.* 2006; Kana and Mizrahi 2010). In *L. monocytogenes,* the PG cleaving proteins Auto and Ami are surface associated and contain two domains: an N-terminal amidase domain (enzymatic domain) and a C-terminal cell wall-anchoring domain (Cabanes *et al.* 2004; Popowska 2004).

Several protein variants (14 SDM proteins) of the N-terminal domain were generated in order to identify the catalytic residues that are critical for the PG cleaving activity. The residue mutation which completely abolished the PG cleaving activity was not identified. However two mutant variants, MUT-3 and MUT-6, in which specific glutamatic acid and aspartate residues were replaced with alanine, had impaired activity following the strategy proposed by Lauer *et al*. (Lauer *et al.* 2001). The partial reduction of PG cleaving activity when the presumptive catalytic residue was altered has previously been shown for other LTGs. For example, the activity of the muralytic Rpf protein of *M. luteus* was reduced, but not completely abolished, when the invariant glutamate residue was altered (Mukamolova *et al.* 2006). The FlgJ protein from *S. typhimurium* has PG cleaving activity, and this activity was partially decreased when the catalytic amino acid (glutamate-223) was substituted (Nambu *et al.* 1999).

To establish the bonds cleaved by ActA, an analysis of the PG cleaved by ActA was attempted. For this, *L. monocytogenes* PG incubated with ActA$_{A30-S157}$ was loaded onto a Prontosil 120 C18 column; however, no soluble muropeptides were detected in HPLC experiment. There are several examples of PG cleaving enzymes where the products of PG cleavage could not be identified via HPLC e.g.LtgG of *B. pseudomallei*, Cwp19 of C.*difficile* and RlpA of *P. aeruginosa* (Jorgenson *et al.* 2014; Wydau-Dematteis *et al.* 2018; Jenkins *et al.* 2019) .

The results of the ActA localization studies performed showed that the protein could be detected in the culture supernatants of *L. monocytogenes* using anti-ActA antibodies, in accordance with other previously published findings (Lathrop *et al.* 2008; Garcia-del Portillo *et al.* 2011). Other *L. monocytogenes* cell wall cleaving enzymes have been detected in culture supernatants e.g. P45 and p60 (Ruhland *et al.* 1993; Schubert *et al.* 2000; Popowska 2004). Rpf-like proteins have been detected in the culture supernatants of actively growing cultures of *M.tuberculosis, M. smegmatis* and *M. bovis* BCG (Mukamolova *et al.* 2002; Loraine *et al.* 2016).

Furthermore, in this work, ActA was detected in the membrane/cell wall fractions of ActA using mass-spectrometry; this provided an opportunity for the investigation into the putative ActA partners. PG cleaving enzymes often make complexes with other enzymes to ensure the controlled enlargement of the PG sacculus by cleaving the bonds in PG and allowing for the insertion of new PG subunits (Höltje 1995; Vollmer and Bertsche 2008). For instance, in *E. coli,* the interaction between a bifunctional penicillin-binding protein(PBP1B) and FtsI (PBP3) has been demonstrated, suggesting that this protein complex is important for the synthesis of PG in the division septum (Vollmer and Bertsche 2008). In *Mycobacteria*, two resuscitation-promoting factors, RpfE and RpfB, have been shown to interact with RipA, a secreted endopeptidase, allowing for the efficient digestion of the mycobacterial cell wall (Hett *et al.* 2007; Hett *et al.* 2008). RipA was also shown to be able to interact with the PG-synthase PonA1 ,a penicillin-binding protein (Squeglia *et al.* 2019).However, due to time constraints, immunoprecipitation experiments and the identification of ActA partners could not be performed.

ActA has been shown to have approximately 50% homology with the RpfA protein. (Iakobachvili 2014). Previously, it has been shown that domain swapping can be used for confirming the functions of specific protein; however, the behaviour of chimeric (hybrids) proteins can be unpredictable (Nixon *et al.* 1998; Foster *et al.* 2002). For example, the RTEM-1 beta-lactamase from *E. coli* and the beta-lactamase from *Proteus vulgaris* have 37% similarity, however, the hybrid protein generated by domain swapping between these two proteins yielded an inactive enzyme (Hosseini-Mazinani *et al.* 1996).

There is currently no indication within the literature that ActA is important for growth. To probe whether ActA may have an effect on stimulating growth, complementation experiments were performed along with an attempt to generate a chimeric construct consisting of the *rpfA* from *M. tuberculosis,* where the Rpf domain was replaced with the N-terminal domain of ActA (pMV306::*rpfA-actA*). We confirmed that the chimeric protein (RpfA-ActA) was secreted in the Δ*rpfABE* strain electroporated with the pMV306::*rpfA-actA* plasmid. However, this strain had an even more pronounced growth defect when compared with the Δ*rpfABE* strain containing an empty pMV306 plasmid, suggesting that the chimeric protein (RpfA-ActA), could not substitute the RpfA protein.

Perhaps the most important finding in this study was the establishment that the N-terminal domain of ActA, possesses the PG cleaving activity. However, our knowledge about the precise

mechanism of this activity, the catalytic residues, and the PG bonds cleaved remains limited. The most impacting factor preventing the elucidation of the aforementioned points was the inability to solve the structure of ActA, despite using several alternative approaches. Currently, there is only one available structure of an ActA fragment with the WASP (Luan *et al.* 2018). However, this does not provide any information with regards to the identification of the active centre of ActA. Perhaps cryo-electron microscopy could be used to solve the structure of the full length version of ActA with its putative partners.

Identification of the ActA partners could be aided by the method of improved digestion and identification of membrane bound proteins that was developed during this project. This method offers novel opportunities for the application of detergents for the digestion of membrane proteins and subsequent mass-spectrometry analysis. Future experiments would help to identify ActA partners.

Another important methodological development from this project was the demonstration that a chimeric construct can be successfully made by using DNA from low GC and high GC-content bacteria: *L. monocytogenes* and *M. tuberculosis* respectively. The chimeric protein was expressed in *M. marinum* to levels comparable to the native RpfA. Due to time constraints, the PG-cleaving activity of the chimeric protein could not be assessed. Nevertheless, the findings have laid the foundation for future experiments for the elucidation of the role of ActA in the remodelling and biosynthesis of PG in *L. monocytogenes*.

Future work

1. Further optimization to solve the crystal structure of the N-terminal domain and determine the active site by adding ligands or other small molecules, e.g. actin, that may enhance nucleation or crystal development (McPherson and Cudney 2014). Moreover, a different technique could be used to solve the structure, such as using cryo-EM.

2. Isolate and analyse PG from a wild type and Δ*actA* mutant *L. monocytogenes* to see whether there is any difference in PG composition. This analysis may indirectly help to establish the specific bonds cleaved by ActA.

3. Standardize the pull-down assays to identifyActA protein partners.

4. Generate a *L. monocytogenes* strain expressing an inactive form of ActA and investigate its virulence, replication in macrophages, motility and biofilm formation to prove whether PG cleaving activity is important for any of these processes.

Chapter 8

Appendix

8.1   The map of pET15b-TEV plasmid

pET15b-TEV plasmid containing 6xHis-Tag sequences and an ampicillin resistant gene
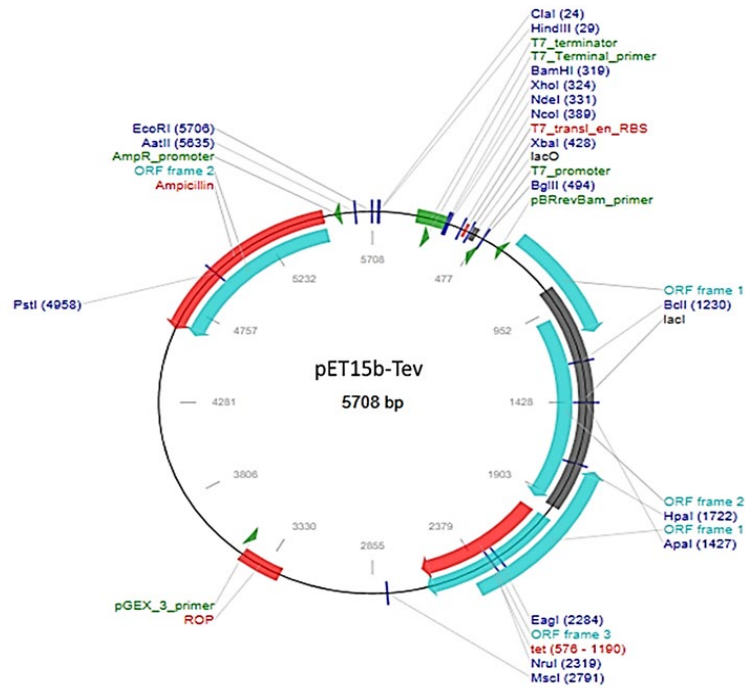
8.2   The map of pLEICS-01 plasmid.

pLEICS-01 plasmid containing 6xHis-Tag sequence and ampicillin resistance cassette.
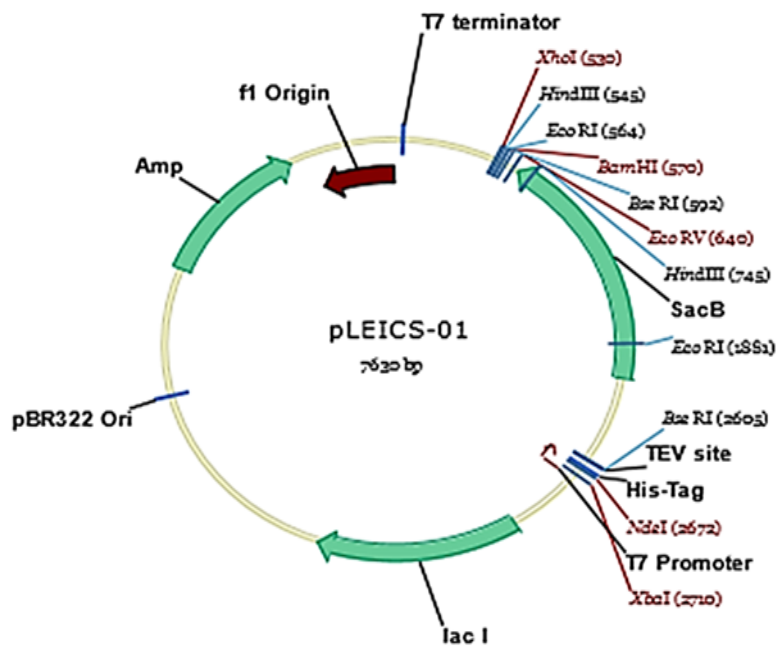
8.3 The map of pET151/D-TOPO plasmid

pET151/D-TOPO plasmid containing 6xHis-Tag sequences and ampicillin resistance gene.

8.4 Blast analysis for the sequence of pLEICS-01-ActA A30-S157

Score	Expect	Identities	Gaps	Strand	Frame
710 bits(384)	0.0()	384/384(100%)	0/384(0%)	Plus/Plus	

Features:

```
Query  117  GCGACAGATAGCGAAGATTCTAGTCTAAACACAGATGAATGGGAAGAAGAAAAAACAGAA
       176
            ||||||||||||||||||||||||||||||||||||||||||||||||||||||||||||
Sbjct  88   GCGACAGATAGCGAAGATTCTAGTCTAAACACAGATGAATGGGAAGAAGAAAAAACAGAA
       147

Query  177  GAGCAACCAAGCGAGGTAAATACGGGACCAAGATACGAAACTGCACGTGAAGTAAGTTCA
       236
            ||||||||||||||||||||||||||||||||||||||||||||||||||||||||||||
Sbjct  148  GAGCAACCAAGCGAGGTAAATACGGGACCAAGATACGAAACTGCACGTGAAGTAAGTTCA
       207

Query  237  CGTGATATTAAAGAACTAGAAAAATCGAATAAAGTGAGAAATACGAACAAAGCAGACCTA
       296
            ||||||||||||||||||||||||||||||||||||||||||||||||||||||||||||
Sbjct  208  CGTGATATTAAAGAACTAGAAAAATCGAATAAAGTGAGAAATACGAACAAAGCAGACCTA
       267

Query  297  ATAGCAATGTTGAAAGAAAAAGCAGAAAAAGGTCCAAATATCAATAATAACAACAGTGAA
       356
            ||||||||||||||||||||||||||||||||||||||||||||||||||||||||||||
Sbjct  268  ATAGCAATGTTGAAAGAAAAAGCAGAAAAAGGTCCAAATATCAATAATAACAACAGTGAA
       327

Query  357  CAAACTGAGAATGCGGCTATAAATGAAGAGGCTTCAGGAGCCGACCGACCAGCTATACAA
       416
            ||||||||||||||||||||||||||||||||||||||||||||||||||||||||||||
Sbjct  328  CAAACTGAGAATGCGGCTATAAATGAAGAGGCTTCAGGAGCCGACCGACCAGCTATACAA
       387

Query  417  GTGGAGCGTCGTCATCCAGGATTGCCATCGGATAGCGCAGCGGAAATTaaaaaaaGAAGG
       476
            ||||||||||||||||||||||||||||||||||||||||||||||||||||||||||||
Sbjct  388  GTGGAGCGTCGTCATCCAGGATTGCCATCGGATAGCGCAGCGGAAATTAAAAAAAGAAGG
       447

Query  477  AAAGCCATAGCATCATCGGATAGT  500
            ||||||||||||||||||||||||
Sbjct  448  AAAGCCATAGCATCATCGGATAGT  471
```

153

8.5 Blast analysis for the sequence of pLEICS-01 -ActA_{A30-N233}

Score	Expect	Identities	Gaps	Strand	Frame
1050 bits(568)	0.0()	568/568(100%)	0/568(0%)	Plus/Minus	

Features:

```
Query  1354     GCGACAGATAGCGAAGATTCTAGTCTAAACACAGATGAATGGGAAGAAGAAAAAACAGAA  1413
                ||||||||||||||||||||||||||||||||||||||||||||||||||||||||||||
Sbjct  2817598  GCGACAGATAGCGAAGATTCTAGTCTAAACACAGATGAATGGGAAGAAGAAAAAACAGAA  2817539

Query  1414     GAGCAACCAAGCGAGGTAAATACGGGACCAAGATACGAAACTGCACGTGAAGTAAGTTCA  1473
                ||||||||||||||||||||||||||||||||||||||||||||||||||||||||||||
Sbjct  2817538  GAGCAACCAAGCGAGGTAAATACGGGACCAAGATACGAAACTGCACGTGAAGTAAGTTCA  2817479

Query  1474     CGTGATATTAAAGAACTAGAAAAATCGAATAAAGTGAGAAATACGAACAAAGCAGACCTA  1533
                ||||||||||||||||||||||||||||||||||||||||||||||||||||||||||||
Sbjct  2817478  CGTGATATTAAAGAACTAGAAAAATCGAATAAAGTGAGAAATACGAACAAAGCAGACCTA  2817419

Query  1534     ATAGCAATGTTGAAAGAAAAAGCAGAAAAAGGTCCAAATATCAATAATAACAACAGTGAA  1593
                ||||||||||||||||||||||||||||||||||||||||||||||||||||||||||||
Sbjct  2817418  ATAGCAATGTTGAAAGAAAAAGCAGAAAAAGGTCCAAATATCAATAATAACAACAGTGAA  2817359

Query  1594     CAAACTGAGAATGCGGCTATAAATGAAGAGGCTTCAGGAGCCGACCGACCAGCTATACAA  1653
                ||||||||||||||||||||||||||||||||||||||||||||||||||||||||||||
Sbjct  2817358  CAAACTGAGAATGCGGCTATAAATGAAGAGGCTTCAGGAGCCGACCGACCAGCTATACAA  2817299

Query  1654     GTGGAGCGTCGTCATCCAGGATTGCCATCGGATAGCGCAGCGGAAATTAAAAAAAGAAGG  1713
                ||||||||||||||||||||||||||||||||||||||||||||||||||||||||||||
Sbjct  2817298  GTGGAGCGTCGTCATCCAGGATTGCCATCGGATAGCGCAGCGGAAATTAAAAAAAGAAGG  2817239

Query  1714     AAAGCCATAGCATCATCGGATAGTGAGCTTGAAAGCCTTACTTATCCGGATAAACCAACA  1773
                ||||||||||||||||||||||||||||||||||||||||||||||||||||||||||||
Sbjct  2817238  AAAGCCATAGCATCATCGGATAGTGAGCTTGAAAGCCTTACTTATCCGGATAAACCAACA  2817179

Query  1774     AAAGTAAATAAGAAAAAAAGTGGCGAAAGAGTCAGTTGCGGATGCTTCTGAAAGTGACTTA  1833
                ||||||||||||||||||||||||||||||||||||||||||||||||||||||||||||
Sbjct  2817178  AAAGTAAATAAGAAAAAAAGTGGCGAAAGAGTCAGTTGCGGATGCTTCTGAAAGTGACTTA  2817119

Query  1834     GATTCTAGCATGCAGTCAGCAGATGAGTCTTCACCACAACCTTTAAAAGCAAACCAACAA  1893
                ||||||||||||||||||||||||||||||||||||||||||||||||||||||||||||
Sbjct  2817118  GATTCTAGCATGCAGTCAGCAGATGAGTCTTCACCACAACCTTTAAAAGCAAACCAACAA  2817059

Query  1894     CCATTTTTCCCTAAAGTATTTAAAAAAA  1921
                ||||||||||||||||||||||||||||
Sbjct  2817058  CCATTTTTCCCTAAAGTATTTAAAAAAA  2817031
```

8.6 Blast analysis for the sequence of pLEICS-01 -ActA$_{G399-N639}$

Score	Expect	Identities	Gaps	Strand	Frame
1360 bits(739)	0.0()	739/739(100%)	0/739(0%)	Plus/Minus	

Features:

```
Query  101     GGTAGACCAACATCTGAAGAATTTAGTTCGCTGAATAGTGGTGATTTTACAGATGACGAA  160
               ||||||||||||||||||||||||||||||||||||||||||||||||||||||||||||
Sbjct  2816506 GGTAGACCAACATCTGAAGAATTTAGTTCGCTGAATAGTGGTGATTTTACAGATGACGAA  2816447
Query  161     AACAGCGAGACAACAGAAGAAGAAATTGATCGCCTAGCTGATTTAAGAGATAGAGGAACA  220
               ||||||||||||||||||||||||||||||||||||||||||||||||||||||||||||
Sbjct  2816446 AACAGCGAGACAACAGAAGAAGAAATTGATCGCCTAGCTGATTTAAGAGATAGAGGAACA  2816387
Query  221     GGAAAACACTCAAGAAATGCGGGTTTTTTACCATTAAATCCGTTTGCTAGCAGCCCGGTT  280
               ||||||||||||||||||||||||||||||||||||||||||||||||||||||||||||
Sbjct  2816386 GGAAAACACTCAAGAAATGCGGGTTTTTTACCATTAAATCCGTTTGCTAGCAGCCCGGTT  2816327
Query  281     CCTTCGTTAAGTCCAAAGGTATCGAAAATAAGCGCACCGGCTCTGATAAGTGACATAACT  340
               ||||||||||||||||||||||||||||||||||||||||||||||||||||||||||||
Sbjct  2816326 CCTTCGTTAAGTCCAAAGGTATCGAAAATAAGCGCACCGGCTCTGATAAGTGACATAACT  2816267
Query  341     AAAAAAACGCCATTTAAGAATCCATCACAGCCATTAAATGTGTTTAATAAAAAAACTACA  400
               ||||||||||||||||||||||||||||||||||||||||||||||||||||||||||||
Sbjct  2816266 AAAAAAACGCCATTTAAGAATCCATCACAGCCATTAAATGTGTTTAATAAAAAAACTACA  2816207
Query  401     ACGAAAACAGTGACTAAAAAACCAACCCCTGTAAAGACCGCACCAAAGCTAGCAGAACTT  460
               ||||||||||||||||||||||||||||||||||||||||||||||||||||||||||||
Sbjct  2816206 ACGAAAACAGTGACTAAAAAACCAACCCCTGTAAAGACCGCACCAAAGCTAGCAGAACTT  2816147
Query  461     CCTGCCACAAAACCACAAGAAACCGTACTTAGGGAAAATAAAACACCCTTTATAGAAAAA  520
               ||||||||||||||||||||||||||||||||||||||||||||||||||||||||||||
Sbjct  2816146 CCTGCCACAAAACCACAAGAAACCGTACTTAGGGAAAATAAAACACCCTTTATAGAAAAA  2816087
Query  521     CAAGCAGAAACAAACAAGCAGTCAATTAATATGCCGAGCCTACCAGTAATCCAAAAAGAA  580
               ||||||||||||||||||||||||||||||||||||||||||||||||||||||||||||
Sbjct  2816086 CAAGCAGAAACAAACAAGCAGTCAATTAATATGCCGAGCCTACCAGTAATCCAAAAAGAA  2816027
Query  581     GCTACAGAGAGCGATAAAGAGGAAATGAAACCACAAACCGAGGAAAAAATGGTAGAGGAA  640
               ||||||||||||||||||||||||||||||||||||||||||||||||||||||||||||
Sbjct  2816026 GCTACAGAGAGCGATAAAGAGGAAATGAAACCACAAACCGAGGAAAAAATGGTAGAGGAA  2815967
Query  641     AGCGAATCAGCTAATAACGCAAACGGAAAAAATCGTTCTGCTGGCATTGAAGAAGGAAAA  700
               ||||||||||||||||||||||||||||||||||||||||||||||||||||||||||||
Sbjct  2815966 AGCGAATCAGCTAATAACGCAAACGGAAAAAATCGTTCTGCTGGCATTGAAGAAGGAAAA  2815907
Query  701     CTAATTGCTAAAAGTGCAGAAGACGAAAAGGCGAAGGAAGAACCAGGGAACCATACGACG  760
               |||||||||||||||||||||||||||| |||||||||||||||||||||||||||||||
Sbjct  2815906 CTAATTGCTAAAAGTGCAGAAGACGAAAAAGCGAAGGAAGAACCAGGGAACCATACGACG  2815847
Query  761     TTAATTCTTGCAATGTTAGCTATTGGCGTGTTCTCTTTAGGGGCGTTTATCAAAATTATT  820
               ||||||||||||||||||||||||||||||||||||||||||||||||||||||||||||
Sbjct  2815846 TTAATTCTTGCAATGTTAGCTATTGGCGTGTTCTCTTTAGGGGCGTTTATCAAAATTATT  2815787
Query  821     CAATTAAGAAAAAATAATT  839
               |||||||||||||||||||
Sbjct  2815786 CAATTAAGAAAAAATAATT  2815768
```

8.7 Purification of ActA $_{A30-S157}$ protein without His-tag

155

Purification of ActA$_{S157}$ with out His-tag
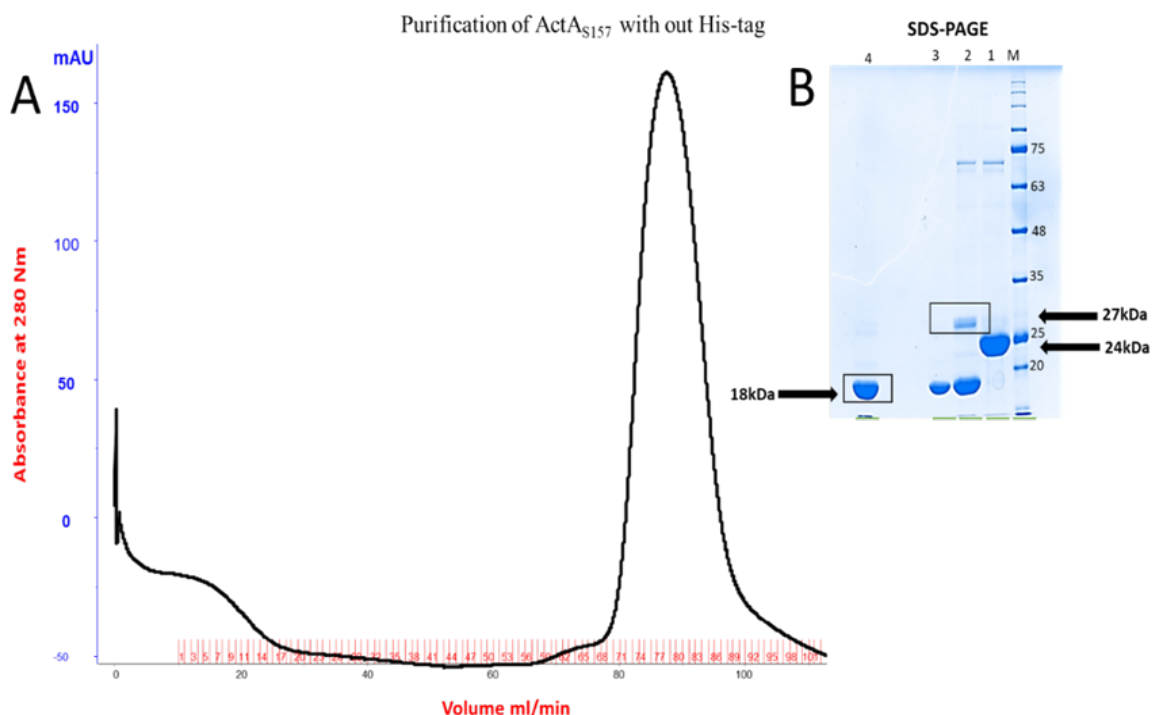
(A) Represents the SEC, a peak at 85 min exhibits the protein with 18 kDa. (B) SDS- PAGE. Lane 1. Purification of ActA $_{A30-S157}$ by nickel column. The protein was eluted in 60 mM imidazole. Lane 2. A mixture of purified ActA$_{A30-S157}$ and TEV-protease. Lane3. Passing the mixture after His-tag digestion through IMAC column. Lane4. Protein fraction after SEC. [M] The Prestained Protein Standards (Geneflow, UK).

8.8   List of the conditions that have been used in crystallization technique

	Original Conditions	Optimisations
1	0.1 M Na HEPES pH 7.0 and 15% w/v PEG 4000	1- 0.1 M Na HEPES pH 7.0 and 10 %, 11%, 12 %, 13%, 14%, 15%, 20% w/v PEG 3350. 2- 0.2 M HEPES pH 7.0 and 15% w/v PEG 4000 3- 0.1 M Na HEPES pH 7.0 and 15% w/v PEG 4000 + additives
2	0.1 M sodium citrate pH 5.0 and 20 % w/v PEG 8000	0.1M sodium citrate pH 5.0 and 22 %, 18%, 15%, 13% w/v PEG 8000
3	0.1 M Na HEPES pH 7.0 and 15% w/v PEG 20 000	1- 0.1 M Na HEPES pH 7.0 and 20%, 18%,16%, 12% w/v PEG 20 000 2- 0.1 M Na HEPES pH 7.0 and 15% w/v PEG 20 000 + additives
4	0.02 M Sodium/potassium phosphate 0.1 M Bis-Tris propane , pH 6.5 and 20% w/v PEG 3350	0.02 M potassium phosphate, 0.1 M Bis-Tris propane pH 6.5 and 18-22% w/v PEG 3350 used

156

8.9 Western blot for ActA protein variants
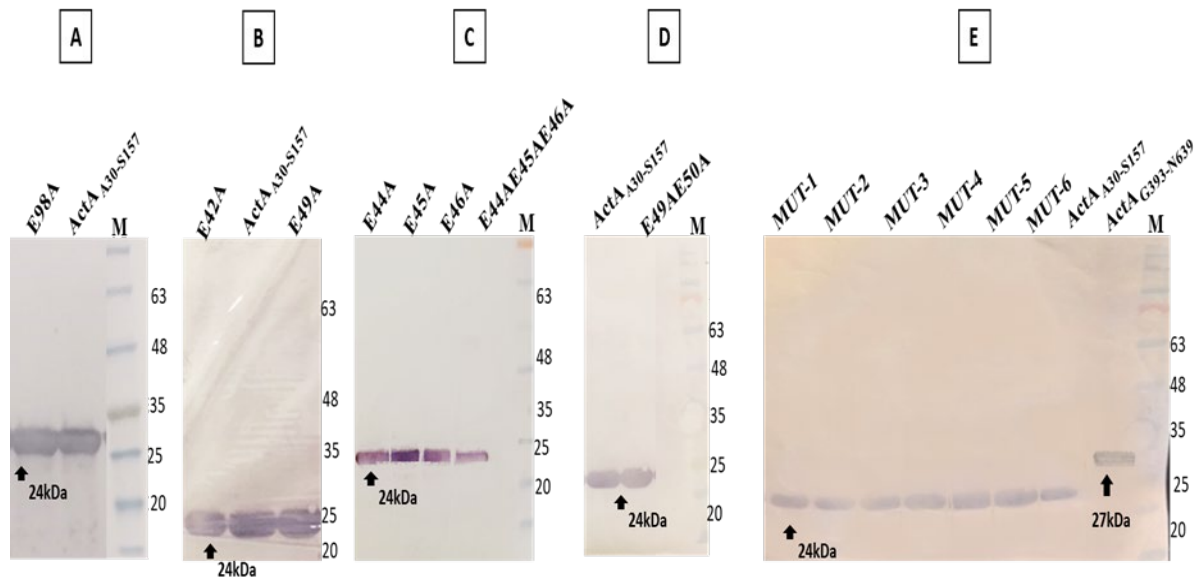
Western blot with anti-His antibody for the ActA protein varients. **(A)** Purified E98A and ActA$_{A30-S157}$ protein. **(B)** E42A, E49A and ActA$_{A30-S157}$ proteins. **(C)** E44A, E45A, E46A and E44AE45AE46A **(D)** E49AE50A and ActA$_{A30-S157}$. **(E)** Shows the proteins generated via Thermo-fisher: ActA$_{A30-S157}$, MUT1, MUT2 , MUT3, MUT 4, MUT5, MUT6 and ActA$_{G393-N639}$ which was used as a negative control .All SDM migrated as ActA$_{A30-S157}$ protein around 24kDa .[M] represents the marker colour Prestained Protein Standard (Geneflow, UK).

8.10 **Mass spectrometry result for the detection of ActA in *L. monocytogenes* wild type and Δ*actA* strains using ultracentrifugation**

8.11 **Mass spectrometry result for the detection of ActA in *L. monocytogenes* wild type and Δ*actA* strains grown in BLEB**

8.12 Blast analysis for the sequence of pGEM-T Easy-F1

Score	Expect	Identities	Gaps	Strand	Frame
1031 bits(558)	0.0()	558/558(100%)	0/558(0%)	Plus/Plus	

Features:

```
Query   7    GGCCATGTGACATTACCCACATAACGGAACGATAACGGGGCGGACACGCTCCGATTGCGA   66
             ||||||||||||||||||||||||||||||||||||||||||||||||||||||||||||
Sbjct   1    GGCCATGTGACATTACCCACATAACGGAACGATAACGGGGCGGACACGCTCCGATTGCGA   60

Query   67   GGGCTTACTACCTGCGCAAATGCCTATATTTCTTGGCGTTCTTGCCGGCGATTGTGACGG   126
             ||||||||||||||||||||||||||||||||||||||||||||||||||||||||||||
Sbjct   61   GGGCTTACTACCTGCGCAAATGCCTATATTTCTTGGCGTTCTTGCCGGCGATTGTGACGG   120

Query   127  AAACGCCGACTTTTCTTAAACGTGACGGAATCGCCTGAAACCGCTACCGTCTCGGGAGGC   186
             ||||||||||||||||||||||||||||||||||||||||||||||||||||||||||||
Sbjct   121  AAACGCCGACTTTTCTTAAACGTGACGGAATCGCCTGAAACCGCTACCGTCTCGGGAGGC   180

Query   187  TCGTCAACCTAACCCAAAATGACGTGCCCTCCCTCGCCGATAGCACGCCGAACTCCATCC   246
             ||||||||||||||||||||||||||||||||||||||||||||||||||||||||||||
Sbjct   181  TCGTCAACCTAACCCAAAATGACGTGCCCTCCCTCGCCGATAGCACGCCGAACTCCATCC   240

Query   247  AGTGGGCGAGGGATTCCGACCGCGGATGGAGGCGGGGGACCCACCAGGTCCGCCGAGATC   306
             ||||||||||||||||||||||||||||||||||||||||||||||||||||||||||||
Sbjct   241  AGTGGGCGAGGGATTCCGACCGCGGATGGAGGCGGGGGACCCACCAGGTCCGCCGAGATC   300

Query   307  GGACCGGAGCCGCATACGGCTCCTTGGGGTGAAGCCAACGTCGTTCGCCGATGTACGACC   366
             ||||||||||||||||||||||||||||||||||||||||||||||||||||||||||||
Sbjct   301  GGACCGGAGCCGCATACGGCTCCTTGGGGTGAAGCCAACGTCGTTCGCCGATGTACGACC   360

Query   367  GCGGCCGGGTGATCCTCTCCACGGCGAATCCAACCCGAACCCGACAGCTGACCTCGTAGG   426
             ||||||||||||||||||||||||||||||||||||||||||||||||||||||||||||
Sbjct   361  GCGGCCGGGTGATCCTCTCCACGGCGAATCCAACCCGAACCCGACAGCTGACCTCGTAGG   420

Query   427  CGTGTACCGAGAGGAATTACCTAACGTATGAGTGGACGCCACCGTAAGCCCACCACATCC   486
             ||||||||||||||||||||||||||||||||||||||||||||||||||||||||||||
Sbjct   421  CGTGTACCGAGAGGAATTACCTAACGTATGAGTGGACGCCACCGTAAGCCCACCACATCC   480

Query   487  AACGTCAGCGTCGCCAAGATCGCCTTTACCGGCGCAGTACTCGGTGGCGGCGGCATCGCC   546
             ||||||||||||||||||||||||||||||||||||||||||||||||||||||||||||
Sbjct   481  AACGTCAGCGTCGCCAAGATCGCCTTTACCGGCGCAGTACTCGGTGGCGGCGGCATCGCC   540

Query   547  ATGGCCGCTCAGGCGACC   564
             ||||||||||||||||||
Sbjct   541  ATGGCCGCTCAGGCGACC   558
```

8.13 Blast analysis for the sequence of pGEM-T Easy-F2

Score	Expect	Identities	Gaps	Strand	Frame
732 bits(396)	0.0()	396/396(100%)	0/396(0%)	Plus/Plus	

Features:

```
Query  1    GGATCCGCGACAGATAGCGAAGATTCTAGTCTAAACACAGATGAATGGGAAGAAGAAAAA  60
            ||||||||||||||||||||||||||||||||||||||||||||||||||||||||||||
Sbjct  1    GGATCCGCGACAGATAGCGAAGATTCTAGTCTAAACACAGATGAATGGGAAGAAGAAAAA  60
Query  61   ACAGAAGAGCAACCAAGCGAGGTAAATACGGGACCAAGATACGAAACTGCACGTGAAGTA  120
            ||||||||||||||||||||||||||||||||||||||||||||||||||||||||||||
Sbjct  61   ACAGAAGAGCAACCAAGCGAGGTAAATACGGGACCAAGATACGAAACTGCACGTGAAGTA  120
Query  121  AGTTCACGTGATATTAAAGAACTAGAAAAATCGAATAAAGTGAGAAATACGAACAAAGCA  180
            ||||||||||||||||||||||||||||||||||||||||||||||||||||||||||||
Sbjct  121  AGTTCACGTGATATTAAAGAACTAGAAAAATCGAATAAAGTGAGAAATACGAACAAAGCA  180
Query  181  GACCTAATAGCAATGTTGAAAGAAAAAGCAGAAAAAGGTCCAAATATCAATAATAACAAC  240
            ||||||||||||||||||||||||||||||||||||||||||||||||||||||||||||
Sbjct  181  GACCTAATAGCAATGTTGAAAGAAAAAGCAGAAAAAGGTCCAAATATCAATAATAACAAC  240
Query  241  AGTGAACAAACTGAGAATGCGGCTATAAATGAAGAGGCTTCAGGAGCCGACCGACCAGCT  300
            ||||||||||||||||||||||||||||||||||||||||||||||||||||||||||||
Sbjct  241  AGTGAACAAACTGAGAATGCGGCTATAAATGAAGAGGCTTCAGGAGCCGACCGACCAGCT  300
Query  301  ATACAAGTGGAGCGTCGTCATCCAGGATTGCCATCGGATAGCGCAGCGGAAATTaaaaaa  360
            ||||||||||||||||||||||||||||||||||||||||||||||||||||||||
Sbjct  301  ATACAAGTGGAGCGTCGTCATCCAGGATTGCCATCGGATAGCGCAGCGGAAATTAAAAAA  360
Query  361  aGAAGGAAAGCCATAGCATCATCGGATAGTCTGCAG  396
            |||||||||||||||||||||||||||||||||||
Sbjct  361  AGAAGGAAAGCCATAGCATCATCGGATAGTCTGCAG  396
```

160

8.14 Blast analysis for the sequence of pGEM-T Easy-F3

Score	Expect	Identities	Gaps	Strand	Frame
1613 bits(873)	0.0()	873/873(100%)	0/873(0%)	Plus/Plus	

Features:

```
Query  1    CTGCAGAACGCAACACCCCGCGAAGTGCTTCCCGCTTCGGCAGCGATGGACGCTCCGTTG   60
            ||||||||||||||||||||||||||||||||||||||||||||||||||||||||||||
Sbjct  1    CTGCAGAACGCAACACCCCGCGAAGTGCTTCCCGCTTCGGCAGCGATGGACGCTCCGTTG   60
Query  61   GACGCGGCCGCGGTCAACGGCGAACCAGCACCGCTGGCCCCGCCGCCCGCCGACCCGGCG   120
            ||||||||||||||||||||||||||||||||||||||||||||||||||||||||||||
Sbjct  61   GACGCGGCCGCGGTCAACGGCGAACCAGCACCGCTGGCCCCGCCGCCCGCCGACCCGGCG   120
Query  121  CCACCCGTGGAACTTGCCGCTAACGACCTGCCCGCACCGCTGGGTGAACCCCTCCCGGCA   180
            ||||||||||||||||||||||||||||||||||||||||||||||||||||||||||||
Sbjct  121  CCACCCGTGGAACTTGCCGCTAACGACCTGCCCGCACCGCTGGGTGAACCCCTCCCGGCA   180
Query  181  GCTcccgccgacccggcaccacccgccgacctggcaccacccgcgcccgccgacgtcgcg   240
            ||||||||||||||||||||||||||||||||||||||||||||||||||||||||||||
Sbjct  181  GCTCCCGCCGACCCGGCACCACCCGCCGACCTGGCACCACCCGCGCCCGCCGACGTCGCG   240
Query  241  ccacccgTGGAACTTGCCGTAAACGACCTGCCCGCACCGCTGGGTGAACCCCTCCCGGCA   300
            ||||||||||||||||||||||||||||||||||||||||||||||||||||||||||||
Sbjct  241  CCACCCGTGGAACTTGCCGTAAACGACCTGCCCGCACCGCTGGGTGAACCCCTCCCGGCA   300
Query  301  GCTcccgccgacccggcaccacccgccgacctggcaccacccgcgcccgccgacctggcg   360
            ||||||||||||||||||||||||||||||||||||||||||||||||||||||||||||
Sbjct  301  GCTCCCGCCGACCCGGCACCACCCGCCGACCTGGCACCACCCGCGCCCGCCGACCTGGCG   360
Query  361  ccacccgcgcccgccgacctggcgccacccgcgcccgccgacctggcaccacccgTGGAA   420
            ||||||||||||||||||||||||||||||||||||||||||||||||||||||||||||
Sbjct  361  CCACCCGCGCCCGCCGACCTGGCGCCACCCGCGCCCGCCGACCTGGCACCACCCGTGGAA   420
Query  421  CTTGCCGTAAACGACCTGCCCGCGCCGCTGGGTGAACCCCTCCCGGCAGCTCCCGCCGAA   480
            ||||||||||||||||||||||||||||||||||||||||||||||||||||||||||||
Sbjct  421  CTTGCCGTAAACGACCTGCCCGCGCCGCTGGGTGAACCCCTCCCGGCAGCTCCCGCCGAA   480
Query  481  CTGGCGGCCACCCGCCGATCTGGCacccgcgtccgccgacctggcgccacccgcgcccgcc   540
            ||||||||||||||||||||||||||||||||||||||||||||||||||||||||||||
Sbjct  481  CTGGCGGCCACCCGCCGATCTGGCACCCGCGTCCGCCGACCTGGCGCCACCCGCGCCCGCC   540
Query  541  gacctggcgccacccgcgcccgccgaactggcgccacccgcgcccgccgacctggcacca   600
            ||||||||||||||||||||||||||||||||||||||||||||||||||||||||||||
Sbjct  541  GACCTGGCGCCACCCGCGCCCGCCGAACTGGCGCCACCCGCGCCCGCCGACCTGGCACCA   600
Query  601  cccgcTGCGGTGAACGAGCAAACCGCGCCGGGCGATCAGCCCGCCACAGCTCCAGGCGGC   660
            ||||||||||||||||||||||||||||||||||||||||||||||||||||||||||||
Sbjct  601  CCCGCTGCGGTGAACGAGCAAACCGCGCCGGGCGATCAGCCCGCCACAGCTCCAGGCGGC   660
Query  661  CCGGTTGGCCTTGCCACCGATTTGGAACTCCCCGAGCCCGACCCCCAACCAGCTGACGCA   720
            ||||||||||||||||||||||||||||||||||||||||||||||||||||||||||||
Sbjct  661  CCGGTTGGCCTTGCCACCGATTTGGAACTCCCCGAGCCCGACCCCCAACCAGCTGACGCA   720
Query  721  CCGCCGCCCGGCGACGTCACCGAGGCGCCCGCCGAAACGCCCCAAGTCTCGAACATCGCC   780
            ||||||||||||||||||||||||||||||||||||||||||||||||||||||||||||
Sbjct  721  CCGCCGCCCGGCGACGTCACCGAGGCGCCCGCCGAAACGCCCCAAGTCTCGAACATCGCC   780
Query  781  TATACGAAGAAGCTGTGGCAGGCGATTCGGGCCCAGGACGTCTGCGGCAACGATGCGCTG   840
            ||||||||||||||||||||||||||||||||||||||||||||||||||||||||||||
Sbjct  781  TATACGAAGAAGCTGTGGCAGGCGATTCGGGCCCAGGACGTCTGCGGCAACGATGCGCTG   840
Query  841  GACTCGCTCGCACAGCCGTACGTCATCGGCTGA     873
            |||||||||||||||||||||||||||||||||
Sbjct  841  GACTCGCTCGCACAGCCGTACGTCATCGGCTGA     873
```

161

Chapter 9

References

Alonzo, F., McMullen, P.D. and Freitag, N.E. (2011) 'Actin polymerization drives septation of *Listeria monocytogenes* namA hydrolase mutants, demonstrating host correction of a bacterial defect', *Infection and immunity*, 79(4), 1458-1470.

Alvarez-Dominguez,C.,Roberts, R. and Stahl, P.D.(1997) 'Internalized *Listeria monocytogenes* modulates intracellular trafficking and delays maturation of the phagosome', *Journal of cell science*, 110(6), 731-743.

Alvarez, D.E. and Agaisse, H. (2016) 'The metalloprotease Mpl supports *Listeria mono-cytogenes* dissemination through resolution of membrane protrusions into vacuoles', *Infection and immunity*, 84(6), 1806-1814.

Arguello, J., Fan, C., Wang, W. and Long, M. (2007) '*Origination of chimeric genes through DNA-level recombination' , in Gene and Protein Evolution* ,Karger Publishers, 131-146.

Auerbuch, V., Loureiro, J.J., Gertler, F.B., Theriot, J.A. and Portnoy, D.A. (2003) 'Ena/VASP proteins contribute to *Listeria monocytogenes* pathogenesis by controlling temporal and spatial persistence of bacterial actin-based motility', *Molecular microbiology*, 49(5), 1361-1375.

Aureli, P., Fiorucci, G.C., Caroli, D., Marchiaro, G., Novara, O., Leone, L. and Salmaso, S. (2000) 'An outbreak of febrile gastroenteritis associated with corn contaminated by *Listeria monocytogenes*', *New England Journal of Medicine*, 342(17), 1236-1241.

Bagnoli, F. and Rappuoli, R. (2017) Protein and Sugar Export and Assembly in Gram-positive Bacteria, Springer.

Bailey, J., Fletcher, D. and Cox, N. (1990) '*Listeria monocytogenes* colonization of broiler chickens', *Poultry science*, 69(3), 457-461.

Baneyx, F. and Mujacic, M. (2004) 'Recombinant protein folding and misfolding in *Escherichia coli*', *Nature biotechnology*, 22(11), 1399.

Bayer, M., Iberer, R., Bischof, K., Rassi, E., Stabentheiner, E., Zellnig, G. and Koraimann, G. (2001) 'Functional and mutational analysis of p19, a DNA transfer protein with muramidase activity', *Journal of bacteriology*, 183(10), 3176-3183.

Béguin, P. (1999) 'Hybrid enzymes', *Current opinion in biotechnology*, 10(4), 336-340.

Behari, J. and Youngman, P. (1998) 'Regulation of hly expression in *Listeria monocytogenes* by carbon sources and pH occurs through separate mechanisms mediated by PrfA', *Infection and immunity*, 66(8), 3635-3642.

Bertsche, U., Weidenmaier, C., Kuehner, D., Yang, S.-J., Baur, S., Wanner, S., Francois, P., Schrenzel, J., Yeaman, M.R. and Bayer, A.S. (2011) 'Correlation of daptomycin resistance in a clinical *Staphylococcus aureus* strain with increased cell wall teichoic acid production and D-alanylation', *Antimicrobial agents and chemotherapy*, 55(8), 3922-3928.

Betts, M.J. and Russell, R.B. (2003) 'Amino acid properties and consequences of substitutions' in *Bioinformatics for geneticists*, 289-316.

Bierne, H. and Cossart, P. (2007) '*Listeria monocytogenes* surface proteins: from genome predictions to function', *Microbiol. Mol. Biol. Rev.*, 71(2), 377-397.

Bierne, H., Garandeau, C., Pucciarelli, M.G., Sabet, C., Newton, S., Garcia-del Portillo, F., Cossart, P. and Charbit, A. (2004) 'Sortase B, a new class of sortase in *Listeria monocytogenes*', *Journal of bacteriology*, 186(7), 1972-1982.

Biester, H. and Schwarte, L. (1939) 'Studies on *Listerella* infection in sheep', *The Journal of Infectious Diseases*, 135-144.

Bitar, A.P., Cao, M. and Marquis, H. (2008) 'The metalloprotease of *Listeria monocytogenes* is activated by intramolecular autocatalysis', *Journal of bacteriology*, 190(1), 107-111.

Bordo, D. and Argos, P. (1991) 'Suggestions for "safe" residue substitutions in site-directed mutagenesis', *Journal of molecular biology*, 217(4), 721-729.

Bubert, A., Kuhn, M., Goebel, W. and Köhler, S. (1992) 'Structural and functional properties of the p60 proteins from different *Listeria* species', *Journal of bacteriology*, 174(24), 8166-8171.

Buchanan, R.L., Gorris, L.G., Hayman, M.M., Jackson, T.C. and Whiting, R.C. (2017) 'A review of *Listeria monocytogenes*: an update on outbreaks, virulence, dose-response, ecology, and risk assessments', *Food Control*, 75, 1-13.

Cabanes, D., Dehoux, P., Dussurget, O., Frangeul, L. and Cossart, P. (2002) 'Surface proteins and the pathogenic potential of *Listeria monocytogenes*', *Trends in microbiology*, 10(5), 238-245.

Cabanes, D., Dussurget, O., Dehoux, P. and Cossart, P. (2004) 'Auto, a surface associated autolysin of *Listeria monocytogenes* required for entry into eukaryotic cells and virulence', *Molecular microbiology*, 51(6), 1601-1614.

Calvo, E., Pucciarelli, M.G., Bierne, H., Cossart, P., Pablo Albar, J. and García-del Portillo, F. (2005) 'Analysis of the *Listeria* cell wall proteome by two-dimensional nanoliquid chromatography coupled to mass spectrometry', *Proteomics*, 5(2), 433-443.

Canova, M.J., Veyron-Churlet, R., Zanella-Cleon, I., Cohen-Gonsaud, M., Cozzone, A.J., Becchi, M., Kremer, L. and Molle, V. (2008) 'The *Mycobacterium tuberculosis* serine/threonine kinase PknL phosphorylates Rv2175c: mass spectrometric profiling of the activation loop phosphorylation sites and their role in the recruitment of Rv2175c', *Proteomics*, 8(3), 521-533.

Carroll, S.A., Hain, T., Technow, U., Darji, A., Pashalidis, P., Joseph, S.W. and Chakraborty, T. (2003) 'Identification and characterization of a peptidoglycan hydrolase, MurA, of *Listeria monocytogenes*, a muramidase needed for cell separation', *Journal of bacteriology*, 185(23), 6801-6808.

Carvalho, F., Sousa, S. and Cabanes, D. (2014) 'How *Listeria monocytogenes* organizes its surface for virulence', *Frontiers in cellular and infection microbiology*, 4, 48.

Centers for Disease Control and Prevention (2011) 'National Center for Zoonotic, Vector-Borne, and Enteric Diseases', "Listeriosis—Technical Information," available: [accessed 12 Aug].

Chambel, L., Sol, M., Fernandes, I., Barbosa, M., Zilhão, I., Barata, B., Jordan, S., Perni, S., Shama, G. and Adrião, A. (2007) 'Occurrence and persistence of *Listeria* spp. in the environment of ewe and cow's milk cheese dairies in Portugal unveiled by an integrated analysis of identification, typing and spatial–temporal mapping along production cycle', *International journal of food microbiology*, 116(1), 52-63.

Chang, A.Y., Chau, V., Landas, J.A. and Pang, Y. (2017) 'Preparation of calcium competent *Escherichia coli* and heat-shock transformation', *JEMI Methods*, 1, 22-25.

Chaturvedi, V., Ertelt, J.M., Jiang, T.T., Kinder, J.M., Xin, L., Owens, K.J., Jones, H.N. and Way, S.S. (2015) 'CXCR3 blockade protects against *Listeria monocytogenes* infection–induced fetal wastage', *The Journal of clinical investigation*, 125(4), 1713-1725.

Chhetri, G., Kalita, P. and Tripathi, T. (2015) 'An efficient protocol to enhance recombinant protein expression using ethanol in *Escherichia coli*', *MethodsX*, 2, 385-391.

Ching, W.-M., Wang, H., Eamsila, C., Kelly, D. and Dasch, G. (1998) 'Expression and refolding of truncated recombinant major outer membrane protein antigen (r56) of Orientia tsutsugamushi and its use in enzyme-linked immunosorbent assays', *Clin. Diagn. Lab. Immunol.*, 5(4), 519-526.

Choi, J. and Lee, S. (2004) 'Secretory and extracellular production of recombinant proteins using *Escherichia coli*', *Applied microbiology and biotechnology*, 64(5), 625-635.

Chrdle, A. and Stárek, M. (2011) '*Listeria* infection of a prosthetic hip joint', *Klinicka mikrobiologie a infekcni lekarstvi*, 17(2), 62-66.

Churchill, R.L., Lee, H. and Hall, J.C. (2006) 'Detection of *Listeria monocytogenes* and the toxin listeriolysin O in food', *Journal of Microbiological Methods*, 64(2), 141-170.

Cicchetti, G., Maurer, P., Wagener, P. and Kocks, C. (1999) 'Actin and phosphoinositide binding by the ActA protein of the bacterial pathogen *Listeria monocytogenes*', *Journal of Biological Chemistry*, 274(47), 33616-33626.

Ciesielski, C.A., Hightower, A.W., Parsons, S.K. and Broome, C.V. (1988) 'Listeriosis in the United States: 1980-1982', *Archives of internal medicine*, 148(6), 1416-1419.

Cohen-Gonsaud, M., Barthe, P., Bagnéris, C., Henderson, B., Ward, J., Roumestand, C. and Keep, N.H. (2005) 'The structure of a resuscitation-promoting factor domain from *Mycobacterium tuberculosis* shows homology to lysozymes', *Nature Structural & Molecular Biology*, 12(3), 270.

Colburn, K.G., Kaysner, C.A., Abeyta, C. and Wekell, M.M. (1990) '*Listeria* species in a California coast estuarine environment', *Appl. Environ. Microbiol.*, 56(7), 2007-2011.

Cole, J.N., Djordjevic, S.P. and Walker, M.J. (2008) 'Isolation and solubilization of Gram-positive bacterial cell wall-associated proteins' in *2D PAGE: Sample Preparation and Fractionation* Springer, 295-311.

Colodner, R., Sakran, W., Miron, D., Teitler, N., Khavalevsky, E. and Kopelowitz, J. (2003) '*Listeria moncytogenes* cross-contamination in a nursery', *American journal of infection control*, 31(5), 322-324.

Conte, M.P., Petrone, G., Di Biase, A.M., Longhi, C., Penta, M., Tinari, A., Superti, F., Fabozzi, G., Visca, P. and Seganti, L. (2002) 'Effect of acid adaptation on the fate of *Listeria monocytogenes* in THP-1 human macrophages activated by gamma interferon', *Infection and immunity*, 70(8), 4369-4378.

Crum, N.F.(2002)'Update on *Listeria monocytogenes* infection',*Current gastroenterology reports*, 4(4), 287-296.

Dahl, J.L., Wei, J., Moulder, J.W., Laal, S. and Friedman, R.L. (2001) 'Subcellular localization of the intracellular survival-enhancing Eis protein of *Mycobacterium tuberculosis*', *Infection and immunity*, 69(7), 4295-4302.

166

Dalton, C.B., Austin, C.C., Sobel, J., Hayes, P.S., Bibb, W.F., Graves, L.M., Swaminathan, B., Proctor, M.E. and Griffin, P.M. (1997) 'An outbreak of gastroenteritis and fever due to *Listeria monocytogenes* in milk', *New England Journal of Medicine*, 336(2), 100-106.

Dawson, S., Evans, M., Willby, D., Bardwell, J., Chamberlain, N. and Lewis, D. (2006) '*Listeria* outbreak associated with sandwich consumption from a hospital retail shop, United Kingdom', *Euro Surveill*, 11(6), 89-91.

De las Heras, A., Cain, R.J., Bielecka, M.K. and Vazquez-Boland, J.A. (2011) 'Regulation of *Listeria* virulence: PrfA master and commander', *Current opinion in microbiology*, 14(2), 118-127.

Dennison, C. (2013) '*A guide to protein isolation*', Springer Science & B*usiness* Media. University of Natal, South Africa.

Dessau, M.A. and Modis, Y. (2011) 'Protein crystallization for X-ray crystallography', *Journal of visualized experiments: JoVE*, (47).

Desvaux, M., Dumas, E., Chafsey, I. and Hebraud, M. (2006) 'Protein cell surface display in Gram-positive bacteria: from single protein to macromolecular protein structure', *FEMS microbiology letters*, 256(1), 1-15.

Desvaux, M. and Hébraud, M. (2006) 'The protein secretion systems in *Listeria*: inside out bacterial virulence', *FEMS microbiology reviews*, 30(5), 774-805.

Dijkstra, R. (1982) 'The occurrence of *Listeria monocytogenes* in surface water of canals and lakes, in ditches of one big polder and in the effluents and canals of a sewage treatment plant', *Zentralblatt fur Bakteriologie, Parasitenkunde, Infektionskrankheiten und Hygiene, Abt. I*, (2/3), 202-205.

Downing, K.J., Mischenko, V.V., Shleeva, M.O., Young, D.I., Young, M., Kaprelyants, A.S., Apt, A.S. and Mizrahi, V. (2005) 'Mutants of *Mycobacterium tuberculosis* lacking three of the five rpf-like genes are defective for growth in vivo and for resuscitation in vitro', *Infection and immunity*, 73(5), 3038-3043.

Dramsi, S., Biswas, I., Maguin, E., Braun, L., Mastroeni, P. and Cossart, P. (1995) 'Entry of *Listeria monocytogenes* into hepatocytes requires expression of inIB, a surface protein of the internalin multigene family', *Molecular microbiology*, 16(2), 251-261.

Dramsi, S. and Cossart, P. (2002) 'Listeriolysin O: a genuine cytolysin optimized for an intracellular parasite', *The Journal of cell biology*, 156(6), 943-946.

Dumon-Seignovert, L., Cariot, G. and Vuillard, L. (2004) 'The toxicity of recombinant proteins in *Escherichia coli*: a comparison of overexpression in BL21 (DE3), C41 (DE3), and C43 (DE3)', *Protein expression and purification*, 37(1), 203-206.

Dyson, M.R. (2010) 'Selection of soluble protein expression constructs: the experimental determination of protein domain boundaries'. *Biochem Soc Trans* , 38 (4): 908–913.

Eklund, M.W., Poysky, F.T., Paranjpye, R.N., Lashbrook, L.C., Peterson, M.E. and Pelroy, G.A. (1995) 'Incidence and sources of *Listeria monocytogenes* in cold-smoked fishery products and processing plants', *Journal of Food Protection®*, 58(5), 502-508.

Farber, J. and Peterkin, P.(1991) '*Listeria monocytogenes*,a food-borne pathogen', *Microbiological reviews*, 55(3), 476-511.

Fenlon, D., Wilson, J. and Donachie, W. (1996) 'The incidence and level of *Listeria monocytogenes* contamination of food sources at primary production and initial processing', *Journal of Applied Bacteriology*, 81(6), 641-650.

Ferreira, V., Wiedmann, M., Teixeira, P. and Stasiewicz, M.J. (2014) '*Listeria monocytogenes* persistence in food-associated environments: epidemiology, strain characteristics, and implications for public health', *Journal of food protection*, 77(1), 150-170.

Footer, M.J., Lyo, J.K. and Theriot, J.A. (2008) 'Close packing of *Listeria monocytogenes* ActA, a natively unfolded protein, enhances F-actin assembly without dimerization', *Journal of Biological Chemistry*, 283(35), 23852-23862.

Forster, B.M. and Marquis, H. (2012) 'Protein transport across the cell wall of monoderm Gram-positive bacteria', *Molecular microbiology*, 84(3), 405-413.

Foster, K.R., Fortunato, A., Strassmann, J.E. and Queller, D.C. (2002) 'The costs and benefits of being a chimera', *Proceedings of the Royal Society of London. Series B: Biological Sciences*, 269(1507), 2357-2362.

Foster, S.J. (1995) 'Molecular characterization and functional analysis of the major autolysin of *Staphylococcus aureus* 8325/4', *Journal of bacteriology*, 177(19), 5723-5725.

Freitag, N.E., Port, G.C. and Miner, M.D. (2009) '*Listeria monocytogenes* from saprophyte to intracellular pathogen', *Nature Reviews Microbiology*, 7(9), 623-628.

Freitag, N.E., Rong, L. and Portnoy, D.A. (1993) 'Regulation of the prfA transcriptional activator of *Listeria monocytogenes*: multiple promoter elements contribute to intracellular growth and cell-to-cell spread', *Infection and immunity*, 61(6), 2537-2544.

Fretz, R., Sagel, U., Ruppitsch, W., Pietzka, A., Stöger, A., Huhulescu, S., Heuberger, S., Pichler, J., Much, P. and Pfaff, G. (2010) 'Listeriosis outbreak caused by acid curd cheese 'Quargel', Austria and Germany 2009', *Eurosurveillance*, 15(5), 19477.

Food Standards Agency (FSA). (2016) 'Guidance on reducing the risk of vulnerable groups contracting listeriosis', available: [accessed 30 Dec].

Gaillard, J.-L., Berche, P., Frehel, C., Gouln, E. and Cossart, P. (1991) 'Entry of *L. monocytogenes* into cells is mediated by internalin, a repeat protein reminiscent of surface antigens from gram-positive cocci', *Cell*, 65(7), 1127-1141.

Garcia-del Portillo, F., Calvo, E., D'Orazio, V. and Pucciarelli, M.G. (2011) 'Association of ActA to peptidoglycan revealed by cell wall proteomics of intracellular *Listeria monocytogenes*', *J Biol Chem*, 286(40), 34675-89.

Geoffroy, C., Gaillard, J.-L., Alouf, J.E. and Berche, P. (1987) 'Purification, characterization, and toxicity of the sulfhydryl-activated hemolysin listeriolysin O from *Listeria monocytogenes*', *Infection and immunity*, 55(7), 1641-1646.

Glaser, P., Frangeul, L., Buchrieser, C., Rusniok, C., Amend, A., Baquero, F., Berche, P., Bloecker, H., Brandt, P. and Chakraborty, T. (2001) 'Comparative genomics of *Listeria* species', *Science*, 294(5543), 849-852.

Glauner, B., Höltje, J. and Schwarz, U. (1988) 'The composition of the murein of Escherichia coli', *Journal of Biological Chemistry*, 263(21), 10088-10095.

Glomski, I.J., Gedde, M.M., Tsang, A.W., Swanson, J.A. and Portnoy, D.A. (2002) 'The *Listeria monocytogenes* hemolysin has an acidic pH optimum to compartmentalize activity and prevent damage to infected host cells', *The Journal of cell biology*, 156(6), 1029-1038.

Goldberg, M.B. (2001) 'Actin-based motility of intracellular microbial pathogens', *Microbiol. Mol. Biol. Rev.*, 65(4), 595-626.

Goldfine, H. and Shen, H. (2007) ' *Listeria monocytogenes: pathogenesis and host response*', New York , USA,.

Gomez, M., Johnson, S. and Gennaro, M.L. (2000) 'Identification of secreted proteins of *Mycobacterium tuberculosis* by a bioinformatic approach', *Infection and immunity*, 68(4), 2323-2327.

Gottlieb, S.L., Newbern, E.C., Griffin, P.M., Graves, L.M., Hoekstra, R.M., Baker, N.L., Hunter, S.B., Holt, K.G., Ramsey, F. and Head, M. (2006) 'Multistate outbreak of

listeriosis linked to turkey deli meat and subsequent changes in US regulatory policy', *Clinical Infectious Diseases*, 42(1), 29-36.

Gräslund, S., Nordlund, P., Weigelt, J., Hallberg, B.M., Bray, J., Gileadi, O., Knapp, S., Oppermann, U., Arrowsmith, C. and Hui, R. (2008) 'Protein production and purification', *Nature methods*, 5(2), 135.

Gray, M.L. and Killinger, A. (1966) '*Listeria monocytogenes* and listeric infections', *Bacteriological reviews*, 30(2), 309.

Greene, S.L. and Freitag, N.E. (2003) 'Negative regulation of PrfA, the key activator of *Listeria monocytogenes* virulence gene expression, is dispensable for bacterial pathogenesis', *Microbiology*, 149(1), 111-120.

Gross, M., Cramton, S.E., Götz, F. and Peschel, A. (2001) 'Key role of teichoic acid net charge in *staphylococcus aureus* colonization of artificial surfaces', *Infection and immunity*, 69(5), 3423-3426.

Guenther, S. and Loessner, M.J. (2011) 'Bacteriophage biocontrol of *Listeria monocytogenes* on soft ripened white mold and red-smear cheeses', *Bacteriophage*, 1(2), 94-100.

Guillet, C., Join-Lambert, O., Le Monnier, A., Leclercq, A., Mechaï, F., Mamzer-Bruneel, M.-F., Bielecka, M.K., Scortti, M., Disson, O. and Berche, P. (2010) 'Human listeriosis caused by *Listeria ivanovii'*, *Emerging infectious diseases*, 16(1), 136.

Gupta, R.K., Srivastava, B.S. and Srivastava, R. (2010) 'Comparative expression analysis of rpf-like genes of *Mycobacterium tuberculosis* H37Rv under different physiological stress and growth conditions', *Microbiology*, 156(9), 2714-2722.

Gupta, R.K. and Srivastava, R. (2012) 'Resuscitation promoting factors: a family of microbial proteins in survival and resuscitation of dormant *Mycobacteria*', *Indian J Microbiol*, 52(2), 114-21.

Guzman, C.A., Rohde, M., Chakraborty, T., Domann, E., Hudel, M., Wehland, J. and Timmis, K.N. (1995) 'Interaction of *Listeria monocytogenes* with mouse dendritic cells', *Infection and immunity*, 63(9), 3665-3673.

Halbedel, S., Reiss, S., Hahn, B., Albrecht, D., Mannala, G.K., Chakraborty, T., Hain, T., Engelmann, S. and Flieger, A. (2014) 'A systematic proteomic analysis of *Listeria monocytogenes* house-keeping protein secretion systems', *Molecular & Cellular Proteomics*, 13(11), 3063-3081.

Hamon, M., Bierne, H. and Cossart, P. (2006) '*Listeria monocytogenes*: a multifaceted model', *Nature Reviews Microbiology*, 4(6), 423-434.

Han, S., Caspers, N., Zaniewski, R.P., Lacey, B.M., Tomaras, A.P., Feng, X., Geoghegan, K.F. and Shanmugasundaram, V. (2011) 'Distinctive attributes of β-lactam target proteins in *Acinetobacter baumannii* relevant to development of new antibiotics', *J Am Chem Soc*, 133(50), 20536-20545.

Hayashi, K. (1975) 'A rapid determination of sodium dodecyl sulfate with methylene blue', *Analytical biochemistry*, 67(2), 503-506.

Heidrich, C., Templin, M.F., Ursinus, A., Merdanovic, M., Berger, J., Schwarz, H., De Pedro, M.A. and Höltje, J.V. (2001) 'Involvement of N-acetylmuramyl-L-alanine amidases in cell separation and antibiotic-induced autolysis of *Escherichia coli*', *Molecular microbiology*, 41(1), 167-178.

Hett, E.C., Chao, M.C., Deng, L.L. and Rubin, E.J. (2008) 'A *Mycobacterial* enzyme essential for cell division synergizes with resuscitation-promoting factor', *PLoS pathogens*, 4(2), e1000001.

Hett, E.C., Chao, M.C., Steyn, A.J., Fortune, S.M., Deng, L.L. and Rubin, E.J. (2007) 'A partner for the resuscitation-promoting factors of *Mycobacterium tuberculosis*', *Molecular microbiology*, 66(3), 658-668.

Hodgkin, E. (2017) '*Listeria* outbreak: three deaths in UK news -what is it? Symptoms of fatal bacteria ' . available at: https://www.express.co.uk/life-style/health/1137699/listeria-outbreak-symptoms-uk-news-what-is-good-food-deaths.

Höltje, J.-V. (1995) 'From growth to autolysis: the murein hydrolases in *Escherichia coli*', *Archives of microbiology*, 164(4), 243-254.

Hosseini-Mazinani, S., Nakajima, E., Ihara, Y., Kameyama, K. and Sugimoto, K. (1996) 'Recovery of active beta-lactamases from *Proteus vulgaris* and RTEM-1 hybrid by random mutagenesis by using a dnaQ strain of *Escherichia coli*', *Antimicrobial agents and chemotherapy*, 40(9), 2152-2159.

Hu, Y.-F., Zhao, D., Yu, X.-L., Hu, Y.-L., Li, R.-C., Ge, M., Xu, T.-Q., Liu, X.-B. and Liao, H.-Y. (2017) 'Identification of bacterial surface antigens by screening peptide phage libraries using whole bacteria cell-purified antisera', *Frontiers in microbiology*, 8, 82.

Iakobachvili , N. (2014) 'Mycobacterial resuscitation promoting factors: roles and mechanisms in infected macrophages', unpublished thesis (degree of Doctor of Philosophy), University of Leicester.

Ivanek, R., Gröhn, Y.T. and Wiedmann, M. (2006) '*Listeria monocytogenes* in multiple habitats and host populations: review of available data for mathematical modeling', *Foodbourne Pathogens & Disease*, 3(4), 319-336.

Jamieson, D.J., Theiler, R.N. and Rasmussen, S.A. (2006) 'Emerging infections and pregnancy', *Emerging infectious diseases*, 12(11), 1638.

Jarvis, N.A., O'Bryan, C.A., Ricke, S.C., Johnson, M.G. and Crandall, P.G. (2016) 'A review of minimal and defined media for growth of *Listeria monocytogenes*', *Food Control*, 66, 256-269.

Jenkins, C.H., Wallis, R., Allcock, N., Barnes, K.B., Richards, M.I., Auty, J.M., Galyov, E.E., Harding, S.V. and Mukamolova, G.V. (2019) 'The lytic transglycosylase, LtgG, controls cell morphology and virulence in *Burkholderia pseudomallei*', *Scientific Reports*, 9(1), 1-13.

Jennings, M.J., Barrios, A.F. and Tan, S. (2016) 'Elimination of truncated recombinant protein expressed in *Escherichia coli* by removing cryptic translation initiation site', *Protein Expr Purif*, 121, 17-21.

Jonquieres, R., Bierne, H., Fiedler, F., Gounon, P. and Cossart, P. (1999) 'Interaction between the protein InlB of *Listeria monocytogenes* and lipoteichoic acid: a novel mechanism of protein association at the surface of Gram-positive bacteria', *Molecular microbiology*, 34(5), 902-914.

Jorgenson, M.A., Chen, Y., Yahashiri, A., Popham, D.L. and Weiss, D.S. (2014) 'The bacterial septal ring protein RlpA is a lytic transglycosylase that contributes to rod shape and daughter cell separation in *Pseudomonas aeruginosa*', *Molecular microbiology*, 93(1), 113-128.

Joseph, J., Fernández-Lloris, R., Pezzat, E., Saubi, N., Cardona, P.-J., Mothe, B. and Gatell, J.M. (2010) 'Molecular characterization of heterologous HIV-1gp120 gene expression disruption in *Mycobacterium bovis* BCG host strain: a critical issue for engineering mycobacterial based-vaccine vectors', *BioMed Research International*, 2010.

Kana, B.D., Gordhan, B.G., Downing, K.J., Sung, N., Vostroktunova, G., Machowski, E.E., Tsenova, L., Young, M., Kaprelyants, A. and Kaplan, G. (2008) 'The resuscitation-promoting factors of *Mycobacterium tuberculosis* are required for virulence and resuscitation from dormancy but are collectively dispensable for growth in vitro', *Molecular microbiology*, 67(3), 672-684.

Kana, B.D. and Mizrahi, V. (2010) 'Resuscitation-promoting factors as lytic enzymes for bacterial growth and signaling', *FEMS Immunology & Medical Microbiology*, 58(1), 39-50.

Karamanos, Y. (1997) 'Endo-N-acetyl-β-D-glucosaminidases and their potential substrates: structure/function relationships', *Research in microbiology*, 148(8), 661-671.

Kespichayawattana, W., Rattanachetkul, S., Wanun, T., Utaisincharoen, P. and Sirisinha, S. (2000) '*Burkholderia pseudomallei* induces cell fusion and actin-associated membrane protrusion: a possible mechanism for cell-to-cell spreading', *Infection and immunity*, 68(9), 5377-5384.

Kleiner-Grote, G.R., Risse, J.M. and Friehs, K. (2018) 'Secretion of recombinant proteins from *E. coli*', *Engineering in Life Sciences*, 18(8), 532-550.

Kocks, C., Gouin, E., Tabouret, M., Berche, P., Ohayon, H. and Cossart, P. (1992) '*L. monocytogenes* induced actin assembly requires the actA gene product, a surface protein', *Cell*, 68(3), 521-531.

Kongo, J., Malcata, F., Ho, A. and Wiedmann, M. (2006) 'Detection and characterization of *Listeria monocytogenes* in Sao Jorge (Portugal) cheese production', *Journal of Dairy Science*, 89(11), 4456-4461.

Kuhn, M. and Goebel, W. (1989) 'Identification of an extracellular protein of *Listeria monocytogenes* possibly involved in intracellular uptake by mammalian cells', *Infection and immunity*, 57(1), 55-61.

Kumar, D., Srivastava, B. and Srivastava, R. (1998) 'Genetic rearrangements leading to disruption of heterologous gene expression in *mycobacteria*: an observation with *Escherichia coli* β-galactosidase in *Mycobacterium smegmatis* and its implication in vaccine development', *Vaccine*, 16(11-12), 1212-1215.

Lamont, R.J. (2004) '*Bacterial invasion of host cells*', Cambridge University Press. United Kingdom

Lasa, I., Gouin, E., Goethals, M., Vancompernolle, K., David, V., Vandekerckhove, J. and Cossart, P. (1997) 'Identification of two regions in the N-terminal domain of ActA involved in the actin comet tail formation by *Listeria monocytogene*s', *The EMBO journal*, 16(7), 1531-1540.

Lathrop, A.A., Banada, P.P. and Bhunia, A.K. (2008) 'Differential expression of InlB and ActA in *Listeria monocytogenes* in selective and nonselective enrichment broths', *J Appl Microbiol*, 104(3), 627-39.

Lauer, P., Theriot, J.A., Skoble, J., Welch, M.D. and Portnoy, D.A. (2001) 'Systematic mutational analysis of the amino-terminal domain of the *Listeria monocytogenes* ActA

protein reveals novel functions in actin-based motility', *Molecular microbiology*, 42(5), 1163-1177.

Le Monnier, A., Abachin, E., Beretti, J.-L., Berche, P. and Kayal, S. (2011) 'Diagnosis of *Listeria monocytogenes* meningoencephalitis by real-time PCR for the *hly* gene', *Journal of clinical microbiology*, 49(11), 3917-3923.

Lebreton, A. and Cossart, P. (2017) 'RNA-and protein-mediated control of *Listeria monocytogenes* virulence gene expression', *RNA biology*, 14(5), 460-470.

Lebreton, A., Stavru, F., Brisse, S. and Cossart, P. (2016) '1926–2016: 90 Years of listeriology', *Microbes and infection*, 18(12), 711-723.

Leder, L., Wendt, H., Schwab, C., Jelesarov, I., Bornhauser, S., Ackermann, F. and Bosshard, H.R. (1994) 'Genuine and apparent cross-reaction of polyclonal antibodies to proteins and peptides', *European journal of biochemistry*, 219(1-2), 73-81.

Leimeister-Wächter, M., Haffner, C., Domann, E., Goebel, W. and Chakraborty, T. (1990) 'Identification of a gene that positively regulates expression of listeriolysin, the major virulence factor of *Listeria monocytogenes*', *Proceedings of the National Academy of Sciences*, 87(21), 8336-8340.

Lenz, L.L., Mohammadi, S., Geissler, A. and Portnoy, D.A. (2003) 'SecA2-dependent secretion of autolytic enzymes promotes *Listeria monocytogenes* pathogenesis', *Proceedings of the National Academy of Sciences*, 100(21), 12432-12437.

Lilie, H., Schwarz, E. and Rudolph, R. (1998) 'Advances in refolding of proteins produced in *E. coli*', *Current opinion in biotechnology*, 9(5), 497-501.

Liu, D. (2008) '*Handbook of Listeria monocytogenes*', Taylor & Francis CRC Press, Boca Raton, Florida, USA.

Loraine, J., Alhumaidan, O., Bottrill, A.R., Mistry, S.C., Andrew, P., Mukamolova, G.V. and Turapov, O. (2019) 'Efficient protein digestion at elevated temperature in the presence of sodium dodecyl sulfate and calcium ions for membrane proteomics', *Analytical chemistry*, 91(15), 9516-9521.

Loraine, J., Pu, F., Turapov, O. and Mukamolova, G.V. (2016) 'Development of an *in-vitro* assay for detection of drug induced resuscitation promoting factor dependent *Mycobacteria* ', *Antimicrobial agents and chemotherapy*, 60(10), 6227-6233.

Low, J. and Donachie, W. (1997) 'A review of *Listeria monocytogenes* and listeriosis', *The Veterinary Journal*, 153(1), 9-29.

Luan, Q., Zelter, A., MacCoss, M.J., Davis, T.N. and Nolen, B.J. (2018) 'Identification of Wiskott-Aldrich syndrome protein (WASP) binding sites on the branched actin filament nucleator Arp2/3 complex', *Proceedings of the National Academy of Sciences*, 115(7), E1409-E1418.

Lundén, J.M., Autio, T.J. and Korkeala, H.J. (2002) 'Transfer of persistent *Listeria monocytogenes* contamination between food-processing plants associated with a dicing machine', *Journal of Food Protection®*, 65(7), 1129-1133.

Maeda, H. (1980) 'A new lysozyme assay based on fluorescence polarization or fluorescence intensity utilizing a fluorescent peptidoglycan substrate', *The Journal of Biochemistry*, 88(4), 1185-1191.

Maguire, B. and Riley Jr, H. (1967) 'Infections due to *Listeria monocytogenes* in infants and children', *American Journal of Medical Sciences*, 254(4), 421-8.

Makino, S.-I., Kawamoto, K., Takeshi, K., Okada, Y., Yamasaki, M., Yamamoto, S. and Igimi, S. (2005) 'An outbreak of food-borne listeriosis due to cheese in Japan, during 2001', *International journal of food microbiology*, 104(2), 189-196.

Makino, T., Skretas, G. and Georgiou, G. (2011) 'Strain engineering for improved expression of recombinant proteins in bacteria', *Microbial cell factories*, 10(1), 32.

Marie Glenn, S. (2012) ' Genes involved in attachment of *Listeria monocytogenes* to abiotic surfaces', (degree of Doctor of Philosophy), University of Leicester.

Marston, F. (1986) 'The purification of eukaryotic polypeptides synthesized in *Escherichia coli*', *Biochemical Journal*, 240(1), 1.

Maurizi, M. (1992) 'Proteases and protein degradation in *Escherichia coli*', *Experientia*, 48(2), 178-201.

Mawuenyega, K.G., Forst, C.V., Dobos, K.M., Belisle, J.T., Chen, J., Bradbury, E.M., Bradbury, A.R. and Chen, X. (2005) '*Mycobacterium tuberculosis* functional network analysis by global subcellular protein profiling', *Mol Biol Cell*, 16(1), 396-404.

McLauchlin, J. (1997) 'The pathogenicity of *Listeria monocytogenes*: a public health perspective', *Reviews in Medical Microbiology*, 8(1), 1-14.

McLaughlan, A.M. and Foster, S.J. (1998) 'Molecular characterization of an autolytic amidase of *Listeria monocytogenes* EGD', *Microbiology*, 144(5), 1359-1367.

McPherson, A. and Cudney, B. (2014) 'Optimization of crystallization conditions for biological macromolecules', *Acta Crystallographica Section F*, 70(11), 1445-1467.

Mead, P.S., Slutsker, L., Dietz, V. and McCaig, L.F. (2000) 'Food-related illness and death in the United States', *Journal of Environmental Health*, 62(7), 9.

Mengaud, J., Lecuit, M., Lebrun, M., Nato, F., Mazie, J.-C. and Cossart, P. (1996) 'Antibodies to the leucine-rich repeat region of internalin block entry of *Listeria monocytogenes* into cells expressing E-cadherin', *Infection and immunity*, 64(12), 5430-5433.

Milenbachs, A.A., Brown, D.P., Moors, M. and Youngman, P. (1997) 'Carbon-source regulation of virulence gene expression in *Listeria monocytogenes*', *Molecular microbiology*, 23(5), 1075-1085.

Milohanic, E., Jonquières, R., Cossart, P., Berche, P. and Gaillard, J.L. (2001) 'The autolysin Ami contributes to the adhesion of *Listeria monocytogenes* to eukaryotic cells via its cell wall anchor', *Molecular microbiology*, 39(5), 1212-1224.

Mirza, S.P., Halligan, B.D., Greene, A.S. and Olivier, M. (2007) 'Improved method for the analysis of membrane proteins by mass spectrometry', *Physiological genomics*, 30(1), 89-94.

Mitchell, G., Ge, L., Huang, Q., Chen, C., Kianian, S., Roberts, M.F., Schekman, R. and Portnoy, D.A. (2015) 'Avoidance of autophagy mediated by PlcA or ActA is required for *Listeria monocytogenes* growth in macrophages', *Infection and immunity*, 83(5), 2175-2184.

Moors, M.A., Auerbuch, V. and Portnoy, D.A. (1999) 'Stability of the *Listeria monocytogenes* ActA protein in mammalian cells is regulated by the N-end rule pathway', *Cellular microbiology*, 1(3), 249-257.

Movahedzadeh, F., Frita, R. and Gutka, H.J. (2011) 'A two-step strategy for the complementation of *M.tuberculosis* mutants', *Genetics and molecular biology*, 34(2), 286-289.

Mukamolova, G.V., Kaprelyants, A.S., Young, D.I., Young, M. and Kell, D.B. (1998) 'A bacterial cytokine', *Proceedings of the National Academy of Sciences*, 95(15), 8916-8921.

Mukamolova, G.V., Murzin, A.G., Salina, E.G., Demina, G.R., Kell, D.B., Kaprelyants, A.S. and Young, M. (2006) 'Muralytic activity of *Micrococcus luteus* Rpf and its relationship to physiological activity in promoting bacterial growth and resuscitation', *Molecular microbiology*, 59(1), 84-98.

Mukamolova, G.V., Turapov, O.A., Young, D.I., Kaprelyants, A.S., Kell, D.B. and Young, M. (2002) 'A family of autocrine growth factors in *Mycobacterium tuberculosis*', *Molecular microbiology*, 46(3), 623-635.

Mushegian, A.R., Fullner, K.J., Koonin, E.V. and Nester, E.W. (1996) 'A family of lysozyme-like virulence factors in bacterial pathogens of plants and animals', *Proceedings of the National Academy of Sciences*, 93(14), 7321-7326.

Mylonakis, E., Paliou, M., Hohmann, E.L., Calderwood, S.B. and Wing, E.J. (2002) 'Listeriosis during pregnancy: a case series and review of 222 cases', *Medicine*, 81(4), 260-269.

Nambu, T., Minamino, T., Macnab, R.M. and Kutsukake, K. (1999) 'Peptidoglycan-hydrolyzing activity of the FlgJ protein, essential for flagellar rod formation in *Salmonella typhimurium*', *Journal of bacteriology*, 181(5), 1555-1561.

Niebuhr, K., Chakraborty, T., Rohde, M., Gazlig, T., Jansen, B., Köllner, P. and Wehland, J. (1993) 'Localization of the ActA polypeptide of *Listeria monocytogenes* in infected tissue culture cell lines: ActA is not associated with actin" comets"', *Infection and immunity*, 61(7), 2793-2802.

Niebuhr, K., Ebel, F., Frank, R., Reinhard, M., Domann, E., Carl, U.D., Walter, U., Gertler, F.B., Wehland, J. and Chakraborty, T. (1997) 'A novel proline-rich motif present in ActA of *Listeria monocytogenes* and cytoskeletal proteins is the ligand for the EVH1 domain, a protein module present in the Ena/VASP family', *The EMBO journal*, 16(17), 5433-5444.

Nixon, A.E., Ostermeier, M. and Benkovic, S.J. (1998) 'Hybrid enzymes: manipulating enzyme design', *Trends in biotechnology*, 16(6), 258-264.

Nyfeldt, A. (1929) 'Etiologie de la mononucleose infectieuse', *CR Soc. Biol*, 101, 590-591.

Olsen, O., Borriss, R., Simon, O. and Thomsen, K.K. (1991) 'Hybrid Bacillus (1-3, 1-4)-β-glucanases: engineering thermostable enzymes by construction of hybrid genes', *Molecular and General Genetics MGG*, 225(2), 177-185.

Ooi, S.T. and Lorber, B. (2005) 'Gastroenteritis due to *Listeria monocytogenes*', *Clinical Infectious Diseases*, 40(9), 1327-1332.

Orsi, R.H. and Wiedmann, M. (2016) 'Characteristics and distribution of *Listeria* spp., including *Listeria* species newly described since 2009', *Applied microbiology and biotechnology*, 100(12), 5273-5287.

Ostermeier, M. and Benkovic, S.J. (2001) 'Evolution of protein function by domain swapping', *Advances in protein chemistry*, 55, 29-77.

Palomares, L.A., Estrada-Moncada, S. and Ramírez, O.T. (2004) 'Production of recombinant proteins' in *Recombinant gene expression* Springer, 15-51.

Peng, C. and Gao, F. (2014) 'Protein localization analysis of essential genes in prokaryotes', *Scientific Reports*, 4, 6001.

Petran, R. and Zottola, E. (1989) 'A study of factors affecting growth and recovery of *Listeria monocytogenes* Scott A', *Journal of food science*, 54(2), 458-460.

Phan-Thanh, L. and Gormon, T. (1997) 'A chemically defined minimal medium for the optimal culture of *Listeria*', *International journal of food microbiology*, 35(1), 91-95.

Public Health England (PHE). (2018) '*Listeria* data 2006 to 2016 ,National laboratory data for residents of England and Wales. Available at: https://assets.publishing.service.gov.uk/government/uploads/system/uploads/attachment_data/file/712007/listeria_data_2006_to_2016_may_2018.pdf

Pilgrim, S., Kolb-Mäurer, A., Gentschev, I., Goebel, W. and Kuhn, M. (2003) 'Deletion of the gene encoding p60 in *Listeria monocytogenes* leads to abnormal cell division and loss of actin-based motility', *Infection and immunity*, 71(6), 3473-3484.

Pina, A.S., Lowe, C.R. and Roque, A.C.A. (2014) 'Challenges and opportunities in the purification of recombinant tagged proteins', *Biotechnology advances*, 32(2), 366-381.

Pinto, D., São-José, C., Santos, M.A. and Chambel, L. (2013) 'Characterization of two resuscitation promoting factors of *Listeria monocytogenes*', *Microbiology*, 159(7), 1390-1401.

PIRIE, J.H. (1940) '*Listeria*: change of name for a genus bacteria', *Nature*, 145(3668), 264.

Pistor, S., Chakraborty, T., Niebuhr, K., Domann, E. and Wehland, J. (1994) 'The ActA protein of *Listeria monocytogenes* acts as a nucleator inducing reorganization of the actin cytoskeleton', *The EMBO journal*, 13(4), 758.

Pistor, S., Grobe, L., Sechi, A.S., Domann, E., Gerstel, B., Machesky, L.M., Chakraborty, T. and Wehland, J. (2000) 'Mutations of arginine residues within the 146-KKRRK-150 motif of the ActA protein of *Listeria monocytogenes* abolish intracellular motility by interfering with the recruitment of the Arp2/3 complex', *Journal of cell science*, 113(18), 3277-3287.

Pizarro-Cerdá, J., Kühbacher, A. and Cossart, P. (2012) 'Entry of *Listeria monocytogenes* in mammalian epithelial cells: an updated view', *Cold Spring Harbor Perspectives in Medicine*, 2(11), a010009.

Popowska, M. (2004) 'Analysis of the peptidoglycan hydrolases of *Listeria monocytogenes*: multiple enzymes with multiple functions', *Polish journal of microbiology*, 53(suppl), 29-34.

Popowska, M. and Markiewicz, Z. (2006) 'Characterization of *Listeria monocytogenes* protein Lmo0327 with murein hydrolase activity', *Archives of microbiology*, 186(1), 69-86.

Portnoy, D.A., Auerbuch, V. and Glomski, I.J. (2002) 'The cell biology of *Listeria monocytogenes* infection the intersection of bacterial pathogenesis and cell-mediated immunity', *The Journal of cell biology*, 158(3), 409-414.

Portnoy, D.A., Chakraborty, T., Goebel, W. and Cossart, P. (1992) 'Molecular determinants of *Listeria monocytogenes* pathogenesis', *Infection and immunity*, 60(4), 1263.

Poussin, M.A. and Goldfine, H. (2010) 'Evidence for involvement of ActA in maturation of the *Listeria monocytogenes* phagosome', *Cell research*, 20(1), 109.

Premaratne, R.J., Lin, W.-J. and Johnson, E.A. (1991) 'Development of an improved chemically defined minimal medium for *Listeria monocytogenes*', *Applied and Environmental Microbiology*, 57(10), 3046-3048.

Racz, P., Tenner, K. and Szivessy, K. (1970) 'Electron microscopic studies in experimental keratoconjunctivitis listeriosa. I. Penetration of *Listeria monocytogenes* into corneal epithelial cells', *Acta microbiologica Academiae Scientiarum Hungaricae*, 17(3), 221-236.

Rafelski, S.M. and Theriot, J.A. (2006) 'Mechanism of polarization of *Listeria monocytogenes* surface protein ActA', *Molecular microbiology*, 59(4), 1262-1279.

Ragon, M., Wirth, T., Hollandt, F., Lavenir, R., Lecuit, M., Le Monnier, A. and Brisse, S. (2008) 'A New Perspective on *Listeria monocytogenes* Evolution', *PLoS Pathog*, 4(9), e1000146.

Ramaswamy, V., Cresence, V.M., Rejitha, J.S., Lekshmi, M.U., Dharsana, K., Prasad, S.P. and Vijila, H.M. (2007) '*Listeria*-review of epidemiology and pathogenesis', *Journal of Microbiology Immunology and Infection*, 40(1), 4.

Ravagnani, A., Finan, C.L. and Young, M. (2005) 'A novel firmicute protein family related to the *Actinobacterial* resuscitation-promoting factors by non-orthologous domain displacement', *BMC genomics*, 6(1), 39.

Read, A., Gauci, C. and Lightowlers, M. (2009) 'Purification of polyclonal anti-conformational antibodies for use in affinity selection from random peptide phage display libraries: A study using the hydatid vaccine EG95', *Journal of Chromatography B*, 877(14-15), 1516-1522.

Réglier-Poupet, H., Pellegrini, E., Charbit, A. and Berche, P. (2003) 'Identification of LpeA, a PsaA-like membrane protein that promotes cell entry by *Listeria monocytogenes*', *Infection and immunity*, 71(1), 474-482.

Ren, Z., Chen, J. and Khalil, R.A. (2017) 'Zymography as a Research Tool in the Study of Matrix Metalloproteinase Inhibitors' in *Zymography* Springer, 79-102.

Rigi, G., Beyranvand, P., Ghaedmohammadi, S., Heidarpanah, S., Akbari Noghabi, K. and Ahmadian, G. (2015) 'Comparison of the extracellular full-length and truncated recombinant protein A production in *Escherichia coli* BL21 (DE3)', *Journal of Paramedical Sciences*, 6(3), 2008-4978.

Ripio, M.-T., Brehm, K., Lara, M., Suarez, M. and Vazquez-Boland, J.-A. (1997) 'Glucose-1-phosphate utilization by *Listeria monocytogenes* is PrfA dependent and coordinately expressed with virulence factors', *Journal of bacteriology*, 179(22), 7174-7180.

Rippey, C., Walsh, T., Gulsuner, S., Brodsky, M., Nord, A.S., Gasperini, M., Pierce, S., Spurrell, C., Coe, B.P. and Krumm, N. (2013) 'Formation of chimeric genes by copy-number variation as a mutational mechanism in schizophrenia', *The American Journal of Human Genetics*, 93(4), 697-710.

Robbins, J.R., Barth, A.I., Marquis, H., De Hostos, E.L., Nelson, W.J. and Theriot, J.A. (1999) '*Listeria monocytogenes* exploits normal host cell processes to spread from cell to cell', *The Journal of cell biology*, 146(6), 1333-1350.

Rocourt, J. and Cossart, P. (1997) 'Food microbiology: fundamentals and frontiers', *American Society for Microbiology, Washington*.

Rogers, R.L., Bedford, T. and Hartl, D.L. (2009) 'Formation and longevity of chimeric and duplicate genes in Drosophila melanogaster', *Genetics*, 181(1), 313-322.

Rogers, R.L. and Hartl, D.L. (2011) 'Chimeric genes as a source of rapid evolution in Drosophila melanogaster', *Molecular biology and evolution*, 29(2), 517-529.

Romano, M., Aryan, E., Korf, H., Bruffaerts, N., Franken, C., Ottenhoff, T. and Huygen, K. (2012) 'Potential of *Mycobacterium tuberculosis* resuscitation-promoting factors as antigens in novel tuberculosis sub-unit vaccines', *Microbes and infection*, 14(1), 86-95.

Rosano, G.L. and Ceccarelli, E.A. (2014) 'Recombinant protein expression in *Escherichia coli*: advances and challenges', *Frontiers in microbiology*, 5, 172.

Rosser, A., Stover, C., Pareek, M. and Mukamolova, G.V. (2017) 'Resuscitation-promoting factors are important determinants of the pathophysiology in *Mycobacterium tuberculosis* infection', *Critical reviews in microbiology*, 43(5), 621-630.

Ruggiero, A., Tizzano, B., Pedone, E., Pedone, C., Wilmanns, M. and Berisio, R. (2009) 'Crystal structure of the resuscitation-promoting factor ΔDUFRpfB from *M. tuberculosis*', *Journal of molecular biology*, 385(1), 153-162.

Ruhland, G.J., Hellwig, M., Wanner, G. and Fiedler, F. (1993) 'Cell-surface location of *Listeria* specific protein p60 detection of Listeria cells by indirect immunofluorescence', *Microbiology*, 139(3), 609-616.

Rydman, P.S. and Bamford, D.H. (2003) 'Identification and mutational analysis of bacteriophage PRD1 holin protein P35', *Journal of bacteriology*, 185(13), 3795-3803.

Salazar, J.K., Carstens, C.K., Bathija, V.M., Narula, S.S., Parish, M. and Tortorello, M.L. (2016) 'Fate of *Listeria monocytogenes* in fresh apples and caramel apples', *Journal of food protection*, 79(5), 696-702.

Schaechter, M. (2009) '*Encyclopedia of microbiology* ', Academic Press. New-York, USA.

Schaub, R.E., Chan, Y.A., Lee, M., Hesek, D., Mobashery, S. and Dillard, J.P. (2016) 'Lytic transglycosylases LtgA and LtgD perform distinct roles in remodeling, recycling and releasing peptidoglycan in *Neisseria gonorrhoeae*', *Molecular microbiology*, 102(5), 865-881.

Scheurwater, E., Reid, C.W. and Clarke, A.J. (2008) 'Lytic transglycosylases: bacterial space-making autolysins', *The international journal of biochemistry & cell biology*, 40(4), 586-591.

Schlech III, W.F., Lavigne, P.M., Bortolussi, R.A., Allen, A.C., Haldane, E.V., Wort, A.J., Hightower, A.W., Johnson, S.E., King, S.H. and Nicholls, E.S. (1983) 'Epidemic listeriosis evidence for transmission by food', *New England Journal of Medicine*, 308(4), 203-206.

Schleifer, K.H. and Kandler, O. (1972) 'Peptidoglycan types of bacterial cell walls and their taxonomic implications', *Bacteriological reviews*, 36(4), 407.

Schmid, M.W., Ng, E.Y., Lampidis, R., Emmerth, M., Walcher, M., Kreft, J., Goebel, W., Wagner, M. and Schleifer, K.-H. (2005) 'Evolutionary history of the genus *Listeria* and its virulence genes', *Systematic and Applied Microbiology*, 28(1), 1-18.

Schnupf, P. and Portnoy, D.A. (2007) 'Listeriolysin O: a phagosome-specific lysin', *Microbes and infection*, 9(10), 1176-1187.

Schubert, K., Bichlmaier, A.M., Mager, E., Wolff, K., Ruhland, G. and Fiedler, F. (2000) 'P45, an extracellular 45 kDa protein of *Listeria monocytogenes* with similarity to protein p60 and exhibiting peptidoglycan lytic activity', *Archives of microbiology*, 173(1), 21-28.

Schuppler, M. and Loessner, M.J. (2010) 'The opportunistic pathogen *Listeria monocytogenes*: pathogenicity and interaction with the mucosal immune system', *International journal of inflammation*, 2010, 12.

Sheehan, B., Klarsfeld, A., Msadek, T. and Cossart, P. (1995) 'Differential activation of virulence gene expression by PrfA, the *Listeria monocytogenes* virulence regulator', *Journal of bacteriology*, 177(22), 6469-6476.

Shleeva, M., Bagramyan, K., Telkov, M., Mukamolova, G., Young, M., Kell, D. and Kaprelyants, A. (2002) 'Formation and resuscitation of 'non-culturable'cells of *Rhodococcus rhodochrous* and *Mycobacterium tuberculosis* in prolonged stationary phase', *Microbiology*, 148(5), 1581-1591.

Siegrist, M.S., Aditham, A.K., Espaillat, A., Cameron, T.A., Whiteside, S.A., Cava, F., Portnoy, D.A. and Bertozzi, C.R. (2015) 'Host actin polymerization tunes the cell division cycle of an intracellular pathogen', *Cell reports*, 11(4), 499-507.

Sinmaz, E. and Tozer, J. (2019) 'Sixth person dies from *Listeria* outbreak linked to NHS sandwiches ', *The Daily Mail* available at: https://www.dailymail.co.uk/news/article-7310001/New-listeria-death-takes-toll-SIX.html

Skoble, J., Portnoy, D.A. and Welch, M.D. (2000) 'Three regions within ActA promote Arp2/3 complex-mediated actin nucleation and *Listeria monocytogenes* motility', *The Journal of cell biology*, 150(3), 527-538.

Smith, G.A. and Portnoy, D.A. (1997) 'How the *Listeria monocytogenes* ActA protein converts actin polymerization into a motile force', *Trends in microbiology*, 5(7), 272-276.

Smith, G.A., Theriot, J.A. and Portnoy, D.A. (1996) 'The tandem repeat domain in the *Listeria monocytogenes* ActA protein controls the rate of actin-based motility, the percentage of moving bacteria, and the localization of vasodilator-stimulated phosphoprotein and profilin', *The Journal of cell biology*, 135(3), 647-660.

Sogawa, K. and Takahashi, K. (1978) 'Use of fluorescamine-labeled casein as a substrate for assay of proteinases', *The Journal of Biochemistry*, 83(6), 1783-1787.

Sokolovic, Z., Schüller, S., Bohne, J., Baur, A., Rdest, U., Dickneite, C., Nichterlein, T. and Goebel, W. (1996) 'Differences in virulence and in expression of PrfA and PrfA-regulated virulence genes of *Listeria monocytogenes* strains belonging to serogroup 4', *Infection and immunity*, 64(10), 4008-4019.

Sousa, M.M., Steen, K.W., Hagen, L. and Slupphaug, G. (2011) 'Antibody cross-linking and target elution protocols used for immunoprecipitation significantly modulate signal-to noise ratio in downstream 2D-PAGE analysis', *Proteome Sci*, 9(45).

Squeglia, F., Moreira, M., Ruggiero, A. and Berisio, R. (2019) 'The Cell Wall Hydrolytic NlpC/P60 Endopeptidases in *Mycobacterial* Cytokinesis: A Structural Perspective', *Cells*, 8(6), 609.

Stamm, L.M., Morisaki, J.H., Gao, L.-Y., Jeng, R.L., McDonald, K.L., Roth, R., Takeshita, S., Heuser, J., Welch, M.D. and Brown, E.J. (2003) '*Mycobacterium marinum* escapes from phagosomes and is propelled by actin-based motility', *Journal of Experimental Medicine*, 198(9), 1361-1368.

Stover, C., De La Cruz, V., Fuerst, T., Burlein, J., Benson, L., Bennett, L., Bansal, G., Young, J., Lee, M.-H. and Hatfull, G. (1991) 'New use of BCG for recombinant vaccines', *Nature*, 351(6326), 456.

Suárez, M., González-Zorn, B., Vega, Y., Chico-Calero, I. and Vázquez-Boland, J.A. (2001) 'A role for ActA in epithelial cell invasion by *Listeria monocytogenes'*, *Cellular microbiology*, 3(12), 853-864.

Sutcliffe, I.C. (2011) 'New insights into the distribution of WXG100 protein secretion systems', *Antonie Van Leeuwenhoek*, 99(2), 127-131.

Swaminathan, B. and Gerner-Smidt, P. (2007) 'The epidemiology of human listeriosis', *Microbes and infection*, 9(10), 1236-1243.

Tao, B., Lee, K., Griffin, H. and Griffin, A. (1994) 'PCR technology current innovations', *Boca Raton: CRC Press*, 71-2.

Tavares, F. and Sellstedt, A. (2000) 'A simple, rapid and non-destructive procedure to extract cell wall-associated proteins from Frankia', *Journal of Microbiological Methods*, 39(2), 171-178.

Telkov, M., Demina, G., Voloshin, S., Salina, E.G., Dudik, T., Stekhanova, T., Mukamolova, G.V., Kazaryan, K., Goncharenko, A. and Young, M. (2006) 'Proteins of the Rpf (resuscitation promoting factor) family are peptidoglycan hydrolases', *Biochemistry (Moscow)*, 71(4), 414-422.

The Food Standards Agency (FSA). (2011) 'Foodborne disease strategy 2010-15 ,an fsa programme for the reduction of foodborne disease in the UK ' available at : https://acss.food.gov.uk/sites/default/files/multimedia/pdfs/fds2015.pdf.

Tilney, L.G. and Portnoy, D.A. (1989) 'Actin filaments and the growth, movement, and spread of the intracellular bacterial parasite, *Listeria monocytogenes*', *The Journal of cell biology*, 109(4), 1597-1608.

Tompkin, R. (2002) 'Control of *Listeria monocytogenes* in the food-processing environment', *Journal of food protection*, 65(4), 709-725.

Travier, L., Guadagnini, S., Gouin, E., Dufour, A., Chenal-Francisque, V., Cossart, P., Olivo-Marin, J.-C., Ghigo, J.-M., Disson, O. and Lecuit, M. (2013) 'ActA promotes *Listeria monocytogenes* aggregation, intestinal colonization and carriage', *PLoS Pathog*, 9(1), e1003131.

Tufariello, J.M., Jacobs Jr, W.R. and Chan, J. (2004) 'Individual *Mycobacterium tuberculosis* resuscitation-promoting factor homologues are dispensable for growth *in vitro* and *in vivo*', *Infection and immunity*, 72(1), 515-526.

Typas, A., Banzhaf, M., Gross, C.A. and Vollmer, W. (2012) 'From the regulation of peptidoglycan synthesis to bacterial growth and morphology', *Nature Reviews Microbiology*, 10(2), 123-136.

Van Asselt, E.J., Dijkstra, A.J., Kalk, K.H., Takacs, B., Keck, W. and Dijkstra, B.W. (1999) 'Crystal structure of *Escherichia coli* lytic transglycosylase Slt35 reveals a lysozyme-like catalytic domain with an EF-hand', *Structure*, 7(10), 1167-1180.

Vázquez-Boland, J.A., Kuhn, M., Berche, P., Chakraborty, T., Domínguez-Bernal, G., Goebel, W., González-Zorn, B., Wehland, J. and Kreft, J. (2001) '*Listeria* pathogenesis and molecular virulence determinants', *Clinical microbiology reviews*, 14(3), 584-640.

Villaverde, A. and Carrió, M.M. (2003) 'Protein aggregation in recombinant bacteria: biological role of inclusion bodies', *Biotechnology letters*, 25(17), 1385-1395.

Voigt, C.A., Martinez, C., Wang, Z.-G., Mayo, S.L. and Arnold, F.H. (2002) 'Protein building blocks preserved by recombination', *Nature Structural & Molecular Biology*, 9(7), 553.

Vollmer, W. and Bertsche, U. (2008) 'Murein (peptidoglycan) structure, architecture and biosynthesis in *Escherichia coli*', *Biochimica et Biophysica Acta (BBA)-Biomembranes*, 1778(9), 1714-1734.

Vollmer, W., Joris, B., Charlier, P. and Foster, S. (2008) 'Bacterial peptidoglycan (murein) hydrolases', *FEMS microbiology reviews*, 32(2), 259-286.

Vos, P., Garrity, G., Jones, D., Krieg, N.R., Ludwig, W., Rainey, F.A., Schleifer, K.-H. and Whitman, W.B. (2011) *Bergey's manual of systematic bacteriology: Volume 3: The Firmicutes*, Springer Science & Business Media.

Wagner, M. and McLauchlin, J. (2008) 'Biology and pathology In: Liu, D., eds. Handbook of *Listeria monocytogenes*', Boca Raton: Taylar & Francis CRC Press.

Wang, J., Sung, W.-K., Krishnan, A. and Li, K.-B. (2005) 'Protein subcellular localization prediction for Gram-negative bacteria using amino acid subalphabets and a combination of multiple support vector machines', *BMC bioinformatics*, 6(1), 174.

Watkins, J. and SLEATH, K.P. (1981) 'Isolation and enumeration of *Listeria monocytogenes* from sewage, sewage sludge and river water', *Journal of Applied Bacteriology*, 50(1), 1-9.

Weagant, S.D., Sado, P.N., Colburn, K.G., Torkelson, J.D., Stanley, F.A., Krane, M.H., Shields, S.C. and Thayer, C.F. (1988) 'The incidence of *Listeria* species in frozen seafood products', *Journal of Food Protection*, 51(8), 655-657.

Weaver, L., Grütter, M. and Matthews, B. (1995) 'The refined structures of goose lysozyme and its complex with a bound trisaccharide show that the "Goose-type" ly'sozymes lack a catalytic aspartate residue', *Journal of molecular biology*, 245(1), 54-68.

Weller, D., Andrus, A., Wiedmann, M. and den Bakker, H.C. (2015) '*Listeria* booriae sp. nov. and *Listeria newyorkensis* sp. nov., from food processing environments in the USA', *International journal of systematic and evolutionary microbiology*, 65(1), 286-292.

Welshimer, H. and Donker-Voet, J. (1971) '*Listeria monocytogenes* in nature', *Appl. Environ. Microbiol.*, 21(3), 516-519.

Werten, M.W., Wisselink, W.H., Jansen-van den Bosch, T.J., de Bruin, E.C. and de Wolf, F.A. (2001) 'Secreted production of a custom-designed, highly hydrophilic gelatin in Pichia pastoris', *Protein engineering*, 14(6), 447-454.

Wiedmann, M., Bruce, J.L., Knorr, R., Bodis, M., Cole, E.M., McDowell, C.I., McDonough, P.L. and Batt, C.A. (1996) 'Ribotype diversity of *Listeria monocytogenes* strains associated with outbreaks of listeriosis in ruminants', *Journal of clinical microbiology*, 34(5), 1086-1090.

Williams, S.K. (2010) '*Listeria monocytogenes* and other *Listeria* species in small and very small ready-to-eat meat processing plants', unpublished thesis, Colorado State University.

Wingfield, P.T. (2015) 'Overview of the purification of recombinant proteins', *Current protocols in protein science*, 80(1), 6.1. 1-6.1. 35.

Wong, K.K., Bouwer, H.A. and Freitag, N.E. (2004) 'Evidence implicating the 5′ untranslated region of *Listeria monocytogenes* actA in the regulation of bacterial actin-based motility', *Cellular microbiology*, 6(2), 155-166.

Wooldridge, K. (2009) 'Bacterial secreted proteins: secretory mechanisms and role in pathogenesis', Horizon Scientific Press.

Wydau-Dematteis, S., El Meouche, I., Courtin, P., Hamiot, A., Lai-Kuen, R., Saubaméa, B., Fenaille, F., Butel, M.-J., Pons, J.-L. and Dupuy, B. (2018) 'Cwp19 is a novel lytic transglycosylase involved in stationary-phase autolysis resulting in toxin release in *Clostridium difficile*', *mBio*, 9(3), e00648-18.

Yakut, N., Soysal, A., Kepenekli Kadayifci, E., Dalgic, N., Yılmaz Ciftdogan, D., Karaaslan, A., Akkoc, G., Ocal Demir, S., Cagan, E. and Celikboya, E. (2018) 'Ventriculoperitoneal shunt infections and re-infections in children: a multicentre retrospective study', *British journal of neurosurgery*, 32(2), 196-200.

Yoshikawa, Y., Ogawa, M., Hain, T., Yoshida, M., Fukumatsu, M., Kim, M., Mimuro, H., Nakagawa, I., Yanagawa, T. and Ishii, T. (2009) '*Listeria monocytogenes* ActA-mediated escape from autophagic recognition', *Nature Cell Biology*, 11(10), 1233.

Zahrl, D., Wagner, M., Bischof, K., Bayer, M., Zavecz, B., Beranek, A., Ruckenstuhl, C., Zarfel, G.E. and Koraimann, G. (2005) 'Peptidoglycan degradation by specialized lytic transglycosylases associated with type III and type IV secretion systems', *Microbiology*, 151(11), 3455-3467.

Zalevsky, J., Grigorova, I. and Mullins, R.D. (2001) 'Activation of the Arp2/3 complex by the *Listeria* ActA protein acta binds two actin monomers and three subunits of the arp2/3 complex', *Journal of Biological Chemistry*, 276(5), 3468-3475.